Integration of biomolecular logic principles with electronic transducers on a chip

Dissertation
zur
Erlangung des Doktorgrades
der Naturwissenschaften
(Dr. rer. nat.)

dem
Fachbereich Pharmazie
der Philipps-Universität Marburg
vorgelegt von
Denise Molinnus
aus **Lebach**

Marburg/Lahn **2018**

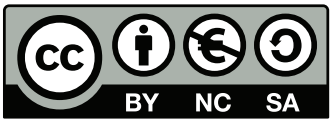

Gutachter: Prof. Dr. Michael J. Schöning

Gutachter: Prof. Dr. Michael Keusgen

Eingereicht am 11.07.2018

Tag der mündlichen Prüfung am 24.09.2018

Hochschulkennziffer: 1180

Erklärung

Ich versichere, dass ich meine Dissertation

"Integration of biomolecular logic principles with electronic transducers on a chip"

selbständig und ohne unerlaubte Hilfe angefertigt und mich dabei keiner anderen als der von mir ausdrücklich bezeichneten Quellen bedient habe. Alle vollständig oder sinngemäß übernommenen Zitate sind als solche gekennzeichnet.

Die Dissertation wurde in der jetzigen oder ähnlichen Form noch bei keiner Hochschule eingereicht und hat noch keinen sonstigen Prüfungszwecken gedient.

Marburg, den 11.07.2018

_____

Denise Molinnus

Abstract

Boolean operations applied in biology and integrated with electronic transducers allow the development of a new class of digital biosensors for the detection of multiple input signals simultaneously and in real-time. With the help of Boolean functions (**AND**, **OR**, etc.), an electrical output signal will be directly delivered, representing a "**1**" or "**0**" binary notation, corresponding to a "true" or "false" statement, respectively. Such digital biosensors have the future potential to create medical devices and systems for intelligent or smart diagnostics.

The present thesis describes the realization of different enzyme-based biomolecular logic gates combined with electronic transducers for the possible application in medicine or food industry. In a first concept, a so called BioLogicChip is developed combining a "sense-act-treat" function integrated on one chip. The present system exemplarily mimics an "artificial pancreas" designed as a closed-loop drug-release system. A glucose sensor is constructed as enzyme-based **AND** logic gate, a temperature-depending hydrogel imitates the actuator function switching ON and OFF with its shrinking or swelling property, and an additional insulin sensor is developed to monitor and control the release of the drug (here: insulin) from the actuator. In this study, the results of the individual components such as the amperometric glucose sensor, the temperature-dependent hydrogel and the amperometric insulin sensor are presented, which are necessary to create such BioLogicChip.

Moreover, a digital adrenaline biosensor is developed to proof the catheter position during adrenal vein sampling. The sensor consists of an oxygen electrode modified by a bi-enzyme system with the enzymes laccase and pyrroloquinoline quinone-dependent glucose dehydrogenase (PQQ-GDH) to realize substrate-recycling principle to detect low adrenaline concentrations (in the nanomolar concentration range). The sensor's behavior at different pH values and at different temperatures is studied. Measurements in Ringer's solution are performed. In addition, the sensitivity of the biosensor to other catecholamines such as noradrenaline, dopamine and dobutamine is investigated. Furthermore, the adrenaline biosensor is successfully examined in human blood plasma. Finally, "proof-of-principle" experiments have been performed by combining the adrenaline biosensor with Boolean operations to get a rapid qualitative statement of the presence or absence of adrenaline, thus validating the correct position of the catheter in a YES/NO form.

This adrenaline biosensor is further miniaturized as a thin-film platinum adrenaline biosensor. Here, the bioelectrocatalytical measurement principle is applied by immobilization of the enzyme PQQ-GDH to detect adrenaline in the nanomolar concentration

range, too. The measurement conditions such as pH value, glucose concentration in the analyte solution and temperature are optimized with regard to a high sensitivity and low detection limit. Also, this sensor has been verified towards other catecholamines (noradrenaline, dopamine and dobutamine). The platinum thin-film adrenaline biosensor is successfully applied in blood plasma for the detection of different spiked adrenaline concentrations. Furthermore, the developed adrenalin biosensor is able to detect the concentration difference between adrenal blood (adrenaline concentration of $\gtrsim$100 nM) and peripheral blood (adrenaline concentration of 1 - 5 nM). A high adrenaline concentration ($\gtrsim$100 nM) would indicate the right position of the catheter into adrenal veins during adrenal vein sampling.

In contrast to the above-mentioned amperometric biosensor examples for biomolecular gates, also a field-effect-based platform is given attention in this thesis. The field-effect electrolyte-insulator-semiconductor (EIS) sensor consists of a layer structure of Al/p-Si/SiO_2/Ta_2O_5 and is used to create an acetoin biosensor for the first time to control different fermentation processes. The sensor chip is modified by the enzyme acetoin reductase from *B. clausii* DSM 8716^T for the catalytical reaction of (R)-acetoin to (R,R)-butanediol and meso-butanediol, respectively, in the presence of NADH. The linear measurement range, the optimal immobilization strategy (cross-linking by using glutaraldehyde and adsorptive binding) as well as the optimal working pH value and long-term stability are investigated by means of constant-capacitance measurements. Finally, the acetoin sensor was successfully applied in wine probes to detect different spiked acetoin concentrations. The sensor shows opportunities to be further developed as digital acetoin biosensor.

Contents

Acronyms

ABTS	2,2'-azino-*bis* (3-ethylbenzthiazoline-6-sulfonic acid)
AC	alternating current
AChE	acetylcholine esterase
AFM	atomic force microscopy
ARP	adenosine triphosphate
AVS	adrenal vein sampling
BioLogicChip	biomolecular logic chip
BSA	bovine serum albumine
CE	counter electrode
ChOx	choline oxidase
CK	creatine kinase
ConCap	constant capacitance
CRTN	phosphprylation of creatine
CT	computer tomography
C-V	capacitance voltage
CV	cyclic voltammetry
DC	direct current
DNA	deoxyribonucleic acid
ESR	esterase
EDX	energy-dispersive X-ray spectroscopy
EIS	electrolyte-insulator-semiconductor
FDA	Food and Drug Administration
GOx	glucose oxidase
HDPE	high-density polyethylene
IHP	inner Helmholtz layer
INV	invertase
LDH	lactate dehydrogenase
LDL	lower detection limit
MIS	metal-insulator semiconductor
MP-11	microperoxidase-11
NAD^+	nicotinamide adenine dinucleotide

NIPAAm	N-isopropylacrylamide
OHP	outer Helmholtz layer
PA	primary aldosteronism
PBS	phosphate buffer solution
PK	pyruvate kinase
PNIPAAm	poly-(N-isopropylacrlyamide)
POC	point-of-care
PQQ-GDH	pyrroloquinoline quinone-dependent glucose dehydrogenase
PZC	point of zero charge
RE	reference electrode
RNA	ribonucleic acid
RS	Ringer's solution
STI	soft tissue injury
UR	urease
WE	working electrode

1 Introduction

Digital electronics strongly influence and assist our daily life. Examples for that are modern telecommunications-, household- or multimedia systems such as mobile phone, coffee machine, rice cooker, tablet computer etc. The centerpiece of all these traditional computer-based devices is Boolean algebra with its 16 two input functions such as **AND, OR, XOR, NAND**, realized as logic gates. With the help of these logic gates, complex logic units are built (e.g., register or memory), peripheral devices are controlled (e.g., monitor, keypad, printer or speakers), memory access of data and program instructions are performed and data are processed [1, 2]. One predominant feature of digital electronics is that Boolean operations are applied to one or more binary input signals to provide a simple and succinct single output signal (true or false) [2]. By combining different Boolean functions as a cascade of Boolean operations, all mathematical algorithms can be described.

Recent research in the field of biosensors is devoted to apply the principle of Boolean operations also in biology. In this case, one or more (bio)chemical input signals, converted by biochemical processes, result in one distinct output signal. Due to Boolean algebra, a "**1**" or "**0**" binary notation will be delivered corresponding to "true" or "false" statements, respectively. Such biomolecular systems are highly attractive and could have a wide field of applications in the areas of chemistry, biotechnology and medicine. Numerous examples were demonstrated by the research groups of Katz, Willner and de Silva [3–7]. Often, logic gates are based on enzymatic reactions with one or more substrates representing chemical input signals. The applied enzymes as biocatalysts correspond to an information processing unit, consequently the resulting product or products of the chemical reaction(s) are representing the chemical output signal(s). Biosensors in combination with Boolean operations are introduced in literature as "biomolecular computing" or "biocomputing" [8].

This introduction gives an idea about the advantages by applying biomolecules in combination with logic gates in chapter 1.1. Additionally, chapter 1.2 summarizes common Boolean operations. Hereafter, a short overview on the current state-of-the-art of several issues of biomolecular gates with different application possibilities is introduced in chapter 1.3. Finally, chapter 1.4 guides through the publications that are collected in the present cumulative thesis and overviews the aims and scope of this work.

1.1 Using molecules in logic devices

Biomolecular logic gates are applications for computation at the nanoscale level by utilizing biologic molecules or materials [9] such as DNA [3, 10–13], enzymes [14–17] or even cells [18, 19]. To create biomolecular logic gates, different molecules can be

combined to perform parallel reactions resulting in a speed of information processing. Furthermore, logic gate systems can be often easily reconfigured by a flexible variation of the input signals. The combination of several biologic gates results in simple computer devices performing basic arithmetic operations such as half-adder/half-substractor or full-adder/full-substractor [20–22]. All common logic operations can be realized with the help of molecules based on chemical approaches. In this context, the binary encoding of information is used, where for each signal below a threshold will be assigned as "**0**" and above the threshold as "**1**" to get a fast "false" or "true" answer, respectively, beneficial, when there is no need for a quantitative but rather a qualitative rapid answer. This binary logic is a general concept and can be applied to any type of signal either chemical, biological or optical. Hence, it can be used for molecular systems to mimic logic functions [8, 23].

Based on these ideas, one of the first realized examples of biomolecular logic gates has been established in the pioneering works by Aviram 1988 and de Silva 1993 [7, 24]. Most common applications of molecular logic gates compromise chemical input signals and optical output signals, mostly with the help of fluorescence. One example is presented by de Silva [7], reporting for the first time about a molecular logic **AND** gate using hydrogen ions and sodium ions as chemical input signals with a receptor that operates as logic device and fluorescence as optical output. The fluorescence signal depends on the binding effect of one or both ions to the receptor. Since then, the complexity of such biomolecular logic gates has steadily increased.

1.2 Basic principles of logic operations

With the application of Boolean logic and by combining different Boolean functions, a simple and precise description of the output signal of a device depending on one or more input signals will be provided. The construction and functionality of different basic logic gates, which are required to describe complex biological reactions, are presented subsequently by consideration of a single 2-input logic circuit with input variables labeled as input A and input B [8, 25]. Typical 2-input logic circuits such as **OR, AND, NOR, NAND** and **XOR** are introduced:

OR logic gate

Fig 1.1 shows the symbol of the **OR** gate with the corresponding truth table. The absence of the respective input signal is taken as logic level input **"0"**, whereas the presence of input signals is named as **"1"**. If either input A or input B, or both are present, taken as the logic level input **"1"** (input signal combinations: **1,0; 0,1; 1,1**), a biochemical reaction takes place. This results in an output signal **"1"**. If neither inputs are available (input signal: **0,0**), no reaction occurs and the logic output signal **"0"** is given.

AND logic gate

In contrast to the **OR** gate, the **AND** gate's output is only **"1"**, if both inputs are present at the same time (input A and input B **(1,1)**), resulting in a biochemical

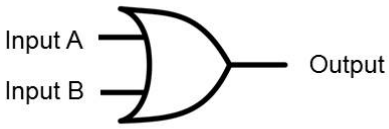

Input A	Input B	Output
0	0	0
1	0	1
0	1	1
1	1	1

Fig. 1.1: Symbol of **OR** logic gate with two inputs (A and B) and the corresponding truth table.

reaction. The absence of one or both input signals (input signal combinations: **1,0; 0,1; 0,0**) forms the output signal **"0"** as shown in Fig. 1.2 (**AND** gate symbol with the corresponding truth table).

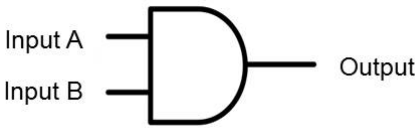

Input A	Input B	Output
0	0	0
1	0	0
0	1	0
1	1	1

Fig. 1.2: Symbol of **AND** logic gate with two inputs (A and B) and the corresponding truth table.

NOR logic gate

The **NOR** (Not OR) gate behaves as the negation of the **OR** gate. According to Fig. 1.3, an output signal **"1"** results only, if input A and input B are absent (input signal combination: **0,0**). If one or both inputs are present (input signal combinations: **1,0; 0,1; 1,1**), no reaction takes place, and a logic output signal **"0"** is resulting.

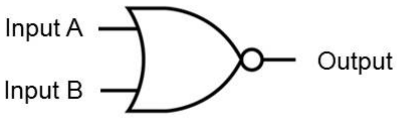

Input A	Input B	Output
0	0	1
1	0	0
0	1	0
1	1	0

Fig. 1.3: Symbol of **NOR** logic gate with two inputs (A and B) and the corresponding truth table.

NAND logic gate

The **NAND** gate (Not AND) delivers an output signal **"1"**, in the case when neither or either of the inputs (input A and input B) are present (input signal combinations: **0,0; 1,0; 0,1**). On the other hand, an output signal **"0"** is generated, if both inputs are present (input signal combinations: **1,1**) as seen in Fig 1.4.

XOR logic gate

The **XOR** gate (excluded OR) allows the output signal **"1"** when either one of the inputs (input A, input B) is present (input signal combinations: **1,0; 0,1**) and a reaction takes place, and is resulting in the output signal **"0"** (= compensation of the signal)

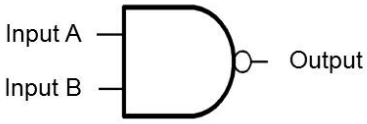

Input A	Input B	Output
0	0	1
1	0	1
0	1	1
1	1	0

Fig. 1.4: Symbol of **NAND** logic gate with two inputs (A and B) and the corresponding truth table.

when neither or both of the inputs (input signal combinations: **0,0; 1,1**) are present (see Fig. 1.5).

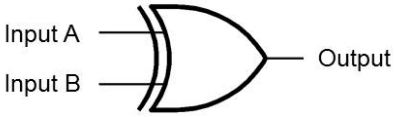

Input A	Input B	Output
0	0	0
1	0	1
0	1	1
1	1	0

Fig. 1.5: Symbol of **XOR** logic gate with two inputs (A and B) and the corresponding truth table.

1.3 State-of-the-art of biomolecular logic gates

Recent developments in the field of biomolecular logic gates based on e.g., **AND**, **OR**, **XOR**, **NOR** (see chapter 1.2) have demonstrated to be able to mimic the operation of electronic logic gates. With the help of biomolecular logic gates, a new research area in advanced diagnostics, therapeutics or drug-release systems is opened [26–31]. In the following, different examples of such biomolecular logic gates are presented.

1.3.1 Biologic gates for biomedical applications

The development of biologic (biomolecular) gates is very promising in the field of biomedical applications. Novel concepts of multi-signal processing can mimic natural biochemical pathways with operations according to the "biocomputing" concept. First approaches were developed for analyzing different biomarker characteristics for certain medical disorders. This is realized by the combination of multi-enzyme cascades with Boolean operations to provide reliable diagnostics of different physiological conditions. Up to now, it is possible to create a network of different logic gates with up to 10 input signals to process biochemical informations [28]. Advantages of "biocomputing" based on enzyme logic gates over optical immunoassays, magnetic resonance imaging or electromyography performed in the hospitals, which are costly, are that such approaches could be helpful, when there is a need of rapid and reliable diagnosis of physiological conditions followed by a timely optimal therapeutic treatment. Furthermore, biochemical information-processing systems by applying cascades of enzyme logic gates is highly promising for point-of-care injury diagnostics, when a rapid determination of pathological situations is necessary. It should also be noted, that only few devices exist in

hospitals that can diagnose multiple injuries simultaneously.

For example, biochemical logic systems composed of enzyme-based logic gates offer great potential for the detection of different injury biomarkers. Depending on the kind of injury, certain proteins are released into blood or urine where they can be detected. Here, particularly relevant is that the detection of only one biomarker would not be meaningful for one specific injury. Only detection of several biomarkers at the same time in the pathological concentration range would be an indication of a certain injury. The analysis of more biomarkers could be performed by implementation of Boolean operations, and by using binary bit pattern(s) consisting of **0** and **1** in order to digitize this process. For biomedical applications, logical **0** represents the normal physiologic state and logical **1** describes the pathological condition. Due to the application of parallel-working, enzyme-based logic gates, different unique bit patterns occur, where each bit pattern describes a specific pathophysiological state, representing one type of injury.

In the last years, different working groups developed biomolecular logic systems for biomedical applications. One recent concept describes the development of enzyme-based logic gates consisting of an **AND** and **XOR** logic gate identifying different types of injuries such as trauma brain injury and hemorrhagic shock by detecting relevant biomarkers such as norepinephrine, oxygen, glucose and lactate [32]. A more complex concept of such digital biosensor is reported in literature, where multiple pathophysiologic conditions can be detected by applying highly parallelized enzyme logic gates resulting in different injury codes depending on the input signals. In this case, an array of **NAND** and **AND** gates to process numerous biomarker inputs such as creatine kinase, lactate dehydrogenase, norepinephrine, glutamate, alanine transaminase, lactate, glucose, gluthathione disulfide, and gluthatione reductase to diagnose soft-tissue injury, traumatic brain, liver injury, abdominal trauma, hermorrhagic shock, and oxidative stress is applied [28, 33, 34]. For a better understanding of the functionality of such enzyme-based logic gates applied in the field of biomedicine, one concept is explained in more detail by Wang's and Katz's group [35] in the following:

Soft tissue injury (STI) can be diagnosed by measuring of already established parameters as input signals such as creatine kinase (CK) and lactate dehydrogenase (LDH) and by mimicking a Boolean **NAND** logic gate. As shown in Fig. 1.6a), an enzyme cascade consisting of CK, pyruvate kinase (PK), and LDH where CK and LDH are input 1 and input 2, respectively, is demonstrated. CK catalyzes the conversion of the reversible phosphorylation of creatine (CRTN) in the presence of adenosine triphosphate (ATP), while LDH catalyzes the reaction of pyruvate to lactate when NADH is oxidized to NAD^+ (nicotinamide adenine dinucleotide). The physiological and pathophysiological level of LDH and CK are detected optically in combination with electrochemical monitoring of the reduced NADH, which represents the output signal. Fig. 1.6c) overviews the truth table of the **NAND** gate with the corresponding input signals and the resulting output signals. In accordance to the functionality of a **NAND** gate (see also chapter 1.2), logical input signals "**0**" and "**1**" represent a normal or an elevated level of CK and LDH, respectively. If both input signals are normal (**0,0**) or only one of them (**0,1; 0,1**), an output signal "**1**" is generated. During an acute cardiac event, the level of the biomarkers CK and LDH can individually rise and fall. On the other hand,

LDH has been routinely employed in the assessment of muscular exertion and fatigue (fitness), but also for tissue breakdown and hemolysis. Only the simultaneous presence of elevated levels of both input signals (CK and LDH) at the same time (**1,1**) would trigger an output signal "**0**", corresponding to a positive STI diagnosis. A threshold level is defined where a NADH concentration below this level represents a positive diagnosis. Meaning, the NADH concentration decreases under this threshold, if both input signals, CK and LDH, are present at the same time, indicating the occurrence of STI.

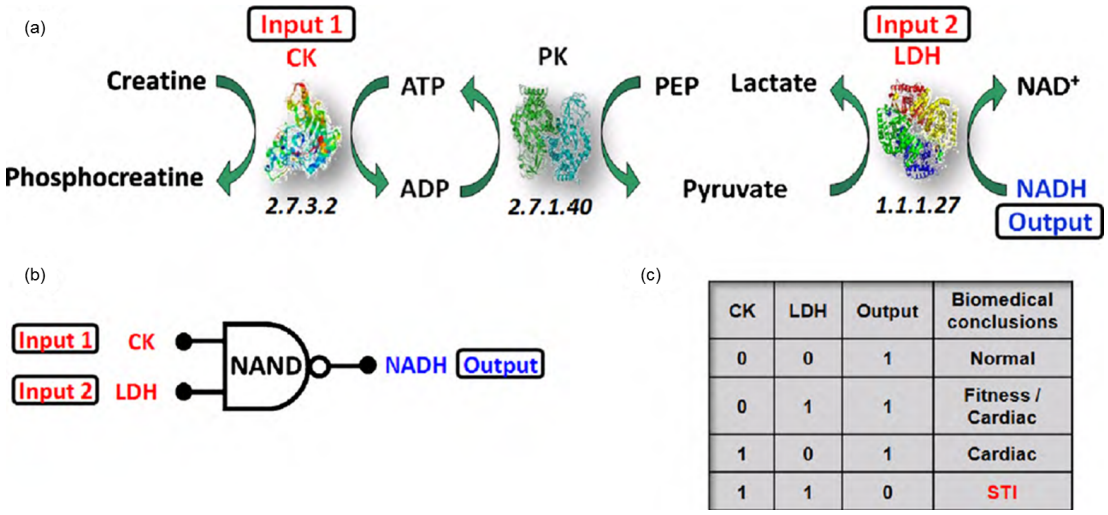

CK	LDH	Output	Biomedical conclusions
0	0	1	Normal
0	1	1	Fitness / Cardiac
1	0	1	Cardiac
1	1	0	STI

Fig. 1.6: (a) Schematic of the enzyme logic gate cascade with the inputs CK (input 1) and LDH (input 2) where NADH serves as output signal; (b) the corresponding **NAND** gate with the two input signals and one output signal; and (c) with the corresponding truth table (original from [35] with permission of Elsevier).

The described concepts can be further developed by combining these biomolecular logic gates with an actuator function to create a "sence-act-treat" system. Since, the resulted output signal could be used to activate either an electrochemical transducer or a chemical actuator, for example, to release a certain drug as demonstrated in Refs. [36, 37].

Nevertheless, most reported "biocomputing" systems are "proof-of-principle" concepts, demonstrating the possibility of detecting different biomarkers even simultaneously and performing logical operations by applying biomolecular systems. But non of the presented concepts is ready yet for practical use. Future studies are still necessary to transfer these concepts to real-life biosensor approaches.

1.3.2 Concatenation of logic gates

(Bio)chemical reactions with (bio)chemical inputs can mimic logical operations or a concatenated set of logic gates. Systems of consecutive operations of several logic gates that operate in series were established, which is essential to solve more complicated problems in practice. In recent years, some interesting examples have been drawn much attention based on enzymatic logic gates. Due to the skillful combination of biocatalysts

relying on substrates that are the product of a preceding logic operation, a cascade of concatenated enzymatic logic gates can be developed [38]. In literature, there are several examples of the creation of such concatenation logic gates composing up to three to four gates [39–46].

One impressive example is reported by Willner's working group [47] in which three logical operations (**OR**, **AND**, **XOR**) are combined containing four different enzymes: acetylcholine esterase (AChE), choline oxidase (ChOx), microperoxidase-11 (MP-11) and glucose dehydrogenase (GDH). As demonstrated in Fig 1.7, acetylcholine (input A) and butyrycholine (input B) are the input signals of the first logical operation with the enzyme AChE. If either one of them is present or both of them, choline (as output product) is generated, catalyzed by the enzyme AChE, which corresponds to an **OR** logic gate. At the same time, choline (product of the first reaction) serves as input signal for the second logic gate which is activated together with oxygen (input C). In this case, only in the presence of choline and oxygen at the same time, H_2O_2 is produced, catalyzed by the enzyme ChOx, resulting in an **AND** logic gate. The third logic gate consists of the enzymes MP-11 and GDH. H_2O_2 from the preceding **AND** gate is used as input for MP-11. The presence of H_2O_2 results in the production of NAD^+. Additionally, glucose reacts with GDH while NADH is produced. A change of the NAD^+/NADH concentration is recognized only, when either H_2O_2 or glucose is present. In the case of the presence of both inputs (H_2O_2 and glucose) together at the same time, MP-11 and GDH are activated. In this case, the oxidation of NADH to NAD^+ catalyzed by MP-11 is compensated by the reduction of NAD^+ to NADH during the reaction of glucose with GDH. Hence, no net changes in the concentration of NAD^+/NADH is formed, like in the absence of both input signals. This chemical reaction constellation can be constituted as **XOR** logic gate. The resulting NADH absorption was photometrically read out at the end as sensor signal.

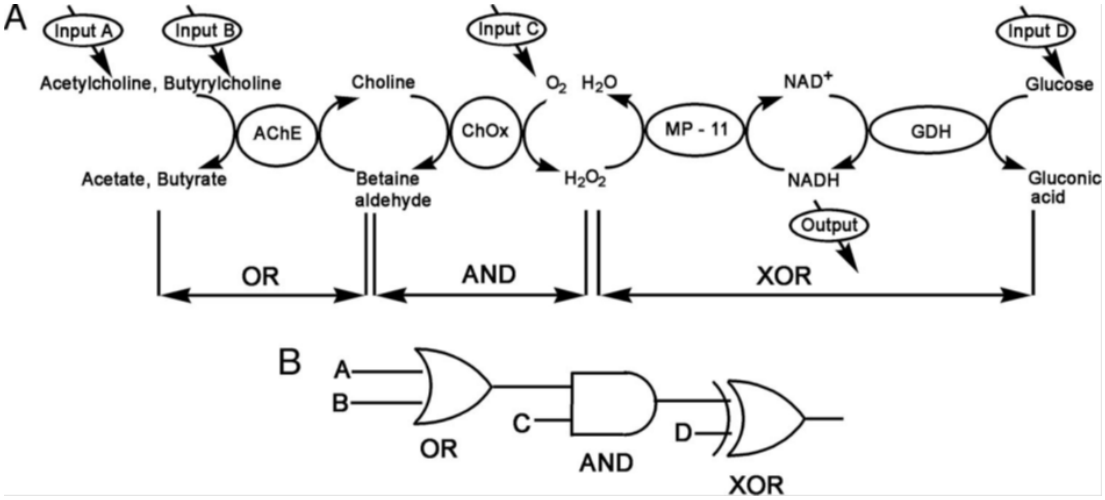

Fig. 1.7: Scheme of three concatenated logic gates with acetolcholine, butyrylcholine, O_2 and glucose as input signals, mimicking an **OR** and **AND**, **XOR** logic gate, respectively (original from [47], copyright (2006) National Academy of Sciences, U.S.A. with permission).

1.3.3 Biologic gates with integrated switchable platforms

Those enzyme-based concatenated logic gates can be used to create various bioelectronic devices such as a molecular keypad lock, encoder/decoder [48], multiplexer/demultiplexer [49], or switchable systems [50, 51], which are just starting to emerge. The application of e.g., keypad-lock systems is attractive when an object or data should be kept secret for some persons. The output signal of such configurations is dependent on the right combination of the inputs on the one hand, but also on the correct order of the input signals, on the other hand. Only with the correct "password", the lock can be opened [52]. One advantage of this system is the easy reconfiguration by combining additional biochemical inputs to increase the complexity of the security system [53]. Different keypad-lock systems can be found in literature based on enzymatic reactions where the output signals were read out optically [52–57].

As an example, the group of Katz [54] developed a novel approach of an enzyme-based biomolecular keypad lock. It consists of a biochemical reaction chain, including the hydrolysis of sucrose catalyzed by the enzyme invertase (INV) to glucose, the oxidation of glucose by the enzyme glucose oxidase (GOx) in the presence of oxygen to yield H_2O_2, followed by the oxidation of a synthetic dye, 2,2'-azino-*bis* (3-ethylbenzthiazoline-6-sulfonic acid) (ABTS) to a colored product $ABTS_{ox}$ catalyzed by the enzyme microperoxidase-11 (MP-11) in the presence of H_2O_2, see Fig. 1.8a). As demonstrated in Fig. 1.8b), the biomolecular keypad-lock system is represented as the network consisting of three concatenated **AND** gates.

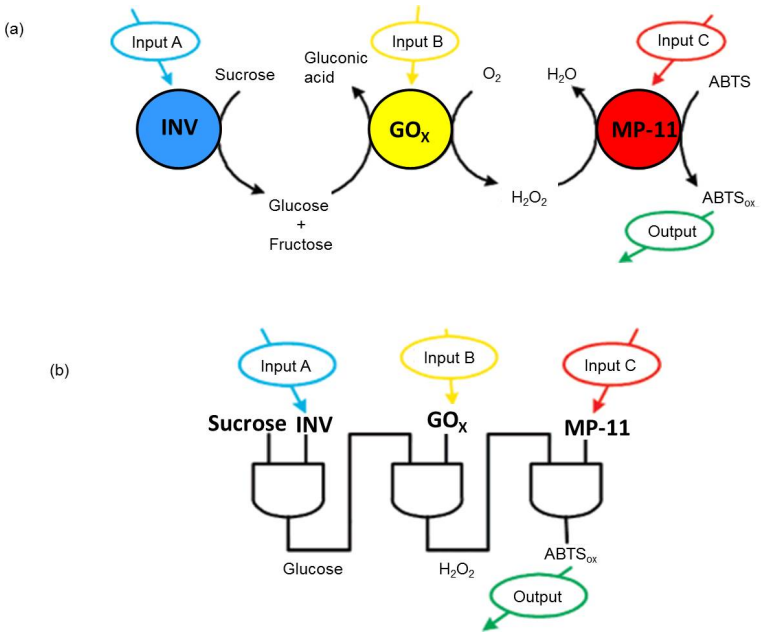

Fig. 1.8: (a) Biomolecular keypad-lock system with the corresponding biocatalytic reaction chain; (b) network of three concatenated **AND** gates (original from [53] with permission of the ACS Publications).

Each **AND** gate is activated by two input signals consisting of a chemical one (sucrose,

glucose or H_2O_2) and a biocatalyst (Inv, GOx or MP-11). The production of $ABTS_{ox}$ at the end of the reaction chain was read out optically.

The logic responses of the system have been studied by the addition of the immobilized enzymes: INV, GOx and MP-11 (input signals: A, B, C, respectively). The presence of the respective enzyme is considered as logic "**1**", while the absence is described as logic "**0**". Eight different combinations of the three (A, B, C) input signals are possible and shown in Fig. 1.9a) with the corresponding output signal, which are detected by the optical detection method, Fig. 1.9b).

(a)

Input A	Input B	Input C	Output
0	0	0	0
0	0	1	0
0	1	0	0
0	1	1	0
1	0	0	0
1	0	1	0
1	1	0	0
1	1	1	1

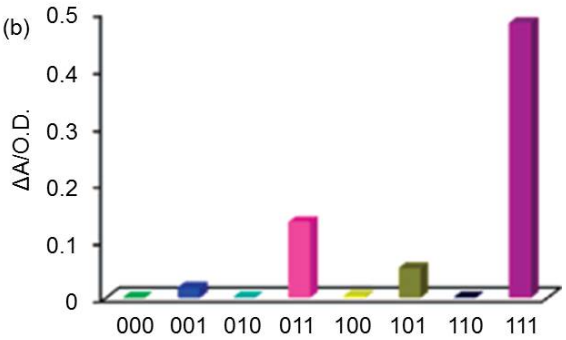

Fig. 1.9: (a) Truth table for the network of three concatenated **AND** gates with the input signals A, B, C; (b) optical detection of the output signals depending on presence/absence of the input signals A, B, C (original from [54] with permission of the ACS Publications).

But, the most important feature of the application of such a keypad-lock system is the dependence of the output signal on the correct order of the different input signals. Here, six different combinations are possible by the variation of the input signals A, B, C which is shown in Fig. 1.10a).

(a)

Input 1	Input 2	Input 3	Output
A	B	C	1
A	C	B	0
B	A	C	0
B	C	A	0
C	A	B	0
C	B	A	0

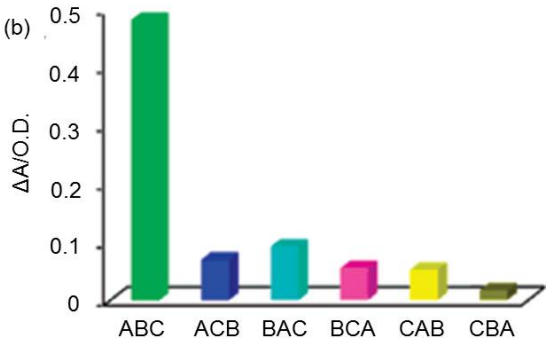

Fig. 1.10: (a) Truth table of the biomolecular keypad lock system by varying the order of the different input signals (A, B, C); (b) optical detection of the output signals depending on the order of the input signals A, B, C (original from [54] with permission of the ACS Publications).

As can be seen from the corresponding measurement results in Fig. 1.10b), only one correct order of the different input signals with the right combination (A,B,C) results in the output signal **1** ("ON"), allowing to open the lock. In contrast to that, all other input combinations correspond to an output signal **0** ("OFF") and the lock stays close.

1.4 Aim and scope of this thesis

Building a computer consisting of enzymatic reactions means, logical operations such as **AND**, **OR**, **NAND**, **XOR** etc., are mimicked by biomolecular reactions. With such devices multiple biochemical signals can be detected simultaneously and converted into one output signal, opening a new avenue of digital biosensors, which is advantageously in medicine for diagnostics or drug-release systems or even in food industry, to only name two examples. Currently, most of the already developed concepts of biomolecular gates use chemicals as input signals and optical detection mode for the output signals (e.g., fluorescence) [38, 50]. This technique has some challenges, due to the fact, that emitted photons have a multidirectional nature; additionally, fluorescence light consists of less efficient emission/re-absorption mechanism which limits the development of more complex, concatenated logical systems [38]. Furthermore, it is also difficult to create reversible logic gate systems with photonic changes as output signal without adding additional chemicals [58].

An alternative strategy is the development of "biocomputing" systems with electronic transducers (e.g., electrodes modified with enzymes) processing an output signal in combination with biomolecular logic gates having the possibility to miniaturize those sensor chips and additionally integrate signal processing. Such systems are advantageously over optical immunoassays performed in the hospitals or other optical detection method because the analyte can be detected label-free. This label-free detection method is beneficial since it has a high possibility to realize more convenient systems for the reason that no labeling with external reagents such as fluorescent dyes is required, which is normally necessary to achieve a highly sensitive and selective reporting of the target analyte. Moreover, this labeling procedure is time-consuming, costly and may cause to non-specific signal issues associated with the labeling itself.

Therefore, this thesis deals with the development and optimization of individual biosensors coupled with electrochemical enzyme logic gate principles. For a possible application in medicine, such a biosensor platform could make a reliable diagnose due to the combination and processing of information with the help of logical interactions, which would be extremely useful for e.g., cancer diagnosis. With this system, different biomarkers as well as selected reactions should be able to detect label-free, and to make a diagnosis with high specificity and reliability. The (bio)chemical signals will be converted to a mathematic algorithm, which is based on "**0**" and "**1**", corresponding to a "biological" computer. The resulting bit pattern(s) correlate with a specific disease, which enables a proper medication for the patient due to an integrated actuator function. By applying logical operations, a reliable and prompt diagnose can be made, corresponding to a "personalized medicine" approach.

Such a biosensor could be also applied in biotechnology to control e.g., fermenta-

tion processes. In contrast to the medical application, typical biotechnological markers should be detected. The converted (bio)chemical signal into the bit pattern(s) corresponds to the state of the fermentation process. Instead of the release of a certain drug, a specific and required substance can be released by triggering the actuator function (e.g., glucose) to optimize the feeding strategy for such fermenter.

In this thesis, different "proof-of-principle" experiments have been realized by applying micro-/nanotechnologies in combination with Boolean operations. Different transducer principles such as amperometry (together with thin-film sensors) and field-effect measurements (together with capacitive field-effect sensors) were applied and the sensor structures were modified with different enzymes. The individual developed systems were characterized and optimized regarding their application in medicine or food industry.

In literature, only a few examples are described with logical systems in combination with such biosensors [44, 59–67]. Fig 1.11 exemplifies an enzyme-based **AND** logic gate in combination with an electrolyte-insulator-semiconductor (EIS) sensor consisting of the enzymes glucose oxidase (GOx), invertase (Inv) and urease (Ur) being in solution. Sucrose and oxygen are used as input signals. The absence of the respective input signal is considered as logic **0**, while the presence of the input signal is described as logic **1**.

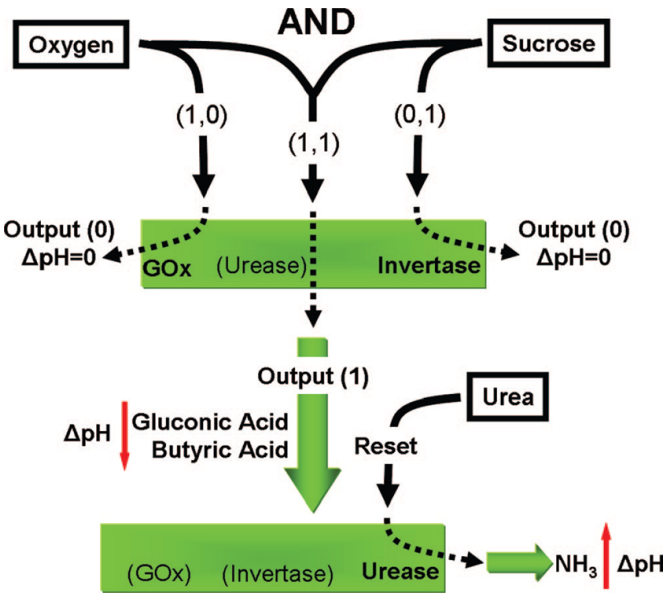

Fig. 1.11: Schematic of an enzyme-based **AND** logic gate activated by the input signals oxygen and succrose, resulting in a pH change as output signal generated from an EIS sensor (original from [62] with permission of the ACS Publications).

As already shown in chapter 1.2, **AND** logic gate means, that only in the simultaneous presence of both input signals, oxygen and sucrose (input signal combination: **1,1**), the biocatalytical reaction cascade proceeds; sucrose is converted into glucose and fructose catalyzed by the enzyme invertase. In a second reaction step, glucose will be converted in the presence of oxygen to gluconic acid resulting in an acidification. This pH change can be detected by the pH-sensitive EIS sensor as the output signal **1**. The biochemical reaction cascade can not be completed, if any or both input signals

are missing (input combinations: **0,0; 0,1; 1,0**), hence, no gluconic acid is produced resulting in an unchanged pH value as output signal **0**. In the presence of both inputs, oxygen and glucose (**1,1**), the pH value of the analyte solution is decreased due to the chemical reaction. With the immobilized enzyme urease, a **RESET** function is integrated and can be activated by addition of urea, resulting in the formation of NH_3 and the pH value is increased.

After an introduction into the state-of-the-art in **chapter 1** and theoretical aspects in **chapter 2**, the main objective of this thesis has been the development of different "proof-of-principle" concepts of enzyme-based biomolecular logic gates in combination with electrochemical transducers. Different applications in fields such as medicine or bio-/food technology are envisaged to get the possibility of on-line measurements. Moreover, with such digital biosensors rapid analytic methods can be created to obtain a qualitative YES/NO decision in a form of binary bit patterns consisting of **1** and **0**. The content of this thesis describes three different applications of individually developed biomolecular logic systems referring to chapter 3 to chapter 8.

Chapter 3 describes a concept of a "sense-act-treat" system, which has been realized to create a closed-loop drug-delivery system for the treatment of e.g., diabetes patients. The combination of continuous monitoring of the glucose concentration with an insulin pump is known as artificial pancreas. Such devices can help to avoid hypoglycemia of diabetes patients that can lead to seizures, coma or even death [68, 69]. Currently, closed-loop hospital settings consist of automatically controlling the blood glucose level, but a combination with an automatic insulin delivery pump is still a grand challenge [70, 71]. Therefore, there is a high motivation for the development of closed-loop drug-delivery systems. The presented concept of a so called "BioLogicChip" can detect multiple input signals simultaneously and thanks to Boolean operations, one electrical output signal is generated consisting of logical **0** or **1**. The chip-based amperometric sensor for the detection of the glucose level by using the enzyme glucose oxidase is combined with a Boolean **AND** logic gate with the inputs glucose and oxygen. Only in the presence of both inputs together, glucose will be catalytically converted by the enzyme. The resulting logic output current will activate a heater with an immobilized temperature-dependent hydrogel. Depending on the current, the temperature of the heater will increase or decrease. Hence, the hydrogel is able to shrink or swell triggered by a low or high glucose concentration, respectively. This hydrogel serves as an actuator and releases a certain amount of drug, e.g., insulin. Furthermore, the required dosage and timing of the insulin release is controlled by the glucose concentration and monitored by an additional insulin sensor.

Therein, the main focus was the development of a concept for the investigation of the on-chip integration of molecular logic principles with the glucose sensor combined with Boolean operations. The working capability of the temperature-dependent hydrogel able to switch "ON/OFF" was studied by measuring the impedance at different temperatures of the interdigitated circular electrode onto which the hydrogel is immobilized. Furthermore, an Ir_xO_y sensor was developed and characterized for the detection of different insulin concentrations.

In **chapter 4**, a digital adrenaline sensor to support medical diagnosis tools such as adrenal vein sampling (AVS) is introduced. Patients with primary aldosteronism (PA) are suffering from aldosteron-producing adenoma, which cause drug-resistant hypertension. These tumors are often less than 1 cm in diameter and therefore, they are not always detectable by a CT (computer tomography) scan [72]. The only reliable diagnosing method is the AVS, which is a straightforward diagnostic test, but only used in a few centers worldwide. This medical examination procedure is not only technically challenging, furthermore, it is invasive and risky [73–75]. Due to the small size of adrenal veins, it is quite difficult to recognize the right veins and to distinguish other vessels [74, 76]. To facilitate AVS, adrenaline can be used as biomarker since the adrenaline concentration in adrenal veins is much higher ($\gtrsim$100 nM) in comparison to peripheral blood (1 - 5 nM) [77, 78]. Hence, an adrenaline concentration of higher than $\sim$100 nM would indicate the right position of the catheter into the adrenal vein. A lower adrenaline concentration would have the consequence that the physician has to correct the catheter‘s position. Consequently, the detection of the adrenaline concentration can be an indication of the position of the catheter during AVS. In this study, the main emphasis was the development of a high-sensitive sensor for the detection of adrenaline in the nanomolar concentration range. To realize this, an oxygen sensor is modified by a bi-enzyme system of laccase and pyrroloquinoline quinone (PQQ)-dependent glucose dehydrogenase (GDH) to implement a substrate-recycling principle. First of all, the functionality of this amperometric sensor system was investigated and optimized in both, in phosphate buffer solution as well as in Ringer‘s solution. Furthermore, a concept of a digital adrenaline biosensor was developed by applying Boolean operations. For the application of the biosensor to support AVS, a precise and quantitative detection of the adrenaline concentration is not necessary, but rather a rapid signal, in a more qualitative YES/NO answer: if the adrenaline concentration is around 100 nM and hence, the catheter position is right, or if there is a low adrenaline concentration (about <5 nM) and the catheter has to be repositioned.

In **chaper 5**, an optimization of the introduced adrenaline biosensor described in chapter 4 is illustrated. Here, a laccase and PQQ-GDH were used having an optimum activity at a pH value relevant for measurements in real blood samples. Additionally, the sensitivity of the developed biosensor has been studied to other catecholamines such as noradrenaline, dobutamine and dopamine. This chapter is additionally provided by first experiments performed in human blood plasma, where different adrenaline concentrations were spiked into.

A continue study is presented in **chapter 6**, where the amperometric adrenaline biosensor system has been further miniaturized. Therefore, a platinum thin-film electrode was modified by an enzyme membrane containing PQQ-GDH to realize the bioelectrocatalytical amplification principle. Here, in a first reaction step, adrenaline will be oxidized to adrenochrome at the electrode surface by an applied potential of +450 mV to the platinum working electrode *vs.* Ag/AgCl reference electrode. Followed by the second reaction step, adrenochrome is reduced back to adrenaline catalyzed by

the enzyme PQQ-GDH in the presence of glucose. Due to this recycling reaction, the sensor signal is amplified. In this study, the main focus was given to the characterization of the chip-based sensor system, where temperature, pH value and glucose concentration were optimized. The long-term stability of the developed biosensor was studied as well as the lower detection limit. Additionally, sensitivity to other catecholamines such as dopamine, noradrenaline and dobutamine has been investigated. To demonstrate the applicability of the adrenaline biosensor to support AVS, it was applied in human blood plasma for the detection of different adrenaline concentrations. Furthermore, preliminary studies were performed to detect the adrenaline-concentration difference between adrenal blood ($\gtrsim$100 nM) and peripheral blood (1 - 5 nM).

A review about the developed biomolecular logic gates combined with different kinds of transducers is reported in **chapter 7**. Here, three different "proof-of principle" studies are focused. At first, a biomolecular logic gate in combination with a field-effect sensor, which has been developed and characterized by A. Poghossian is therefore only shortly discussed. Three enzymes (glucose oxidase, esterase and urease) are immobilized onto one chip. This logic gate is structured as **OR** logic gate with the input signals glucose and ethyl butyrate, and has also an integrated **RESET** function realized by the enzyme urease with urea as substrate.

The second example describes the digital adrenaline biosensor from **chapter 4** with two concatenated **AND** logic gates consisting of the enzymes laccase building the first **AND** logic gate with the input signals adrenaline and oxygen and PQQ-GDH as part of the second **AND** logic gate with the input signals adrenochrome and glucose, resulting in a substrate recycling in the presence of all input signals together. By defining an internal threshold level for the output signal, a YES/NO decision can be given.

The last example shows an enzyme-based molecular logic gate with biosensor/actuator function integrated onto one chip, the so called "BioLogicChip". The concept of this "sense-act-treat" system is already introduced in **chapter 3**. The system consists of a glucose sensor designed as enzyme-based **AND** logic gate, a temperature-dependent hydrogel immobilized onto a thermoresistive heater serving as actuator to release a certain amount of insulin triggered by logical operation and an amperometric insulin sensor to monitor the release of the drug. The characterization of the individual components is overviewed.

Chapter 8 deals with the development of a novel acetoin biosensor to control and monitor fermentation processes, because acetoin is a major fermentation product of bacilli and *Enterobacteriaceae*. Acetoin is an important contributor to e.g., wine or beer flavor and aroma but it is also naturally contained in fruits, corn, meat and some fermented foods. Furthermore, acetoin has a significant importance for microorganisms in avoiding acidification, when participating in the regulation of the NADH/NAD^+ ratio and in storing carbon [79, 80].

The presence of acetoin is usually indicated by a "buttery", "butteryscotch", "honey" or "toffee" tone [81, 82] and plays an important role during the fermentation process of alcoholic beverages. The acetoin level during fermentation could be e.g., an indicator of the degree of the beer's maturity and hence, the maturation time. In general, many

fermentation processes can be controlled more precisely by on-line monitoring of the acetoin concentration.

In this contribution, a pH-sensitive capacitive EIS field-effect structure with the enzyme acetoin reductase from *B. clausii* DSM 8716^T (developed in our institute) for the detection of acetoin in the presence of NADH is introduced for the first time. Two different immobilization strategies, namely cross-linking by using glutaraldehyde and adsorptive immobilization were studied. Typical biosensor properties such as linear concentration range, pH optimum, reproducibility and long-term stability were investigated. In addition, the newly developed acetoin biosensor was applied in white wine samples for the detection of different, spiked acetoin concentrations. This acetoin biosensor can be further developed as on-line digital system by applying Boolean operations to get a YES/NO answer, if the fermentation process or the beer maturity is completed, or not.

At the end, **chapter 9** is concluding this thesis with the final summary of the obtained results from the introduced, conceptualized enzyme-based logic gates with their achievements in different application fields, and an outlook including current ideas and future strategies.

References

[1] R. C. Jaeger. *Microelectronic Circuit Design*. McGraw-Hill Series in Electrical and Computer Engineering. New York: McGraw-Hill, 1997.

[2] G. Boole. *An Investigation of the Laws of Thought, on which are Founded the Mathematical Theories of Logic and Probability*. New York: Reprinted by Dover Publications, Inc., 1954.

[3] I. Willner, B. Shlyahovsky, M. Zayats, and B. Willner. "DNAzymes for sensing, nanobiotechnology and logic gate applications". *Chemical Society Reviews* 37 (2008), 1153–1165.

[4] R. Freeman, T. Finder, and I. Willner. "Multiplexed analysis of Hg^{2+} and Ag^{+} ions by nucleic acid functionalized CdSe/ZnS quantum dots and their use for logic gate operations". *Angewandte Chemie* 48 (2009), 7818–7821.

[5] X. Liu, R. Aizen, R. Freeman, O. Yehezkeli, and I. Willner. "Multiplexed aptasensors and amplified DNA sensors using functionalized graphene oxide: Application for logic gate operations". *ACS Nano* 6 (2012), 3553–3563.

[6] S. Lilienthal, M. Klein, R. Orbach, I. Willner, F. Remacle, and R. D. Levine. "Continuous variables logic *via* coupled automata using a DNAzyme cascade with feedback". *Chemical Science* 8 (2017), 2161–2168.

[7] P. A. de Silva, N. H. Q. Gunaratne, and C. P. McCoy. "A molecular photoionic AND gate based on fluorescent signalling". *Nature* 364 (1993), 42–44.

[8] E. Katz. *Biomolecular Information Processing*. Weinheim, Germany: Wiley-VCH Verlag GmbH & Co. KGaA, 2012.

[9] D. C. Magri, G. J. Brown, G. D. McClean, and A. P. de Silva. "Communicating chemical congregation: A molecular AND logic gate with three chemical inputs as a "lab-on-a-molecule" prototype". *Journal of the American Chemical Society* 128 (2006), 4950–4951.

[10] R. Orbach, L. Mostinski, F. Wang, and I. Willner. "Nucleic acid driven DNA machineries synthesizing Mg^{2+}-dependent DNAzymes: An interplay between DNA sensing and logic-gate operations". *Chemistry* 18 (2012), 14689–14694.

[11] R. Orbach, F. Remacle, R. D. Levine, and I. Willner. "Logic reversibility and thermodynamic irreversibility demonstrated by DNAzyme-based Toffoli and Fredkin logic gates". *Proceedings of the National Academy of Sciences of the United States of America* 109 (2012), 21228–21233.

[12] M. N. Stojanovic, T. E. Mitchell, and D. Stefanovic. "Deoxyribozyme-based logic gates". *Journal of the American Chemical Society* 124 (2002), 3555–3561.

[13] M. Massey, I. L. Medintz, M. G. Ancona, and W. R. Algar. "Time-gated FRET and DNA-based photonic molecular logic gates: AND, OR, NAND, and NOR". *Journal of the American Chemical Society* 2 (2017), 1205–1214.

[14] E. Honarvarfard, M. Gamella, A. Poghossian, M. J. Schöning, and E. Katz. "An enzyme-based reversible Controlled NOT (CNOT) logic gate operating on a semiconductor transducer". *Applied Materials Today* 9 (2017), 266–270.

[15] J. Zhou, M. A. Arugula, J. Halámek, M. Pita, and E. Katz. "Enzyme-based NAND and NOR logic gates with modular design". *The Journal of Physical Chemistry. B* 113 (2009), 16065–16070.

[16] T. Hou, T. Zhao, W. Li, F. Li, and P. Gai. "A label-free visual platform for self-correcting logic gate construction and sensitive biosensing based on enzyme-mimetic coordination polymer nanoparticles". *Journal of Materials Chemistry B* 5 (2017), 4607–4613.

[17] E. Katz. "Enzyme-based logic gates and networks with output signals analyzed by various methods". *ChemPhysChem* 18 (2017), 1688–1713.

[18] Z. Li, M. A. Rosenbaum, A. Venkataraman, T. K. Tam, E. Katz, and L. T. Angenent. "Bacteria-based AND logic gate: A decision-making and self-powered biosensor". *Chemical Communications* 47 (2011), 3060–3062.

[19] M. A. TerAvest, Z. Li, and L. T. Angenent. "Bacteria-based biocomputing with cellular computing circuits to sense, decide, signal, and act". *Energy and Environmental Science* 4 (2011), 4907–4916.

[20] A. Coskun, E. Deniz, and E. U. Akkaya. "Effective PET and ICT switching of boradiazaindacene emission: A unimolecular, emission-mode, molecular half-subtractor with reconfigurable logic gates". *Organic Letters* 7 (2005), 5187–5189.

[21] J. Wang, J. Sun, and Q. Sun. "Single-PPLN-based simultaneous half-adder, half-subtracter, and OR logic gate: Proposal and simulation". *Optics Express* 15 (2007), 1690–1699.

[22] D. Margulies, G. Melman, and A. Shanzer. "A molecular full-adder and full-subtractor, an additional step toward a moleculator". *Journal of the American Chemical Society* 128 (2006), 4865–4871.

[23] U. Pischel. "Chemical approaches to molecular logic elements for addition and subtraction". *Angewandte Chemie* 46 (2007), 4026–4040.

[24] A. Aviram. "Molecules for memory, logic, and amplification". *Journal of the American Chemical Society* 110 (1988), 5687–5692.

[25] N. Wagner and G. Ashkenasy. "Systems chemistry: Logic gates, arithmetic units, and network motifs in small networks". *Chemistry* 15 (2009), 1765–1775.

[26] J. Liu, H. Zhou, J.-J. Xu, and H.-Y. Chen. "Dual-biomarker-based logic-controlled electrochemical diagnosis for prostate cancers". *Electrochemistry Communications* 32 (2013), 27–30.

[27] T. Konry and D. R. Walt. "Intelligent medical diagnostics via molecular logic". *Journal of the American Chemical Society* 131 (2009), 13232–13233.

[28] J. Halámek, V. Bocharova, S. Chinnapareddy, J. R. Windmiller, G. Strack, M.-C. Chuang, J. Zhou, P. Santhosh, G. V. Ramirez, M. A. Arugula, J. Wang, and E. Katz. "Multi-enzyme logic network architectures for assessing injuries: Digital processing of biomarkers". *Molecular BioSystems* 6 (2010), 2554–2560.

[29] Y.-H. Lai, S.-C. Sun, and M.-C. Chuang. "Biosensors with built-in biomolecular logic gates for practical applications". *Biosensors* 4 (2014), 273–300.

[30] K. Radhakrishnan, J. Tripathy, and A. M. Raichur. "Dual enzyme responsive microcapsules simulating an "OR" logic gate for biologically triggered drug delivery applications". *Chemical Communications* 49 (2013), 5390–5392.

[31] S. Mailloux, J. Halámek, and E. Katz. "A model system for targeted drug release triggered by biomolecular signals logically processed through enzyme logic networks". *The Analyst* 139 (2014), 982–986.

[32] M. Pita, J. Zhou, K. M. Manesh, J. Halámek, E. Katz, and J. Wang. "Enzyme logic gates for assessing physiological conditions during an injury: Towards digital sensors and actuators". *Sensors and Actuators B: Chemical* 139 (2009), 631–636.

[33] J. Halámek, J. R. Windmiller, J. Zhou, M.-C. Chuang, P. Santhosh, G. Strack, M. A. Arugula, S. Chinnapareddy, V. Bocharova, J. Wang, and E. Katz. "Multiplexing of injury codes for the parallel operation of enzyme logic gates". *The Analyst* 135 (2010), 2249–2259.

[34] M. Zhou, F. Wang, and S. Dong. "Boolean logic gates based on oxygen-controlled biofuel cell in "one pot"". *Electrochimica Acta* 56 (2011), 4112–4118.

[35] J. R. Windmiller, G. Strack, M.-C. Chuang, J. Halámek, P. Santhosh, V. Bocharova, J. Zhou, E. Katz, and J. Wang. "Boolean-format biocatalytic processing of enzyme biomarkers for the diagnosis of soft tissue injury". *Sensors and Actuators B: Chemical* 150 (2010), 285–290.

[36] E. Katz and J. Halámek. "New approach in forensic analysis – Biomolecular computing based analysis of significant forensic biomarkers". *Annals of Forensic Research and Analysis* 1 (2014), 1002–1006.

[37] S. Mailloux, J. Halámek, L. Halámková, A. Tokarev, S. Minko, and E. Katz. "Biomolecular release triggered by glucose input–bioelectronic coupling of sensing and actuating systems". *Chemical Communications* 49 (2013), 4755–4757.

[38] J. Andréasson and U. Pischel. "Molecules with a sense of logic: A progress report". *Chemical Society Reviews* 44 (2015), 1053–1069.

[39] R. Baron, O. Lioubashevski, E. Katz, T. Niazov, and I. Willner. "Logic gates and elementary computing by enzymes". *The Journal of Physical Chemistry A* 110 (2006), 8548–8553.

[40] S. Erbas-Cakmak and E. U. Akkaya. "Cascading of molecular logic gates for advanced functions: A self-reporting, activatable photosensitizer". *Angewandte Chemie* 52 (2013), 11364–11368.

[41] G. de Ruiter and M. E. van der Boom. "Orthogonal addressable monolayers for integrating molecular logic". *Angewandte Chemie* 51 (2012), 8598–8601.

[42] L. Feng, Z. Lyu, A. Offenhäusser, and D. Mayer. "Multi-level logic gate operation based on amplified aptasensor performance". *Angewandte Chemie* 54 (2015), 7693–7697.

[43] A. P. de Silva. "Molecular logic gate arrays". *Chemistry – An Asian Journal* 6 (2011), 750–766.

[44] E. Katz, A. Poghossian, and M. J. Schöning. "Enzyme-based logic gates and circuits-analytical applications and interfacing with electronics". *Analytical and Bioanalytical Chemistry* 409 (2017), 81–94.

[45] D.-H. Qu, F.-Y. Ji, Q.-C. Wang, and H. Tian. "A double INHIBIT logic gate employing configuration and fluorescence changes". *Advanced Materials* 18 (2006), 2035–2038.

[46] F. Kramer, L. Halámková, A. Poghossian, M. J. Schöning, E. Katz, and J. Halámek. "Biocatalytic analysis of biomarkers for forensic identification of ethnicity between Caucasian and African American groups". *The Analyst* 138 (2013), 6251–6257.

[47] T. Niazov, R. Baron, E. Katz, O. Lioubashevski, and I. Willner. "Concatenated logic gates using four coupled biocatalysts operating in series". *Proceedings of the National Academy of Sciences of the United States of America* 103 (2006), 17160–17163.

[48] J. Andréasson, S. D. Straight, T. A. Moore, A. L. Moore, and D. Gust. "Molecular all-photonic encoder-decoder". *Journal of the American Chemical Society* 130 (2008), 11122–11128.

[49] J. Andréasson, S. D. Straight, S. Bandyopadhyay, R. H. Mitchell, T. A. Moore, A. L. Moore, and D. Gust. "A molecule-based 1: 2 digital demultiplexer". *The Journal of Physical Chemistry C* 111 (2007), 14274–14278.

[50] A. J. M. Huxley, M. Schroeder, H. Q. N. Gunaratne, and A. P. de Silva. "Modification of fluorescent photoinduced electron transfer (PET) sensors/switches to produce molecular photo-ionic triode action". *Angewandte Chemie* 53 (2014), 3622–3625.

[51] S. Liu, L. Wang, W. Lian, H. Liu, and C.-Z. Li. "Logic gate system with three outputs and three inputs based on switchable electrocatalysis of glucose by glucose oxidase entrapped in chitosan films". *Chemistry - An Asian Journal* 10 (2015), 225–230.

[52] D. Margulies, C. E. Felder, G. Melman, and A. Shanzer. "A molecular keypad lock: A photochemical device capable of authorizing password entries". *Journal of the American Chemical Society* 129 (2007), 347–354.

[53] G. Strack, M. Ornatska, M. Pita, and E. Katz. "Biocomputing security system: Concatenated enzyme-based logic gates operating as a biomolecular keypad lock". *Journal of the American Chemical Society* 130 (2008), 4234–4235.

[54] J. Halámek, T. K. Tam, S. Chinnapareddy, V. Bocharova, and E. Katz. "Keypad lock security system based on immune-affinity recognition integrated with a switchable biofuel cell". *The Journal of Physical Chemistry Letters* 1 (2010), 973–977.

[55] M. Kumar, A. Dhir, and V. Bhalla. "A molecular keypad lock based on the thiacalix[4]arene of 1,3-alternate conformation". *Organic Letters* 11 (2009), 2567–2570.

[56] Z. Guo, W. Zhu, L. Shen, and H. Tian. "A fluorophore capable of crossword puzzles and logic memory". *Angewandte Chemie* 119 (2007), 5645–5649.

[57] Y. Wang, Y. Huang, B. Li, L. Zhang, H. Song, H. Jiang, and J. Gao. "A cell compatible fluorescent chemosensor for Hg^{2+} based on a novel rhodamine derivative that works as a molecular keypad lock". *RSC Advances* 1 (2011), 1294–1300.

[58] F. Moseley, J. Halámek, F. Kramer, A. Poghossian, M. J. Schöning, and E. Katz. "An enzyme-based reversible CNOT logic gate realized in a flow system". *The Analyst* 139 (2014), 1839–1842.

[59] A. Poghossian, E. Katz, and M. J. Schöning. "Enzyme logic AND-Reset and OR-Reset gates based on a field-effect electronic transducer modified with multienzyme membrane". *Chemical Communications* 51 (2015), 6564–6567.

[60] M. Suresh, A. Ghosh, and A. Das. "A simple chemosensor for Hg^{2+} and Cu^{2+} that works as a molecular keypad lock". *Chemical Communications* (2008), 3906–3908.

[61] A. Poghossian, K. Malzahn, M. H. Abouzar, P. Mehndiratta, E. Katz, and M. J. Schöning. "Integration of biomolecular logic gates with field-effect transducers". *Electrochimica Acta* 56 (2011), 9661–9665.

[62] M. Krämer, M. Pita, J. Zhou, M. Ornatska, A. Poghossian, M. J. Schöning, and E. Katz. "Coupling of biocomputing systems with electronic chips: Electronic interface for transduction of biochemical information". *The Journal of Physical Chemistry C* 113 (2009), 2573–2579.

[63] V. Bocharova, T. K. Tam, J. Halámek, M. Pita, and E. Katz. "Reversible gating controlled by enzymes at nanostructured interface". *Chemical Communications* 46 (2010), 2088–2090.

[64] A. Poghossian, M. Krämer, M. H. Abouzar, M. Pita, E. Katz, and M. J. Schöning. "Interfacing of biocomputing systems with silicon chips: Enzyme logic gates based on field-effect devices". *Procedia Chemistry* 1 (2009), 682–685.

[65] E. Katz, V. M. Fernández, and M. Pita. "Switchable bioelectrocatalysis controlled by pH changes". *Electroanalysis* 27 (2015), 2063–2073.

[66] I. Tokarev and S. Minko. "Stimuli-responsive hydrogel thin films". *Soft Matter* 5 (2009), 511–524.

[67] I. Tokarev, V. Gopishetty, J. Zhou, M. Pita, M. Motornov, E. Katz, and S. Minko. "Stimuli-responsive hydrogel membranes coupled with biocatalytic processes". *ACS Applied Materials and Interfaces* 1 (2009), 532–536.

[68] M. Breton, A. Farret, D. Bruttomesso, S. Anderson, L. Magni, S. Patek, C. Dalla Man, J. Place, S. Demartini, S. Del Favero, C. Toffanin, C. Hughes-Karvetski, E. Dassau, H. Zisser, F. J. Doyle, G. de Nicolao, A. Avogaro, C. Cobelli, E. Renard, and B. Kovatchev. "Fully integrated artificial pancreas in type 1 diabetes: Modular closed-loop glucose control maintains near normoglycemia". *Diabetes* 61 (2012), 2230–2237.

[69] J. R. Castle, J. M. Engle, J. El Youssef, R. G. Massoud, K. C. J. Yuen, R. Kagan, and W. K. Ward. "Novel use of glucagon in a closed-loop system for prevention of hypoglycemia in type 1 diabetes". *Diabetes Care* 33 (2010), 1282–1287.

[70] F. J. Doyle, L. M. Huyett, J. B. Lee, H. C. Zisser, and E. Dassau. "Closed-loop artificial pancreas systems: Engineering the algorithms". *Diabetes Care* 37 (2014), 1191–1197.

[71] B. W. Bequette. "A critical assessment of algorithms and challenges in the development of a closed-loop artificial pancreas". *Diabetes Technology and Therapeutics* 7 (2005), 28–47.

[72] S. Monticone, A. Viola, D. Rossato, F. Veglio, M. Reincke, C. Gomez-Sanchez, and P. Mulatero. "Adrenal vein sampling in primary aldosteronism: Towards a standardised protocol". *The Lancet Diabetes and Endocrinology* 3 (2015), 296–303.

[73] G. P. Rossi, R. J. Auchus, M. Brown, J. W. M. Lenders, M. Naruse, P. F. Plouin, F. Satoh, and W. F. Young. "An expert consensus statement on use of adrenal vein sampling for the subtyping of primary aldosteronism". *Hypertension* 63 (2013), 151–160.

[74] T. Dekkers, J. Deinum, L. J. Schultzekool, D. Blondin, O. Vonend, A.R.R.M. Hermus, M. Peitzsch, L. C. Rump, G. Antoch, F.C.G.J. Sweep, S. R. Bornstein, J. W. M. Lenders, H. S. Willenberg, and G. Eisenhofer. "Plasma metanephrine for assessing the selectivity of adrenal venous sampling". *Hypertension* 62 (2013), 1152–1157.

[75] W. F. Young, A. W. Stanson, G. B. Thompson, C. S. Grant, D. R. Farley, and J. A. van Heerden. "Role for adrenal venous sampling in primary aldosteronism". *Surgery* 136 (2004), 1227–1235.

[76] N. Daunt. "Adrenal vein sampling: How to make it quick, easy, and successful". *Radiographics* 25 Suppl 1 (2005), 143–158.

[77] P. Collste, B. Brismar, A. Alveryd, I. Björkhem, C. Hårdstedt, L. Svensson, and J. Ostman. "The catecholamine concentration in central veins of hypertensive patients - an aid not without problems in locating phaeochromocytoma". *Acta Chirurgica Scandinavica, Supplementum* 530 (1986), 67–71.

[78] E. L. Bravo, R. C. Tarazi, F. M. Fouad, D. G. Vidt, and R. W. Gifford. "Clonidine-suppression test: A useful aid in the diagnosis of pheochromocytoma". *New England Journal of Medicine* 305 (1981), 623–626.

[79] Z. Xiao and P. Xu. "Acetoin metabolism in bacteria". *Critical Reviews in Microbiology* 33 (2007), 127–140.

[80] X. Zhang, T. Bao, Z. Rao, T. Yang, Z. Xu, S. Yang, and H. Li. "Two-stage pH control strategy based on the pH preference of acetoin reductase regulates acetoin and 2,3-butanediol distribution in *Bacillus subtilis*". *PloS One* 9 (2014), e91187.

[81] Z. Xiao, X. Wang, Y. Huang, F. Huo, X. Zhu, L. Xi, and J. R. Lu. "Thermophilic fermentation of acetoin and 2,3-butanediol by a novel *Geobacillus* strain". *Biotechnology for Biofuels* 5 (2012), 88–89.

[82] P. Romano and G. Suzzi. "Origin and production of acetoin during wine yeast fermentation". *Applied Microbiology and Biotechnology* 2 (1996), 309–315.

2 Theory

Biosensors represent a subgroup of chemical sensors and transform biochemical information into an analytically useful signal, e.g., into an electrical signal [1]. Sensors in combination with enzymes are getting more and more attractive to develop biochemical sensors due to the enzyme‘s exceptional, natural substrate specificity or extremely high selectivity to a given substrate. Due to the application of enzymes, the biochemical reaction can be accelerated by lowering the activation energy without getting the enzymes changed. In the following chapters 2.1 to 2.3, an overview of the applied measurement principles considered for the enzyme-based electrochemical biosensors in this thesis is provided.

2.1 Field-effect potentiometric sensors

The potentiometric measurement method is a classical analytical technique and used for numerous practical applications, see exemplarily [2–6] and references therein. Here, the potential difference between an ion-selective electrode and a reference electrode is the measured quantity and depends on the activity of the ions containing in the analyte solution under ideally zero current conditions. In this context, the focus is given on the electrolyte-insulator-semiconductor (EIS) system, which is highly attractive for the detection of potential differences [7, 8].

2.1.1 Basic principle of a metal-insulator-semiconductor field-effect structure (MIS)

The structure of capacitive field-effect EIS sensors corresponds to metal-insulator-semiconductor an (MIS) capacitors, furthermore, their functionality can be derived from an MIS device, which is shown in Fig 2.1.

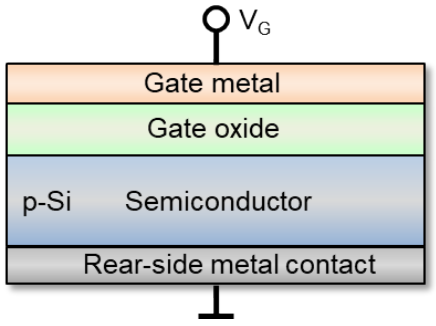

Fig. 2.1: Schematic of an MIS structure with V_G as gate voltage (adapted from refs. [9]).

The MIS sensor consists of e.g., a p-type semiconductor substrate composing of silicon, which is covered by a thermally grown thin insulating layer out of SiO_2 that is assumed to be ideal thus, no current passes through this layer. On top of this structure, there is a metal gate layer [9, 10]. The thickness of the insulator layer is usually approximately 50 - 100 nm. In order to measure the capacitance of the MIS structure, a DC (direct current) voltage is applied through to the metal gate layer superimposed by an additional AC (alternating current) voltage to measure the capacitance [11, 12].

There are three distinct operation states (accumulation, depletion, inversion) of an MIS capacitor depending on the applied gate voltage V_G. For the case of a p-type semiconductor, a typical course of a theoretical capacitance-voltage (C-V) curve is shown in Fig. 2.2, whereas the appropriate operation regime with the energy-band diagram of the MIS structure is depicted in Fig 2.3:

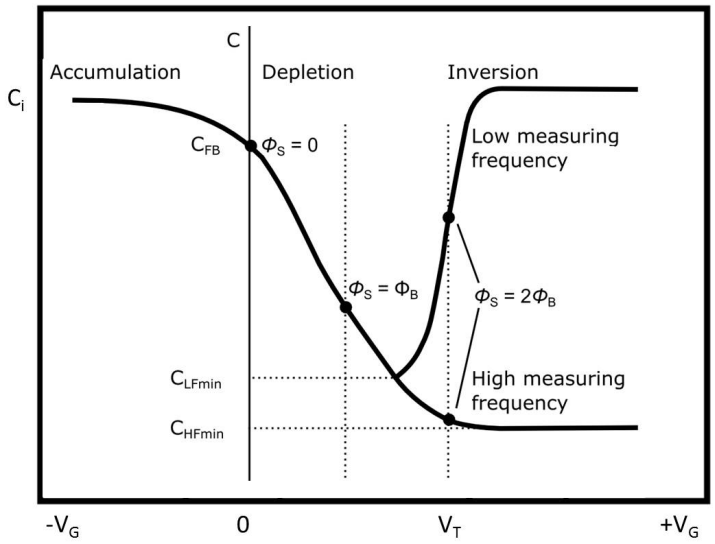

Fig. 2.2: Theoretical capacitance-voltage (C-V) curve of a p-type MIS structure at high and low measuring frequencies. ϕ_s: semiconductor-surface potential, C_i: insulator capacitance, C_{FB}: flat-band capacitance, C_{LFmin}: low-frequency minimum capacitance, $C_{HF_{min}}$: high-frequency minimum capacitance, V_T: threshold voltage (adapted from [9]).

Accumulation regime: A negative gate voltage $V_G<0$ is applied to the metal electrode. In response to that, positively charged holes accumulate from the silicon to the semiconductor surface (semiconductor/gate insulator interface). Due to the increase of the hole concentrations at the semiconductor surface, the valence band will bend closer to the Fermi level E_F at the interface semiconductor-insulator. The energy-band distance between valence band E_v and the conducting gap E_c remains always constant, thus, E_c is also adjusted upwards close to the interface. Under this condition, the device behaves as a conventional plate capacitor with $C \cong C_i$ (C_i: insulator capacitance) [9, 10, 14].

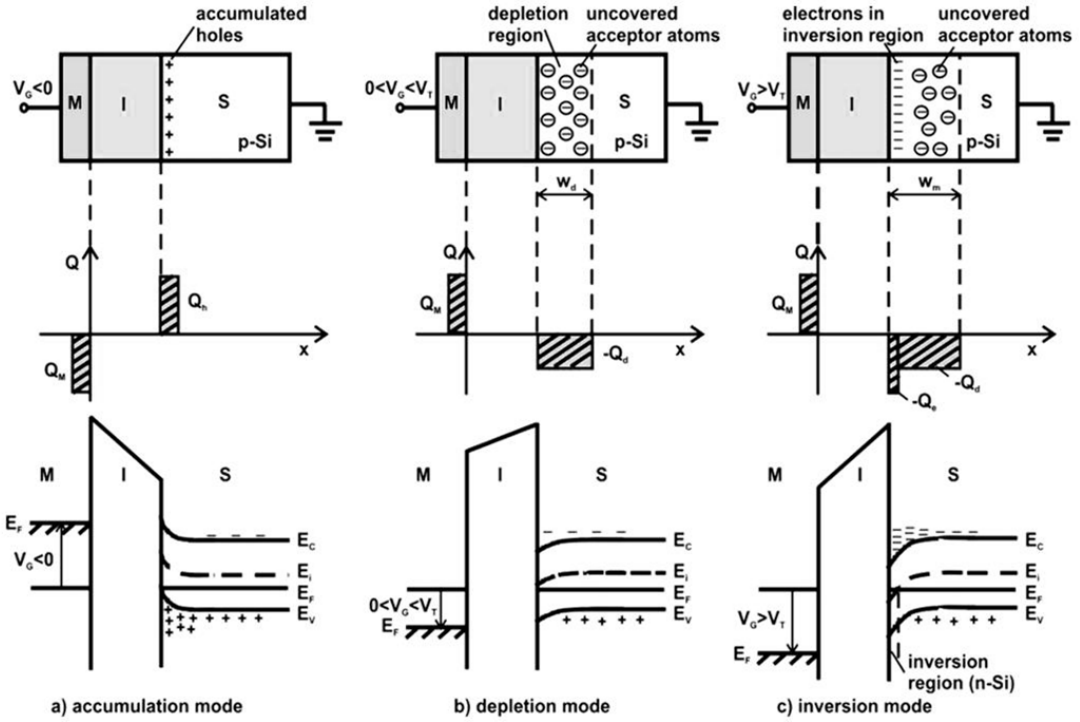

Fig. 2.3: Charge distribution and energy-band diagram of the MIS structure in accumulation (a), depletion (b) and inversion (c) mode, respectively. M: metal, I: insulator, S: semiconductor, Q_m: charge on the metal gate, Q_h: charge of the accumulation holes, Q_d: charge in the depletion region (charge of the uncovered acceptors), w_d: width of depletion region, w_m: maximum width of the depletion region, Q_e: electron charge in the inversion region. The (+) symbols near the valence band at the semiconductor-insulator interface represent the accumulated holes. The (-) symbols near the conducting band represent the electrons in the inversion layer (adapted from [9, 10, 13]).

Depletion regime: This regime arises when a slightly positive charge ($V_G>0$) is applied to the metal gate and hence, the holes are repelled from the semiconductor surface. Consequently, the space-charge region of positive charge carriers is depleted. The decrease of the hole concentration at the semiconductor surface implies the increase of the distance between the Fermi level and the valence band. Hence, the energy band bends downwards resulting in two different layers, the insulator layer and the layer of the depletion region. In this regime, the MIS structure can be described as two capacitors in series, the insulator capacitance and the applied voltage-dependent space-charge capacitance of the semiconductor C_{SC} (see equation 2.1):

$$\frac{1}{C} = \frac{1}{C_i} + \frac{1}{C_{SC}} \tag{2.1}$$

The voltage regime, at which the energy bands are horizontally throughout the semiconductor up to the surface, is called flat-band voltage when the net charge density in Si is zero [9].

Inversion regime: With increasing of the applied gate voltage ($V_G \gg 0$), the thickness of the depletion area increases. Considering the energy-band diagram, Fig 2.3c), the energy-band edges bend down further at the interface semiconductor-insulator. If the Fermi level bends below the intrinsic energy level (E_i), an inversion layer of n-type silicon arises although the substrate is p-doped [9, 12]. When the AC frequency is low (below around 100 Hz), the gate-charge fluctuations are slowly enough that the inversion charge is able to follow this variation. Hence, the total capacitance is again equal to that of the insulator. At higher frequencies, the inversion-charge fluctuation is too slow to achieve an equilibrium. As a result, the depletion-layer width increases until reaching a constant final value.

2.1.2 Solid-liquid interface

Electrical double layer

Whenever a solid surface comes into contact with a liquid, there is a potential difference at the solid-liquid boundary. The excess charge from electrons and dipoles from the electrolyte results in an electric field across the phase boundary. The layer where these charges are existing is called electrical double layer [15] (see Fig. 2.4).

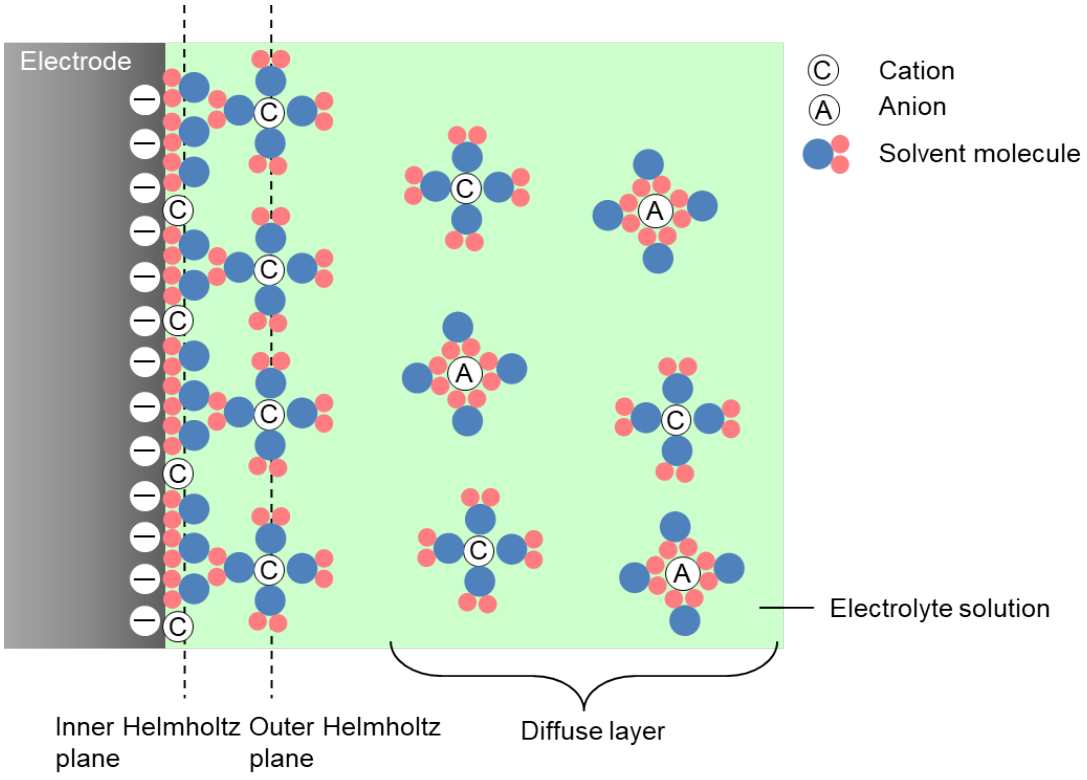

Fig. 2.4: Schematic of the electrical double layer with inner and outer Helmholtz plane (adapted from [16]).

However, there are three hypotheses describing the phenomena of the electrical double layer:

- The simplest hypothesis describes an inner layer which is close to the electrode and contains solvent molecules as well as specifically adsorbed ions linked at the electrode surface by van der Waals- or chemical forces. The layer arising through the center of these molecules, parallel to the electrode surface, known as *inner Helmholtz layer* (IHP), is shown in Fig. 2.4. Solvated ions are nonspecifically adsorbed directly at the surface where the surface charges are neutralized. The plane passing through the center of these ions is defined as outer *Helmholtz layer* (OHP). Both *Helmholtz layers* are also referred as *compact layer* [11, 16, 17].

- But, the *Helmholtz* model does not consider the thermal motion of ions, which results in detaching of the ions from the compact layer and form a diffuse double layer that is called *Gouy-Chapmann layer* (second theory) [11, 16]. This layer describes a three-dimensional area consisting of distributed ions and spreads over from the OHP into the bulk solution; it comprises the compensation of the forces of the electrical field and forces induced by thermal motion [16].

- The third theory combines the ideas of *Helmholtz-* and *Gouy-Chapman* model and is known as *Stern* model. Here, the ions which are directly adsorbed to the surface build an immobile *Helmholtz* plane, while the mobile ions outside of this plane are distributed as described in *Gouy-Chapman* theory [17].

2.1.3 Enzyme-based electrolyte-insulator-semiconductor (EIS) structure

EIS-enzyme sensors are based on pH changes due to enzyme-substrate interactions. Such an EIS structure with the immobilized enzyme is shown in Fig. 2.5.

The basic structure of EIS sensors is similar to that of the MIS system with the difference in the layer over the insulator, which is replaced by a transducer layer, an electrolyte and a reference electrode. The pH sensitivity of the EIS sensor can be explained by the site-binding theory in the following.

Site-binding theory

With the site-binding theory, the pH sensitivity of a field-effect device can be explained. The transducer layer of e.g., an EIS sensor consists of a pH-sensitive material such as $SiO_2, Al_2O_3,$ or Ta_2O_5 containing neutral surface-hydroxyl groups (MOH). Bringing the transducer surface in contact with the analyte solution, depending on the pH value, the neutral surface-hydroxyl sites are able to bind ($MOH_2{}^+$) or release (MO^-) protons. The surface reactions are shown with $H_B{}^+$ as protons in the bulk-analyte solution in equation 2.2 and equation 2.3 [9, 18]:

$$MOH \rightleftharpoons MO^- + H_B{}^+ \tag{2.2}$$

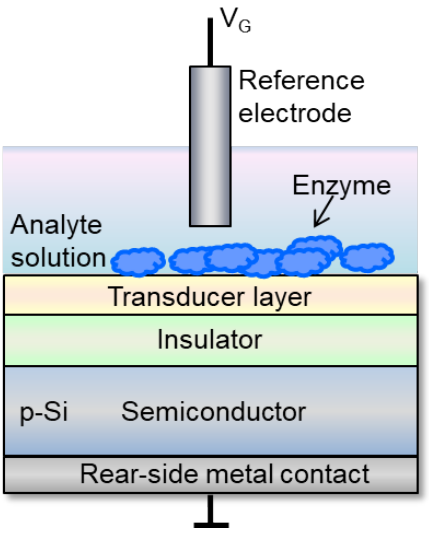

Fig. 2.5: Schematic of an EIS sensor with an immobilized enzyme (adapted from refs. [9]).

$$MOH_2^+ \rightleftharpoons MOH + H_B^+ \tag{2.3}$$

Fig. 2.6 illustrates different conditions of the surface charge depending on the pH value of the analyte solution. Each material has a net neutral charge at a certain pH value, named point of zero charge pH_{PZC}. In Tab. 2.1, different materials with their pH_{PZC} values are listed [19–21].

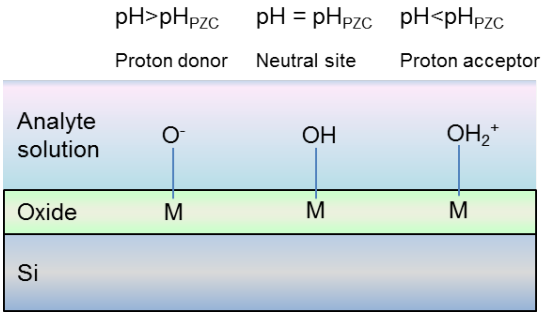

Fig. 2.6: Schematic of the electrolyte-oxide interface with the corresponding surface groups depending on the pH value of the analyte (adapted from [21]).

At pH values higher than the pH_{PZC}, the oxide surface is negatively charged, whereas at pH values lower than the pH_{PZC}, the surface is positively charged. Hence, a pH change of the analyte solution will lead to a potential change of the oxide surface.

The resulting pH-dependent electrical surface charge of the gate insulator will cause a modulation of the capacitance of the EIS structure [21]. The pH sensitivity of the EIS system at the interface oxide-electrolyte towards the pH change in the analyte solution

Tab. 2.1: Literature values of pH_{PZC} for different materials.

	SiO_2	Ta_2O_5	Si_3N_4	Al_2O_3
pH_{PZC}	2.5	2.8	3.2	7.5

(δpH_B) can be described with the following equations equation 2.4 and equation 2.5 [8, 21]:

$$\frac{\delta\varphi}{\delta pH_B} = -2.3\frac{kT}{q}\alpha \tag{2.4}$$

with

$$\alpha = \frac{1}{(2.3kTC_{dif}/q^2\beta_{int}) + 1} \tag{2.5}$$

where $\delta\varphi$ is the potential change, k represents the Boltzmann constant, T is the absolute temperature and q describes the elementary charge. α is a dimensionless sensitivity parameter, which can assume values ranging from 0 to 1, and depends on the intrinsic surface-buffer capacity β_{int} and the differential double-layer capacitance C_{dif}. Herein, β_{int} defines the number of possible binding sites at the oxide surface and C_{dif} is mainly determined by the ion concentration of the analyte solution.

As a result of equation 2.4 and equation 2.5, the maximum Nernstian sensitivity of 59.1 mV/pH (at 25 °C) can be achieved with an α value of approximately 1. This is the case, when the oxide has a high surface-buffer capacity β_{int} (high density of surface-active sites) and a low double-layer capacitance (low electrolyte concentration). One common example of such an oxide is Ta_2O_5, having a large surface-site density ($\sim 10^{15}$ cm^{-2}), resulting in a high pH sensitivity. On the other side, SiO_2 possesses less surface sites ($5 \cdot 10^{14}$ cm^{-2}). Hence, a lower pH sensitivity is expected [8, 21, 22].

The Nernstian equation is defined as followed [7] (see equation 2.6):

$$E = E^0 + \frac{RT}{zF}ln(a_s) \tag{2.6}$$

where E is termed as electrode potential, E^0 is the standard electrode potential. z and a_s are the ionic charge and ion activity, respectively, R is the gas constant, and T is the absolute temperature.

Measurement procedure

The capacitance of the EIS sensor is modulated in the same way as already described for the MIS structure. In contrast to the MIS structure, the charge-carrier distribution in an EIS system at the semiconductor surface is not only controlled by an external DC voltage, furthermore, it is also depending on the electrochemical interaction between the analyte solution and the pH-sensitive layer (transducer layer). Electrochemical interactions cause a horizontal shift of the C-V curve (a typical C-V curve is shown in Fig. 2.2), depending on the change of the pH value in the analyte solution. At a fixed capacitance value within the linear region of the C-V curve, typically about 60% of the

maximum capacitance, the potential change over time can be determined [11] resulting in the constant capacitance (ConCap) mode. For more details, see also chapter 2.5.1.

For the development of an enzymatic field-effect sensor with high sensitivity and selectivity, a selected enzyme is immobilized on the EIS chip. One example is demonstrated in [23], where different concentrations of urea are detected by a modified EIS sensor with the enzyme urease. Due to the enzymatic reaction, with increasing of the urea concentration, the OH^--ion concentration is also increased (increase of the pH value), resulting in a bias-voltage shift to higher values. The dynamic response of the ConCap measurements at a fixed capacitance demonstrates also, that with increasing of OH^--ion concentration from the enzymatic reaction (catalytic hydrolysis of urea into ammonium ions), the potential is increased.

Another example of an enzyme-based EIS sensor is discussed in [24]. Here, the enzyme penicillinase is immobilized onto the sensor surface for the catalytical reaction of penicillin, resulting in an increase of the H^+-ion concentration (decrease of the pH value). Due to this reaction, the bias voltage shifts to lower values, i.e. to the left along the voltage axis. With increasing of the penicillin concentration, the potential is decreased during the ConCap measurements.

2.2 Basic principle of cyclic voltammetry

Cyclic voltammetry provides information about a redox system, where a linear potential scan is applied in order to measure the resulting current for the reaction of an analyte. For a cyclic voltammetric experiment, a three-electrode arrangement is usually chosen, which is schematically illustrated in Fig. 2.7.

The redox electrode at which the electrochemical reaction occurs is the working electrode (WE). The material of the WE can influence the performance of the voltammetric measurement. Hence, the WE electrode should provide a high signal-to-noice ratio as well as reproducible response (signal) values. The selection of the material depends on the redox behavior of the target analyte but also from the backround current over the potential region that is required for the measurement. Furthermore, some other material aspects have to be taken into account such as conductivity of the electrode, surface reproducibility, mechanical properties, cost, availability, and toxicity. The most frequently used WE materials are carbon or noble metals (e.g., platinum and gold) [16]. An Ag/AgCl electrode is typically applied as reference electrode (RE). The RE should be placed close to the WE to reduce potential drops because of the resistance of the analyte solution. The measurement set-up also consists of a counter electrode (CE), e.g., out of platinum, to avoid current flow through the RE. The cell current is directed through the CE, the solution and the WE to adjust the potential difference between WE and RE.

In cyclic voltammetry, the potential is applied to the WE and measured against the RE, resulting in two circuits: the current-flow circuit containing WE and CE and the current-free one, where the potential difference between WE and RE is measured. The current flow through the RE is negligible, its potential can be regarded as constant. Hence, the measured potential change can be considered as potential change of the WE

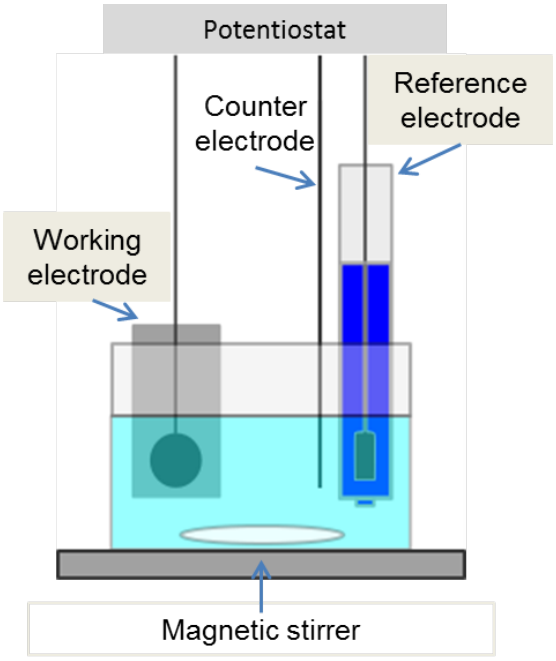

Fig. 2.7: Schematic of a three-electrode measurement set-up with WE, CE and RE to perform voltammetric measurements.

resulting in a triangular potential waveform shown in Fig 2.8a) [11, 16, 25].

Due to the electrochemical reaction at the electrode surface, the analyte concentration is decreased at this surface and should be compensated by diffusion of the species from the analyte solution. But in most cases, the reaction at the electrode surface is faster than the supply by diffusion. With the help of Fick's law, the time-dependent concentration profile of the analyte can be described as equation 2.7 [11]:

$$j(r,t) = -D\nabla(r,t) \tag{2.7}$$

where the flux j of the analyte at point r and time t is proportional to the analyte concentration. D describes the proportional factor and is called diffusion coefficient.

The corresponding current, resulting from the applied potential at the WE, is recorded by using a potentiostat. An exemplary measurement curve is shown in Fig. 2.8b) for a reversible system (see equation 2.8):

$$Ox + ne^- \rightleftharpoons Red \tag{2.8}$$

Here, Ox depicts the oxidized species and Red the reduced one. With decreasing the potential, Ox is reduced resulting in an increase of the current in the negative direction. As depletion of the Ox concentration at the electrode surface, the current peak will decay. With reversal of the scan-rate direction, the potential increases, Red is oxidized, which is indicated by a peak of the current in the positive direction [25]. The peak

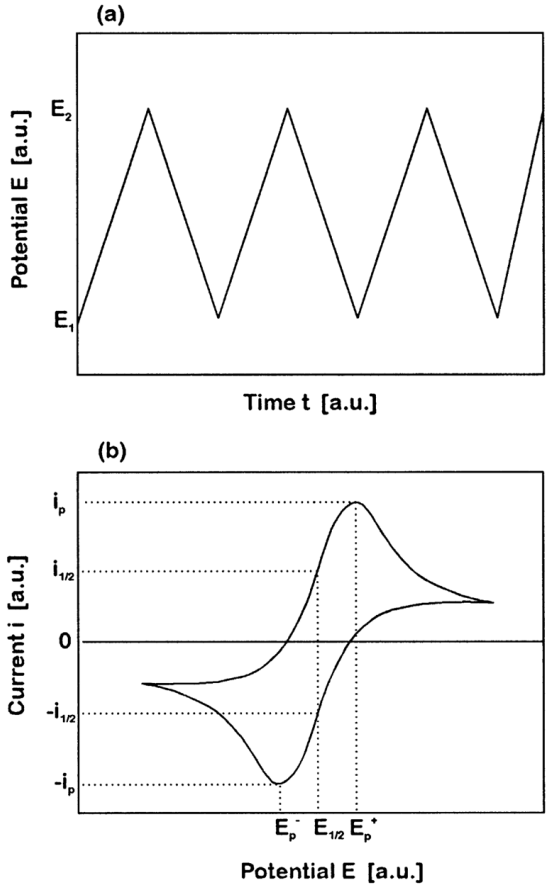

Fig. 2.8: (a) Triangular wave form generated for cyclic voltammetry sweeping forth and back between two fixed values E_1 and E_2; (b) the current potential yields a peak-shaped curve with a half-wave potential $E_{1/2} \approx E^0$ with the resulting current $i_{1/2}$ and $-i_{1/2}$. E_p^- and E_p^+ describes the anodic and cathodic peak potential, respectively, with the corresponding current $-i_p$ and i_p, the peak current i_p is proportional to the analyte's bulk concentration c_0; (adapted from [11]).

current for reversible systems at 25 °C is given by the Randles-Sevcik equation 2.9:

$$i_p = (2.69 \cdot 10^{15}) n^{\frac{3}{2}} A c D^{\frac{1}{2}} v^{\frac{1}{2}} \tag{2.9}$$

with n as the number of electrons, A depicts the surface area of the electrode, c is the analyte concentration, D the diffusion coefficient, and v the scan rate. The measured current is directly proportional to the reaction concentration and the square root of the scan rate. Both, the anodic and the cathodic peak potentials are independent of the scan rate. For reversible processes, the magnitude of both peaks is similar.

2.3 Basic principle of amperometric sensors

Since the development of the first enzyme-based glucose sensor by Clark in 1962 [26], many efforts have been done for the development of several amperometric sensors for

different kinds of applications such as environmental analysis or medicine, see examples in [27–32]. Usually, the amperometric measurement set-up is the same as already shown in Fig. 2.7.

Amperometry is based on the detection of a current through a working electrode over time. This involves a change of the applied potential to the working electrode from a value, where no Faradaic reaction occurs to a potential value that facilitates reduction or oxidation of a certain electroactive species in an unstirred solution (see Fig. 2.9a)). Here, the mass transport is controlled by diffusion. The measured current represents the concentration change only close to the electrode surface. Consequently, the diffusion layer increases corresponding to the depletion of the analyte, indicated by a decrease of the current slope depending on time. Hence, the Faradaic current i_F decays with time which is described by the Cottrell equation 2.10 [16, 33]:

$$i_F = nFAc\sqrt{\frac{D}{\pi T}} \tag{2.10}$$

whereby n is the number of electrons, F describes the Faradaic constant, D is the diffusion coefficient, A represents the surface area of the electrode, T is the time and c is the concentration of the analyte solution. The obtained curve of the Faradaic current (i_f) over time is shown in Fig. 2.9b).

Despite this Faradaic current which provides the analytical information and is a result of electrochemical reaction at the electrode surface, there is an additional current, the so-called capacitive current i_c (or non-Faradaic current) that occurs due to the compensation of the charges at the electrode-electrolyte boundary. Here, ions in the analyte solution migrate to or from the interface to compensate the changes of the electrode charge resulting in a zero charge. As typical for a capacitor, the current decreases exponentially with time [12, 16] (see equation 2.11):

$$i_c = \frac{E_s - E_i}{R_s} exp(-\frac{t}{R_s C}) \tag{2.11}$$

where R_s represents the electrical resistance of the analyte solution and C corresponds to the capacitance of the electrical double layer at the electrolyte-electrode interface.

If there is an electrochemical reaction in the system, the measuring quantity i_t (total current) is the Faradaic current together with the capacitive current, as depicted in Fig. 2.9. That leads to a superimposition of the Faradaic current by the capacitive current at low analyte concentrations. Hence, the chronoamperometric signal contains both currents for a small value t (t<50 ms). By considering the different rates of decay of i_f and i_c, the capacitive current decays much faster. Consequently, after a certain time, this current can be neglected and the Faradaic current displays the quantity value [12, 16].

2.3.1 Oxygen sensor

One of the most studied electrochemical reactions is the amperometric detection of oxygen. The applications of oxygen electrodes are ranging from biology to medicine or industrial purposes, energy production or safety [34]. Nowadays, noble metals such as

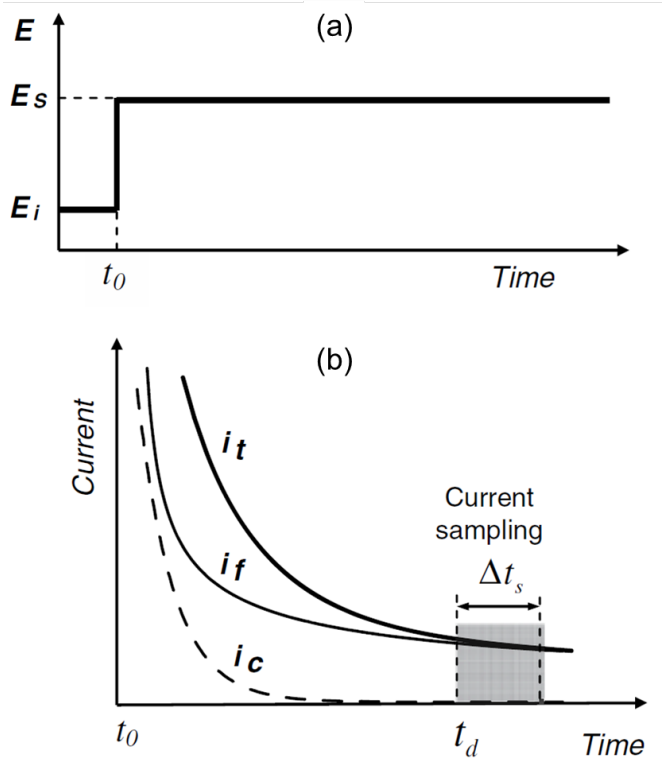

Fig. 2.9: Principle of the chronoamperometric method with (a) potential-time waveform where E_i is the applied potential, here, no electrochemical reaction occurs, E_s promotes the reduction or oxidation of an electrochemical species at time t_0; (b) resulting current where i_f describes the Faradaic current, i_c is the capacitive current and i_t depicts the total current, t_d is the time delay after which the current sampling lessens the contribution of the capacitive current to the total current and Δt_s is the width of the sampling interval; (adapted from [12]).

Pt and AU, or C are used as electrode material where one four-electron reduction is obtained due to the reaction of molecular oxygen [34] (see equation 2.12):

$$O_2 + 2H_2O + 4e^- \Rightarrow 4OH^-(E_I) \tag{2.12}$$

while the following reactions occur at the silver anode in equation 2.13 and equation 2.14:

$$4Ag \Rightarrow 4Ag^+ + 4e^- \tag{2.13}$$

and

$$4Ag^+ + 4Cl^- \Rightarrow 4AgCl \tag{2.14}$$

The first amperometric oxygen sensor was developed by L.L. Clark to determine the oxygen concentration in blood. The sensor consisted of a platinum disk cathode, a silver anode and an internal buffer KCl solution. The big advantage of the Clark-oxygen electrode is that both, cathode and anode, are covered by an oxygen-permeable membrane [35]. According to the application of the electrode and to achieve a high

sensitivity, several membranes are available for oxygen sensors, namely e.g., Teflon, polyethylene, or silicon rubber. Such membrane has two tasks, on the one hand, the electrode surface should be protected against clogging, and on the other hand, a diffusion barrier for e.g., organic impurities should be provided to ensure a stable current. Oxygen diffuses through this oxygen-permeable membrane from the analyte solution and will be reduced as mentioned in equation 2.12 [12]. The obtained steady-state current is proportional to the oxygen concentration in the analyte solution and can be calculated under consideration of the diffusion in equation 2.15 [34]:

$$i = \frac{3\pi F_{r_0} D_s S_s P(r_1)}{D_s(r_1 - r_0)/D_m r_1 + S_m r_0 r_1} \tag{2.15}$$

Here, r_0 and r_1 describe the outer radius of the membrane and the radius of the electrode, respectively. The subscripts s and m stand for the solution and membrane, respectively. S is the solubility of oxygen in the analyte solution and membrane. $P(r_1)$ describes the oxygen partial pressure at the membrane surface.

In general, for amperometric measurements, an external potential is applied to the WE against the RE promoting the analyte reaction. One alternative approach is a galvanic oxygen sensor having a similar design as amperometric gas sensors, with the difference that the chemical reaction occurs without an externally applied potential [12]. A galvanic oxygen sensor typically consists of two electrodes which are in contact with the electrolyte solution through an oxygen-permeable membrane. Similar to the working principle of the Clark-oxygen sensor, oxygen diffuses through the membrane, where the reduction reaction takes place at the cathode. But in the case of the galvanic sensor, the applied potential is close to zero. The potential of the cathode, which is necessary for the reduction reaction, is established by selecting anode materials such as lead or cadmium, which are sufficiently electronegative in the electrochemical series in combination with e.g., a silver cathode. The electrons, which are required for the reduction of oxygen, are provided by the anode, where an equal magnitude oxidation takes place. As the oxygen-reduction reaction is a cathodic one, lead from the anode is oxidized to form lead oxide. If the whole anode material is consumed, oxygen can not longer be detected by this sensor. The lifetime of a typical galvanic oxygen sensor is therefore approximately between one and two years [12, 36].

2.4 Enzyme-immobilization techniques

The immobilization method of the applied enzymes to the sensor surface plays a decisive role and has an influence on the overall sensor performance. In general, the highly selective primary interaction of enzyme and substrate can be destroyed by the application of an inappropriate immobilization strategy. The operational stability and long-term use of enzymatic biosensors represent an important task. Both factors can also be associated with the applied immobilization strategy, which can be distinguished into four principal techniques, namely adsorption, entrapment, covalent binding and cross-linking [37, 38].

The physical adsorption-immobilization method is characterized by weaker, monocovalent interactions such as hydrogen bonds, hydrophobic interactions, van der Waals forces, affinity binding, or ionic binding of the enzyme with the surface of the electrode, or mechanical binding of the enzyme. It is a reversible immobilization method where the enzyme can be removed from the sensor surface under gentle conditions, which is beneficial when the enzyme‘s activity has decayed and the sensor can be loaded with fresh enzyme [39]. This method has the advantage that a high amount of enzyme can be loaded onto the electrode surface. Furthermore, the enzyme‘s natural structure and functionality will be hardly influenced. On the other hand, this technique is easy and fast to handle but it has a low long-term stability due to the relatively weak non-specific forces, often resulting in an enzyme leakage from the matrix [39].

There are several substances, which can be used for the entrapment of enzymes such as polyacrilamide, calcium alginate, agar, agarose, chitosan polymer or gel. Entrapment is an irreversible immobilization method. However, due to the application of these materials, a poor mechanical strength can be a consequence, but also, the materials can have an influence on the diffusion limitation of the substrate/product [37, 39]. Therefore, more recently, two anion-exchange polymers have been suggested to immobilize enzymes, e.g., Nafion or Eastman AQ can incorporate the enzymes by separation of anionic-interfering species such as ascorbic- or urin acid. A big advantage by using such polymers is the possibility to immobilize the enzyme directly onto the electrode surface resulting in a thinner layer than conventional precast membranes [37].

Covalent binding and cross-linking pertain to the chemical immobilization methods. Cross-linking is performed by using, for example, glutaraldehyde or cyanoric chloride to perform intermolecular cross-linkages between the enzyme molecules by means of bi- or multifunctional reagents. In the case of covalent binding, which is the most commonly used method, the enzymes are covalently bound to the sensor surface via their side chains, which are not essential for their catalytical activity. The activity and stability of the covalently bound enzyme depends on several factors: size and shape of the electrode surface, composition of the electrode material, specific condition during coupling and the direction of the enzyme binding. Both methods, cross-linking and covalent binding are irreversible immobilization methods [39]. These techniques are useful, when the sensor surface is so small that the appropriate membrane should be fabricated directly on the sensor. Also, the enzyme loading onto the sensor surface can be controlled better, giving a more stable and reproducible enzyme activity [25].

Alternatively, electrochemically prepared polymer films are applied for the immobilization of enzymes. In this case, the films consist of aromatic organic compounds (e.g., pyrrole, tiophene, phenylene diamine or phenol) which are deposited onto the electrode surface that is already loaded by the enzyme previously by adsorption or cross-linked, or the polymer includes the enzyme as a counterion [40]. The thickness of such polymer films is usually in the nanometer range. Furthermore, these polymer membranes can also improve the selectivity due to their functionality as permselective membrane and provide a barrier against electrode fouling [37].

2.5 Measurement techniques

In the following paragraph, the measurement techniques to perform the experiments in this thesis are shortly described.

2.5.1 Capacitance-voltage- and constant-capacitance measurements

For the detection of different analytes, corresponding enzymes are immobilized onto the EIS-sensor surface; the set-up is used to perform capacitance-voltage- (C-V) and constant-capacitance (ConCap) measurements. As already mentioned in chapter 2.1, to obtain the characteristic C-V curve, a DC-bias voltage is applied between the rear-side contact of the EIS structure and the reference electrode, which is superimposed by a small AC voltage (usually 10 - 50 mV). For sensor measurements, the important part of the EIS sensor is the depletion region. Fig. 2.10, left, shows typical C-V plots for a *p*-doped EIS sensor.

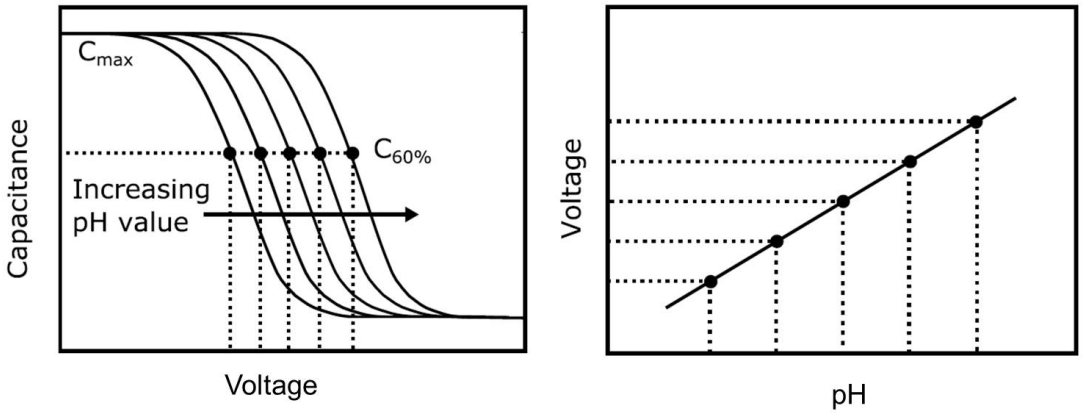

Fig. 2.10: Typical C-V curves of an EIS sensor depending on the pH changes of the analyte solution (left) and corresponding calibration curve at a fixed capacitance (right).

With increasing or decreasing of the pH value of the analyte solution due to the enzymatic reaction at the membrane-electrolyte surface, the curves are shifted to the left or right along the voltage axis. To obtain the calibration plot from the C-V curves, a fixed capacitance (about 60% of the maximum capacitance) is chosen. The resulting voltage is plotted versus the corresponding pH value of the analyte solution, which is depicted in Fig. 2.10, right.

In the ConCap-measurement mode, the dynamic response of the sensor signal, depending on the pH value of the analyte solution at a fixed bias voltage, is recorded over time, which is demonstrated in Fig. 2.11, left. To obtain the calibration plot from the ConCap curve, the steady-state voltage signal is plotted versus the corresponding pH value of the analyte solution (see Fig. 2.11, right). Both curves, obtained from the C-V curves as well as from the ConCap plot, should yield the same calibration behavior.

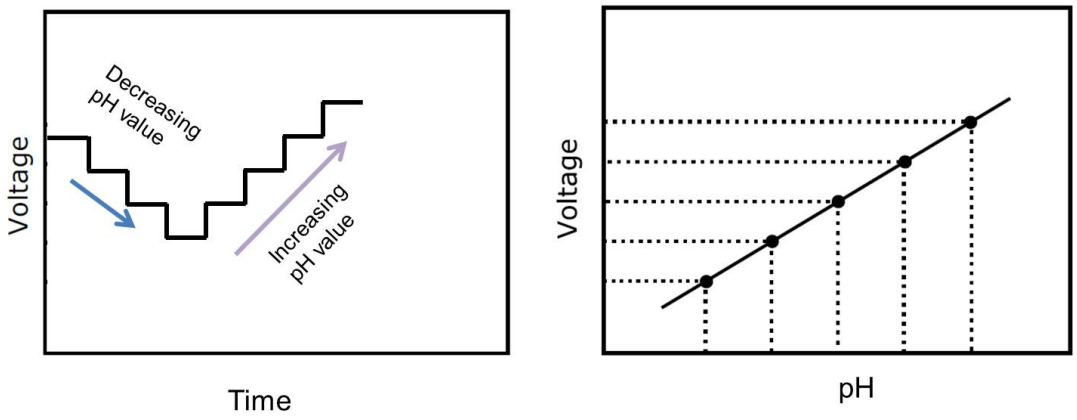

Fig. 2.11: Typical ConCap plot of an EIS sensor depending on the pH changes of the analyte solution (left) and corresponding calibration curve at a fixed capacitance (right).

2.5.2 Amperometry

For amperometric measurements, an oxidation/reduction potential for the electroactive species of interest has been adjusted. Therefore, at first, a cyclic voltammogram has to be recorded, which is shown in Fig. 2.8b). A potential is selected where the electroactive compound is depleted at the electrode surface and the transfer of the species is diffusion-limited. Hence, it should be a value between $E_{1/2}$ and E_p^+ for oxidation reactions and between $E_{1/2}$ and E_p^- for reduction reactions. The resulting Faradaic current is plotted over time. With stepwise increasing of the analyte concentration, the current is also gradually increased. An example of a typical (chrono)amperometric measurement is depicted in Fig. 2.12, left, with the derived calibration curve in Fig 2.12, right. The calibration curve is obtained by plotting the current measured at the end of each concentration step (steady-state condition) against the corresponding analyte concentration.

References

[1] A. Hulanicki, S. Glab, and F. Ingman. "Chemical sensors: Definitions and classification". *Pure and Applied Chemistry* 63 (1991), 1247–1250.

[2] J. Bobacka, A. Ivaska, and A. Lewenstam. "Potentiometric ion sensors". *Chemical Reviews* 108 (2008), 329–351.

[3] A. J. Bandodkar, V. W. S. Hung, W. Jia, G. Valdés-Ramírez, J. R. Windmiller, A. G. Martinez, J. Ramírez, G. Chan, K. Kerman, and J. Wang. "Tattoo-based potentiometric ion-selective sensors for epidermal pH monitoring". *The Analyst* 138 (2013), 123–128.

[4] T. Yoshinobu, H. Iwasaki, Y. Ui, K. Furuichi, Y. Ermolenko, Y. Mourzina, T. Wagner, N. Näther, and M. J. Schöning. "The light-addressable potentiometric sensor for multi-ion sensing and imaging". *Methods* 37 (2005), 94–102.

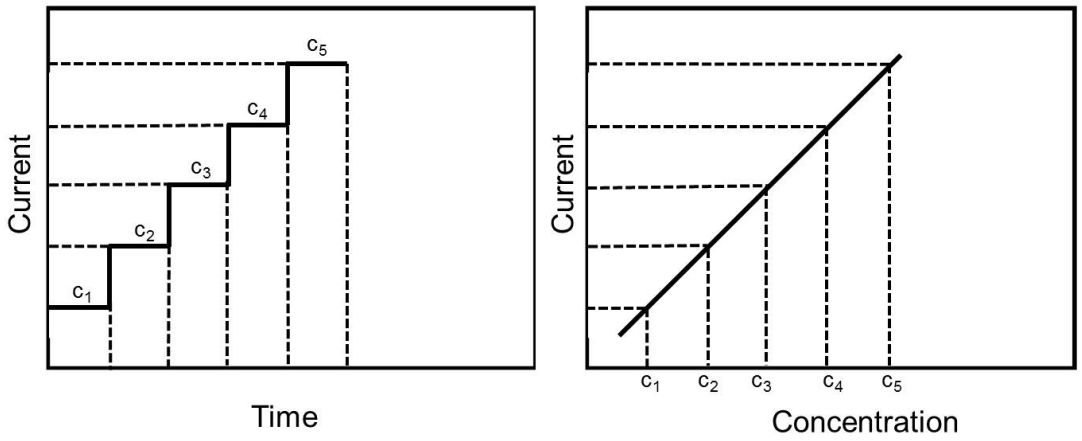

Fig. 2.12: Typical (chrono)amperometric curve for detection of the current depending on the titration of different analyte concentrations ($c_1 < c_5$) (left); corresponding calibration curve (right).

[5] A. Poghossian, T. Yoshinobu, A. Simonis, H. Ecken, H. Lüth, and M. J. Schöning. "Penicillin detection by means of field-effect based sensors: EnFET, capacitive EIS sensor or LAPS?" *Sensors and Actuators B: Chemical* 78 (2001), 237–242.

[6] D. Rolka, A. Poghossian, and M. J. Schöning. "Integration of a capacitive EIS Sensor into a FIA system for pH and penicillin determination". *Sensors* 4 (2004), 84–94.

[7] P. Bergveld and A. Sibbald. *Analytical and Biomedical Applications of Ion-Selective Field-Effect Transistors*. Vol. 23. Wilson and Wilson's Comprehensive Analytical Chemistry. Amsterdam: Elsevier, 1988.

[8] P. Bergveld. "Thirty years of ISFETOLOGY". *Sensors and Actuators B: Chemical* 88 (2003), 1–20.

[9] A. Poghossian and M. J. Schöning. "Silicon-based chemical and biological field-effect sensors". In: *Encyclopedia of Sensors*. Ed. by C. A. Grimes, E. C. Dickey, and Pishko M. V. Stevenson Ranch, CA.: ASP, American Scientific Publ., 2006.

[10] S. M. Sze and K. K. Ng. *Physics of Semiconductor Devices*. 3. ed. Hoboken, NJ: Wiley-Interscience, 2007.

[11] M. J. Schöning, O. Glück, M. Thust, M. Ali, B. Pahlavanpour, M. Eklund, E. E. Uzgiris, J. Y. Gui, Laird., and C. K. "Composition Measurement". In: *The Measurement, Instrumentation, and Sensors Handbook*. Ed. by J. G. Webster. The Eectrical Engineering Handbook Series. Boca Raton, FL: CRC Press, 1999, 1835–1883.

[12] F.-G. Banica. *Chemical Sensors and Biosensors: Fundamentals and Applications*. 1. publ. Chichester: Wiley, 2012.

[13] E. H. Nicollian and J. R. Brews. *MOS (Metal Oxide Semiconductor) Physics and Technology*. A Wiley-interscience publication. New York, NY: Wiley, 1982.

[14] D. A. Neamen. *Semiconductor Physics and Devices: Basic Principles*. 4. ed. New York, NY: McGraw-Hill, 2012.

[15] C. H. Hamann, A. Hamnett, and W. Vielstich. *Electrochemistry*. 2., Completely Rev. and Updated ed. Weinheim: Wiley-VCH-Verl., 2007.

[16] D. L. Langhus. "Analytical Electrochemistry, 2nd Edition (Wang, Joseph)". *Journal of Chemical Education* 78 (2001), 457.

[17] H.-J. Butt, K. Graf, and M. Kappl. *Physics and Chemistry of Interfaces*. 1., Auflage, neue Ausg. Weinheim: Wiley-VCH, 2006.

[18] R. van Hal, J. Eijkel, and P. Bergveld. "A novel description of ISFET sensitivity with the buffer capacity and double-layer capacitance as key parameters". *Sensors and Actuators B: Chemical* 24 (1995), 201–205.

[19] L. Bousse, S. Mostarshed, B. van der Shoot, N. de Rooij, P. Gimmel, and W. Göpel. "Zeta potential measurements of Ta_2O_5 and SiO_2 thin films". *Journal of Colloid and Interface Science* 147 (1991), 22–32.

[20] J. P. Fitts, X. Shang, G. W. Flynn, T. F. Heinz, and K. B. Eisenthal. "Electrostatic surface charge at aqueous/alpha-Al_2O_3 single-crystal interfaces as probed by optical second-harmonic generation". *The Journal of Physical Chemistry. B* 109 (2005), 7981–7986.

[21] A. Poghossian. "Determination of the pH_{pzc} of insulators surface from capacitance–voltage characteristics of MIS and EIS structures". *Sensors and Actuators B: Chemical* 44 (1997), 551–553.

[22] R. van Hal, J. Eijkel, and P. Bergveld. "A general model to describe the electrostatic potential at electrolyte oxide interfaces". *Advances in Colloid and Interface Science* 69 (1996), 31–62.

[23] J. R. Siqueira, D. Molinnus, S. Beging, and M. J. Schöning. "Incorporating a hybrid urease-carbon nanotubes sensitive nanofilm on capacitive field-effect sensors for urea detection". *Analytical Chemistry* 86 (2014), 5370–5375.

[24] M. Thust, M. J. Schöning, J. Vetter, P. Kordos, and H. Lüth. "A long-term stable penicillin-sensitive potentiometric biosensor with enzyme immobilized by heterobifunctional cross-linking". *Analytica Chimica Acta* 323 (1996), 115–121.

[25] A. E. G. Cass, ed. *Biosensors: A Practical Approach; Series*. Vol. 60. The Practical Approach Series. Oxford: IRL Press, 1990.

[26] L. C. Clark and C. Lyons. "Electrode systems for continous monitoring in cardiovascular surgery". *Annals of the New York Academy of Sciences* 102 (1962), 29–45.

[27] P. Kanyong, F. D. Krampa, Y. Aniweh, and G. A. Awandare. "Enzyme-based amperometric galactose biosensors: A review". *Mikrochimica Acta* 184 (2017), 3663–3671.

[28] V. K. Nigam and P. Shukla. "Enzyme based biosensors for detection of environmental pollutants - a review". *Journal of Microbiology and Biotechnology* 25 (2015), 1773–1781.

[29] A. P. F. Turner. "Biosensors: Fundamentals and applications - historic book now open access". *Biosensors and Bioelectronics* 65 (2015), A1.

[30] J. Shan and Z. Ma. "A review on amperometric immunoassays for tumor markers based on the use of hybrid materials consisting of conducting polymers and noble metal nanomaterials". *Mikrochimica Acta* 184 (2017), 969–979.

[31] I. Czolkos, E. Dock, E. Tønning, J. Christensen, M. Winther-Nielsen, C. Carlsson, R. Mojzíková, P. Skládal, U. Wollenberger, L. Nørgaard, T. Ruzgas, and J. Emnéus. "Prediction of wastewater quality using amperometric bioelectronic tongues". *Biosensors and Bioelectronics* 75 (2016), 375–382.

[32] J. C. Gonzalez-Rivera and J. F. Osma. "Fabrication of an amperometric flow-injection microfluidic biosensor based on laccase for in situ determination of phenolic compounds". *BioMed Research International* 2015 (2015), 845261.

[33] K. Cammann, ed. *Instrumentelle analytische Chemie: Verfahren, Anwendungen, Qualitätssicherung*. 1., Aufl., Nachdr. Heidelberg: Spektrum Akad. Verl., 2010.

[34] J. Janata. *Principles of Chemical Sensors*. 2nd ed. Dordrecht and New York: Springer, 2009.

[35] L. L. Clark JR. "Monitor and control of blood and tissue oxygen tensions". *American Society of Artificial Internal Organs* 2 (1956), 41–48.

[36] L. Nei and R. G. Compton. "An improved Clark-type galvanic sensor for dissolved oxygen". *Sensors and Actuators B: Chemical* 30 (1996), 83–87.

[37] A. Mulchandani and K. Rogers, eds. *Enzyme and Microbial Biosensors: Techniques and Protocols*. Vol. 6. Methods in Biotechnology. Totowa NJ: Humana Press, 1998.

[38] J. M. Guisan, ed. *Immobilization of Enzymes and Cells*. Second Edition. Vol. 22. Methods in Biotechnology. Totowa, NJ: Humana Press Inc, 2006.

[39] N. R. Mohamad, N. H. C. Marzuki, N. A. Buang, F. Huyop, and R. A. Wahab. "An overview of technologies for immobilization of enzymes and surface analysis techniques for immobilized enzymes". *Biotechnology, Biotechnological Equipment* 29 (2015), 205–220.

[40] N. C. Foulds and C. R. Lowe. "Enzyme entrapment in electrically conducting polymers. Immobilisation of glucose oxidase in polypyrrole and its application in amperometric glucose sensors". *Journal of the Chemical Society, Faraday Transactions 1: Physical Chemistry in Condensed Phases* 82 (1986), 1259–1264.

3 Concept for a biomolecular logic chip with an integrated sensor and actuator function (*Physica Status Solidi A*, 212, 6 (2015), 1382–1388)

D. Molinnus, M. Bäcker, H. Iken, A. Poghossian, M. Keusgen and M. J. Schöning

Published in: *Physica Status Solidi A*, Vol. 212, 6 (2015), 1382–1388.

Submitted: 2014-12-12; Accepted: 2015-04-14; Published: 2015-05-04

3.1 Abstract

A concept for a new generation of an integrated multifunctional biosensor/actuator system is developed, which is based on biomolecular logic principles. Such a system is expected to be able to detect multiple biochemical input signals simultaneously and in real-time and convert them into electrical output signals with logical operations such as **OR**, **AND**, etc. The system can be designed as a closed-loop drug release device triggered by an enzyme logic gate, while the release of the drug induced by the actuator at the required dosage and timing will be controlled by an additional drug sensor. Thus, the system could help to make an accurate and specific diagnosis. The presented concept is exemplarily demonstrated by using an enzyme logic gate based on a glucose/glucose oxidase system, a temperature-responsive hydrogel mimicking the actuator function and an insulin (drug) sensor. In this work, the results of functional testing of individual amperometric glucose and insulin sensors as well as an impedimetric sensor for the detection of the hydrogel swelling/shrinking are presented.

3.2 Introduction

As medical diagnostic techniques continue to progress toward therapies based on biomarkers as an indicator for a particular disease state, the development of highly sensitive, specific, and cost-effective sensors and systems for the detection of clinically relevant biomarkers are important issues in clinical diagnostics [1–3]. Some well-known examples of biomarkers are prostate-specific antigen for prostate cancer, cardiac troponin, or creatine kinase for myocardial infarction, C-reactive protein as an indicator of inflammation, etc. [4, 5]. Recently, enzyme biomarkers have also been used for a forensic identification of ethnic groups [6]. However, biomarkers often relate to several different disorders, making the diseases specification sophisticated. The diagnostic value of biomarkers for the disease specification can be increased by the detection of panels of biomarkers [7, 8].

Recent research efforts in the field of molecular logic gates and biocomputing using a variety of recognition elements, including enzymes, DNA (deoxyribonucleic acid), RNA (ribonucleic acid), and biochemical pathways in living cells, show a great potential for this new technology (see e.g., Refs. [9–15]). Molecular logic and computation potentially could also be applied to create medical devices and systems for intelligent or smart diagnostics [16–19]. For example, **AND** and **INHIBIT** logic gates that respond to the presence of both interleukin-8 protein and bacterial DNA in a sample have been realized in [17]. In addition, a multi-enzyme logic-gate network has been developed to assess the traumatic brain injury and soft tissue injury [18, 19]. Moreover, biomolecular logic principles have been utilized for the development of a "Sense-and-Act" system for biologically triggered drug-release applications [20, 21].

In this work, we present a novel and very promising platform for on-chip integration of molecular logic principles with a multi-functional biosensor/actuator system – so-called biomolecular logic chip (BioLogicChip). Such a chip is expected to be able to detect multiple biochemical input signals (e.g., panel of biomarkers or cascade of biochemical reactions) simultaneously and in real-time in a microfluidic system and convert them into electrical output signals with logical operations such as **OR**, **AND**, etc. The resulting bit patterns consisting of "zeroes" and "ones" correlate with a specific disease. With these logic operations, the actuator function can be addressed and stimulated, resulting in the release of the respective agent (e.g., drugs for the treatment of the patient). The BioLogicChip represents a "sense/act/treat" logic biosensor/actuator system capable for a highly specific and reliable diagnosis and drug administration as it responds only to specific combinations of biochemical input signals that are processed by the biomolecular logic gate.

3.3 Concept for the BioLogicChip

The proposed concept is exemplarily demonstrated by using the enzyme logic gate based on a glucose/glucose oxidase system and a temperature-responsive hydrogel mimicking the actuator function (e.g., hydrogel valve) shown in Fig. 3.1. Here, the chip is designed as a closed-loop drug-release device triggered by the enzyme logic gate. The glucose level is measured by an amperometric sensor using the enzyme glucose oxidase, whereat

glucose and oxygen serve as input signals to mimic the Boolean **AND** logic operation. The absence of the respective analytes in the solution is considered as the input signal **0**, while addition of analytes is used as the input signal **1**. If both input signals or either one of them are missing (input signal **0,0; 0,1; 1,0**), no enzymatic reaction occurs and the logic output signal is **0**. In the presence of both the glucose and oxygen (input signal **1,1**), an oxidation of glucose catalyzed by glucose oxidase results in the production of gluconic acid and hydrogen peroxide, yielding a glucose concentration-dependent current change (logic output signal **1**). The logic output current will activate the heater on which a temperature-responsive hydrogel is positioned. Thus, the temperature-dependent shrinking/swelling of the hydrogel could be activated in accordance to the logic output of the enzyme logic gate. If hydrogel is designed, for instance, as fluidic valve closing some compartment containing the drug of interest, it can act as an actuator releasing the particular drug (e.g., insulin in order to reduce the glucose level) in the solution as the hydrogels shrinks. Alternatively, drug molecules could be incorporated within the hydrogel. The release of the drug at the required dosage and timing will be controlled by the glucose level and monitored by an additional drug sensor (here, an insulin sensor). In this work, the results of functional testing of the individual amperometric glucose and insulin sensors as well as an impedimetric sensor for the detection of the temperature-induced hydrogel shrinking are presented.

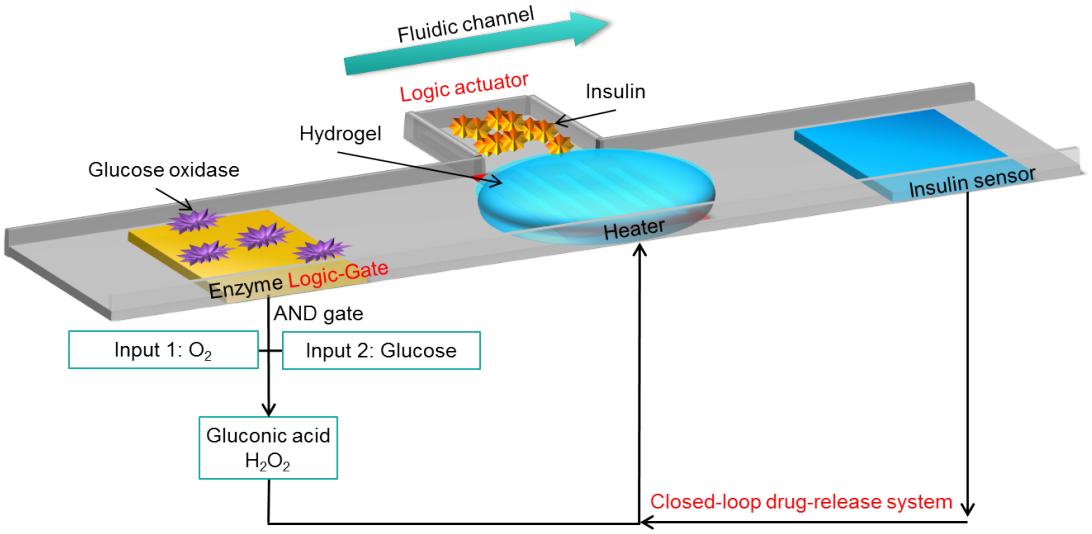

Fig. 3.1: Schematic of a BioLogicChip consisting of an enzyme logic gate based on a glucose/glucose oxidase system, a temperature-responsive hydrogel valve mimicking the actuator function (drug release from the closed compartment in the solution as the hydrogel shrinks) and a drug (insulin) sensor for the control of the drug release. The chip is exemplarily designed as a closed-loop drug-release device triggered by the enzyme logic gate.

3.4 Experimental

3.4.1 Chemicals

Glutaraldehyde, bovine serum albumine (BSA), bovine insulin (≥ 27 USP units/mg), enzyme glucose oxidase (EC 1.1.4., from *Aspergillus niger*), glucose monohydrate, and the buffer components were purchased from Sigma–Aldrich (St. Louis). Hydrochlorid acid was bought from Merck Titrisol (Darmstadt, Germany). N-isopropylacrylamide (NIPAAm, 99%, Sigma–Aldrich), cross-linking agent N,N'-methylenebis (acrylamide) (BIS, 98%, Merck), and the photoinitiator Irgacure 2959 (Ciba) were used as received, without any additional purfication.

3.4.2 Preparation of sensors structures

The sensor chips were fabricated by means of conventional silicon- and thin-film technologies. First, 500 nm (SiO_2) was grown by thermal wet oxidation of a p-Si wafer. Then, 20 nm titanium as adhesion layer and subsequently, 200 nm platinum as electrode material for the amperometric glucose sensor were deposited on the (SiO_2) surface by electron-beam evaporation and patterned by means of lift-off technique. The wafer was cut into separate chips with size of 1 x 2 cm^2. The schematic layer structure and photograph of the chip are shown in Fig. 3.2. This basis structure was also used for the preparation of the amperometric insulin sensor. After the surface cleaning with acetone, isopropanol and deionized water, the chips were glued onto the substrate holder, electrically connected by means of an ultrasonic wedge bonder and encapsulated with silicone rubber (TSE 399C, Momentive Performance Materials, Switzerland). The contact area of the Pt electrodes with the analyte was approximately 0.4 cm^2.

The glucose biosensor was prepared by attaching an enzyme membrane on the platinum electrode. For this, 125.7 μL phosphat buffer (pH 7.4) containing GOD with a concentration of 166.6 U/mL was mixed with 20 μL of BSA (10 vol%) and 20 μL glutaraldehyde (2 vol%) solutions. The resulting volumetric ratio of all three components was 1–2–2 (enzyme–BSA–glutaraldehyde) [22]. A total of 30 μL of the membrane cocktail was then dropped on the platinum electrode resulting in an enzyme loading of approximately 1 U/electrode. After drying, the chip was rinsed with buffer solution to remove unbound components and stored at 4 °C until required.

The impedimetric sensor for the hydrogel-shrinking detection is based on a platinum interdigitated circle structure and was fabricated as described before for the glucose sensor. The circular structure consists of 24 fingers with a width of 100 μm and a gap between the electrodes of 150 μm (see Fig. 3.3).

The temperature-responsive hydrogel was prepared from a pre-polymer solution consisting of 100 mM NIPAAm, 1 mM BIS and 0.45 mmol Irgacure dissolved in 60 mL deionized water under stirring. The poly-(N-isopropylacrylamide) (PNIPAAm) hydrogel film was prepared by the photopolymerization method described in [23]. With the help of a photomask during the UV light exposure, the size of the hydrogel was defined. After drying at room temperature, the thickness of the hydrogel was approximately 10 μm in the dry state.

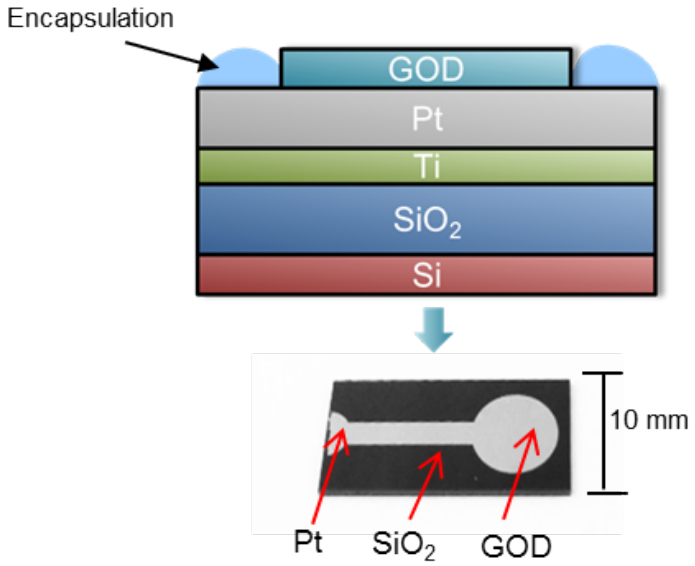

Fig. 3.2: Layer structure of the amperometric glucose sensor (top) and photograph of the biosensor chip (bottom).

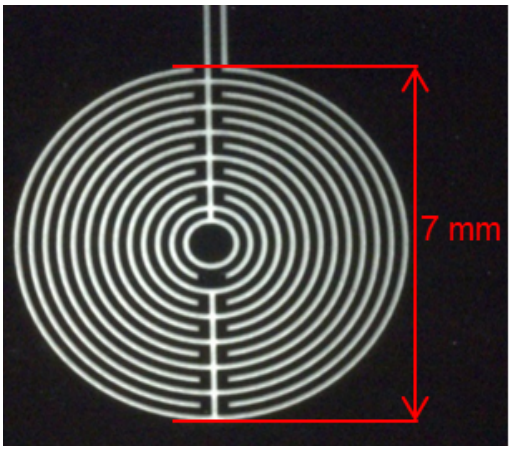

Fig. 3.3: Platinum interdigitated circle structure.

Different metal electrodes have been discussed in literature for the amperometric detection of insulin [24]. For example, a modified glassy carbon electrode with a composite of ruthenium oxide and cyanoruthenate has shown promising results in the flow-injection analysis under acidic conditions [25]. The application of natural antibodies and even more directly imprinted polymers and antibody replicae for the detection of insulin have been reported in [26]. However, insulin had a limited stability in buffer solutions at pH>4. A more stable amperometric detector for insulin has been prepared by electroplating the equated iridium complexes on the classy carbon electrode. The nanometer-thick film of Ir_xO_y could be used for the fast amperometric determination of

insulin at low concentrations (<1 μM) dissolved in pH 7.4 buffer solution [27]. Therefore, Ir_xO_y was chosen as an electrode material for the insulin oxidation. In this work, the Ir_xO_y layer was fabricated by thermal oxidation (at 700 °C [28]) for 1 h of a 20 nm thick iridium film deposited on top of the Si–SiO_2–Ti–Pt structure. The schematic layer structure and photograph of the insulin sensor is shown in Fig. 3.4.

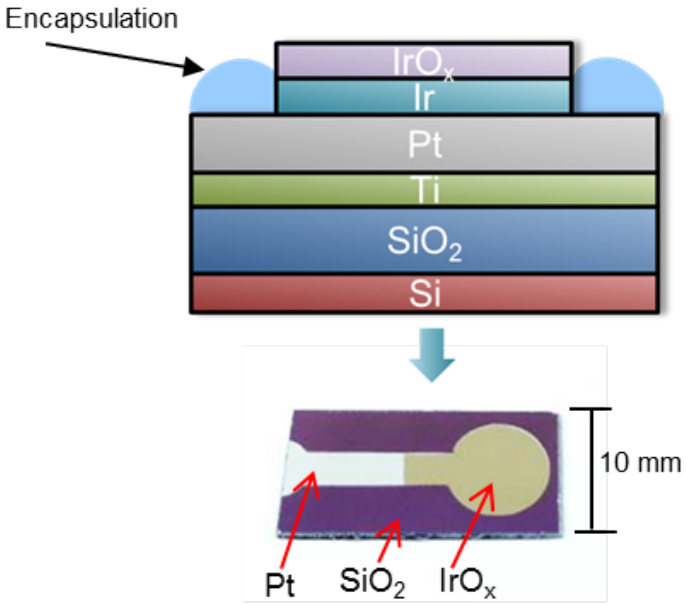

Fig. 3.4: Layer structure of the amperometric insulin sensor (top) and photograph of the prepared chip (bottom).

3.4.3 Electrochemical sensor characterization

For the electrochemical characterization of the amperometric glucose and insulin sensor, the Pt and Ir_xO_y working electrodes were connected to a potentiostat (PalmSens, Palm Instruments BV, Netherlands). A three-electrode arrangement was used, where a conventional liquid-junction Ag/AgCl electrode (Metrohm) was utilized as a reference electrode and a platinum wire as a counter electrode. To oxidize the hydrogen peroxide that is produced during the enzymatic reaction, a constant potential of +600 mV *vs.* Ag/AgCl was applied to the platinum working electrode and the current was monitored as a function of time. This potential value for hydrogen peroxide oxidation has been determined from the linear-sweep voltammetry measurements in the diffusion-controlled plateau region. For the oxidation of the insulin, a constant potential of +800 mV [28] was applied on the Ir_xO_y electrode. The experiments were performed at room temperature.

The swelling/shrinking behavior of the temperature-responsive PNIPAAm hydrogel was studied at different temperatures (28 - 42 °C) using an impedance measurement system IM6e (Zahner Elektrik GmbH, Germany).

3.5 Results and discussion

3.5.1 Enzyme-based AND logic gate

Before experiments with the **AND** enzyme logic gate, the glucose sensitivity of the prepared amperometric glucose biosensor has been tested. Fig. 3.5 depicts the response of the glucose sensor recorded in solutions with different glucose concentrations from 0.2 - 2.34 mM (a) and the corresponding calibration curve (b). As expected, the current increases with increasing the glucose concentration. The sensor exhibits a sensitivity of 9.15 $\pm$ 0.15 μA/mM in a linear concentration range of 0.2 - 2.34 mM glucose, which is comparable with results reported for glucose oxidase modified electrodes based on Au films [29].

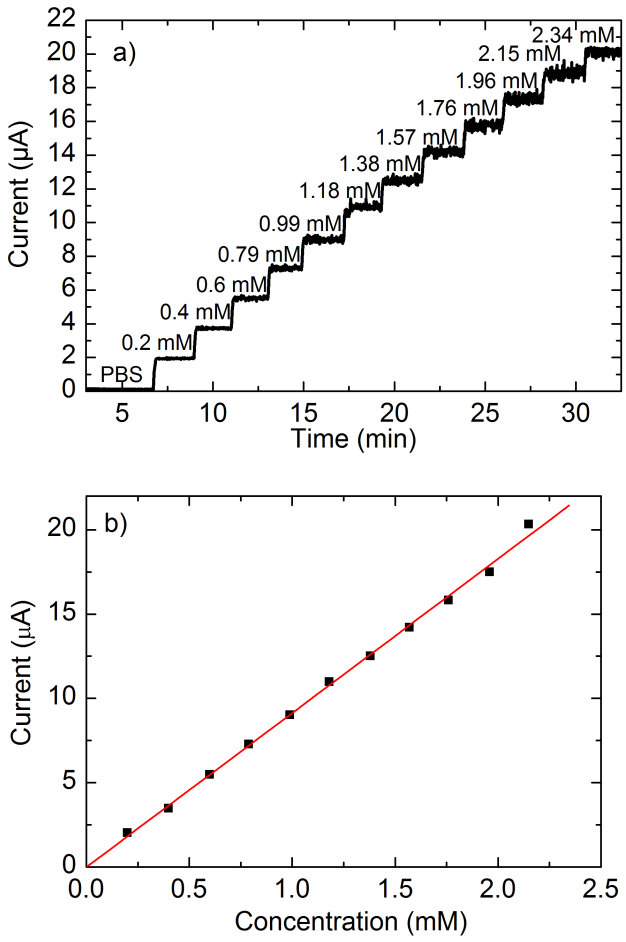

Fig. 3.5: Amperometric detection (a) and sensitivity plot (b) of glucose in the concentration range of 0.2 - 2.34 mM, determined by the glucose biosensor.

Figure 3.6 shows the logic output signal of the enzyme biosensor **AND** gate with glucose and oxygen as input signals. In this experiment, the sensor with the immobilized

glucose oxidase was consecutively exposed to (a) glucose- and oxygen-free buffer solution, (b) glucose-free buffer in the presence of dissolved oxygen (with a concentration obtained in the solution under equilibrium with air), (c) oxygen-free glucose solution (10 mM), and (d) buffer solution containing both the glucose (10 mM) and dissolved oxygen. To obtain oxygen-free solution, nitrogen was bubbled through the solution for 30 min before starting the measurement. In addition, the presence or absence of oxygen in solution was controlled by an oxygen sensor (Atlas Scientific). As can be seen, a large signal ($\sim$17 μA) has been registered only if both substrates (glucose and oxygen) are present in the solution (input **1,1**). Thus, only in the presence of glucose and dissolved oxygen the enzymatic reaction is completed, resulting in a final product (hydrogen peroxide) detected by the amperometric sensor. As a result, the sensor generates an electronic signal corresponding to the logic output signal produced by the enzymes. If both or either one of the inputs are missing (inputs **0,0; 0,1; 1,0**), no enzymatic reaction occurs and therefore, no (or only a very small) current change was detected. The truth table with respective input signal combinations is also reviewed in Fig. 3.6.

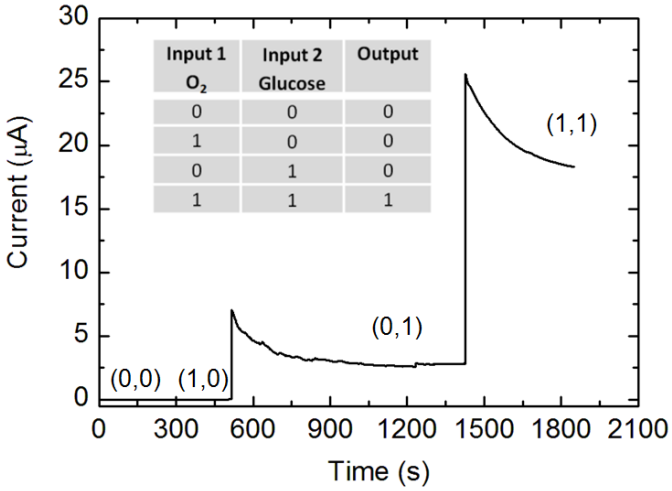

Fig. 3.6: Ouput signal of an enzyme-based **AND** logic gate by different combinations of glucose and oxygen inputs, determined by the glucose biosensor.

3.5.2 Impedimetric detection of hydrogel shrinking

Hydrogels are cross-linked polymer structures capable for absorbing a large amount of water. Stimuli-responsive hydrogels are able to swell or shrink and thus, to change their volume significantly in response to external stimuli (e.g., pH, ionic strength, temperature) [30, 31]. At low temperatures, the PNIPAAm hydrogel is in a highly swollen state. Above the phase-transition temperature (around 32 - 34 °C [23]), the polymer network chains collapse.

To examine the feasibility of the prepared hydrogel film to work as a drug-release device enabling to switch "ON/OFF", impedance of the interdigitated circular electrodes

was measured at different temperatures reaching from 28 °C to 42 °C. The open-circuit impedance measurement was performed at a frequency of 1053 Hz and is presented in Fig. 3.7. At temperatures lower than the phase-transition temperature, the impedance has a constant value of 2.5 kΩ. The impedance is increased sharply at temperatures above 33.4 °C and achieves to a value of 14.8 kΩ at 42 °C. The high impedance at high temperatures corresponds to the collapsed and hydrophobic gel phase containing little water, while the low impedance at low temperatures corresponds to a swollen state with high water content. In contrast, comparative impedance measurements with the interdigitated circular electrodes without the immobilized hydrogel depicted a linearity decrease of the impedance by increasing of the temperature due to the increase of the conductivity of water. These experiments clearly demonstrate the feasibility of the PNIPAAm hydrogel films as temperature-responsive actuator. Future experiments envisage combining the hydrogel actuator together with a drug reservoir releasing the agent (e.g., insulin) of interest.

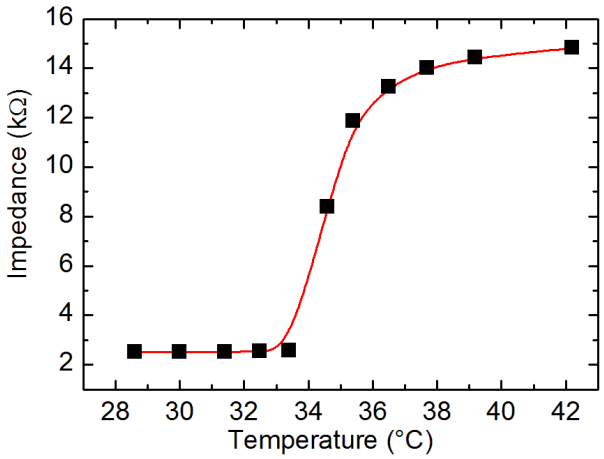

Fig. 3.7: Characterization of the temperature-dependent swelling/shrinking behavior of the PNIPAAm hydrogel film by impedance measurements at temperatures between 28 °C and 42 °C.

3.5.3 Insulin sensor

Morphological characterization

The prepared Ir_xO_y film was characterized by energy-dispersive X-ray spectroscopy [EDX, Magellan 400 (FEI)] and atomic force microscopy (AFM, NanoWizard® II, JPK Instruments, Germany). With the use of EDX images (data not shown), the oxidation of iridium could be confirmed. To obtain further details of the surface morphology of the iridium layer, the sensor surface was investigated with AFM. For this, areas of 5.0 x 5.0 μm^2 were scanned prior to and after 1 h oxidation (see Fig. 3.8). The oxidation procedure resulted in a raise of surface roughness, indicated by increasing average roughness values R_a of 1.2 nm (before oxidation) to 4.7 nm (after oxidation).

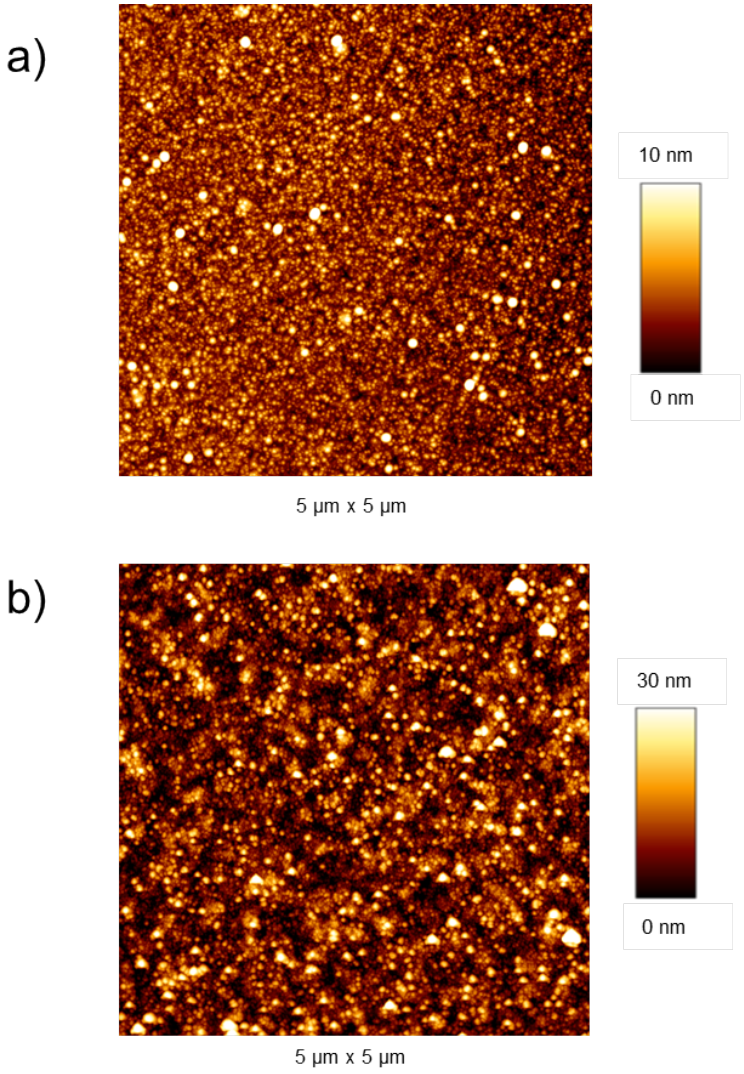

Fig. 3.8: AFM height images of the iridium layer before oxidation (a) and after 1 h oxidation (b).

Electrochemical characterization

Insulin is a peptide hormone and can be directly electrochemically detected, among other things, by its oxidation at modified electrodes [25, 32]. The measurement of the oxidation of insulin is a preferred mode of determination since it avoids interferences associated with the reduction of oxygen at the sensing electrode. The electrochemical oxidation of insulin was subjected by using an Ir_xO_y-modified electrode. The resulting sensor signal was recorded by amperometric measurements. Therefore, a stock solution of 0.42 mM insulin was prepared freshly prior to measurement by dissolving powdered insulin from porcine pancreas in 2.5 mL of 0.02 M HCl. This stock solution was further diluted with 0.05 M phosphate buffer (pH 7.4) solution to define working solutions with desired concentrations [27]. Figure 3.9 exemplarily presents the calibration curve from

the oxidation of insulin measured by the Ir_xO_y sensor with an oxidation time of 1 h of the iridium layer. The sensor was able to detect insulin in the concentration range of 0.1 - 0.5 μM with a sensitivity of 4.36 $\pm$ 0.91 nA/μM. Insulin at higher concentrations cannot be detected. This may be a consequence of approaching the solubility limit of insulin since insulin is known to be sparingly soluble at neutral pH. The measurement shows a feasible application of using the Ir_xO_y electrode to monitor the insulin at lower concentrations.

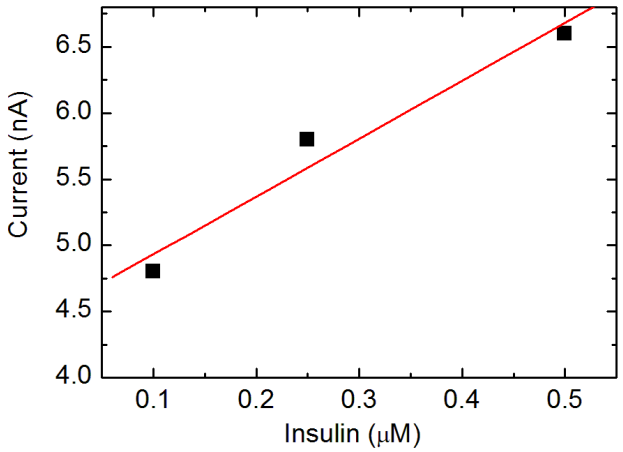

Fig. 3.9: Sensitivity plot of insulin in the concentration range of 0.1 - 0.5 μM measured by the Ir_xO_y sensor.

3.6 Conclusions

In this work, a concept for the BioLogicChip – a "sense/act/treat" logic biosensor/actuator system capable for a highly specific and reliable diagnosis and drug administration – is presented. The BioLogicChip is expected to be able to detect multiple biochemical input signals and convert them into logic output signals correlating with a specific disease. With these logic operations (**AND**, **OR**, etc.), the actuator function can be stimulated, resulting in the release of a particular agent (e.g., drugs). The proposed concept has been demonstrated through the example of a closed-loop drug-release system triggered by the enzyme logic based on a glucose/glucose oxidase system and the logic actuator based on a temperature-responsive hydrogel. In proof-of-concept experiments, the amperometric Pt glucose sensor for the enzyme logic function, an impedimetric sensor for the detection of swelling/shrinking of the temperature-responsive PNIPAAm hydrogel film (mimicking the actuator function) and an Ir_xO_y-based amperometric insulin sensor (for the drug-release control) have been prepared and successfully tested. Future work will be directed to integrate single sensors and actuators onto one chip and combine them with a microfluidic device as well as to develop a "sense/act/treat" system based on multiple enzyme logic gates and actuators triggered by a cascade of enzymatic reactions.

Acknowledgments

D. Molinnus gratefully thanks FH Aachen for the Ph.D. scholarship and Dr. Elmar Neumann (Research Centre Jülich), C. Huck and F. Kramer for technical support.

References

[1] K.-I. Chen, B.-R. Li, and Y.-T. Chen. "Silicon nanowire field-effect transistor-based biosensors for biomedical diagnosis and cellular recording investigation". *Nano Today* 6 (2011), 131–154.

[2] X. Luo and J. J. Davis. "Electrical biosensors and the label free detection of protein disease biomarkers". *Chemical Society Reviews* 42 (2013), 5944–5962.

[3] A. Poghossian and M. J. Schöning. "Label-free sensing of biomolecules with field-effect devices for clinical applications". *Electroanalysis* 26 (2014), 1197–1213.

[4] I. E. Tothill. "Biosensors for cancer markers diagnosis". *Seminars in Cell Biology* 20 (2009), 55–62.

[5] G.-J. Zhang and Y. Ning. "Silicon nanowire biosensor and its applications in disease diagnostics: A review". *Analytica Chimica Acta* 749 (2012), 1–15.

[6] F. Kramer, L. Halámková, A. Poghossian, M. J. Schöning, E. Katz, and J. Halámek. "Biocatalytic analysis of biomarkers for forensic identification of ethnicity between Caucasian and African American groups". *The Analyst* 138 (2013), 6251–6257.

[7] A. Kim, C. S. Ah, C. W. Park, J.-H. Yang, T. Kim, C.-G. Ahn, S. H. Park, and G. Y. Sung. "Direct label-free electrical immunodetection in human serum using a flow-through-apparatus approach with integrated field-effect transistors". *Biosensors and Bioelectronics* 25 (2010), 1767–1773.

[8] V. Krivitsky, L.-C. Hsiung, A. Lichtenstein, B. Brudnik, R. Kantaev, R. Elnathan, A. Pevzner, A. Khatchtourints, and F. Patolsky. "Si nanowires forest-based on-chip biomolecular filtering, separation and preconcentration devices: nanowires do it all". *Nano Letters* 12 (2012), 4748–4756.

[9] Y.-H. Lai, S.-C. Sun, and M.-C. Chuang. "Biosensors with built-in biomolecular logic gates for practical applications". *Biosensors* 4 (2014), 273–300.

[10] E. Katz and V. Privman. "Enzyme-based logic systems for information processing". *Chemical Society Reviews* 39 (2010), 1835–1857.

[11] M. Pita, M. Krämer, J. Zhou, A. Poghossian, M. J. Schöning, V. M. Fernández, and E. Katz. "Optoelectronic properties of nanostructured ensembles controlled by biomolecular logic systems". *ACS Nano* 2 (2008), 2160–2166.

[12] A. Poghossian, K. Malzahn, M. H. Abouzar, P. Mehndiratta, E. Katz, and M. J. Schöning. "Integration of biomolecular logic gates with field-effect transducers". *Electrochimica Acta* 56 (2011), 9661–9665.

[13] N. H. Voelcker, K. M. Guckian, A. Saghatelian, and M. R. Ghadiri. "Sequence-addressable DNA logic". *Small* 4 (2008), 427–431.

[14] E. Shapiro and B. Gil. "Cell biology. RNA computing in a living cell". *Science* 322 (2008), 387–388.

[15] P. Nurse. "Life, logic and information". *Nature* 454 (2008), 424–426.

[16] J. Liu, H. Zhou, J.-J. Xu, and H.-Y. Chen. "Dual-biomarker-based logic-controlled electrochemical diagnosis for prostate cancers". *Electrochemistry Communications* 32 (2013), 27–30.

[17] T. Konry and D. R. Walt. "Intelligent medical diagnostics via molecular logic". *Journal of the American Chemical Society* 131 (2009), 13232–13233.

[18] J. Halámek, V. Bocharova, S. Chinnapareddy, J. R. Windmiller, G. Strack, M.-C. Chuang, J. Zhou, P. Santhosh, G. V. Ramirez, M. A. Arugula, J. Wang, and E. Katz. "Multi-enzyme logic network architectures for assessing injuries: Digital processing of biomarkers". *Molecular BioSystems* 6 (2010), 2554–2560.

[19] J. Halámek, J. R. Windmiller, J. Zhou, M.-C. Chuang, P. Santhosh, G. Strack, M. A. Arugula, S. Chinnapareddy, V. Bocharova, J. Wang, and E. Katz. "Multiplexing of injury codes for the parallel operation of enzyme logic gates". *The Analyst* 135 (2010), 2249–2259.

[20] K. Radhakrishnan, J. Tripathy, and A. M. Raichur. "Dual enzyme responsive microcapsules simulating an "OR" logic gate for biologically triggered drug delivery applications". *Chemical Communications* 49 (2013), 5390–5392.

[21] S. Mailloux, J. Halámek, and E. Katz. "A model system for targeted drug release triggered by biomolecular signals logically processed through enzyme logic networks". *The Analyst* 139 (2014), 982–986.

[22] M. Bäcker, D. Rakowski, A. Poghossian, M. Biselli, P. Wagner, and M. J. Schöning. "Chip-based amperometric enzyme sensor system for monitoring of bioprocesses by flow-injection analysis". *Biotechnology Journal* 163 (2013), 371–376.

[23] M. Bäcker, M. Raue, S. Schusser, C. Jeitner, L. Breuer, P. Wagner, A. Poghossian, A. Förster, T. Mang, and M. J. Schöning. "Microfluidic chip with integrated microvalves based on temperature- and pH-responsive hydrogel thin films". *Physica Status Solidi A* 209 (2012), 839–845.

[24] A. Salimi, L. Mohamadi, R. Hallaj, and S. Soltanian. "Electrooxidation of insulin at silicon carbide nanoparticles modified glassy carbon electrode". *Electrochemistry Communications* 11 (2009), 1116–1119.

[25] J. A. Cox and T. J. Gray. "Flow injection amperometric determination of insulin based upon its oxidation at a modified electrode". *Analytical Chemistry* 61 (1989), 2462–2464.

[26] R. Schirhagl, U. Latif, D. Podlipna, H. Blumenstock, and F. L. Dickert. "Natural and biomimetic materials for the detection of insulin". *Analytical Chemistry* 84 (2012), 3908–3913.

[27] M. Pikulski and W. Gorski. "Iridium-based electrocatalytic systems for the determination of insulin". *Analytical Chemistry* 72 (2000), 2696–2702.

[28] M. F. Smiechowski and V. F. Lvovich. "Iridium oxide sensors for acidity and basicity detection in industrial lubricants". *Sensors and Actuators B: Chemical* 96 (2003), 261–267.

[29] M. Delvaux, A. Walcarius, and S. Demoustier-Champagne. "Bienzyme HRP-GOx-modified gold nanoelectrodes for the sensitive amperometric detection of glucose at low overpotentials". *Biosensors and Bioelectronics* 20 (2005), 1587–1594.

[30] I. Tokarev and S. Minko. "Stimuli-responsive hydrogel thin films". *Soft Matter* 5 (2009), 511–524.

[31] T. Khaleque, S. Abu-Salih, J. R. Saunders, and W. Moussa. "Experimental methods of actuation, characterization and prototyping of hydrogels for bioMEMS/NEMS applications". *Journal of Nanoscience and Nanotechnology* 11 (2011), 2470–2479.

[32] R. T. Kennedy, L. Huang, M. A. Atkinson, and P. Dush. "Amperometric monitoring of chemical secretion from individual pancreatic β-cells". *Analytical Chemistry* 65 (1993), 1882–1887.

4 Towards an adrenaline biosensor based on substrate-recycling amplification in combination with an enyzme logic gate (*Sensors and Actuators B: Chemical*, 237, (2016), 190–195)

D. Molinnus, M. Sorich, A. Bartz, P. Siegert, H. S. Willenberg, F. Lisdat, A. Poghossian, M. Keusgen and M. J. Schöning

Published in: *Sensors and Actuators B: Chemicals,* Vol. 237, (2016), 190–195.

Submitted: 2016-04-29; Accepted: 2016-06-10; Published: 2016-06-14

4.1 Abstract

An amperometric biosensor using a substrate-recycling principle was realized for the detection of low adrenaline concentrations (1 nM) by measurements in phosphate buffer and Ringer's solution at pH 6.5 and pH 7.4, respectively. In "proof-of-principle" experiments, a Boolean logic-gate principle has been applied to develop a digital adrenaline biosensor based on an enzyme **AND** logic gate. The obtained results demonstrate that the developed digital biosensor is capable for a rapid qualitative determination of the presence/absence of adrenaline in a YES/NO statement. Such digital biosensor could be used in clinical diagnostics for the control of a correct insertion of a catheter in the adrenal veins during adrenal venous-sampling procedure.

4.2 Introduction

Inadequate high aldosterone secretion by an aldosterone-producing adenoma is one of the most frequent causes of hypertension [1]. Patients with primary aldosteronism (PA) have considerably higher cardiovascular morbidity and mortality than patients with essential hypertension [2, 3]. Because of the therapeutical aspects, patients with PA undergo an adrenal venous-sampling (AVS) procedure for aldosteronoma localization and differential diagnosis. The technique used is invasive and complicated because adrenal veins are in general difficult to cannulate [4]. Since adrenaline concentration in adrenal veins is much higher ($\gtrsim$100 nM) than in the periphery ($\lesssim$1.2 nM) [5, 6], the concentration difference of adrenaline can be used as an indicator for the correct insertion and positioning of the catheter in the adrenal veins and successful AVS procedure [7, 8]. This requires a fast adrenaline detection method with a high sensitivity and low detection limit in the nanomolar concentration range.

Adrenaline belongs to the substance group of catecholamines. Several methods have been developed for the determination of catecholamines, mainly high-performance liquid chromatography, fluorescence spectroscopy, capillary electrophoresis, chemiluminescence [9–11] and electrochemical detection [12, 13]. Electrochemical detection using biosensors offer faster and more versatile analytical methods for clinical or biomedical applications. However, for very low analyte concentrations sensitivity is often not sufficient; consequently, different amplifications methods have been developed. Electrochemical recycling of the analyte between two closely arranged electrodes (preferentially interdigitated electrodes) allows a repeated participation of analyte molecules in the signal generation [14]. An alternative is chemical recycling by coupling a chemical reaction to the electrochemical detection reaction [15]. With the application of a proper biological molecule the sensor's selectivity and sensitivity can be further improved. This can be reached by combining the enzymatic reaction with an electrochemical conversion [16] or most efficiently by using two enzymes [17]. In biochemical recycling approach, the analyte is converted by one enzyme in a product which can be converted back to the original substrate by a second enzyme and thus amplifying the response by several orders of magnitude, as described in [18, 19]. Other examples are ultrasensitive sensors for the detection of phenolic substances ranging from micromolar to nanomolar levels which were developed by combining oxidase enzymes with a pyrroloquinoline quinone (PQQ)-dependent glucose dehydrogenase (GDH) [20, 21]. However, maximum sensitivity with the applied enzymes used in [20, 21] was obtained at pH 6.0, which limits the application of these biosensors for the detection of adrenaline in biological liquids such as blood.

The present study describes an adrenaline biosensor based on a laccase/PQQ-GDH bi-enzyme system and the substrate-recycling principle with optimal working characteristics in the pH range relevant for blood samples. In contrast to [20, 21], we utilize a genetically modified laccase variant, which is active in a broad pH range between pH 3.5 to pH 8.0 and stable in phosphate buffer solution (PBS) [22]. The sensor has been tested in PBS and Ringer's solution (RS), a substitute for blood plasma or other physiological liquids. In addition, in "proof-of-principle" experiments, the possibility of construction of a digital adrenaline biosensor based on a Boolean **AND** logic gate with

a YES/NO output has been demonstrated for the first time.

4.3 Experimental

4.3.1 Materials

Glutaraldehyde, bovine serum albumin (BSA), glycerol, $CaCl_2$ and the buffer components (monosodium phosphate and disodiumphosphate) were purchased from Sigma–Aldrich (USA). The laccase was provided by AB Enzymes GmbH (Germany). Glucose dehydrogenase (from *Acinetobacter calcoaceticus*) was provided by Roche Diagnostics (Germany). Cellulose acetate filter with a pore size of 0.2 μm was obtained from Sartorius Stedim Biotech GmbH (Germany). Adrenaline solution (1 mg/mL) was purchased from Sanofi–Aventis GmbH (Germany). PQQ was bought from Wako (Japan) and RS (8.6 g/L NaCl, 0.3 g/L KCl, 0.33 g/L $CaCl_2 \cdot 2H_2O$) was purchased from Bernburg (Germany).

4.3.2 Modification of the oxygen sensor with enzyme membrane

For the realization of the adrenaline biosensor, a commercial galvanic oxygen sensor (Atlas Scientific, USA) was modified by a bi-enzyme (laccase/GDH) membrane. Unlike the polarographic oxygen sensor, the galvanic sensor does not need a constant voltage applied to it. In the galvanic oxygen sensor, the electrodes are dissimilar enough to self-polarize and reduce oxygen molecules without an applied voltage. The enzyme membrane was prepared from the membrane cocktail consisting of 15 μL of the laccase (1.82 U/μL) solution, 15 μL of GDH (0.03 U/μL) solution combining 20 μM PQQ and 1 mM $CaCl_2$ [23], 60 μL of BSA (10 vol%) and 60 μL mixture of glutaraldehyde (2 vol%) and glycerol (10 vol%) solutions, respectively. All components were mixed with the resulting volumetric ratio of 1/2/2 (enzymes/BSA/glutaraldehyde-glycerol). Detail information for determination of the enzyme activity is described in [24, 25]. A total of 100 μL of the membrane cocktail was then dropped onto a Teflon block. After drying for 24 h at 4 °C, the enzyme membrane with a thickness of approximately 130 μm was fixed with the help of a cellulose acetate filter (dialysis membrane) and silicon rubber (TSE 399C, Momentive PerformanceMaterials, Switzerland) onto the high-density polyethylene (HDPE) layer of the oxygen sensor (see Fig. 4.1).

4.3.3 Measuring setup

For the electrochemical characterization, the adrenaline biosensor was connected to a potentiometer (2007 Multimeter, Keithley Instruments) and exposed to the solution containing different concentrations of adrenaline (see Fig. 4.1) The sensor measures the oxygen consumption due to the oxidation of adrenaline by the laccase. The produced output voltage (delivered by the galvanic oxygen sensor) is proportional to the oxygen consumption in the solution due to the enzymatic reaction. The sensitivity of the biosensor to adrenaline was investigated in both PBS and RS containing 20 mM glucose. Adrenaline solutions with various concentrations from 1 nM to 1 μM were prepared from a stock solution of 0.1 mM adrenaline, stored at 4 °C in the dark. At each adrenaline

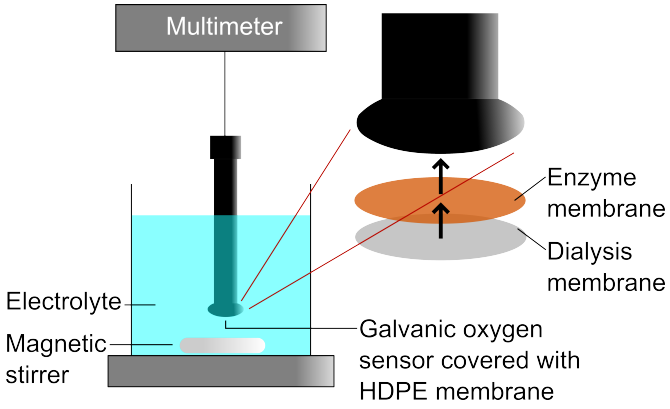

Fig. 4.1: Measurement setup for the detection of adrenaline (schematically).

concentration, the sensor signal was recorded for about 20 min. All experiments were carried out at room temperature under continuous stirring.

4.4 Results and discussion

4.4.1 Substrate-recycling principle

In order to measure low adrenaline concentrations (in the nanomolar concentration range), the substrate-recycling principle based on a bi-enzyme system (laccase/PQQ-GDH) has been proposed in [17, 20, 21]. PQQ acts here as a prostethic group for the GDH and binds via Ca^{2+} ions to the apoenzyme. Fig. 4.2 schematically shows the substrate-recycling principle for the enzymatic signal amplification of the adrenaline biosensor: In the presence of dissolved oxygen, the enzyme laccase oxidizes adrenaline to adrenochrome; in a second oxidation reaction, GDH transforms glucose into gluconolactone, while adrenochrome is reduced back to adrenaline, the substrate of the first reaction.

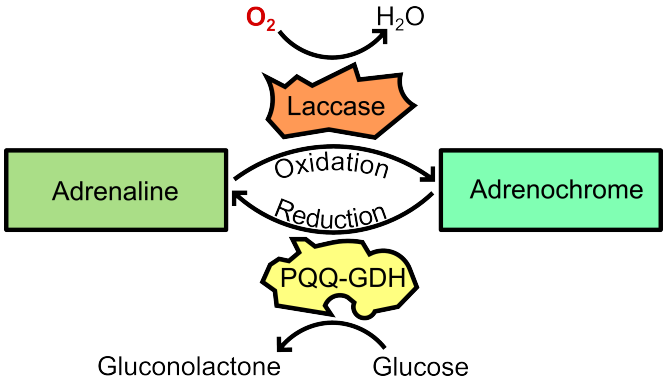

Fig. 4.2: Scheme of the substrate-recycling principle for the amplification of the adrenaline-sensor signal.

Thus, the combination of both enzymes laccase and GDH results in an amplification

of the adrenaline signal. The amount of dissolved oxygen consumed during the enzymatic reactions serves as measuring parameter to evaluate the adrenaline concentration and is detected by means of a galvanic oxygen sensor modified with the bi-enzyme (laccase/GDH) membrane.

4.4.2 Electrochemical sensor characterization

In experiments with the genetically modified laccase only, the maximum adrenaline sensitivity in PBS has been achieved at a pH value around pH 8.0 [26]. On the other hand, the highest activity of PQQ-GDH is known to be in a weakly acidic to neutral pH range [23, 27]. Hence, it has to be tested whether the combination of these two enzymes can result in an enzyme system with high sensitivity around the neutral pH range – as requested for the intended application (e.g., in adrenal veins). Therefore, the pH behavior of the adrenaline sensor was investigated in the range of pH 6.0 - pH 8.0. Fig. 4.3 summarizes the normalized adrenaline sensitivity of the developed biosensor, where the data points represent the adrenaline sensitivity averaged for three measurements in the concentration range of 300 - 1000 nM adrenaline. It can be clearly seen that high sensitivity can be obtained at pH values $\gtrsim$6.5. This verifies that the use of the genetically modified laccase with a different pH behavior is beneficial for a recycling system with PQQ-GDH making the sensor applicable at around neutral pH. The figure also illustrates that in PBS a decrease in response at pH 7.4 was found which did not occur when RS was used. This can be explained by the fact that phosphate ions can compete with Ca^{2+} ions necessary for the PQQ-binding in the GDH [28]. However, this does not limit the use of the system for the intended application under physiological conditions.

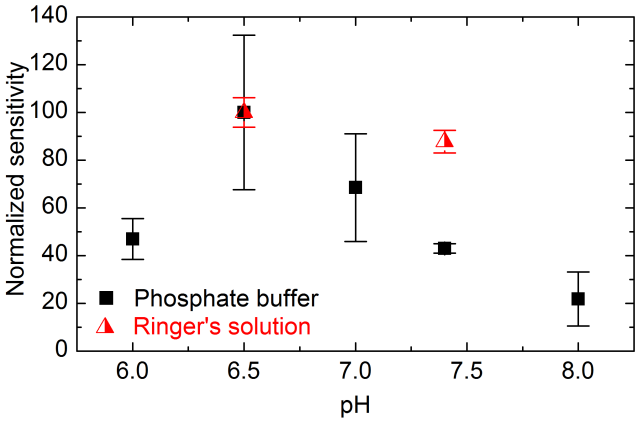

Fig. 4.3: Normalized sensitivity of the adrenaline biosensor with the enzymes laccase and GDH measured in PBS and RS, respectively, at different pH values.

In further experiments, the lower detection limit of the adrenaline biosensor has been studied in PBS as well as in RS with pH 6.5 at which the maximum sensitivity has been observed. Fig. 4.4a demonstrates the dynamic response of the developed adrenaline biosensor measured in both PBS and RS with different adrenaline concentrations (1 -

300 nM). As expected, the sensor signal measured in both solutions decreases with increasing adrenaline concentration due to the oxygen consumption during the oxidation reaction of adrenaline by the enzyme laccase. The inset in Fig. 4.4a depicts the calibration curves of the adrenaline biosensor in PBS and RS, respectively. The calibration curves were nearly linear in a wide concentration range of 5 - 100 nM adrenaline with a slope of -0.15 mV/nM and -0.12 mV/nM in PBS and RS, respectively. As can be recognized from the zoomed curves in Fig. 4.4b, the developed biosensor is capable for measurements of very low adrenaline concentrations with detection limits of about 1 nM.

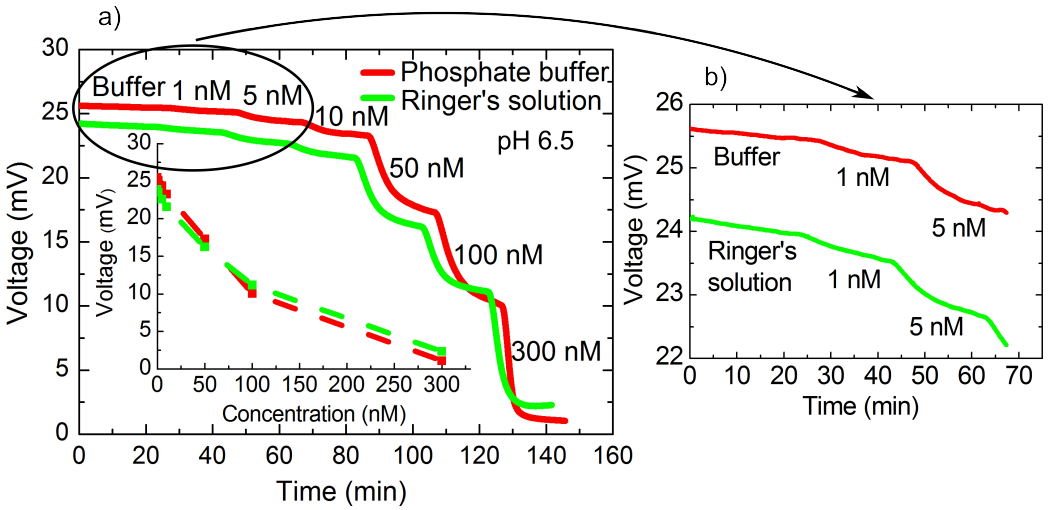

Fig. 4.4: a) Dynamic response of the adrenaline biosensor with laccase/PQQ-GDH measured in PBS as well as in RS of pH 6.5 (1 mM $CaCl_2$), containing different adrenaline concentrations of 1 - 300 nM; inset figure represents the calibration curves of the sensor; b) zoomed dynamic response for the evaluation of the lower detection limit.

In order to verify the applicability of the developed sensor at physiological pH conditions, additional measurements were performed in PBS as well as in RS at pH 7.4. The results of these experiments are compiled in Fig. 4.5 As expected, the adrenaline sensitivity measured in PBS of pH 7.4 was about two times smaller (-0.06 mV/nM in the linear range of 5 - 100 nM) than that of measured in PBS of pH 6.5. This is consistent with results shown in Fig. 4.3. On the other hand, the sensitivity of the adrenaline sensor measured in RS at pH 7.4 (-0.11 mV/nM) was about the same as in RS at pH 6.5. This is a result of the better match of the pH optima of laccase and PQQ-GDH used in this study compared to previous developments [20] and the absence of inhibiting ions in the RS.

In comparison to reported detection limits of 293 nM [12] and 0.5 nM [20] in buffer solution of pH 6.5 and pH 6.0, respectively, the developed biosensor provides a detectable signal at physiological level of pH 7.4 even at an adrenaline concentration of 1 nM (see Fig. 4.5b). These experiments underline the possibility of application of the developed adrenaline biosensor in biological liquids, in particular, in blood samples.

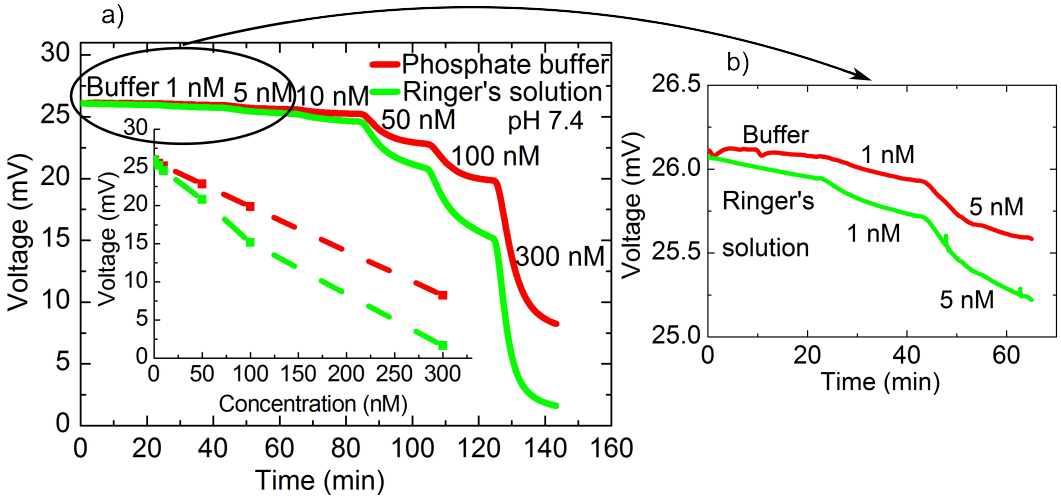

Fig. 4.5: a) Dynamic response of the adrenaline biosensor with laccase/PQQ-GDH measured in PBS as well as in RS of pH 7.4 (1 mM $CaCl_2$), containing different adrenaline concentrations of 1 - 300 nM; inset figure represents the calibration curves of the sensor; b) zoomed dynamic response for the evaluation of the lower detection limit.

4.4.3 Digital adrenaline biosensor based on AND logic gate

Typically, biosensors provide quantitative information on the concentration of analytes. Recent advances in molecular logic gates [29–37] have opened opportunities for development of so-called digital biosensors. In contrary to quantitative measurements with conventional biosensors, digital biosensors enable processing of multiple biochemical input signals according to Boolean logic and finally, generate qualitative binary output signals in the form of YES/NO decisions [38–40]. The potential of this approach for biomedical applications has recently been demonstrated by introducing digital biosensors for diagnostic and forensic applications [41, 42]. The digital biosensor concept could be beneficial when there is no need for precise, quantitative measurements of biomarker concentrations, but rather a rapid qualitative answer on the presence (or elevated concentration)/absence of a biomarker is required (e.g., directly during a surgical operation). In the following, preliminary results on the development of such digital adrenaline biosensor based on the substrate-recycling principle in combination with enzyme logic gates with YES/NO output are presented.

As first "proof-of-principle", such digital adrenaline biosensor can be represented as two concatenated enzyme-based **AND** logic gates (**AND 1** and **AND 2**), containing two enzymes: laccase and GDH (see Fig. 4.6). In order to digitalize chemical processes, the reacting species are considered as logic input signals reflecting two levels of their concentrations. The presence of the particular analytes in the solution corresponds to the input signal **1**, while absence of analytes is considered as the input signal **0**. The enzyme-based **AND 1** gate is activated by two chemical input signals: adrenaline (input 1) and dissolved oxygen (input 2). In the presence of dissolved oxygen, the enzyme laccase oxidizes adrenaline to adrenochrome. At low adrenaline concentrations,

the amount of dissolved oxygen consumed during enzymatic reactions is small. As a consequence, small changes in sensor signal can be expected as schematically shown in Fig. 4.6 (lower diagram I). The second **AND 2** gate is activated by glucose (input 3) and adrenochrome (product of adrenaline-oxidation reaction, input 4) and serves for amplification of the sensor signal. During the second oxidation reaction, PQQ-GDH transforms glucose into gluconolactone, while adrenochrome is reduced back to adrenaline, the substrate of the first reaction (which can be started again). Due to the substrate recycling, the consumption of dissolved oxygen is thus increased, resulting in a high sensor signal change (see diagram II). The reaction cascade cannot start if adrenaline or/and dissolved oxygen is missing, and the substrate-recycling reaction cannot be completed if glucose is missing, all resulting in a logic output signal **0**.

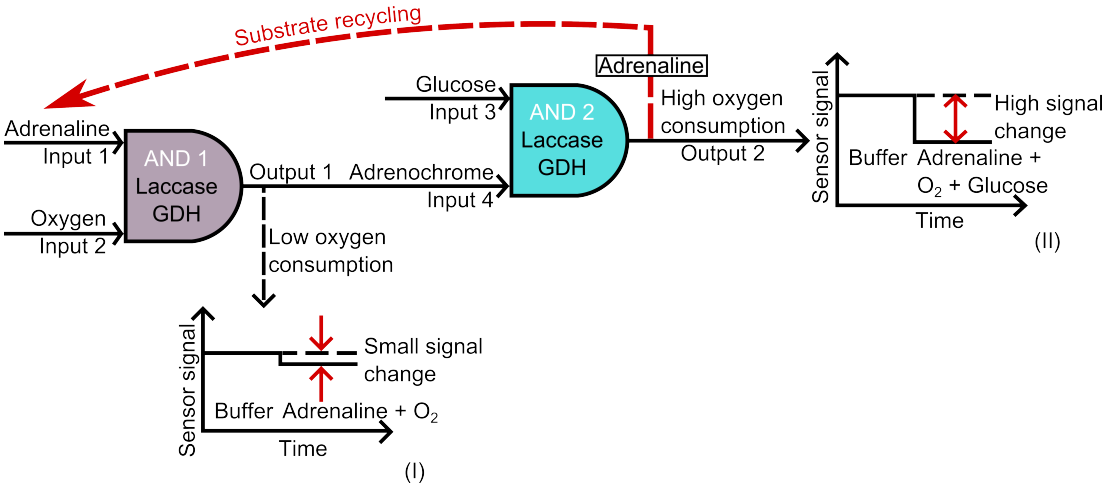

Fig. 4.6: Schematic of a digital adrenaline biosensor based on substrate-recycling principle. The digital biosensor consists of two concatenated enzyme-based **AND** logic gates (**AND 1** and **AND 2**) containing two enzymes (laccase and GDH). The expected changes in sensor signal by low and high oxygen consumption are added, too (see schematic diagrams I and II).

Fig. 4.7 illustrates the normalized output signal of the digital adrenaline biosensor based on the substrate-recycling principle. In this experiment, the developed adrenaline biosensor with the immobilized laccase/PQQ-GDH was consecutively exposed to i) PBS with dissolved oxygen (with a concentration obtained in the solution under equilibrium with air), ii) PBS containing dissolved oxygen and glucose, iii) PBS containing adrenaline and dissolved oxygen, iv) PBS containing adrenaline, glucose and dissolved oxygen. These experiments allow not only the functional testing of the dissolved oxygen sensor, but also to study the sensor signal in solutions containing different combinations of input analytes (adrenaline, dissolved oxygen and glucose).

As can be seen, the highest output was recorded in solution containing dissolved oxygen, thus verifying correct functioning of the galvanic dissolved oxygen sensor. In the absence of adrenaline in the solution, the addition of glucose does not affect the sensor output, because no oxidation reaction takes place. As expected, a small signal output has been observed in the solution containing adrenaline and dissolved oxygen; this case corresponds to the adrenaline sensor without substrate-recycling amplification. On the

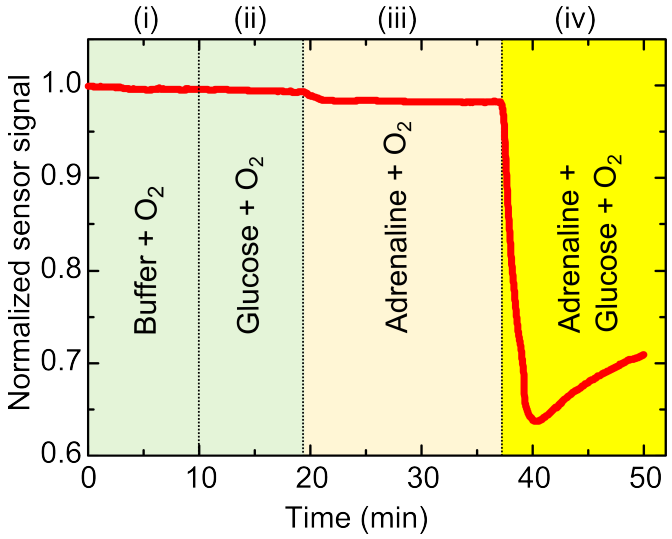

Fig. 4.7: Normalized output signal of the digital adrenaline biosensor recorded in PBS (pH 6.5) containing different combinations of input analytes (adrenaline (1 μM), dissolved oxygen (air saturation) and glucose (20 mM)).

other hand, due to the substrate-recycling reaction and high oxygen consumption, a high signal change of about 35% has been recorded in the presence of adrenaline, dissolved oxygen and glucose in the solution. Thus, only in the presence of these three analytes in the solution, the cascade of enzymatic reactions is completed, resulting in a signal amplification and logic output **1**. Hence, the developed digital sensor could be able to distinguish elevated adrenaline concentrations in form of a YES/NO output as an indicator for the correct insertion and positioning of the catheter in the adrenal veins.

It is worth mentioning that in the described model study, the logic **0**/**1** values of the chemical input signals correspond to the complete absence/presence of the analyte or species contributing to the biochemical reactions. For practical applications, the logic **0** and **1** chemical input signals should be considered as physiologically normal (~1 nM for adrenaline) and pathologically elevated (or abnormal exceeding a predefined threshold taken from clinical data) concentrations, respectively, that requires a calibration of digital biosensors. Here, the advantage of differential measurements in the adrenal and femoral veins can be exploited in order to detect the increase in adrenaline concentration in adrenal veins.

4.5 Conclusions

Detection of adrenaline in biological liquids, particularly in blood samples, is of high interest in clinical diagnostics. In this study, an amperometric adrenaline biosensor based on an improved laccase/PQQ-GDH bi-enzyme system has been developed and tested in both PBS and RS with different pH values. A lower detection limit of about 1 nM adrenaline has been achieved at physiological pH values by using the modified enzyme laccase (exhibiting a high activity in a wide pH range) in combination with

PQQ-GDH and the substrate-recycling principle for signal amplification.

In addition, in a "proof-of-concept" experiment, the possibility of creation of a digital adrenaline biosensor based on two concatenated enzyme-based **AND** logic gates has been demonstrated. The important feature of those digital biosensors is their rapid qualitative analysis in response to the presence/absence of various combinations of analytes or biomarkers. In the future, such digital adrenaline biosensor could be used in clinical diagnostics as a novel tool for the control of the correct insertion and positioning of the catheter in the adrenal veins during AVS procedure. It will be able to distinguish the adrenaline concentration in adrenal veins and in the periphery, and finally generate a rapid qualitative output signal on the pathophysiological/physiological concentrations in the form of a binary YES/NO.

Future works will be directed to test functioning of the digital adrenaline biosensor in real blood samples considering also cross-selectivity towards different catecholamines.

Acknowledgments

This research is supported by a Ph.D. scholarship from FH Aachen. The authors would like to thank AB Enzymes for providing a fungal laccase and M. Bäcker for valuable discussions.

References

[1] J. W. Funder, R. M. Carey, C. Fardella, C. E. Gomez-Sanchez, F. Mantero, M. Stowasser, W. F. Young Jr., and V. M. Montori. "Case detection, diagnosis, and treatment of patients with primary aldosteronism: an endocrine society clinical practice guideline". *Journal of Clinical Endocrinology and Metabolism* 93 (2008), 3266–3281.

[2] P. Mulatero, S. Monticone, C. Bertello, A. Viola, D. Tizzani, A. Iannaccone, V. Crudo, J. Burrello, A. Milan, F. Rabbia, and F. Veglio. "Long-term cardio- and cerebrovascular events in patients with primary aldosteronism". *Journal of Clinical Endocrinology and Metabolism* 98 (2013), 4826–4833.

[3] C. Catena, G. Colussi, E. Nadalini, A. Chiuch, S. Baroselli, R. Lapenna, and L. A. Sechi. "Cardiovascular outcomes in patients with primary aldosteronism after treatment". *Archives of Internal Medicine* 168 (2008), 80–85.

[4] W. F. Young and A. W. Stanson. "What are the keys to successful adrenal venous sampling (AVS) in patients with primary aldosteronism?" *Clinical Endocrinolody* 70 (2009), 14–17.

[5] P. Collste, B. Brismar, A. Alveryd, I. Björkhem, C. Hårdstedt, L. Svensson, and J. Ostman. "The catecholamine concentration in central veins of hypertensive patients - an aid not without problems in locating phaeochromocytoma". *Acta Chirurgica Scandinavica, Supplementum* 530 (1986), 67–71.

[6] E. L. Bravo, R. C. Tarazi, F. M. Fouad, D. G. Vidt, and R. W. Gifford. "Clonidine-suppression test: A useful aid in the diagnosis of pheochromocytoma". *New England Journal of Medicine* 305 (1981), 623–626.

[7] G. P. Rossi, R. J. Auchus, M. Brown, J. W. M. Lenders, M. Naruse, P. F. Plouin, F. Satoh, and W. F. Young. "An expert consensus statement on use of adrenal vein sampling for the subtyping of primary aldosteronism". *Hypertension* 63 (2013), 151–160.

[8] T. Dekkers, J. Deinum, L. J. Schultzekool, D. Blondin, O. Vonend, A.R.R.M. Hermus, M. Peitzsch, L. C. Rump, G. Antoch, F.C.G.J. Sweep, S. R. Bornstein, J. W. M. Lenders, H. S. Willenberg, and G. Eisenhofer. "Plasma metanephrine for assessing the selectivity of adrenal venous sampling". *Hypertension* 62 (2013), 1152–1157.

[9] E. Nalewajko, A. Wiszowata, and A. Kojło. "Determination of catecholamines by flow-injection analysis and high-performance liquid chromatography with chemiluminescence detection". *Journal of Pharmaceutical and Biomedical Analysis* 43 (2007), 1673–1681.

[10] S. García Palop, A. Mellado Romero, and J. Martínez Calatayud. "Oxidation of adrenaline and noradrenaline by solved molecular oxygen in a FIA assembly". *Journal of Pharmaceutical and Biomedical Analysis* 27 (2002), 1017–1025.

[11] S. Wei, G. Song, and J.-M. Lin. "Separation and determination of norepinephrine, epinephrine and isoprinaline enantiomers by capillary electrophoresis in pharmaceutical formulation and human serum". *Journal of Pharmaceutical and Biomedical Analysis* 1098 (2005), 166–171.

[12] D. Brondani, C. W. Scheeren, J. Dupont, and I. C. Vieira. "Biosensor based on platinum nanoparticles dispersed in ionic liquid and laccase for determination of adrenaline". *Sensors and Actuators B: Chemical* 140 (2009), 252–259.

[13] T. J. Castilho, M. d. P. Sotomayor, and L. T. Kunota. "Amperometric biosensor based on horseradish peroxidase for biogenic amine determinations in biological samples". *Journal of Pharmaceutical and Biomedical Analysis* 37 (2005), 785–791.

[14] F. W. Scheller, C. G. Bauer, A. Makower, U. Wollenberger, A. Warsinke, and F. F. Bier. "Coupling of immunoassays with enzymatic recycling electrodes". *Analytical Letters* 34 (2001), 1233–1245.

[15] X. Yang, G. Johansson, D. Pfeiffer, and F. W. Scheller. "Enzyme electrodes for ADP/ATP with enhanced sensitivity due to chemical amplification and intermediate accumulation". *Electroanalysis* 3 (1991), 659–663.

[16] F. Lisdat, U. Wollenberger, M. Paeschke, and F. W. Scheller. "Sensitive catecholamine measurement using a monoenzymatic recycling system". *Analytica Chimica Acta* 368 (1998), 233–241.

[17] A. L. Ghindilis, A. Makower, C. G. Bauer, F. F. Bier, and F. W. Scheller. "Determination of *p*-aminophenol and catecholamines at picomolar concentrations based on recycling enzyme amplification". *Analytica Chimica Acta* 304 (1995), 25–31.

[18] F. W. Scheller, N. Siegbahn, B. Danielsson, and K. Mosbach. "High-sensitivity enzyme thermistor determination of L-lactate by substrate recycling". *Analytical Chemistry* 57 (1985), 1740–1743.

[19] D. Cybulski, K. B. Male, J. M. Scharer, M. Moo-Young, and J. H. T. Luong. "Substrate recycling scheme for tetrachloro-*p*-benzoquinone using bilirubin oxidase and NADH: Application for pentachlorophenol assay". *Environmental Science and Technology* 33 (1999), 796–800.

[20] F. Lisdat, U. Wollenberger, A. Makower, H. Hörtnagl, D. Pfeiffer, and F. W. Scheller. "Catecholamine detection using enzymatic amplification". *Biosensors and Bioelectronics* 12 (1997), 1199–1211.

[21] J. Szeponik, B. Möller, D. Pfeiffer, F. Lisdat, U. Wollenberger, A. Makower, and F. W. Scheller. "Ultrasensitive bienzyme sensor for adrenaline". *Biosensors and Bioelectronics* 12 (1997), 947–952.

[22] M. Paloheimo, L. Valtakari, T. Puranen, K. Kruus, J. Kallio, A. Mantyla, R. Fagerstrom, P. Ojapalo, and J. Vehmaanpera. "Laccase enzyme and use thereof". US7927849 B2. 2011.

[23] V. Laurinavicius, J. Razumiene, A. Ramanavicius, and A. D. Ryabov. "Wiring of PQQ-dehydrogenases". *Biosensors and Bioelectronics* 20 (2004), 1217–1222.

[24] K.-S. Shin and Y.-J. Lee. "Purification and characterization of a new member of the laccase family from the white-rot basidiomycete *Coriolus hirsutus*". *Archives of Biochemistry and Biophysics* 384 (2000), 109–115.

[25] A. J. J. Olsthoorn and J. A. Duine. "Production, characterization, and reconstitution of recombinant quinoprotein glucose dehydrogenase (soluble type; EC 1.1.99.17) apoenzyme of *Acinetobacter calcoaceticus*". *Archives of Biochemistry and Biophysics* 336 (1996), 42–48.

[26] D. Molinnus, A. Bartz, M. Bäcker, P. Siegert, H. Willenberg, A. Poghossian, M. Keusgen, and M. J. Schöning. "Detection of adrenaline based on substrate recycling amplification". *Procedia Engineering* 120 (2015), 540–543.

[27] A. J. J. Olsthoorn and J. A. Duine. "On the mechanism and specificity of soluble, quinoprotein glucose dehydrogenase in the oxidation of aldose sugars". *Biochemistry* 37 (1998), 13854–13861.

[28] B. Kosar-Grašić, B. Purgarić, and H. Füredi-Milhofer. "Precipitation of calcium phosphates from electrolyte solutions—VI The precipitation diagram of calcium hydrogen phosphate". *Journal of Inorganic and Nuclear Chemistry* 40 (1978), 1877–1880.

[29] E. Katz. *Biomolecular Information Processing*. Weinheim, Germany: Wiley-VCH Verlag GmbH & Co. KGaA, 2012.

[30] D. Molinnus, M. Bäcker, H. Iken, A. Poghossian, M. Keusgen, and M. J. Schöning. "Concept for a biomolecular logic chip with an integrated sensor and actuator function". *Physica Status Solidi A* 212 (2015), 1382–1388.

[31] A. Poghossian, E. Katz, and M. J. Schöning. "Enzyme logic AND-Reset and OR-Reset gates based on a field-effect electronic transducer modified with multi-enzyme membrane". *Chemical Communications* 51 (2015), 6564–6567.

[32] F. Moseley, J. Halámek, F. Kramer, A. Poghossian, M. J. Schöning, and E. Katz. "An enzyme-based reversible CNOT logic gate realized in a flow system". *The Analyst* 139 (2014), 1839–1842.

[33] A. Poghossian, K. Malzahn, M. H. Abouzar, P. Mehndiratta, E. Katz, and M. J. Schöning. "Integration of biomolecular logic gates with field-effect transducers". *Electrochimica Acta* 56 (2011), 9661–9665.

[34] K. Szaciłowski. "Digital information processing in molecular systems". *Chemical Reviews* 108 (2008), 3481–3548.

[35] E. Katz and V. Privman. "Enzyme-based logic systems for information processing". *Chemical Society Reviews* 39 (2010), 1835–1857.

[36] M. Pita, M. Krämer, J. Zhou, A. Poghossian, M. J. Schöning, V. M. Fernández, and E. Katz. "Optoelectronic properties of nanostructured ensembles controlled by biomolecular logic systems". *ACS Nano* 2 (2008), 2160–2166.

[37] E. Katz. "Biocomputing - tools, aims, perspectives". *Current Opinion in Biotechnology* 34 (2015), 202–208.

[38] E. Katz, J. Wang, M. Privman, and J. Halámek. "Multianalyte digital enzyme biosensors with built-in Boolean logic". *Analytical Chemistry* 84 (2012), 5463–5469.

[39] J. Wang and E. Katz. "Digital biosensors with built-in logic for biomedical applications - biosensors based on a biocomputing concept". *Analytical and Bioanalytical Chemistry* 398 (2010), 1591–1603.

[40] Y.-H. Lai, S.-C. Sun, and M.-C. Chuang. "Biosensors with built-in biomolecular logic gates for practical applications". *Biosensors* 4 (2014), 273–300.

[41] K. M. Manesh, J. Halámek, M. Pita, J. Zhou, T. K. Tam, P. Santhosh, M.-C. Chuang, J. R. Windmiller, D. Abidin, E. Katz, and J. Wang. "Enzyme logic gates for the digital analysis of physiological level upon injury". *Biosensors and Bioelectronics* 24 (2009), 3569–3574.

[42] F. Kramer, L. Halámková, A. Poghossian, M. J. Schöning, E. Katz, and J. Halámek. "Biocatalytic analysis of biomarkers for forensic identification of ethnicity between Caucasian and African American groups". *The Analyst* 138 (2013), 6251–6257.

5 Detection of adrenaline in blood plasma as biomarker for adrenal venous sampling (*Electroanalysis,* 30, 5 (2018), 937–942)

D. Molinnus, G. Hardt, P. Siegert, H. S. Willenberg, A. Poghossian, M. Keusgen and M. J. Schöning

Published in: *Electroanalysis,* Vol. 30, 5 (2018), 937–942.

Submitted: 2018-01-09; Accepted: 2018-02-01; Published: 2018-02-14

5.1 Abstract

An amperometric bi-enzyme biosensor based on substrate-recycling principle for the amplification of the sensor signal has been developed for the detection of adrenaline in blood. Adrenaline can be used as biomarker verifying successful adrenal venous-sampling procedure. The adrenaline biosensor has been realized via modification of a galvanic oxygen sensor with a bi-enzyme membrane combining a genetically modified laccase and a pyrroloquinoline quinone-dependent glucose dehydrogenase. The measurement conditions such as pH value and temperature were optimized to enhance the sensor performance. A high sensitivity and a low detection limit of about 0.5 - 1 nM adrenaline have been achieved in phosphate buffer at pH 7.4, relevant for measurements in blood samples. The sensitivity of the biosensor to other catecholamines such as noradrenaline, dopamine and dobutamine has been studied. Finally, the sensor has been successfully applied for the detection of adrenaline in human blood plasma.

5.2 Introduction

Primary aldosteronism (PA) is an adrenal disease of salt retention and the most frequent cause of secondary hypertension. Patients with PA have a significant higher cardiovascular morbidity and mortality risk than patients with essential hypertension, even when they are selected to have comparable blood-pressure values [1, 2]. For subtype diagnosis of PA, adrenal venous sampling (AVS) is the method of choice. Success of AVS is dependent on the accuracy and speed of catheter insertion into the adrenal veins. Rapid assessment of cortisol is used to prove a correct AVS procedure. However, the determination of cortisol is hampered by its binding to protein and long biological half-life. In addition, the determination of cortisol by an immunoassay takes relatively long [3]. Alternatively, adrenaline (epinephrine) can serve as biomarker, because of its higher concentration difference in adrenal ($\gtrsim$100 nM; sometimes up to 1000 nM) and peripheral blood (1 - 5 nM) [4, 5]. An adrenaline concentration of about 100 nM or more would be a safe indication of correct catheter position in adrenal veins, thereby accelerating the medical examination and preventing unnecessary exposure of the patient to X-rays. On the other hand, if the adrenaline concentration in adrenal venous blood is significantly lower than 100 nM, the catheter tip has to be repositioned during AVS procedure.

At present, numerous sensors have been proposed for the detection of adrenaline by using e.g., an enzyme laccase-modified oxygen sensor with a lower detection limit (LDL) of 3 μM [6], screen-printed electrodes modified with a thin iridium oxide film capable for the detection of adrenaline down to 30 nM [7] or carbon fiber microelectrodes having a LDL of about 50 nM adrenaline [8]. However, their application to support medical examinations is limited due to insufficient lower detection limit. For medical application of the adrenaline biosensor to support AVS procedure, a sensor with a high sensitivity and a low detection limit (in the nanomolar concentration range) is required. Hence, different signal-amplification principles by applying substrate recycling have been proposed to improve the biosensor performance [9–11], utilizing a bi-enzyme system (laccase/PQQ-GHD). As shown in Fig. 5.1, in a first reaction, adrenaline is oxidized by the laccase under oxygen consumption to adrenochrome. This oxygen consumption is measured by the galvanic oxygen sensor. Then, glucose is converted into gluconolactone, while adrenochrome is reduced back to adrenaline (i.e., original product) catalyzed by the PQQ-GDH [12]. The second reaction step is oxygen-independent. Thus, by applying the bi-enzyme laccase and PQQ-GDH system, adrenaline can be recycled (up to several 1000 times), resulting in a higher oxygen consumption and an amplification of the adrenaline biosensor signal. Thus, by applying this measurement principle, the lower detection limit can significantly be improved. The resulting output voltage delivered by the galvanic oxygen sensor is related to the oxygen consumption due to the oxidation of adrenaline by the laccase and is proportional to the adrenaline concentration in solution.

It has been demonstrated that with such signal amplification methods a LDL in the low nanomolar or even subnanomolar concentration range can be achieved [13–17]. For instance, enzymatic amplification was applied to develop an ultrasensitive adrenaline biosensor with detection limit of about 0.5 nM [10]. Recently, we introduced an amperometric laccase/PQQ-GDH bi-enzyme adrenaline biosensor with LDL of 1 nM using

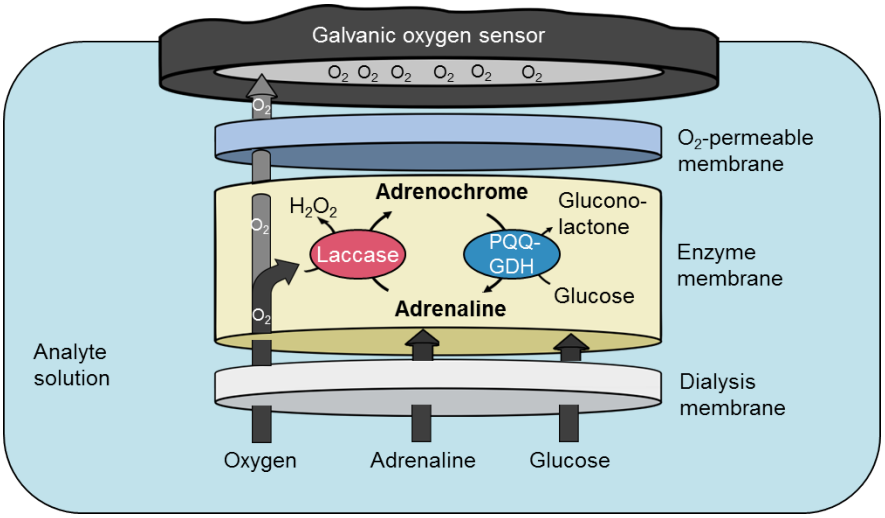

Fig. 5.1: Schematic of the biosensor set-up for the detection of adrenaline based on substrate-recycling principle for sensor-signal amplification employing the enzymes laccase for the oxidation of adrenaline to adrenochrome and PQQ-GDH for the reduction of adrenochrome to adrenaline.

substrate-recycling principle and a commercial oxygen sensor [18]. However, maximum sensitivity and LDL values of above described biosensor based on substrate-amplification principle were achieved at pH 6 - 6.5, that could also limit its application in biomedicine, in particular for adrenaline detection directly in untreated whole blood samples or in blood plasma.

In the present work, we report on a high-sensitive and low-detection limit bi-enzyme adrenaline biosensor based on substrate-recycling amplification principle using a genetically modified laccase variant and a PQQ-GDH both having optimum activity in pH range relevant for blood samples [19, 20]. The biosensor has been tested in phosphate buffer solution (PBS) with different pH values and adrenaline concentrations at various temperatures, in order to find out optimal measurement conditions for enhanced sensor performance. In addition, the sensitivity of the biosensor to other catecholamine such as noradrenaline, dopamine and dobutamine has been studied. The results of preliminary experiments on adrenaline detection in blood plasma have been presented, too.

5.3 Experimental

5.3.1 Materials

The genetically modified laccase ($27\,U/\mathrm{mg}$) was provided by AB Enzymes GmbH (Germany) [19] and quinoprotein GDH ($760\,U/\mathrm{mg}$, E.C. 1.1.5.2, from microorganism not specified by the company) was bought from Sorachim SA (Switzerland) [20]. PQQ was purchased from Wako (Japan). Glutaraldehyde, bovine serum albumin (BSA), glycerol, $CaCl_2$ and the PBS buffer components (monosodium phosphate and disodium phosphate) were obtained from Sigma-Aldrich (USA). Cellulose acetate filter (pore size: $0.2\,\mu\mathrm{m}$) was bought from Sartorius Stedim Biotech (Germany).

Adrenaline solution (1 mg/mL) was purchased from Infectopharm (Germany), noradrenaline (1 mg/mL) was bought from Sanofi (Germany), dopamine (250 mg/mL) was acquired from Carinopharm (Germany) and dobutamine (250 mg/50 mL) from Fresenius (Germany). Adrenaline, noradrenaline, dopamine and dobutamine stock solutions of 1 μM and 100 μM were freshly prepared and stored at 4 °C in the dark.

5.3.2 Preparation of the enzyme membrane and measuring set-up

The adrenaline biosensor was prepared by means of modification of a commercial galvanic oxygen sensor (Atlas Scientific, USA) with a bi-enzyme membrane composed of a laccase/PQQ-GDH system. In contrast to [18], the GDH used in this work has a higher activity, is stable in the pH range of pH 3.5 - 8.5 with a maximum activity in PBS at pH 7.0 and optimum temperature range of 30 - 37 °C [20]. For the preparation of the bi-enzyme membrane, a suspension consisting of 15 μL laccase (2.21 U/μL) solution, 15 μL of GDH (1.18 U/μL) solution solved in PBS (10 mM, pH 7.4), together with 20 μM PQQ, 1 mM $CaCl_2$ [21], 60 μL of BSA (10 vol%) and 60 μL of a glutaraldehyde (2 vol%) / glycerol (10 vol%) solution was prepared. 100 μL of the mixture was placed onto a Teflon block to dry at room temperature. The membranes were stored at 4 °C before using. For the preparation of the adrenaline biosensor, the membrane was mounted between a cellulose acetate filter and an O_2-permeable, high-density polyethylene (HDPE) layer of the commercial oxygen sensor (see Fig. 5.1). Additionally, the cellulose acetate filter was fixed with silicon rubber (RTV 118Q, Momentive Performance Materials, Switzerland). Between the measurements, the sensor has been stored in PBS (10 mM, pH 7.4) containing 20 μM PQQ and 1 mM $CaCl_2$.

The principle of the galvanic oxygen sensor is the use of carefully selected electrode materials to realize a self-polarization sufficient for electrochemical reduction of oxygen at the working electrode. This causes a current depending on the oxygen concentration in the analyte solution, which is converted into an output voltage. The main advantage of this galvanic principle is that there is no need for an external source. The commercial galvanic oxygen sensor used in this study consists of a zinc rod which serves as anode submerged in an electrolyte. The cathode is a silver disk which is covered by the HDPE membrane. For more details about the sensor, see [22]. Electrochemical experiments were carried out by connecting the adrenaline bi-enzyme biosensor to a potentiometer (2007 Multimeter, Keithley Instruments). The biosensor was exposed to the solution containing different concentrations of adrenaline or other catecholamines and the output signal was recorded for 20 min under continuous stirring. In all experiments, the analyte solution contained 20 mM glucose that is a sufficient amount to ensure the recycling process [17].

5.4 Results and discussions

It is known that the pH value and temperature of the solution may strongly influence the enzyme activity and thus, also the biosensor performance. Therefore, before measurements in blood plasma, the adrenaline biosensor was studied in PBS at different

pH values and temperatures in order to determine optimal measurement conditions for further characterization in terms of sensitivity, detection limit and stability.

5.4.1 Determination of optimum pH and temperature

The genetically modified laccase used in this work is stable in a broad pH range [19] and the mono-enzyme adrenaline biosensor using only laccase has a pH optimum at pH 8.0 as experimentally determined in [6]. On the other hand, the used GDH has a maximum activity at pH 7.0 [20]. From the point of view of biosensor characteristics and its application, more important is the optimum pH (further referred as pHs) at which the sensor modified with the bi-enzyme membrane demonstrates maximum sensitivity. This pHs could differ from the pH optimum of the particular enzymes and has to be examined. Intuitively, it can be expected, that pHs of the bi-enzyme recycling adrenaline biosensor could be between the pH optimum for laccase and GDH, respectively.

Fig. 5.2 (top) depicts exemplarily the calibration curves of the bi-enzyme adrenaline biosensor measured in PBS with different pH values from pH 6.5 to pH 8.5 at room temperature. At each pH value, the sensor signal was recorded for different adrenaline concentrations in PBS between 5 nM and 100 nM. The dependence of the adrenaline sensitivity on the pH value is shown in Fig. 5.2 (bottom), where each data point represents the average sensitivity evaluated from the twice-repeated series of measurements with two biosensors. In contrast to [18], in this study, a maximum sensitivity (0.17 mV/nM) was observed at pH 7.4. Moreover, the adrenaline sensitivity at pH 7.4 was three times higher than that of reported (0.06 mV/nM in the adrenaline concentration range of 5 - 100 nM, at pH 7.4) in [18]. The sensitivity is decreased down to about 0.05 mV/nM and 0.03 mV/nM at pH values of 6.5 and 8.5, respectively. These results demonstrate that the developed adrenaline biosensor could be beneficial for the application in biological liquids at physiological pH level of pH 7.4.

For future application of the adrenaline biosensor to support AVS procedure, it should be also able to work in real blood samples at temperatures up to 37 °C. Generally, fungal laccases are known to be thermally unstable [19]. However, the laccase variant used in this work is stable at temperatures lower than 50 °C with an optimum temperature of 37 °C. The applied PQQ-GDH has its optimum activity at temperatures of about 30 - 37 °C [20]. To determine working temperature of the adrenaline biosensor with the bi-enzyme (laccase/PQQ/GDH) membrane, the temperature behavior of the sensor has been studied in PBS (pH_s 7.4, containing different concentrations of adrenaline from 5 nM to 100 nM) in a temperature range from 20 °C to 35 °C. For better controlling of the temperature, a Peltier tempering unit (Lauda-Brinkman, LP, USA) with an integrated Pt 1000 and a magnetic stirrer has been applied. At each adjusted temperature, the sensor signal was measured at varius adrenaline concentrations and then, the adrenaline sensitivity was evaluated. All measurements were repeated twice with two biosensors. The highest sensitivity of the biosensor to adrenaline was observed at a temperature of 30 °C. At lower and higher temperatures, the sensitivity is strongly decreasing to less than 40% of the maximum sensitivity (data not shown).

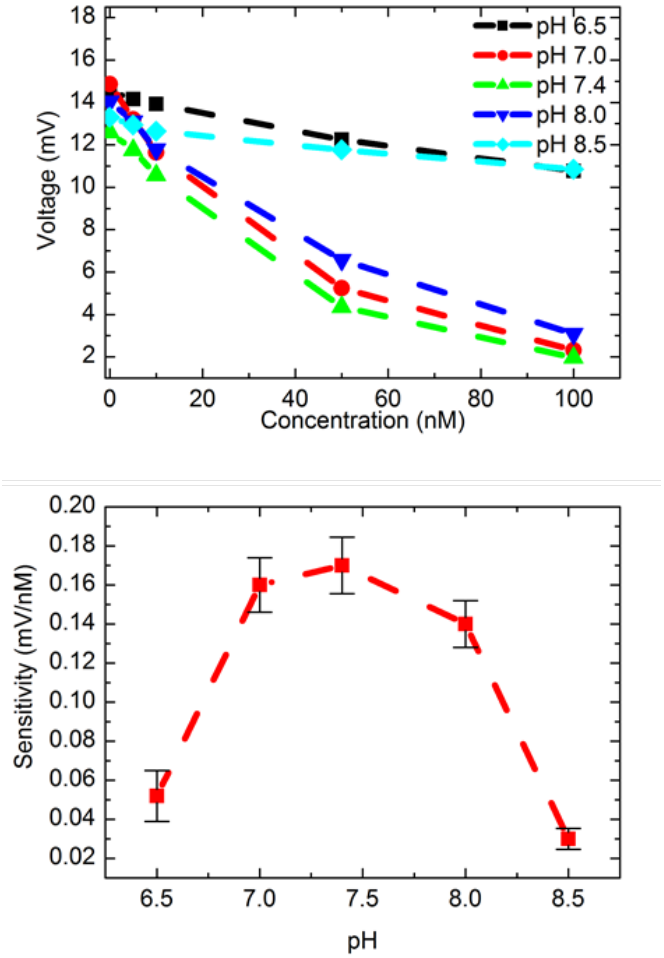

Fig. 5.2: (Top) Calibration curves of the adrenaline biosensor modified with the enzymes laccase and PQQ-GDH recorded in PBS (pH 6.5 - pH 8.5) with different adrenaline concentrations from 5 nM to 100 nM at room temperature. (Bottom) Dependence of the average adrenaline sensitivity (set of two series of measurements with two biosensors each) on the pH value of the solution.

5.4.2 Detection limit and long-term stability

In further experiments, three adrenaline biosensors were characterized in PBS at optimal measuring conditions (pH 7.4, and 30 °C) in terms of lower detection limit and long-term stability. An example of the dynamic response of the sensor in PBS containing different adrenaline concentrations from 1 nM to 100 nM is shown in Fig. 5.3 with the corresponding calibration curve (inset graph). As expected, with increasing adrenaline concentration, the sensor signal is decreased due to the oxygen consumption during the oxidation reaction of adrenaline catalyzed by the enzyme laccase. The adrenaline sensitivity was about 0.67 mV/nM in the linear range of 1 - 10 nM adrenaline. As can be seen, even at an adrenaline concentration of 1 nM, the biosensor provides a detectable signal of about 1.0 mV (some biosensors were able to detect even 0.5 nM adrenaline).

Thus, the developed biosensor is capable for adrenaline detection in the low nanomolar and even subnanomolar concentration range. The LDL by using a signal-to-noise ratio of S/N = 3 [23] was estimated to be 0.1 nM.

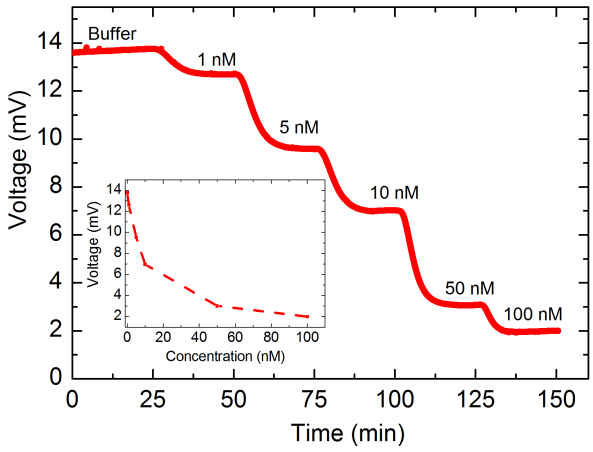

Fig. 5.3: Dynamic response of the adrenaline biosensor measured in PBS of pH 7.4 at 30 °C with the corresponding calibration curve (inset graph).

The long-term stability of the developed adrenaline biosensor has been examined in PBS over one week. The biosensor was stable during the first three days of measurements with sensitivity-value fluctuations within not more than 0.02 mV/nM. However, after seven days, the adrenaline sensitivity decreased to about 35% of the original sensitivity on the first day. Further experiments regarding to the composition of the enzyme membrane and membrane attachment to the oxygen sensor are needed in order to enhance the long-term stability of the adrenaline biosensor.

5.4.3 Sensitivity to other catecholamines

Adrenaline, noradrenaline, dopamine and dobutamine belong to the group of catecholamines with different substituent groups on the aromatic ring and the terminal amino group [24]. Adrenaline, noradrenaline and dopamine are present in blood, whereas dobutamine belongs to the group of synthesized catecholamines [25, 26]. Due to their similar chemical structure, the presence of different catecholamines in solution can influence the biosensor signal during adrenaline measurements. Therefore, the sensitivity of the developed biosensor to noradrenaline, dopamine and dobutamine has been proven. All measurements were repeated two times with two different sensors each see Fig. 5.4.

Fig. 5.4 (top) depicts exemplarily the dynamic response of the biosensor measured at different noradrenaline, dopamine and dobutamine concentrations between 1 nM and 100 nM in PBS of pH 7.4 at 30 °C and the corresponding calibration curvse (Fig. 5.4 bottom), respectively. As can be seen, the sensor was practically insensitive to noradrenaline, dopamine and dobutamine up to concentrations of about 50 nM, 10 nM and 100 nM, respectively. The developed sensor has no cross-sensitivity towards dopamine

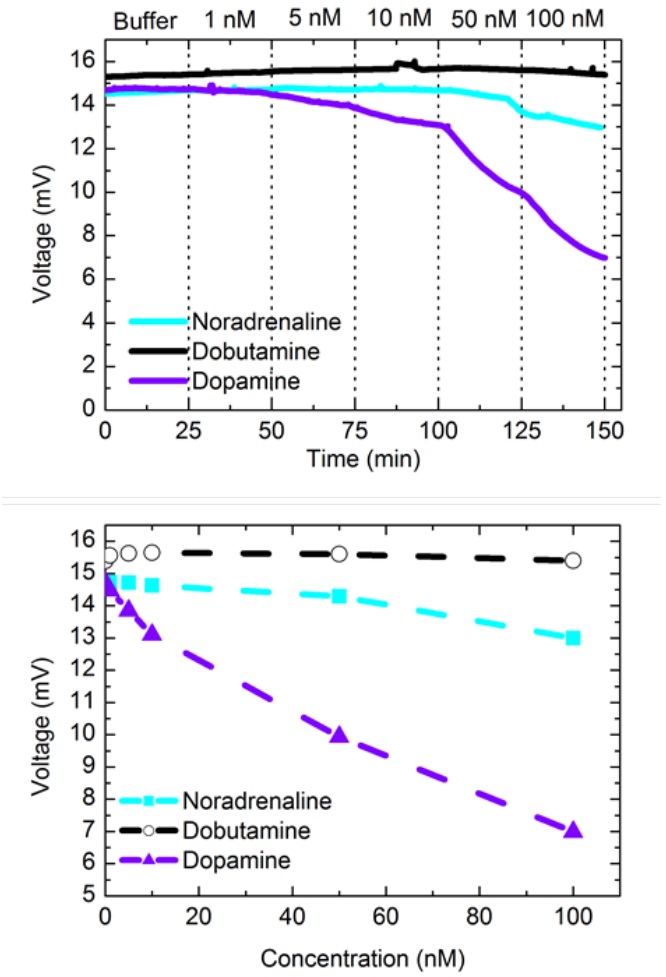

Fig. 5.4: Dynamic response of the developed biosensor measured in PBS of pH 7.4 at 30 °C containing different catecholamines with concentrations from 1 nM to 100 nM (top) with the corresponding calibration curves (bottom).

and noradrenaline at concentrations that are relevant in adrenal venous blood, which are in the picomolar concentration range [27, 28]. These experiments demonstrated that the developed biosensor is suitable for the detection of adrenaline in complex media (e.g., in blood) containing different catecholamines.

5.4.4 Detection of adrenaline in blood plasma

The adrenaline detection in blood is of high interest for a future application of the adrenaline biosensor to support medical tumor diagnosis, especially during AVS procedure. Therefore, the developed adrenaline bi-enzyme sensor has been characterized in real blood plasma (peripheral blood) containing different adrenaline concentrations

from 1 nM to 150 nM. Before starting with the experiments, blood of patients was centrifuged for three minutes and adjusted to about 30 °C. Then, 20 mM of glucose has been added to blood plasma, following by spiking with different concentrations of adrenaline. The measurements in blood plasma were repeated twice with two sensors each. The results of these preliminary experiments are presented in Fig. 5.5. As expected, with increasing adrenaline concentration, the sensor signal is decreased due to the oxygen consumption. Compared with measurements in buffer solution, the initial potential is lower due to less dissolved oxygen content in blood compared to buffer solution [29, 30]. Nevertheless, a detectable signal of about 0.1 mV could be measured at an adrenaline concentration of 1 nM in blood plasma. The average adrenaline sensitivity was about 0.01 mV/nM in the concentration range of 1 nM - 100 nM. These experiments have shown the suitability of the biosensor for the detection of the adrenaline level in real blood samples, in particular, in both adrenal blood with a concentration of $\gtrsim$100 nM adrenaline and in peripheral blood with 1 - 5 nM adrenaline.

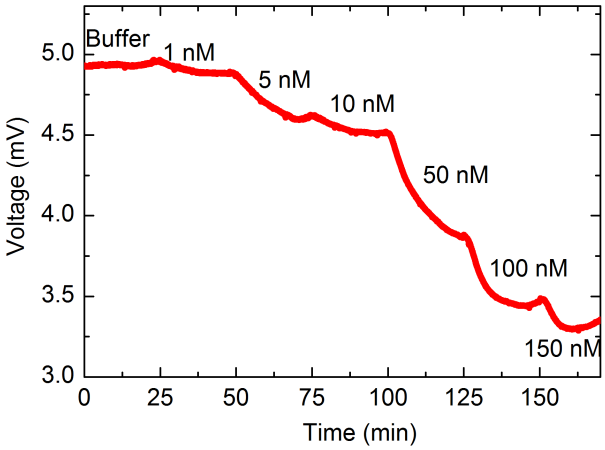

Fig. 5.5: Dynamic response of the biosensor measured in human blood plasma (pH 7.4 at 30 °C) with different adrenaline concentrations from 1 nM to 150 nM.

5.5 Conclusions

An amperometric bi-enzyme adrenaline biosensor has been developed with the aim of future applications for adrenaline detection in blood samples during AVS procedure. The biosensor was investigated in PBS with different pH values (pH 6.5 - 8.5) and adrenaline concentrations (1 nM - 100 nM) and at various temperatures (20 - 35 °C). A high sensitivity and a lower detection limit of 0.5 - 1 nM were achieved due to a) enzymatic amplification of the sensor signal using substrate-recycling principle; b) utilization of the enzymes laccase and PQQ-GDH both exhibiting a high activity at pH values relevant for blood samples; and c) optimization of measuring conditions (pH 7.4, 30 °C). The adrenaline biosensor was practically insensitive to other catecholamines such as noradrenaline, dopamine and dobutamine at concentrations up to several orders

of magnitude higher than their content in adrenal venous blood. Finally, the developed adrenaline biosensor has been successfully tested in blood plasma samples spiked with different concentrations of adrenaline (1 - 150 nM). The achieved results demonstrate the ability of the biosensor to detect adrenaline at concentrations corresponding to adrenaline levels in both peripheral and adrenal blood.

Acknowledgments

This research is supported by a Ph.D. scholarship from FH Aachen. The authors thank F. Lisdat for valuable discussions and AB Enzymes for providing the enzyme.

References

[1] P. Milliez, X. Girerd, P.-F. Plouin, J. Blacher, M. E. Safar, and J.-J. Mourad. "Evidence for an increased rate of cardiovascular events in patients with primary aldosteronism". *Journal of the American College of Cardiology* 45 (2005), 1243–1248.

[2] M. Stowasser, J. Sharman, R. Leano, R. D. Gordon, G. Ward, D. Cowley, and T. H. Marwick. "Evidence for abnormal left ventricular structure and function in normotensive individuals with familial hyperaldosteronism type I". *The Journal of Clinical Endocrinology and Metabolism* 90 (2005), 5070–5076.

[3] D. Blondin, I. Quack, M. Haase, S. Kücükköylü, and H. S. Willenberg. "Indication and technical aspects of adrenal blood sampling". *RoFo: Fortschr. Röntgenstr.* 187 (2015), 19–28.

[4] P. Collste, B. Brismar, A. Alveryd, I. Björkhem, C. Hårdstedt, L. Svensson, and J. Ostman. "The catecholamine concentration in central veins of hypertensive patients - an aid not without problems in locating phaeochromocytoma". *Acta Chirurgica Scandinavica, Supplementum* 530 (1986), 67–71.

[5] E. L. Bravo, R. C. Tarazi, F. M. Fouad, D. G. Vidt, and R. W. Gifford. "Clonidine-suppression test: A useful aid in the diagnosis of pheochromocytoma". *New England Journal of Medicine* 305 (1981), 623–626.

[6] D. Molinnus, A. Bartz, M. Bäcker, P. Siegert, H. Willenberg, A. Poghossian, M. Keusgen, and M. J. Schöning. "Detection of adrenaline based on substrate recycling amplification". *Procedia Engineering* 120 (2015), 540–543.

[7] A. Salimi, V. Alizadeh, and R. G. Compton. "Disposable amperometric sensor for neurotransmitters based on screen-printed electrodes modified with a thin iridium oxide film". *Analytical Sciences* 21 (2005), 1275–1280.

[8] S.-Y. Ly, Y.-H. Kim, I.-K. Han, I.-G. Moon, W.-W. Jung, S.-Y. Jung, H.-J. Sin, T.-K. Hong, and M.-H. Kim. "Anodic square-wave stripping voltammetric analysis of epinephrine using carbon fiber microelectrode". *Microchemical Journal* 82 (2006), 113–118.

[9] A. L. Ghindilis, A. Makower, C. G. Bauer, F. F. Bier, and F. W. Scheller. "Determination of *p*-aminophenol and catecholamines at picomolar concentrations based on recycling enzyme amplification". *Analytica Chimica Acta* 304 (1995), 25–31.

[10] F. Lisdat, U. Wollenberger, A. Makower, H. Hörtnagl, D. Pfeiffer, and F. W. Scheller. "Catecholamine detection using enzymatic amplification". *Biosensors and Bioelectronics* 12 (1997), 1199–1211.

[11] J. Szeponik, B. Möller, D. Pfeiffer, F. Lisdat, U. Wollenberger, A. Makower, and F. W. Scheller. "Ultrasensitive bienzyme sensor for adrenaline". *Biosensors and Bioelectronics* 12 (1997), 947–952.

[12] U. Wollenberger, F. Lisdat, A. Rose, and K. Streffer. "Phenolic Biosensors". In: *Bioelectrochemistry*. Ed. by P. N. Bartlett. Chichester, UK: John Wiley & Sons, Ltd, 2008, 219–248.

[13] F. Mizutani, S. Yabuki, and M. Asai. "Highly-sensitive measurement of hydroquinone with an enzyme electrode". *Biosensors and Bioelectronics* 6 (1991), 305–310.

[14] A. Eremenko, A. Makower, W. Jin, P. Rüger, and F. W. Scheller. "Biosensor based on an enzyme modified electrode for highly-sensitive measurement of polyphenols". *Biosensors and Bioelectronics* 10 (1995), 717–722.

[15] F. W. Scheller, C. G. Bauer, A. Makower, U. Wollenberger, A. Warsinke, and F. F. Bier. "Coupling of immunoassays with enzymatic recycling electrodes". *Analytical Letters* 34 (2001), 1233–1245.

[16] F. W. Scheller, N. Siegbahn, B. Danielsson, and K. Mosbach. "High-sensitivity enzyme thermistor determination of L-lactate by substrate recycling". *Analytical Chemistry* 57 (1985), 1740–1743.

[17] D. Cybulski, K. B. Male, J. M. Scharer, M. Moo-Young, and J. H. T. Luong. "Substrate recycling scheme for tetrachloro-*p*-benzoquinone using bilirubin oxidase and NADH: Application for pentachlorophenol assay". *Environmental Science and Technology* 33 (1999), 796–800.

[18] D. Molinnus, M. Sorich, A. Bartz, P. Siegert, H. S. Willenberg, F. Lisdat, A. Poghossian, M. Keusgen, and M. J. Schöning. "Towards an adrenaline biosensor based on substrate recycling amplification in combination with an enzyme logic gate". *Sensors and Actuators B: Chemical* 237 (2016), 190–195.

[19] M. Paloheimo, L. Valtakari, T. Puranen, K. Kruus, J. Kallio, A. Mantyla, R. Fagerstrom, P. Ojapalo, and J. Vehmaanpera. "Laccase enzyme and use thereof". US7927849 B2. 2011.

[20] Sorachim. 2017. URL: `http://www.sorachim.com/enzymes/glucose-dehydrogenase-pqq-dependent.html`.

[21] V. Laurinavicius, J. Razumiene, A. Ramanavicius, and A. D. Ryabov. "Wiring of PQQ-dehydrogenases". *Biosensors and Bioelectronics* 20 (2004), 1217–1222.

[22] EXP Tech. 2017. URL: `https://www.exp-tech.de/zubehoer/labor/chemie/6455/dissolved-oxygen-kit`.

[23] A. Shrivastava and V. Gupta. "Methods for the determination of limit of detection and limit of quantitation of the analytical methods". *Chronicles of Young Scientists* 2 (2011), 21–25.

[24] X. Lin, Y. Ni, and S. Kokot. "A novel electrochemical sensor for the analysis of β-agonists: The poly(acid chrome blue K)/graphene oxide-nafion/glassy carbon electrode". *Journal of Hazardous Materials* 260 (2013), 508–517.

[25] Y.-Y. Ling, Q.-A. Huang, D.-X. Feng, X.-Z. Li, and Y. Wei. "Electrochemical oxidation of dobutamine on a magnesium oxide microflowers? Nafion composite film modified glassy carbon electrode". *Analytical Methods* 5 (2013), 4580–4584.

[26] V. Ambade, M. M. Arora, P. Singh, B. L. Somani, and D. Basannar. "Adrenaline, noradrenaline and dopamine level estimation in depression: does it help?" *Medical Journal Armed Forces India* 65 (2009), 216–220.

[27] G. Planz, R. Planz, M. Persigehl, H. D. Bundschu, and R. Heintz. "Adrenalin- und Noradrenalinkonzentration im Blut der Nebennieren- und Nierenvenen des Menschen bei normalem Blutdruck und bei essentieller Hypertonie". *Klinische Wochenschrift* 56 (1978), 1109–1112.

[28] Y. Baba, M. Nakajo, and S. Hayashi. "Adrenal venous catecholamine concentrations in patients with adrenal masses other than pheochromocytoma". *Endocrine* 43 (2013), 219–224.

[29] R. N. Pittman. "Regulation of tissue oxygenation". *1st edn. Morgan and Claypool Life Science, San Rafael* 3 (2011), 1–100.

[30] G. A. Truesdale, A. L. Downing, and G. F. Lowden. "The solubility of oxygen in pure water and sea-water". *Journal of Applied Chemistry* 5 (1955), 53–62.

6 Chip-based biosensor for the detection of low adrenaline concentrations to support adrenal venous sampling (*Sensors and Actuators B: Chemical*, 272, (2018), 21–27)

D. Molinnus, G. Hardt, L. Käver, H. S. Willenberg, J. C. Kröger, A. Poghossian, M. Keusgen and M. J. Schöning

Published in: *Sensors and Actuators B: Chemical,* Vol. 272, (2018), 21–27.

Submitted: 2018-02-02; Accepted: 2018-05-23; Published: 2018-05-24

6.1 Abstract

A chip-based amperometric biosensor referring on using the bioelectrocatalytical amplification principle for the detection of low adrenaline concentrations is presented. The adrenaline biosensor has been prepared by modification of a platinum thin-film electrode with an enzyme membrane containing the pyrroloquinoline quinone-dependent glucose dehydrogenase and glutaraldehyde. Measuring conditions such as temperature, pH value, and glucose concentration have been optimized to achieve a high sensitivity and a low detection limit of about 1 nM adrenaline measured in phosphate buffer at neutral pH value. The response of the biosensor to different catecholamines has also been proven. Long-term stability of the adrenaline biosensor has been studied over 10 days. In addition, the biosensor has been successfully applied for adrenaline detection in human blood plasma for future biomedical applications. Furthermore, preliminary experiments have been carried to detect the adrenaline-concentration difference measured in peripheral blood and adrenal venous blood, representing the adrenal vein-sampling procedure of a physician.

6.2 Introduction

Catecholamines such as adrenaline (epinephrine), noradrenaline (norepinephrine) and dopamine belong to a class of chemical neurotransmitters and hormones. They are capable for many profound changes in the body, e.g., regulation of physiological processes and the development of neurological, psychiatric, endocrine and cardiovascular diseases [1, 2]. The determination of adrenaline concentrations in blood plasma or urine can help to diagnose different diseases such as hypertension, pheocromocytoma or neuroblastoma [3]. For example, adrenal vein sampling (AVS) is a necessary medical diagnostic test of adrenal gland tumors, where blood from both adrenal glands (left and right) is drained [4, 5]. However, adrenal glands are difficult to cannulate which is especially true for the small right adrenal vein (1 - 15 mm length in cadaver studies) (see Fig. 6.1).

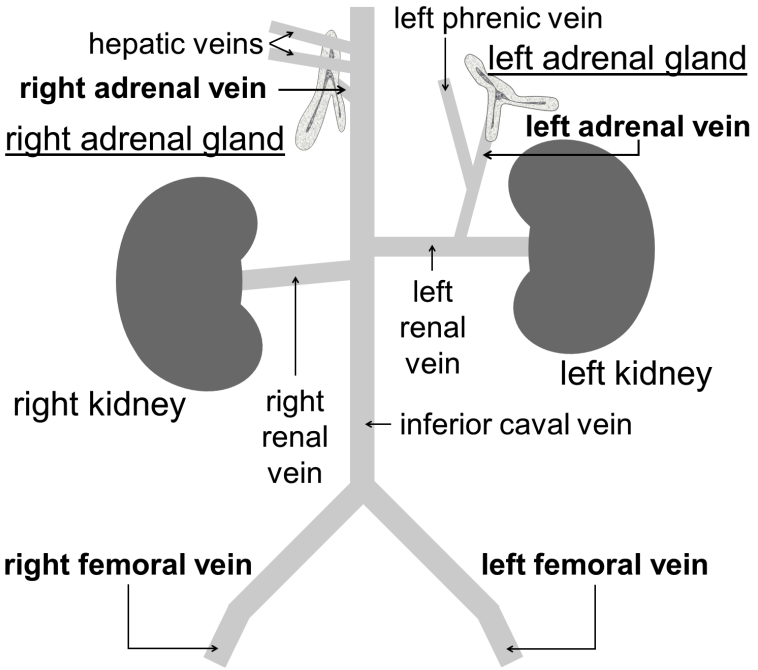

Fig. 6.1: Schematic of the anatomy of the human body, which illustrates the left and right adrenal veins with the corresponding adrenal glands; the catheter has to be pushed through the femoral vein into both adrenal veins.

This can become an obstacle in the study and significantly extend the exposure time to radiation and is consuming human resources. It may also lead to a mistakable cannulation of nearby accessory hepatic veins or to dilution of adrenal venous blood with that from other larger veins. Classically, a catheter tip is placed in the right adrenal vein where blood is sampled from the femoral vein collected simultaneously. Thereafter (in view centers at the same time through a second catheter), the left adrenal vein is cannulated, and again, blood specimen from the left adrenal outflow and from the femoral vein are obtained and subjected to hormone analysis. The ratio of the cortisol

concentration in the adrenal veins to that of the femoral vein informs the physician on the extent of dilution of adrenal venous blood with peripheral extraadrenal blood and is a measure of selectivity of the study. Since cortisol has a relative long half-live and is bound to protein, the ratio of adrenal venous to peripheral cortisol can be as low as 2. However, one possible new approach is the detection of a certain biomarker to confirm the right position of the catheter in adrenal veins. In this case, adrenaline can be used as such biomarker. Since the adrenaline concentration in adrenal vein samples is known to be significantly higher ($\gtrsim$100 nM) than in peripheral samples ($\lesssim$1 nM) [6, 7], a presence of high adrenaline concentration of about 100 nM would confirm the right position of the catheter during AVS.

Common methods for the detection of adrenaline in medicine are high-performance liquid chromatography, fluorescence spectroscopy or capillary electrophoresis [8–13]. Although these methods are highly sensitive, they are not suitable for point-of-care testing at the patient due to the complex and labor-intensive procedures [14]. In the last few years, different biosensors have been developed for the detection of adrenaline. One strategy is the application of amperometric biosensors that are based on substrate-recycling principle by combining phenol-oxidizing enzymes such as e.g., tyrosinase, phenoloxidase or laccase in combination with pyrroloquinoline quinone (PQQ)-dependent glucose dehydrogenase (GDH) [15–18]. By using the substrate-recycling principle, the analyte is oxidized by one enzyme into a product, which can be reduced back to the original substrate by the second enzyme. Due to the recycling process, catecholamines can be detected down to the nanomolar concentration range [18–20]. Recently, we have reported on a biosensor based on laccase and PQQ-GDH by using substrate-recycling principle for the detection of adrenaline with a lower detection limit of about 1 nM at pH 7.4 in both phosphate buffer and Ringer‘s solution [21]. In this case, a genetically modified laccase variant has been applied which is active in a broader pH range, making the sensor applicable for the detection of adrenaline at a pH value in the physiological range. This is beneficial, when the adrenaline biosensor is applied in biological liquids, in particular in blood samples. However, because the sensor signal is proportional to the oxygen consumption due to the enzymatic reaction, small oxygen changes in the surrounding have influence on the sensor response. In addition, the oxygen concentration of real blood samples can vary and hence, the sensor signal could be falsified. Alternatively, the detection of catecholamines can be also performed by applying a monoenzymatic recycling electrode modified by e.g., laccase, PQQ-GDH or tyrosinase [22–24]. In this case, the analyte is oxidized or reduced at the electrode surface by an applied potential and the resulting product is transformed back to the initial analyte catalyzed by an enzyme. One example is shown in [23], where a screen-printed electrode is modified by the enzyme laccase or PQQ-GDH allowing the detection of different catecholamines in the nanomolar concentration range. With this sensor system, dopamine (not adrenaline) could be detected down to a concentration of 50 nM at pH 5.5 by applying the enzyme laccase, or 2 nM at pH 8.5 by applying the enzyme PQQ-GDH. Nevertheless, the described sensors have an insufficient lower detection limit, in particular for the detection of adrenaline, and their pH optimum does not conform to the pH value of biological liquids.

In this study, we report on a high-sensitive thin-film adrenaline biosensor based on the

bioelectrocatalytical amplification principle by using a PQQ-GDH, which enables the detection of adrenaline in the nanomolar concentration range at physiological conditions (pH 7.4). The enzyme from company Sorachim was designed to have a pH optimum at about pH 7.0 [25]. With the developed biosensor set-up – to our knowledge – for the first time successful measurements in real blood samples have been performed. The measuring conditions (pH, temperature and glucose concentration) have been optimized to enhance the biosensor performance. In addition, the long-term stability as well as the sensitivity to other catecholamines (noradrenaline, dopamine and dobutamine) has been investigated. Finally, preliminary results obtained with this biosensor could distinguish between peripheral and adrenal venous blood by the different content of adrenaline concentrations.

6.3 Experimental

6.3.1 Materials

The quinoprotein GDH was bought from Sorachim SA (Switzerland, 757 U/mg) [25]. The cofactor PQQ was purchased from Wako (Japan). For the preparation of PBS, the components (monosodium phosphate and disodiumphosphate) were obtained from Sigma-Aldrich (USA), as well as glutaraldehyde, bovine serum albumin (BSA), glycerol, $CaCl_2$ and sulfuric acid. Adrenaline solution (1 mg/mL) was purchased from Infectopharm (Germany), noradrenaline (1 mg/mL) was obtained from Sanofi (Germany), dopamine (250 mg/mL) was bought from Carinopharm (Germany) and dobutamine (250 mg/50 mL) from Fresenius (Germany). The stock solutions of the used catecholamines of 1 μM and 100 μM, respectively, were freshly prepared before measurements and stored at 4 °C in the dark.

6.3.2 Preparation of the sensor structures

The platinum thin-film sensor chips were fabricated by means of conventional silicon- and thin-film technologies. In brief, a 500 nm SiO_2 layer was grown by thermal wet oxidation of a p-Si wafer. Afterwards, an adhesion layer (20 nm titanium) and a 200 nm thick platinum layer, which serves as electrode material, were deposited on the SiO_2 surface by electron-beam evaporation and patterned by means of lift-off technique. The completed wafer was separated into 1 cm x 2 cm chips. The chips were glued into a substrate holder. The electrical connecting was done by an ultrasonic wedge bonder. For the details of the sensor structure, see [26]. It is known that in electrochemical experiments the quality and the purity of the electrode surface will have an effect on the measurements. Therefore, each sensor was electrochemically cleaned immediately before modification with the enzyme membrane. For the cleaning process, the electrode potential was cycled in sulfuric acid solution (50 mM) until a stable cyclic voltammetry (CV) scan has been achieved [27]. Sample potential was cycled from -400 mV to 1400 mV (*vs.* Ag/AgCl reference electrode) at a rate of 0.1 V/s. Up to 12 cycles had to be approximately performed. The adrenaline biosensor was prepared by modification of the platinum thin-film electrode with the enzyme membrane containing

PQQ-GDH. For the preparation of the enzyme membrane cocktail, 8 μL of the GDH (1.18 U/μL) solution was solved in PBS (10 mM, pH 7.4) together with 20 μM PQQ, 1 mM $CaCl_2$, 8 μL BSA (10 vol%) and 8 μL glutaraldehyde (2 vol%) / glycerol (10 vol%) solution. Different volumetric ratios were tested to achieve a high sensitivity and a low detection limit of 1 nM adrenaline for the adrenaline biosensor. At first, a volumetric ratio of 1-1-1 (enzyme-BSA-glutaraldehyde/glycerol) was studied. But in this case, the enzyme membrane did not get sufficiently dry and could not be used for the detection of adrenaline; the membrane had a sticky-like behavior. Therefore, the enzyme membrane with the PQQ-GDH was prepared in accordance to the protocol described in [21]. Here, the same membrane cocktail was prepared as already described above, but with less amount of GDH solution (4 μL), resulting in a volumetric ratio of 1-2-2 (enzyme-BSA-glutaraldehyde/glycerol). 20 μL of the membrane cocktail was pipetted onto the platinum electrode. Here, the membrane gave the best sensor results (see also chapter 6.5). When further decreasing the amount of enzyme solution, less enzyme activity is immobilized onto the sensor surface. Consequently, the sensitivity towards adrenaline is decreased, too. After drying, the encapsulation of the electrode with silicon rubber (TSE 399C, Momentive Performance Materials, Switzerland) was followed. The resulting active area of the Pt electrode with the covered enzyme membrane was approximately 0.4 cm^2. If not in use, the sensors were stored in air at 4 °C in the dark.

6.4 Measurement procedure

Fig. 6.2 illustrates the measurement set-up with the layer structure of the Pt sensor chip and the bioelectrocatalytical principle of substrate recycling by using PQQ-GDH.

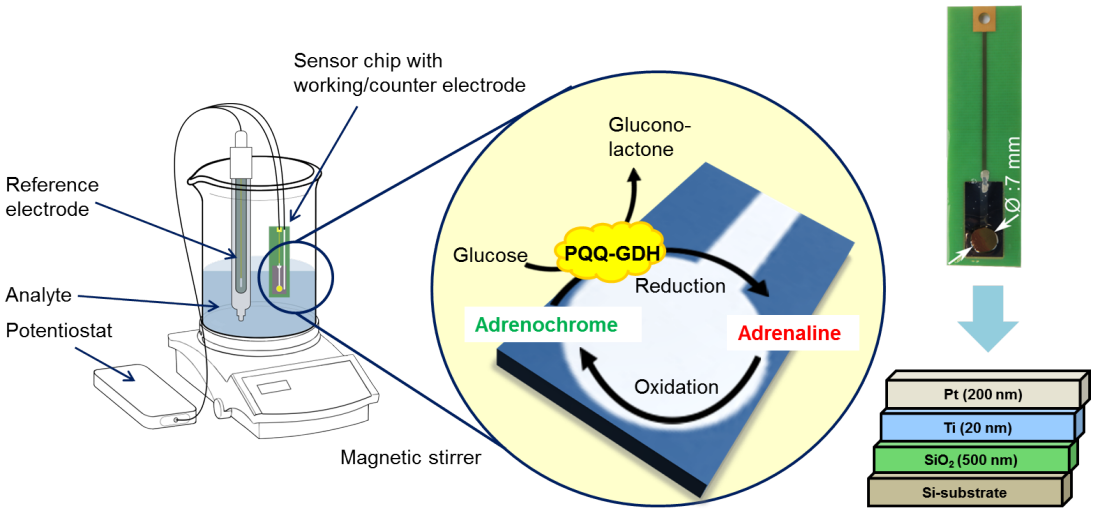

Fig. 6.2: Schematic of the measurement set-up with a photograph of the assembled sensor chip and its layer structure; the zoomed picture is illustrating the working principle of the adrenaline biosensor based on the bioelectrocatalytical substrate amplification.

The adrenaline biosensors were electrochemically characterized in a three-electrode arrangement using a potantiostat (PalmSens, Palm Instrumet BV, Netherlands). A platinum wire (MaTeck, Germany) was used as counter electrode, and an external liquid-junction Ag/AgCl electrode (Metrohm, Germany) as reference electrode. The electrodes were mounted into a Peltier-tempering unit (Lauda-Brinkman, LP, USA) including the stirring function with an integrated Pt 1000 sensor to control the temperature. All measurements were carried out in 20 mL analyte solution. By an applied constant potential of +450 mV to the platinum working electrode *vs.* Ag/AgCl, adrenaline is in a first reaction step oxidized to adrenochrome at the electrode surface. Afterwards, in a second reaction, in the presence of glucose, adrenochrome is reduced back to adrenaline catalyzed by the enzyme PQQ-GDH. The recycling of adrenaline implies an amplification of the sensor signal. The generated current is related to the different adrenaline concentrations. For the measurements, the sensor chip was exposed into analyte solution with different adrenaline concentrations and the sensor signal was recorded for about 25 min.

6.5 Results and discussions

6.5.1 Electrochemical characterization of the adrenaline biosensor

The freshly drained blood during AVS procedure has a temperature around 37 °C. Therefore, the developed biosensor should be able to detect adrenaline at body temperature. The temperature behavior of the sensor with the immobilized PQQ-GDH has been investigated in PBS of pH 7.4 containing 20 mM glucose in a temperature range between 22 °C and 40 °C. At each temperature, adrenaline concentrations were varied between 1 nM and 150 nM. Fig. 6.3a) shows the sensitivity of the developed biosensor with data points representing the average of two performed measurement cycles. The adrenaline biosensor depicts a relatively broad temperature optimum from 30 °C to 37 °C with sensitivity values between 4.0 nA/nM and 4.5 nA/nM. The influence of the pH value of the buffer solution has been studied in the range from pH 6.5 to pH 8.0. The sensor signal was recorded at different adrenaline concentrations between 1 nM and 150 nM in PBS containing 20 mM glucose. The experiments were performed at 30 °C. The results of these experiments are depicted in Fig. 6.3b). Each data point represents again the average of the adrenaline sensitivity of two performed measurements. Maximum sensitivity of 4.5 nA/nM could be reached at a pH value of 7.4, demonstrating that the biosensor is capable for measurement cycles in biological solutions having physiological pH conditions. The bioelectrocatalytical measurement principle allows the detection of adrenaline in the nanomolar concentration range. The reaction involves the oxidation of adrenaline at the electrode surface by an applied potential of +450 mV. In a second reaction step, the oxidation product (adrenochrome) is reduced back to adrenaline catalyzed by the enzyme PQQ-GDH, while glucose is oxidized to gluconolactone. Hence, the addition of glucose is necessary to complete the bioelectrocatalytical measurement system. Fig. 6.3c) demonstrates the dependence of the mean sensitivity of the adrenaline biosensor on glucose concentrations between 5 mM and 50 mM. The measurements were performed in PBS of pH 7.4 at 30 °C with adrenaline concentrations

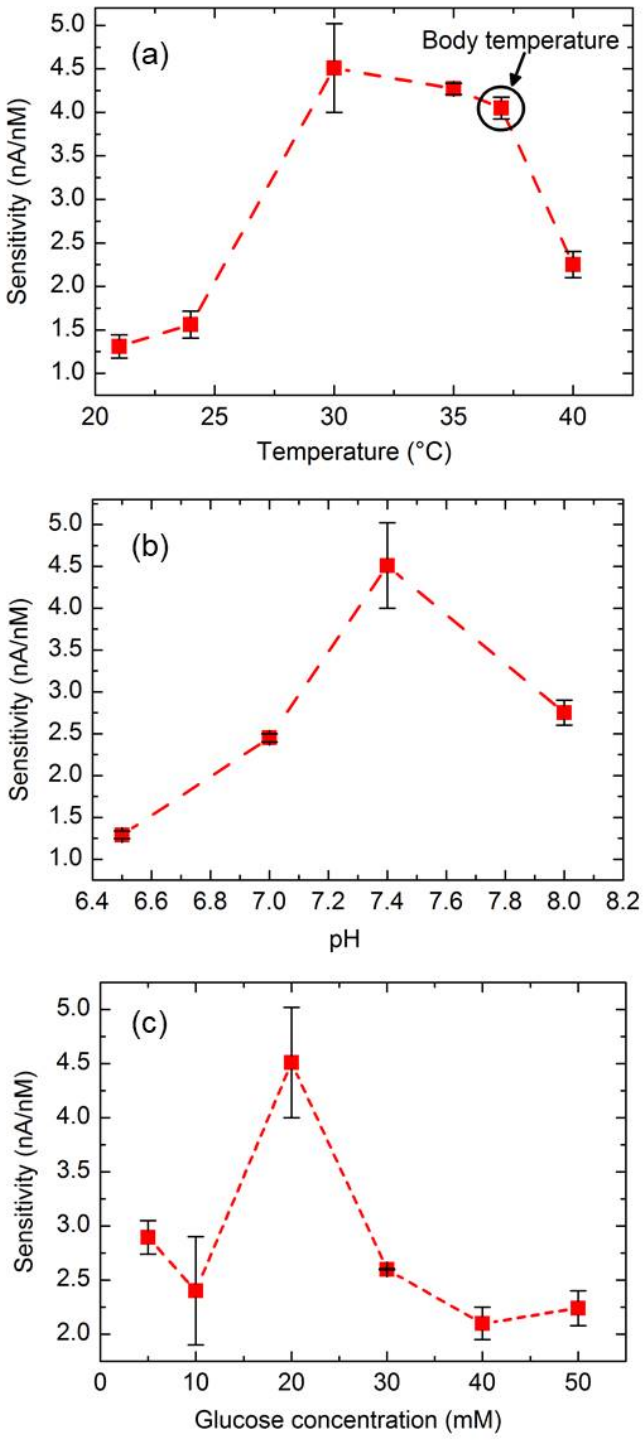

Fig. 6.3: Mean values of the adrenaline sensitivity (set of two series of measurements) of the thin-film biosensor recorded in PBS with different adrenaline concentrations from 1 nM to 150 nM: (a) at different temperatures (22 - 40 °C) at pH value of 7.4 and with 20 mM glucose; (b) at different pH values (pH 6.5 - 8.0) at 30 °C and with 20 mM glucose; (c) containing different glucose concentrations (5 - 50 nM) at pH value of 7.4 and at 30 °C.

between 1 nM and 150 nM. The highest sensitivity of 4.5 nA/nM has been observed at a glucose concentration of 20 mM, which is also comparable with results described in literature [28]. At a glucose concentration of 5 mM (typical glucose concentration in blood), the sensitivity decrease is about 35%. But, even at these glucose concentrations corresponding to the glucose level in blood, a lower detection limit for the adrenaline biosensor of 1 nM could be achieved. Thus, the sensor should be sufficiently sensitive enough for the detection of adrenaline in real blood samples taken from adrenal- and peripheral veins without an additional amount of glucose. From Fig. 6.3, optimal measurement conditions in terms of maximum sensitivity can be defined as: pH 7.4, temperature of 30 °C and 20 mM glucose concentration. Therefore, further experiments were performed at optimal measurements conditions.

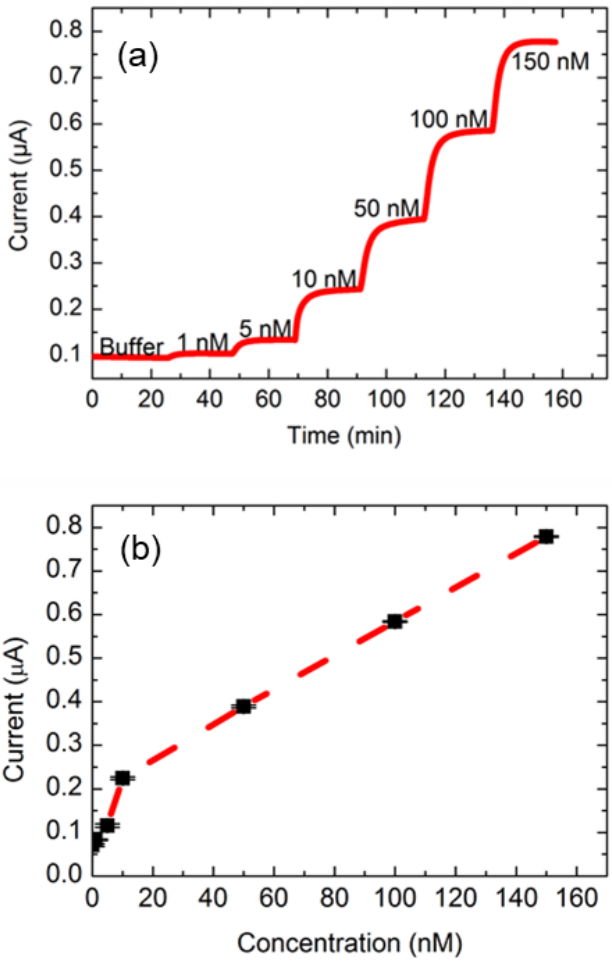

Fig. 6.4: Dynamic response of the adrenaline biosensor at different concentrations of adrenaline measured in PBS of pH 7.4 at 30 °C containing 20 mM glucose (a); corresponding calibration curve with standard deviation of the adrenaline biosensor (b).

Fig. 6.4 presents an example of the dynamic response with the corresponding calibration curve of the adrenaline biosensor at different adrenaline concentrations from

1 nM to 150 nM. As expected, with increasing the adrenaline concentration, the current is increased due to the oxidation of adrenaline at the sensor surface. A sensitivity of 8.8 nA/nM in the concentration range between 1 nM and 10 nM adrenaline and 4.2 nA/nM in the concentration range between 50 and 150 nM adrenaline could be achieved. A sensor-signal change at an adrenaline concentration of 1 nM has been clearly detected that is sufficient for the adrenaline detection in adrenal blood (>100 nM adrenaline) and peripheral blood (1 nM adrenaline).

6.5.2 Study of cross-sensitivity of the adrenaline biosensor to different catecholamines

Adrenaline, noradrenaline and dopamine are natural catecholamines and are present in human blood. The catecholamine molecules consist of a catechol nucleus and they differ in their side-chain amine [2, 29, 30].

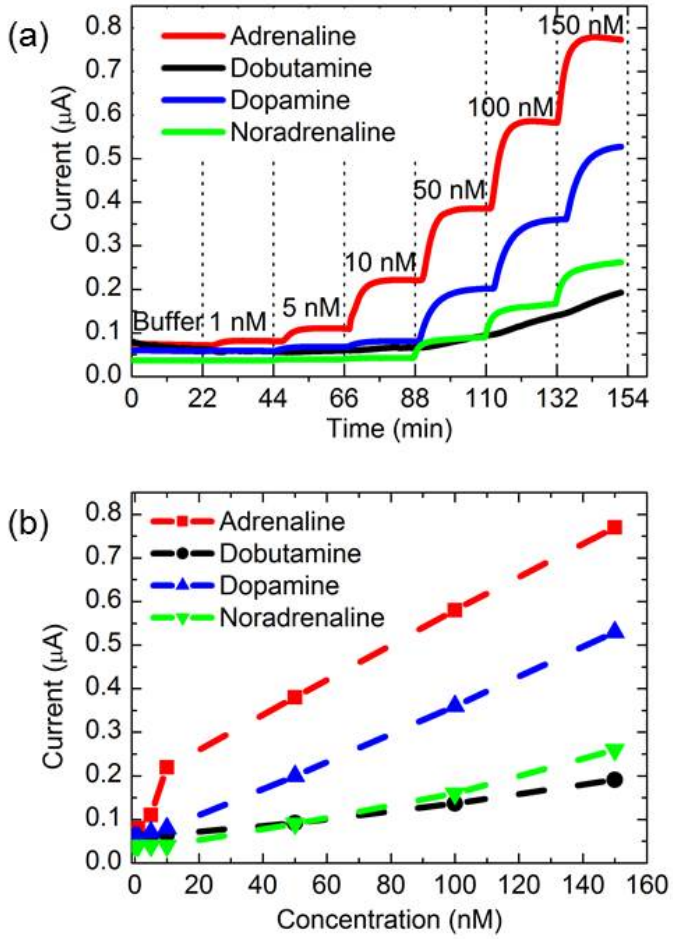

Fig. 6.5: Dynamic response of the biosensor measured in PBS of pH 7.4 at 30 °C containing different catecholamines in the concentration range from 1 nM to 150 nM (a); corresponding calibration plots of the biosensor (b).

In contrast, dobutamine is a synthesized catecholamine and is used in human and veterinary medicine as a therapeutic drug for e.g., coronary heart disease [31].

Since the natural and synthesized catecholamines are very similar in their chemical structure, the sensitivity of the developed biosensor to adrenaline and to other catecholamines has been compared. Fig. 6.5 demonstrates exemplarily the dynamic responses of the biosensor measured at different adrenaline, dobutamine, dopamine, and noradrenaline concentrations, respectively, between 1 nM and 150 nM (Fig. 6.5a)) with the corresponding calibration curves (Fig. 6.5b)). The response of the biosensor to adrenaline, dopamine and noradrenaline shows a typical concentration-dependent behavior. The highest sensitivity was observed for adrenaline. No significant sensor-signal change was recorded during measurements performed in dobutamine solution.

Despite of a cross-selectivity of the adrenaline biosensor towards dopamine and noradrenaline, it can be applied for adrenaline measurements in real samples such as adrenal veins, because of the very low level of dopamine (<1.5 nM) and noradrenaline (<0.2 nM) in adrenal veins [9]. Hence, their presence in blood practically does not influence the biosensor signal during adrenaline measurements performed in human blood during AVS.

6.5.3 Long-term stability of the adrenaline biosensor

To study the stability of the adrenaline biosensor, four sensors were periodically characterized over a time period of 10 days. At each day, sensitivity of the adrenaline biosensor was tested under optimal measuring conditions at different adrenaline concentrations between 1 nM and 150 nM. Fig. 6.6 summarizes the mean values of the obtained sensitivities of the four individual adrenaline biosensors over 10 days with the corresponding standard deviation shown as error bars.

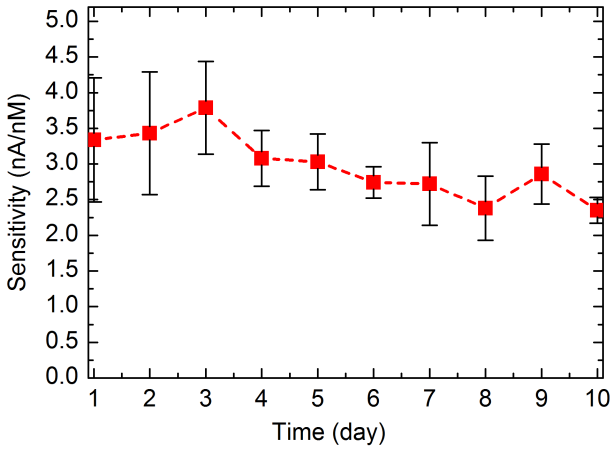

Fig. 6.6: Stability of the adrenaline biosensor (N = 4 sensors) over a time period of 10 days with standard deviation.

Within the first four days, the sensors show practically a constant sensitivity of about 3.5 nA/nM. After ten days, the sensitivity value decreases to about 25% to an average

sensitivity of about 2.5 nA/nM.

6.5.4 Application of the adrenaline biosensor in real blood samples

The main goal of this work was the development of a chip-based adrenaline biosensor with lower detection limit in the nanomolar concentration range and its capability for adrenaline measurements in human blood samples. In the future, such a sensor could be applied to support AVS for adrenal secretory tumor diagnosis. Therefore, preliminary experiments have been performed to detect adrenaline in human blood plasma. A 39-year old obese patient known to have hypokalemic hypertension due to primary aldosteronism underwent AVS. During the study, freshly extracted blood from the femoral vein and the right adrenal outflow was centrifuged for about three minutes to produce plasma before starting with the measurements. Part of the obtained peripheral blood plasma (pH 7.4) was spiked with different concentrations of adrenaline from 50 nM to 1000 nM. Additionally, 20 mM glucose has been added to the blood plasma (pH 7.4). Measurements were carried out at 30 °C.

The results of these experiments are shown in Fig. 6.7a). The dynamic response of the adrenaline biosensor in blood plasma shows similar sensor behavior as in buffer solution. With increasing the adrenaline concentration, the sensor signal is also increased due to the resulting oxidation current. The zoomed curve in Fig. 6.7a) demonstrates that a lower detection limit of about 50 nM could be reached. The higher current value recorded in blood plasma without adrenaline indicates the existence of other substances in blood plasma contributing to the total current, influencing the biosensor signal.

For future application, the adrenaline biosensor should be able to detect the adrenaline-concentration difference between peripheral blood ($\lesssim$1 nM adrenaline) and adrenal venous blood ($\gtrsim$100 nM adrenaline) to proof the position of the catheter. Experiments with plasma of the above mentioned patient have been performed to study the biosensor behavior in blood samples of both origins. The measurements have been carried out under optimum conditions (30 °C, 20 mM glucose). The pH value of the blood plasma was controlled by a pH meter (Mettler-Toledo, Germany) and was at pH 7.4.

Fig. 6.7b) demonstrates the results of these experiments. The generated current of both blood plasma samples was recorded for about 40 min. The sensor signal was stable after 15 min conditioning. These first measurements could validate that the developed chip-based adrenaline biosensor is able to distinguish the adrenaline concentration in peripheral and adrenal blood. The difference between the two blood samples (peripheral and adrenal venous) at 40 min would correspond to a change of about 200 nM adrenaline assuming that the current changes for the adrenaline-spiked blood samples in Fig. Fig. 6.7a) are valid. Of interest, the selectivity indices (ratio of adrenal to femoral vein cortisol plasma concentrations) were 47.4 and 2.0 for the right and left adrenal veins (determined by means of an immunoassay as an additional clinical diagnosis method), respectively, and are in line with the biosensor results. The AVS study showed a lateralization of aldosterone secretion to the adrenal gland which carried a small tumors lesion. Its removal led to biochemical cure and clinical improvement [32].

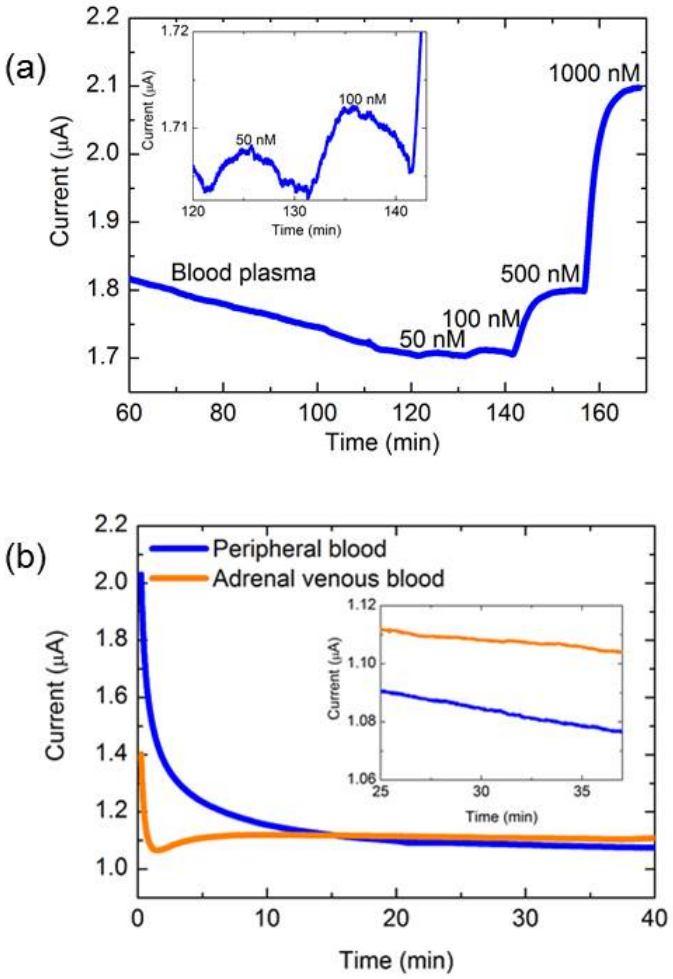

Fig. 6.7: Dynamic response of the adrenaline biosensor measured in human blood plasma (pH 7.4 at 30 °C) spiked with different adrenaline concentrations from 50 nM to 150 nM and zoomed curve demonstrating the lower detection limit (a); response of the biosensor measured in peripheral and adrenal venous blood sample and zoomed curve demonstrating the signal difference recorded in peripheral and adrenal venous blood (b).

6.6 Conclusions

A high-sensitive, amperometric chip-based adrenaline biosensor modified with an enzyme membrane consisting of PQQ-GDH has been developed and characterized regarding the pH-, temperature- and glucose-concentration optimum. Due to the applied bioelectrocatalysis as measuring principle, adrenaline is recycled resulting in a signal amplification. Other working groups used already the bioelectrocatalysis as measurement principle. For example, [22] applied the enzyme tyrosinase for the recycling reaction of catechol, where 0,04 μM could be detected at a pH value of pH 6.0. The group of Lisdat et al. [23] applied the enzyme laccase for the detection of dopamine, noradrenaline and adrenaline, where dopamine could be detected with the highest sensitivity and a lower

detection limit of 50 nM at pH 5.5. Additionally, they performed also experiments by applying the enzyme PQQ-GDH for the recycling of dopamine, resulting in a lower detection limit of 2 nM at pH 8.5 with a glucose concentration of 10 mM in the analyte solution. In summary, all these developed biosensors possess an insufficient lower detection limit for the measurement of adrenaline during AVS. Furthermore, the adjusted pH value in those works does not correspond to the blood pH value. Hence, in this study, a chip-based biosensor has been developed for the detection of 1 nM adrenaline measured in PBS at physiological pH value of pH 7.4. Additionally, the sensor has been studied regarding its cross-selectivity against dopamine, noradrenaline and dobutamine. The highest sensitivity has been observed during adrenaline measurements. Preliminary experiments have been carried out in human blood plasma, where an adrenaline concentration of 50 nM could be measured. Furthermore, the adrenaline biosensor has been studied in peripheral blood and adrenal blood and the biosensor was able to detect the adrenaline-concentration difference (around 200 nM) between both real blood samples.

Declaration

The clinical part of the work was done under the ethical standards of the SHIP-PAGE study (steroid hormones in patients with pituitary, adrenal or gonadal endocrinopathies) for individuals investigated for primary aldosteronism (Ethics Committee of the Rostock University Medical Center, #A2016-0088) and the study has been carried out in accordance with The Code of Ethics of the World Medical Association (Declaration of Helsinki).

Acknowledgments

D. Molinnus gratefully thanks FH Aachen for the Ph.D. scholarship. The authors thank H. Iken for the preparation of the sensors.

References

[1] G. Eisenhofer, I. J. Kopin, and D. S. Goldstein. "Catecholamine metabolism: a contemporary view with implications for physiology and medicine". *Pharmacological Review* 56 (2004), 331–349.

[2] D. Carlström. "The structure of the catecholamines. IV. The crystal structure of (−)-adrenaline hydrogen (+)-tartrate". *Acta Crystallogr. B Struct. Sci.* 29 (1973), 161–167.

[3] M. Tsunoda. "Recent advances in methods for the analysis of catecholamines and their metabolites". *Analytical and Bioanalytical Chemistry* 386 (2006), 506–514.

[4] D. Blondin, I. Quack, M. Haase, S. Kücükköylü, and H. S. Willenberg. "Indication and technical aspects of adrenal blood sampling". *RoFo: Fortschr. Röntgenstr.* 187 (2015), 19–28.

[5] N. Daunt. "Adrenal vein sampling: How to make it quick, easy, and successful". *Radiographics* 25 Suppl 1 (2005), 143–158.

[6] E. L. Bravo, R. C. Tarazi, F. M. Fouad, D. G. Vidt, and R. W. Gifford. "Clonidine-suppression test: A useful aid in the diagnosis of pheochromocytoma". *New England Journal of Medicine* 305 (1981), 623–626.

[7] P. Collste, B. Brismar, A. Alveryd, I. Björkhem, C. Hårdstedt, L. Svensson, and J. Ostman. "The catecholamine concentration in central veins of hypertensive patients - an aid not without problems in locating phaeochromocytoma". *Acta Chirurgica Scandinavica, Supplementum* 530 (1986), 67–71.

[8] V. Ambade, M. M. Arora, P. Singh, B. L. Somani, and D. Basannar. "Adrenaline, noradrenaline and dopamine level estimation in depression: does it help?" *Medical Journal Armed Forces India* 65 (2009), 216–220.

[9] Y. Baba, M. Nakajo, and S. Hayashi. "Adrenal venous catecholamine concentrations in patients with adrenal masses other than pheochromocytoma". *Endocrine* 43 (2013), 219–224.

[10] A. Lund. "Simultaneous fluorimetric determinations of adrenaline and noradrenaline in blood". *Acta Pharmacologica et Toxicologica* 6 (1950), 137–146.

[11] E. Nalewajko, A. Wiszowata, and A. Kojło. "Determination of catecholamines by flow-injection analysis and high-performance liquid chromatography with chemiluminescence detection". *Journal of Pharmaceutical and Biomedical Analysis* 43 (2007), 1673–1681.

[12] S. García Palop, A. Mellado Romero, and J. Martínez Calatayud. "Oxidation of adrenaline and noradrenaline by solved molecular oxygen in a FIA assembly". *Journal of Pharmaceutical and Biomedical Analysis* 27 (2002), 1017–1025.

[13] S. Wei, G. Song, and J.-M. Lin. "Separation and determination of norepinephrine, epinephrine and isoprinaline enantiomers by capillary electrophoresis in pharmaceutical formulation and human serum". *Journal of Pharmaceutical and Biomedical Analysis* 1098 (2005), 166–171.

[14] C. D. Forster and I. A. Macdonald. "The assay of the catecholamine content of small volumes of human plasma". *Biomedical Chromatography* 13 (1999), 209–215.

[15] P. N. Bartlett, ed. *Bioelectrochemistry: Fundamentals, Experimental Techniques and Applications*. Chichester: Wiley & Sons, 2008.

[16] U. Wollenberger, F. Schubert, D. Pfeiffer, and F. W. Scheller. "Enhancing biosensor performance using multienzyme systems". *Trends in Biotechnology* 11 (1993), 255–262.

[17] J. Szeponik, B. Möller, D. Pfeiffer, F. Lisdat, U. Wollenberger, A. Makower, and F. W. Scheller. "Ultrasensitive bienzyme sensor for adrenaline". *Biosensors and Bioelectronics* 12 (1997), 947–952.

[18] F. Lisdat, U. Wollenberger, A. Makower, H. Hörtnagl, D. Pfeiffer, and F. W. Scheller. "Catecholamine detection using enzymatic amplification". *Biosensors and Bioelectronics* 12 (1997), 1199–1211.

[19] A. L. Ghindilis, A. Makower, C. G. Bauer, F. F. Bier, and F. W. Scheller. "Determination of *p*-aminophenol and catecholamines at picomolar concentrations based on recycling enzyme amplification". *Analytica Chimica Acta* 304 (1995), 25–31.

[20] A. Makower, A. V. Eremenko, K. Streffer, U. Wollenberger, and F. W. Scheller. "Tyrosinase-glucose dehydrogenase substrate-recycling biosensor: A highly-sensitive measurement of phenolic compounds". *Journal of Chemical Technology & Biotechnology* 65 (1996), 39–44.

[21] D. Molinnus, M. Sorich, A. Bartz, P. Siegert, H. S. Willenberg, F. Lisdat, A. Poghossian, M. Keusgen, and M. J. Schöning. "Towards an adrenaline biosensor based on substrate recycling amplification in combination with an enzyme logic gate". *Sensors and Actuators B: Chemical* 237 (2016), 190–195.

[22] P. Önnerfjord. "Tyrosinase graphite-epoxy based composite electrodes for detection of phenols". *Biosensors and Bioelectronics* 10 (1995), 607–619.

[23] F. Lisdat, W. O. Ho, U. Wollenberger, F. W. Scheller, T. Richter, and U. Bilitewski. "Recycling systems based on screen-printed electrodes". *Electroanalysis* 10 (1998), 803–807.

[24] U. Wollenberger and B. Neumann. "Quinoprotein glucose dehydrogenase modified carbon paste electrode for the detection of phenolic compounds". *Electroanalysis* 9 (1997), 366–371.

[25] Sorachim. 2017. URL: `http://www.sorachim.com/enzymes/glucose-dehydrogenase-pqq-dependent.html`.

[26] D. Molinnus, M. Bäcker, H. Iken, A. Poghossian, M. Keusgen, and M. J. Schöning. "Concept for a biomolecular logic chip with an integrated sensor and actuator function". *Physica Status Solidi A* 212 (2015), 1382–1388.

[27] C. Spégel, A. Heiskanen, J. Acklid, A. Wolff, R. Taboryski, J. Emnéus, and T. Ruzgas. "On-chip determination of dopamine exocytosis using mercaptopropionic acid modified microelectrodes". *Electroanalysis* 19 (2007), 263–271.

[28] I. W. Schubart, G. Göbel, and F. Lisdat. "A pyrroloquinolinequinone-dependent glucose dehydrogenase (PQQ-GDH)-electrode with direct electron transfer based on polyaniline modified carbon nanotubes for biofuel cell application". *Electrochimica Acta* 82 (2012), 224–232.

[29] D. Carlström and R. Bergin. "The structure of the catecholamines. I. The crystal structure of noradrenaline hydrochloride". *Acta Crystallographica* 23 (1967), 313–319.

[30] R. Bergin and D. Carlström. "The structure of the catecholamines. II. The crystal structure of dopamine hydrochloride". *Acta Crystallogr. B Struct. Sci.* 24 (1968), 1506–1510.

[31] Y.-Y. Ling, Q.-A. Huang, D.-X. Feng, X.-Z. Li, and Y. Wei. "Electrochemical oxidation of dobutamine on a magnesium oxide microflowers? Nafion composite film modified glassy carbon electrode". *Analytical Methods* 5 (2013), 4580–4584.

[32] T. A. Williams, J. W. M. Lenders, P. Mulatero, J. Burrello, M. Rottenkolber, C. Adolf, F. Satoh, L. Amar, M. Quinkler, J. Deinum, F. Beuschlein, K. K. Kitamoto, U. Pham, R. Morimoto, H. Umakoshi, A. Prejbisz, T. Kocjan, M. Naruse, M. Stowasser, T. Nishikawa, W. F. Young, C. E. Gomez-Sanchez, J. W. Funder, M. Reincke, T. A. Williams, R. J. Auchus, D. K. Bartsch, R. Baudrand, P. Björklund, M. J. Brown, R. M. Carey, C. Catena, J. M. Connell, T. Dekkers, T. J. Fahey, F. Fallo, C. E. Fardella, G. Giacchetti, G. Giraudo, P. Hellman, A. Januszewicz, K. K. Kitamoto, G. A. Kline, F. Mantero, B. S. Miller, P.-F. Plouin, A. Prejbisz, C. L. Rump, L. A. Sechi, F. Veglio, J. Widimský, and H. S. Willenberg. "Outcomes after adrenalectomy for unilateral primary aldosteronism: An international consensus on outcome measures and analysis of remission rates in an international cohort". *The Lancet Diabetes and Endocrinology* 5 (2017), 689–699.

7 Coupling of biomolecular logic gates with electronic transducers: from single enzyme logic gates to sense/act/treat chips (*Electroanalysis*, 29, (2017), 1840–1849)

D. Molinnus, A. Poghossian, M. Keusgen, E. Katz and M. J. Schöning

Published in: *Electroanalysis,* Vol. 29, (2017), 1840–1849.

Submitted: 2017-04-07; Accepted: 2017-04-25; Published: 2017-05-19

7.1 Abstract

The integration of biomolecular logic principles with electronic transducers allows designing novel digital biosensors with direct electrical output, logically triggered drug-release, and closed-loop sense/act/treat systems. This opens new opportunities for advanced personalized medicine in the context of theranostics. In the present work, we will discuss selected examples of recent developments in the field of interfacing enzyme logic gates with electrodes and semiconductor field-effect devices. Special attention is given to an enzyme **OR/Reset** logic gate based on a capacitive field-effect electrolyte-insulator-semiconductor sensor modified with a multi-enzyme membrane. Further examples are a digital adrenaline biosensor based on an **AND** logic gate with binary YES/NO output and an integrated closed-loop sense/act/treat system comprising an amperometric glucose sensor, a hydrogel actuator, and an insulin (drug) sensor.

7.2 Introduction

Recent developments in the field of biocomputing using different biomolecules have resulted in a variety of biochemical Boolean logic gates (**AND, NAND, OR, XOR, NOR, INHIB,** etc.) and more complex digital logic devices such as adders, subtractors, multiplexers, and keypad locks (see e.g., recent reviews [1–7] and references therein). Typical biomolecules in this context are enzymes and DNA (deoxyribonucleic acid) molecules. Although the idea to construct biocomputers from biomolecules, ions or even living cells has attracted significant interest, the current biochemical computing devices are not yet competitive with electronic computing systems [5, 8, 9]. Most of the developments on molecular logic gates and circuits reported so far are "proof-of-principle" experiments, demonstrating basic concepts or mimicking the operation of their electronic analogues. Moreover, biomolecular logic gates usually work in bulk solutions and often utilize optical output signals (fluorescent or colorimetric), which makes it difficult to implement multiple logic devices together in the same analyte [10]. Hence, transferring biomolecular logic principles to solid substrates and their integration with electrochemical/electronic devices is not an easy task [5, 9, 11].

Analyzing the chemical output signals of biomolecular logic systems is in most cases only possible with a limited number of techniques such as optical analysis of the chemical products. The interfacing of biomolecular logic systems with biosensing- and signal-reading devices still receives comparatively little attention. However, future progress in the design of biomolecular logic systems, particularly when extrapolating this to "molecular computers", will necessarily rely on the integration of molecular signal-processing systems with various output-reading methodologies. A route on which already progress has been achieved is the coupling of biomolecular logic systems to electrochemical interfaces and signal-responsive materials. The integration of these logic systems with electronic transducers, e.g., electrodes [12, 13] and semiconductor field-effect devices [10, 11, 14, 15], is indeed promising to move from "proof-of-concept" studies to ready-to-use logic devices with direct electrical output. These molecular logic elements might even enable gate-to-gate communication with the possibility of addressing and switching between "ON" and "OFF" states. Moreover, interfacing of biomolecular logic systems with electronic transducers and stimuli-responsive materials may result in novel digital biosensors and actuators [8, 16], logically triggered drug-release systems [12, 17–20], and closed-loop intelligent sense/act/treat biochips [21, 22]. Such biochips are considered as highly attractive for personalized medicine and theranostics.

This work summarizes selected examples of recent developments and ongoing research in the field of biomolecular logic gates that are combined with electronic transducers, mainly focusing on work performed at the Institute of Nano- and Biotechnologies (Aachen University of Applied Sciences, Germany). Special attention is given to enzyme logic gates based on a capacitive field-effect electrolyte-insulator-semiconductor (EIS) sensor modified with a multi-enzyme membrane and a digital adrenaline biosensor based on the substrate-recycling principle. In addition, a concept for an integrated closed-loop sense/act/treat system is introduced. The present article provides a compact overview on selected results regarding the combination of biomolecular enzyme-based logic gates with electronic transducers. In addition, more technical details are collected in the

Supporting Information to allow readers following the conceptual explanations together with the technological background.

7.3 Enzyme logic gates based on field-effect EIS sensor

Interfacing biomolecular logic gates with field-effect devices is a highly forward-looking approach to directly convert biochemical (logic) signals into processed electrical output signals. Such systems can be understood as electrochemical analogues of electronic logic elements. In previous experiments, capacitive field-effect devices have been widely used for measuring the concentration of different ions and products of enzymatic reactions [23–25] as well as for the detection of various charged macromolecules (DNA, proteins, polyelectrolytes) and nanoobjects (e.g., gold nanoparticles, carbon nanotubes) [26–31]. Consequently, also EIS sensors can be favorably applied as a universal platform for developing various chemical and biomolecular logic gates. The main focus of the present work lies on enzyme logic gates because biochemical reactions are often catalyzed by enzymes (e.g., in living cells). In addition, enzyme logic gates are particularly promising to create digital biosensors and can be easily integrated with electronic devices using various well-established enzyme-immobilization techniques.

The possibility to couple enzyme logic gates with a field-effect capacitive EIS sensor was first demonstrated in [14, 15], where Al–p-Si–SiO_2 structures modified with pH-responsive gold nanoparticles were applied for designing single **AND-Reset** and **OR-Reset** logic gates. In these logic gates, either enzymes [15] or their substrates [14] were used as input signal, while the product (H^+ ions) of the enzymatic reactions, activated by different combinations of chemical input signals, provided the output signal. The pH-induced charge changes of the gold-nanoparticle shells and SiO_2-gate surface of the EIS sensor resulted in an electronic signal (typically, shift of capacitance-voltage curves along the voltage axis) corresponding to the logic output produced by the enzymes. These primary studies have shown that enzyme logic systems can indeed be successfully interfaced with field-effect transducers. In subsequent experiments, **AND-Reset** and **OR-Reset** logic gates were developed using EIS sensors modified with a multi-enzyme membrane. The operation principle of these devices is based on local pH changes due to a cascade of enzymatic reactions. At the same time, the pH of the bulk solution remained constant [10, 11]. The results for the single **OR-Reset** gate are exemplarily presented below.

Figure 7.1 shows schematically the capacitive EIS sensor with the immobilized enzyme membrane; to perform the measurements, the set-up is completed with the analyte, an Ag/AgCl reference electrode and an impedance analyzer. The EIS chips (with sizes of 10 mm x 10 mm) consisting of an Al (300 nm) –p–Si–SiO_2 (30 nm) –Ta_2O_5 (60 nm) structure were prepared from a p-doped Si wafer (thickness: ∼400 μm, resistivity: 1–10 Ωcm, Si-Mat, Germany). The enzyme membrane for the **OR-Reset** logic gate combines three enzymes: glucose oxidase (GOD), esterase (Est) and urease (Ur). The multi-enzyme membrane was prepared by drop-coating of the membrane mixture onto the Ta_2O_5 surface. For details of chip fabrication and multi-enzyme membrane immobilization, see the Supporting Information.

The operating principle of the enzyme logic **OR-Reset** gate is based on local pH

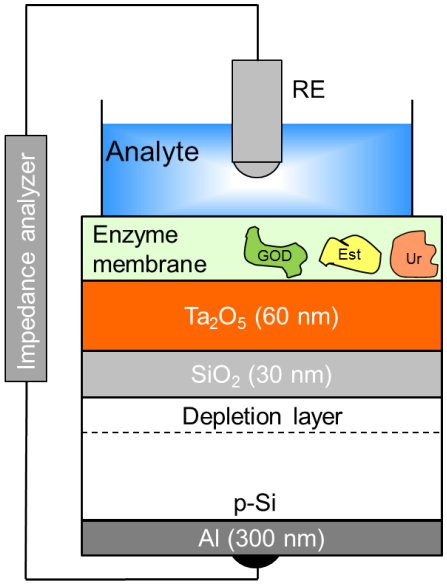

Fig. 7.1: Layer structure and measurement set-up of EIS sensor modified with immobilized multi-enzyme membrane. RE: reference electrode.

variations due to enzymatic reactions near the Ta_2O_5 surface of the EIS-sensor chip. Therefore, the pH sensitivity of the enzyme-modified EIS sensor has been additionally studied before enzyme logic-gate measurements. In comparison to blank (without enzyme membrane) Ta_2O_5 gate field-effect sensors, for which a pH sensitivity of 55 - 58 mV/pH was reported previously (see [32, 33]), the pH sensitivity of the enzyme-modified EIS structure was slightly lower (~48 mV/pH between pH 3 and pH 9).

Figure 7.2 (top) sketches the enzyme-based **OR-Reset** logic gate, which was activated by the substrates glucose or/and ethyl butyrate, respectively, while urea was used to implement the **Reset** function [10]. The input signal combination **(1,0)** corresponds to the presence of glucose, the input signal combination **(0,1)** to the presence of ethyl butyrate, and input **(1,1)** means that both analytes are present. For the **OR** logic-gate experiments, the multi-enzyme EIS sensor was exposed to buffer (pH 7.5), glucose (1 mM), ethyl butyrate (1 mM) or a mixture of glucose/ethyl butyrate solutions as biochemical inputs. The resulting EIS-sensor signal, corresponding to the logic output of the enzymatic reactions, was monitored by dynamic constant-capacitance measurements (ConCap [30]) using an impedance analyzer (Zahner Elektrik, Germany).

Both, the catalytic conversion of glucose by GOD (when dissolved oxygen is present) or ethyl butyrate by Est, form acids, in that case gluconic acid, butyric acid, or both of them. These acids induce a local pH decrease at the Ta_2O_5 surface of the EIS sensor [10, 11]. The latter modulates the electronic output signal of the EIS sensor in accordance with the logic output derived from the biochemical reactions, which are activated by different combinations of chemical input signals. A typical dynamic ConCap response, see Figure 7.2 (bottom), shows exemplary signal changes of 127 mV (glucose signal) and 167 mV (ethyl butyrate signal) [10]. The signal changes towards more negative voltages underline the local acidification at the Ta_2O_5 surface of the EIS sensor.

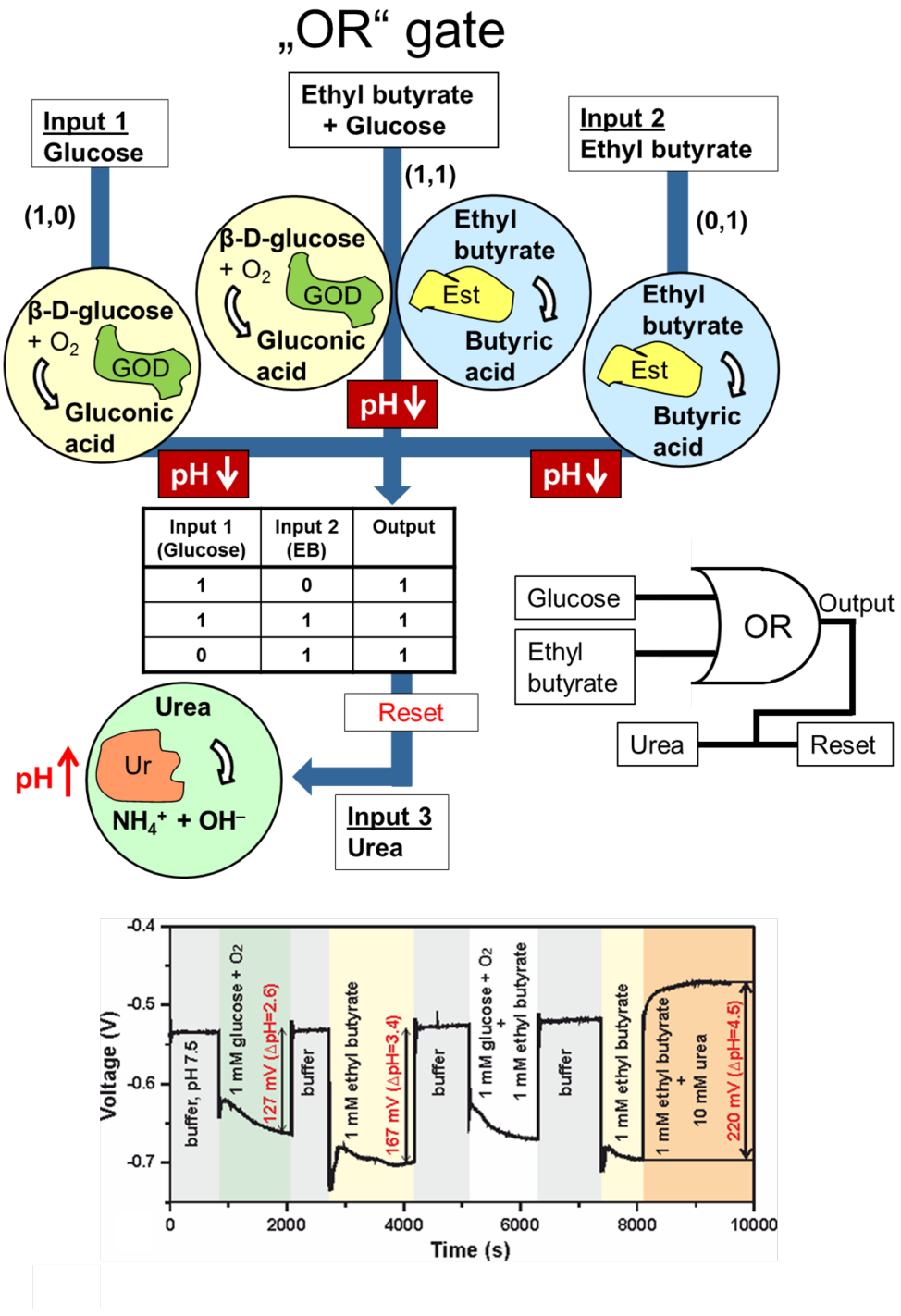

Fig. 7.2: Schematic of the enzyme **OR-RESET** logic gate including enzymatic reactions and truth table (top); ConCap signal buffer (pH 7.5), 1 mM glucose, 1 mM ethyl butyrate (EB), mixture of 1 mM glucose / 1 mM ethyl butyrate or mixture of 1 mM ethylbutyrate / 10 mM solutions (bottom). Part of the figure (bottom graph) is reproduced from Ref. [10] with permission of the Royal Society of Chemistry.

Referring to the pH sensitivity of the enzyme-modified EIS sensor with ∼48 mV/pH, the achieved signal changes in Figure 7.2 correspond to a local pH change (decrease) of ΔpH≈2.6 (for glucose) and ΔpH≈3.4 (for ethyl butyrate). At the same time, control experiments (data not shown) evidenced that the pH of the bulk solution remained practically constant at pH 7.5. In addition, after each measurement cycle in either glucose- or ethyl butyrate solution, the sensor signal was measured in pH buffer (pH 7.5) to check the reproducibility of the EIS sensor signal (see Figure 7.2, bottom).

To guarantee reversible operation, such logic gate must be returned (switched) back to its initial state (so-called **Reset** function) [10, 34]. Then, the system will be ready to respond to the next incoming chemical signals. In previous experiments with enzyme logic gates coupled to EIS sensors, the **Reset** function was activated via changing the pH value of the bulk solution. This can be done by adding urea to a Ur-containing solution [14] or by exposing the logic transducer again to the original buffer solution [11]. Ideally, activation of the **Reset** function directly at the EIS sensor surface by local enzymatic reactions (i.e., a local pH change) could be highly advantageous because of the possibility to address and to switch a particular gate in a logic network [10]. An example of such local **Reset** function is presented in Figure 7.2 (bottom), where the EIS sensor covered with multi-enzyme membrane containing Ur is exposed to 10 mM urea solution. A fast signal change of ∼220 mV was registered, which corresponds to a local pH increase by ΔpH≈4.5 directly at the Ta_2O_5 surface of the EIS sensor while the pH of the bulk solution remained unchanged.

The present example demonstrates the successful integration of the biomolecular logic gate with a silicon-based EIS field-effect sensor. Only logic pH changes, derived from the local enzymatic reactions in close vicinity to the sensor surface, were detected as the logic output signal while the bulk pH remains constant. This way, the suggested approach could allow individual addressing and switching of the respective logic gates, even in complex networks, via local pH variations induced by generating H^+ or OH^- ions through water electrolysis or enzymatic reactions. In addition, logic output signals of the field-effect device can be applied to activate down-stream electrochemical reactions or logic actuators releasing species for next logic steps.

7.4 Digital adrenaline biosensor based on AND logic gates

Developing digital biosensors that use logic principles to differentiate between clinical conditions on basis of critical biochemical parameters and disease-specific biomarkers attracts more and more research groups [8]. In contrast to conventional biosensors, which usually provide precise, quantitative information on the concentration of analytes, digital biosensors deliver qualitative output signals in a binary YES/NO format (see e.g., [7, 8, 16, 18]). Digital biosensors could be especially useful in application fields in which there is no need for a quantitative determination of analyte concentrations, but where rapid qualitative information is required regarding the presence (exceeding a predefined threshold level) or absence of a certain analyte. Recently, a digital adrenaline biosensor has been introduced which employs the substrate-recycling principle in combination with enzyme logic gates [35]. Such a digital biosensor is considered as a benefit in clinical medicine during the adrenal venous sampling (AVS) procedure for adrenal tumor

localization and differential diagnosis [36]. Typically, the adrenaline concentration in adrenal veins is about 100-times higher ($\gtrsim$100 nM) than in the periphery [37, 38]. Thus, the adrenaline-concentration difference can serve as qualitative indicator (binary YES/NO signal) for correct catheter positioning during the AVS procedure [39, 40]. The developed adrenaline biosensor was able to detect very low adrenaline concentrations (1 nM) in both phosphate buffer (PBS) and Ringer's solutions (substitute for blood plasma). However, in model logic-gate experiments, the logic **0** of the input signal was taken as the physical absence of adrenaline, although for practical applications it should correspond to the normal physiological concentration. In addition, as logic **1** of the input signal, an adrenaline concentration of 1 μM was selected, exceeding the pathophysiological or elevated level of adrenaline in adrenal veins significantly.

In this work, we present a digital adrenaline biosensor with logic **0** and **1** values of the input signals corresponding to the normal physiological adrenaline concentration in the periphery and an elevated level of adrenaline in adrenal veins, respectively. To detect nanomolar adrenaline concentrations, the substrate-recycling principle based on a bi-enzyme system of laccase/pyrroloquinoline quinone (PQQ)-dependent glucose dehydrogenase (GDH) was used [41–43]. In this biochemical recycling approach, the analyte is converted by one enzyme into a product, which can be converted back to the original substrate by a second enzyme and thus, allows amplifying the response signal by several orders of magnitude.

The schematics of a digital adrenaline biosensor based on substrate-recycling amplification is shown in Figure 7.3. This biosensor consists of two concatenated **AND** logic gates (**AND 1** and **AND 2**) with enzymes laccase and PQQ-dependent GDH, respectively.

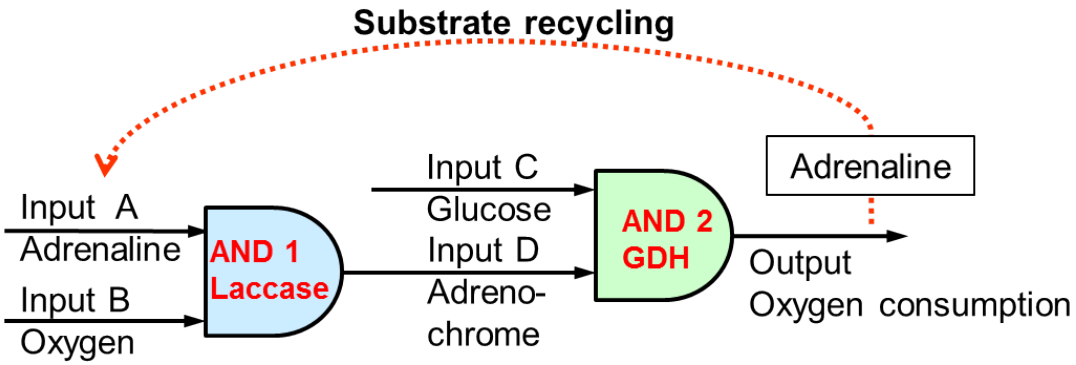

Fig. 7.3: Digital adrenaline biosensor (schematically) with two concatenated **AND** logic gates (**AND 1** and **AND 2**) containing the enzyme laccase and GDH for the substrate recycling.

AND 1 gate is activated by adrenaline (input A) and dissolved oxygen (input B), whereas **AND 2** gate is activated by glucose (input C) and adrenochrome (product of the adrenaline-oxidation reaction, input D). Laccase oxidizes adrenaline to adrenochrome only when dissolved oxygen is present (**AND 1** gate). For **AND 2** gate, PQQ-GDH oxidizes glucose to gluconolactone, while adrenochrome is reduced to adrenaline, which can serve again as input A and trigger the reaction continuously

(substrate-recycling principle). As a result, the oxygen consumption is increased, yielding a high sensor-signal change (logic **1**). In contrast, the enzymatic reaction cascade is hindered if either dissolved oxygen or glucose are missing. In such situation, a low or even no sensor-signal change is expected (logic **0**) [35]. The quantity of dissolved oxygen consumed during the oxidation of adrenaline by laccase depends on the adrenaline concentration in solution and has been detected using a commercial galvanic oxygen sensor modified with the bi-enzyme (laccase/GDH) membrane. Details of the preparation of the bi-enzyme membrane are described in the Supporting Information.

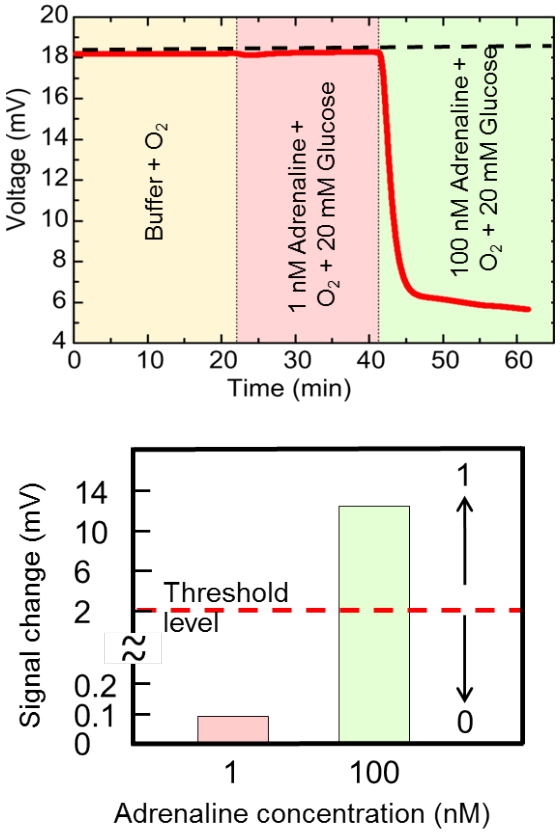

Fig. 7.4: (top) Output signal of the digital adrenaline biosensor recorded in adrenaline-free PBS, pH 7.4 (concentration of dissolved oxygen under equilibrium with air) and in PBS containing 20 mM glucose and adrenaline with concentrations of 1 nM and 100 nM, respectively. At each adrenaline concentration, the sensor signal was measured for about 20 min. All experiments were carried out at room temperature under continous stirring; (bottom) the bar charts are showing changes in the output signal of the adrenaline sensor and the dashed line defines the threshold level for the output signal.

Figure 7.4 (top) shows the output signal of the digital adrenaline biosensor recorded in adrenaline-free PBS, pH 7.4 (concentration of dissolved oxygen under equilibrium with air) and in PBS containing 20 mM glucose and adrenaline with concentrations of 1 nM and 100 nM, respectively. This corresponds to the normal physiological adrenaline concentration in the periphery and to the elevated level of adrenaline in adrenal veins.

As can be seen, a small signal change of about 0.1 mV was detected in PBS containing 1 nM adrenaline. In case of the solution containing 100 nM, a larger signal change of 12 mV was recorded. For practical applications, the logic **0** and **1** chemical input signals should be considered as physiologically normal (1 nM adrenaline in the periphery blood) and as elevated (in adrenal veins, exceeding a defined threshold from clinical data), respectively. Alternatively, the threshold level separating the logic **0** and **1** values can be personally tailored for each patient. Since the difference between the signal changes corresponding to logic **0** and **1** is significant, the threshold level in Figure 7.4 (bottom) is exemplarily fixed at 2 mV (dashed line). Only in the correct positioning of the catheter, causing the output signal to exceed the predefined threshold, would result in a logical **1** value. Hence, the developed digital sensor is able to distinguish elevated adrenaline concentrations in form of a YES/NO output as an indicator for the correct insertion and positioning of the catheter in the adrenal veins.

7.5 On-chip integration of molecular gates with biosensor/actuator system

One of the most promising areas for biomolecular logic gates and systems is their application in the logically triggered activation of actuator devices. Coupling of logic output with actuators, capable for release and/or delivery of therapeutic agents (drugs), might lead to intelligent sense/act and sense/act/treat theranostic (therapeutic and diagnostic) devices [8, 17, 44–46]. Recently, we proposed a challenging concept based on the on-chip integration of biomolecular gates with a biosensor/actuator system – a so-called biomolecular logic chip (BioLogicChip) [22]: The BioLogicChip will be capable of detecting multiple analytes (e.g., a panel of biomarkers) and subsequently convert them into electrical output signals in accordance to defining specific combinations of logic **"0"** and **"1"**, which are characteristic for particular diseases. Based on the logic operations, the actuator system can be activated to release a particular substance (e.g., drug for patient treatment). Thus, the BioLogicChip represents an integrated closed-loop sense/act/treat logic system, allowing a highly specific and reliable diagnosis as well as a personalized drug administration for optimal therapeutic intervention. The BioLogicChip responds to defined combinations of biochemical signals, processed together by corresponding biomolecular logic gates [22].

The concept for a BioLogicChip is schematically shown in Figure 7.5, tailored as closed-loop insulin-release actuator triggered by an enzyme **AND** logic gate, which relies on a glucose/GOD system. Besides the amperometric glucose biosensor, it features a temperature-responsive hydrogel for the actuator function (hydrogel valve). Further elements are a thermoresistive heater for heating-up the hydrogel above the phase-transition temperature, an impedance sensor for detecting hydrogel shrinking, a drug reservoir, and an amperometric insulin sensor for the drug-release control.

The **AND** logic gate provides a logic **"1"** only in case that both substrates, i.e. glucose and dissolved oxygen, are present. Depending on a predefined threshold value, this logic **"1"** will then activate the heater and cause the temperature-dependent shrinking (or swelling) of the hydrogel. Since the hydrogel works as an actuator valve that is opening

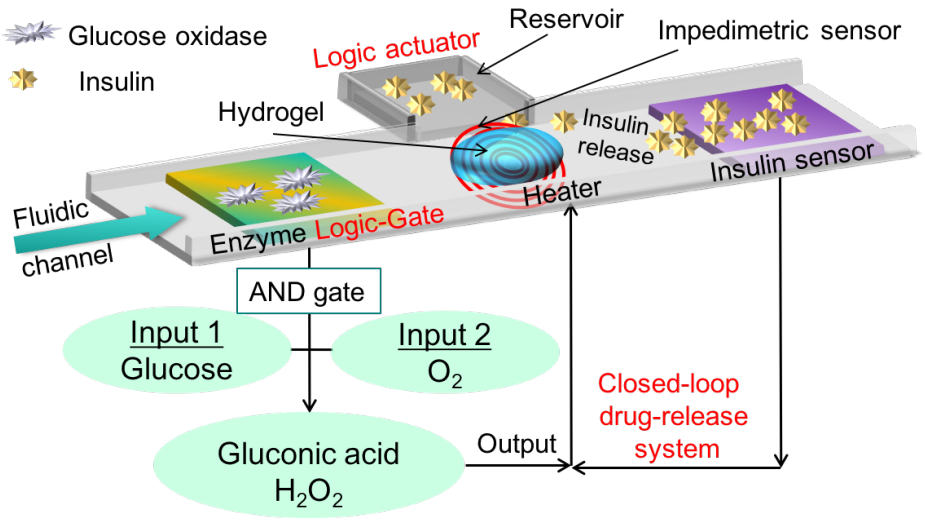

Fig. 7.5: Concept of BioLogicChip (schematically) designed as closed-loop drug-release device triggered by an enzymatic **AND** logic gate. The chip consists of an enzymatic biosensor (glucose/GOD), an actuator (hydrogel valve) for drug release from a closed reservoir in a microfluidic channel when hydrogel is shrinking, a thermoresistive heater (to heat hydrogel above phase-transition temperature), an impedance sensor (to detect hydrogel shrinking), and an insulin sensor (to monitor insulin release).

(or closing) a reservoir containing insulin, it can induce an insulin release to reduce the glucose level of a patient with a therapeutic status. The insulin release (dosage, timing) will be monitored by a downstream-placed insulin sensor and a feedback control of the glucose level using a glucose biosensor [22]. Chapter 7.5.1 to chapter 7.5.3 briefly describe the individual sensors, i.e. the glucose- and insulin biosensors as well as the impedimetric sensor (to monitor the temperature-induced hydrogel shrinking). Details of materials used, sensors preparation, and measurement set-up can be found in a recent article [22] and in the Supporting Information.

7.5.1 Glucose sensor

Figure 7.6 (top) depicts a cross-section of the layer structure (inset graph) and sensor signal (current), depending on glucose concentrations in the range 0.5 - 15 mM.

The three-electrode set-up used in this experiment consisted of a liquid-junction Ag/AgCl reference electrode, a platinum counter electrode, and a sensor chip (platinum working electrode). For amperometric H_2O_2 detection – as a product of glucose oxidation by GOD – a potential of +600 mV was applied. With increasing glucose concentration, the H_2O_2 concentration raises, yielding a higher current output as sensor signal. The average sensitivity was found to be 4.4 ± 0.15 mA/mM in the glucose

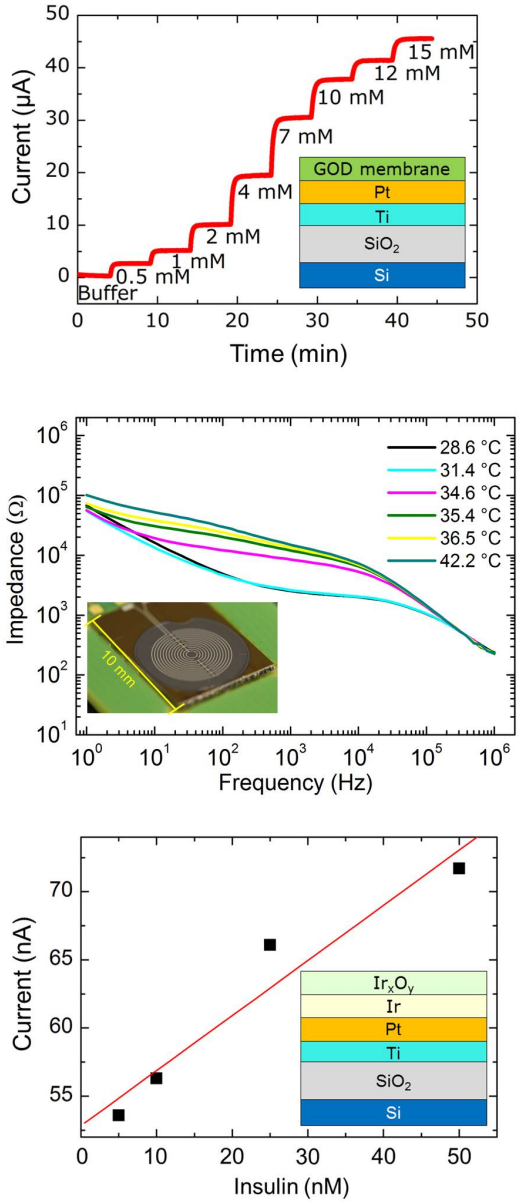

Fig. 7.6: (top) Cross-section of the layer structure (inset graph) and sensor signal (current) depending on the glucose concentration (0.5 - 15 mM) measured at an applied potential of 600 mV on the working electrode; (middle) open-circuit impedance-spectroscopy characteristics of the interdigitated circular electrodes covered with a PNIPAAm hydrogel film measured at different temperatures (inset shows photograph of impedimetric sensor); (bottom) cross-section of the layer structure (inset graph) and calibration curve of the insulin sensor measured at an applied potential of 800 mV on the working electrode.

concentration range from 0.5 to 7 mM. When integrated into the BioLogicChip, at elevated glucose concentrations, the glucose sensor will activate the actuator function by applying a logic output signal to the heater.

7.5.2 Hydrogel-shrinking sensor

Hydrogels are cross-linked polymer structures, which can absorb a large volume of water. Depending on external stimuli, they can change their volume (swelling or shrinking) more than 100-fold [47, 48]. For developing a hydrogel-based actuator, we used the temperature-responsive hydrogel poly(N-isopropylacrylamide) (PNIPAAm), which is often used for fluidic applications [49, 50]. The swelling/shrinking properties of the PNIPAAm film (serving as a hydrogel valve) were studied using an impedimetric sensor based on interdigitated circular Pt electrodes. Figure 7.6 (middle) shows the open-circuit impedance spectroscopic characteristics of the interdigitated circular electrodes (covered with a PNIPAAm film) measured at different temperatures. The inset depicts a photograph of this impedimetric sensor. For simplicity, we compare impedance values at different temperatures recorded in the frequency range in which the temperature dependence of the impedance signal is well visible (e.g., at 1000 Hz). Temperatures below the phase-transition temperature (around 32 - 34 °C [49]) correspond to the highly swollen state (high water content) of the PNIPAAm hydrogel, resulting in a low impedance of about 2.5 kΩ. Above the phase-transition temperature, the hydrogel collapses and switches to the shrinking state with low water content. Consequently, the impedance increases starting at 34.6 °C to reach a value of 14.8 kΩ at 42.2 °C. The temperature-induced swelling/shrinking behavior of the PNIPAAm enables its application as temperature-responsive actuator. It can be designed as a hydrogel valve combined with an insulin reservoir or, alternatively, insulin molecules can be incorporated inside the hydrogel and subsequently released.

7.5.3 Insulin sensor

Recently, it was demonstrated that nanometer-thick films of Ir_xO_y prepared by thermal oxidation of an iridium film (700 °C [51] for 1 h in air) can be applied for amperometric insulin detection. In this experiment, the insulin concentration in buffer solution (pH 7.4) was varying between 0.1 μM and 0.5 μM [22]. Further experiments showed that the performance of this insulin sensor can be improved by increasing the oxidation time of iridium. Figure 7.6 (bottom) displays a schematic cross-section of the layer structure of this insulin sensor (a 20 nm thick iridium film was thermally oxidized for 5 h at 700 °C) together with the output signal depending on the insulin concentration. For insulin oxidation, a potential of +800 mV [22] was applied to the Ir_xO_y working electrode *vs.* the Ag/AgCl reference electrode. The calibration curve is nearly linear in the insulin concentration range from 5 nM to 50 nM with a sensitivity of 0.4 ± 0.07 nA/nM. The estimated lower detection limit was determined to be about 5 nM. These results show the feasibility of the developed Ir_xO_y-based amperometric sensor for the detection of very low insulin concentrations.

The next development step will be the integration of all three components (i.e., glucose sensor, temperature-responsive hydrogel for insulin release, and insulin sensor) on one

chip. Such a closed-loop chip could be a very promising platform for the treatment of diabetes patients in the future.

Other studies have already shown that closed-loop control systems were comparable with conventional insulin-pump therapy [52]. Similar to artificial pancreas technologies, the development of such BioLogicChip designed as closed-loop drug-release device triggered by an enzymatic **AND** logic gate could prevent in a future application the variation of the glucose level during the continuous glucose sensing [53]. The Medtronic MiniMed 670G system is the first FDA (Food and Drug Administration) -approved closed-loop system that monitors glucose and automatically adjusts the delivery of insulin based on the glucose level [54]. The system consists of a continuous glucose monitor and an additional insulin pump. In contrast to the Medtronic system, the BioLogicChip contains an additional insulin sensor, which allows the control of insulin concentration and dynamic of insulin release. Furthermore, in most cases of artificial pancreas systems, multiple handheld devices to monitor the glucose level, compute hormone delivery rates and control hormone delivery pumps might be problematic due to the complexity of such systems [55]. In this way, an integration of all functionalities onto one chip might be advantageous.

7.6 Conclusions

In this work, we have presented selected examples of integrating enzyme logic principles with electronic transducers (semiconductor field-effect devices and electrodes). An enzyme **OR/Reset** logic gate consisting of a field-effect EIS structure covered with a multi-enzyme membrane has been developed and studied experimentally. The working principle of this **OR/Reset** gate is based on local pH changes at the surface of the EIS sensor, arising from a cascade of enzymatic reactions. This approach possibly enables the activation of downstream electrochemical reactions as well as addressable switching "ON" and "OFF" of particular logic gates inside the logic network via local pH changes. A digital adrenaline biosensor based on two concatenated **AND** logic gates with the binary YES/NO output has been developed, where the logic **0** and **1** values of the input signals correspond to the normal physiological adrenaline concentration in the periphery and elevated level of adrenaline in adrenal veins, respectively. Due to the substrate-recycling principle, the developed biosensor is able to detect very low adrenaline concentrations down to the nanomolar range. Only in the case of correct catheter position, causing the output signal to exceed a predefined threshold level, the output signal would result in a logical **1** value. In future, this digital biosensor is intended for clinical diagnostics as a novel tool for the control of a correct insertion and positioning of a catheter in the adrenal veins during AVS procedure.

In addition, an integrated sense/act/treat system designed as a closed-loop drug-release device was studied. The system combines a digital glucose sensor based on a logic **AND** gate, a hydrogel actuator with heating element, a drug reservoir, and a drug sensor. We expect that such a sense/act/treat system can be used in personalized medicine for diagnosis and drug administration to optimize therapeutic interventions, owing to the fact that it responds only to specific combinations of biochemical signals processed by the biomolecular logic gates.

While the present paper summarized recent experimental achievements on digital logic systems in the authors' laboratory, much broader research activities have taken place in other laboratories in the area of non-conventional computing, particularly with respect to enzyme-based logic gates and circuits [17, 56–80]. The results reported by all these laboratories will certainly trigger further developments in the integration of various logic systems with electronic transducers and actuators. Overall, the transition of logic elements from mostly optical means for reading output signals to electronic transduction tools would be beneficial for developing many novel logic elements for information processing, biosensing, and bioactuation.

Acknowledgments

D. Molinnus gratefully thanks FH Aachen for the Ph.D. scholarship. The authors thank P. Wagner for valuable discussions.

7.7 Supporting information

7.7.1 Enzyme logic gates based on a field-effect EIS sensor

Materials

The enzymes esterase (Est, EC 3.1.1.1), glucose oxidase (GOD, EC 1.1.3.4) and urease (Ur, EC 3.5.1.5) were purchased from Sigma–Aldrich and Sinus Biochemicals. Other reagents and chemicals (pH-buffer solutions, KCl, bovine serum albumin (BSA), glutaraldehyde, glycerol, β-D-glucose, ethyl butyrate, urea) were purchased from Fluka and Sigma–Aldrich. The analyte solutions for the logic gate experiments were prepared by dissolving glucose or ethyl butyrate in a working buffer (1 mM phosphate buffer, pH 7.5, adjusted with 100 mM KCl).

Preparation of EIS sensors

The EIS chips consisting of an Al–p-Si–SiO_2–Ta_2O_5 structure were fabricated from a p-Si wafer by standard microfabrication processes. First, a high-quality SiO_2 layer with a thickness of 30 nm was prepared by thermal dry oxidation of Si under O_2 atmosphere at 1000 °C for about 30 min. Afterwards, a Ta_2O_5 layer with a thickness of approximately 60 nm was prepared by electron-beam evaporation of 30 nm Ta, followed by thermal oxidation in oxygen atmosphere at 530 °C for about 45 min. To create the Ohmic contact to the Si, the SiO_2 layer on the rear side of the wafer was etched and then, a 300 nm thick Al layer was deposited by electron-beam evaporation and annealed in nitrogen atmosphere at 400 °C for 10 min. Finally, the wafer was cut into single chips with the sizes of 10 mm × 10 mm.

Modification of the EIS sensor with the multi-enzyme membrane

The enzymes were immobilized on the Ta_2O_5 surface by cross-linking with BSA and glutaraldehyde. To prepare a membrane solution, the enzyme cocktail consisting of

GOD (5.9 kU/ml), Est (0.4 kU/ml), and BSA (40 mg/ml) was mixed in the ratio of 1:1 v/v with 1% v/v glutaraldehyde solution comprising 10% v/v glycerol. The multi-enzyme membrane was prepared via drop-coating method by applying 2 μL of the particular membrane solution onto the Ta_2O_5 surface, followed by drying in air at room temperature for 30 min and rinsing in ultrapure water to remove non-immobilized components. For the Ur immobilization, 1 μL of the solution containing Ur (70 kU/ml) in phosphate saline buffer (1 mM, pH 7.5) mixed in the ratio of 1:1 with 1% aqueous glutaraldehyde solution comprising 10% glycerol was applied onto the surface of the EIS structure.

Measurement setup

For the experiments, the EIS-sensor chip was mounted into a home-made measuring cell, sealed by an O-ring, and contacted on its front side by the electrolyte and the reference electrode (conventional liquid-junction Ag/AgCl electrode, Metrohm). The contact area of the EIS sensor with the solution was about 0.5 cm^2. For measurements, a DC polarization voltage was applied via the reference electrode and a small AC voltage (20 mV) was applied to the system in order to measure the capacitance of the sensor using an impedance analyzer (Zahner Elektrik, Germany). For the **OR** enzyme logic-gate experiments, the particular analyte solution (1 mM ethyl butyrate or glucose, pH 7.5) was applied to the sensor surface as biochemical input, and the logic output signals have been read out by means of the ConCap method. All potential values are referred to the reference electrode.

7.7.2 Digital adrenaline biosensor based on AND logic gates

Materials

Glutaraldehyde, BSA, glycerol, $CaCl_2$ and the buffer components (monosodium phosphate and disodiumphosphate) were purchased from Sigma–Aldrich (USA). The laccase was provided by AB Enzymes GmbH (Germany). Glucose dehydrogenase (GDH) was provided by Roche Diagnostics (Germany). Cellulose acetate filter with a pore size of 0.2 μm was obtained from Sartorius Stedim Biotech GmbH (Germany). Adrenaline solution (1 mg/mL) was purchased from Sanofi–Aventis GmbH (Germany). Pyrroloquinoline quinone (PQQ) was bought from Wako (Japan) and Ringer's solution (8.6 g/L NaCl, 0.3 g/L KCl, 0.33 g/L $CaCl_2 \cdot 2H_2O$) was purchased from Bernburg (Germany).

Modification of the oxygen sensor with enzyme membrane

For the realization of the adrenaline biosensor, a commercial galvanic oxygen sensor (Atlas Scientific, USA) was modified by a bienzyme (laccase/GDH) membrane. The enzyme membrane was prepared from the membrane cocktail consisting of 15 μL of the laccase (1.82 U/μL) solution, 15 μL of GDH (0.03 U/μL) solution combining 20 μM PQQ and 1 mM $CaCl_2$, 60 μL of BSA (10 vol%) and 60 μL mixture of glutaraldehyde (2 vol%) and glycerol (10 vol%) solutions, respectively. All components were mixed with the resulting volumetric ratio of 1/2/2 (enzymes/BSA/glutaraldehyde-glycerol).

A total of 100 μL of the membrane cocktail was then dropped onto a Teflon block. After drying for 24 hat 4 °C, the enzyme membrane with a thickness of ∼130 μm was fixed with the help of a cellulose acetate filter (dialysis membrane, pore size 0.2 μm, Sartorius Stedim Biotech GmbH, Germany) and silicon rubber (TSE 399C, Momentive Performance Materials, Switzerland) onto the high-density polyethylene layer of the oxygen sensor.

Measurement setup

For the electrochemical characterization, the adrenaline biosensor was connected to a potentiometer (2007 Mulitmeter, Keithley Instruments) and exposed to the solution containing different concentrations of adrenaline. Adrenaline solutions with various concentrations were prepared from a stock solution of 0.1 mM adrenaline. The output voltage of the galvanic oxygen sensor is proportional to the oxygen consumption in the solution.

7.7.3 Integration of molecular logic principles with a multi-functional biosensor/actuator system

Materials

Glutaraldehyde, BSA, bovine insulin (27 USP units/mg), GOD (EC 1.1.4., from *Aspergillus niger*), glucose monohydrate, and the buffer components were purchased from Sigma–Aldrich (St. Louis). Hydrochlorid acid was bought from Merck Titrisol (Darmstadt, Germany). N-isopropylacrylamide (NIPAAm, 99%, Sigma–Aldrich), cross-linking agent N,N'-methylenebis(acrylamide) (BIS, 98%, Merck), and the photoinitiator Irgacure 2959 (Ciba) were used as received.

Preparation of glucose sensor

The sensor chips consisting of a p-Si–SiO_2–Ti–Pt structure were fabricated by means of silicon- and thin-film technologies. First, 50 nm SiO_2 was grown by thermal wet oxidation of a p-Si wafer. Then, 20 nm titanium as adhesion layer and subsequently, 200 nm platinum as electrode material for the amperometric glucose sensor were deposited on the SiO_2 surface by electron-beam evaporation and patterned by means of lift-off technique. The wafer was cut into separate chips with a size of 1×2 cm^2. This basis structure was also used for the preparation of the amperometric insulin sensor. After the surface cleaning with acetone, isopropanol and deionized water, the chips were glued onto the substrate holder, electrically connected by means of an ultrasonic wedge bonder and encapsulated with silicone rubber (TSE 399C, Momentive Performance Materials, Switzerland). The contact area of the Pt electrodes with the analyte was ∼0.4 cm^2.

The glucose biosensor was prepared by attaching an enzyme membrane on the platinum electrode. For this, 126 μL phosphat buffer (pH 7.4) containing GOD with a concentration of 166.6 U/mL was mixed with 20 μL of BSA (10 vol%) and 20 μL glutaraldehyde (2 vol%) solutions. The resulting volumetric ratio of all three components

was 1:2:2 (enzyme:BSA:glutaraldehyde). A total of 30 μL of the membrane cocktail was then dropped on the platinum electrode resulting in an enzyme loading of about 1 U/electrode. After drying, the chip was rinsed with buffer solution to remove unbound components and stored at 4 °C.

Preparation of impedimetric sensor for the detection of hydrogel shrinking

The impedimetric sensor for the hydrogel-shrinking detection is based on a platinum interdigitated circle structure and was fabricated as described before for the glucose sensor. The circular structure consists of 24 fingers with a width of 100 μm and a gap between the electrodes of 150 μm. The temperature-responsive hydrogel was prepared from a pre-polymer solution consisting of 100 mM NIPAAm, 1 mM BIS and 0.45 mM Irgacure dissolved in 60 mL deionized water under stirring. The poly-(N-isopropylacrylamide) (PNIPAAm) hydrogel film was prepared by the photopolymerization method. After drying at room temperature, the thickness of the hydrogel was approximately 10 μm in the dry state.

Preparation of insulin sensor

The insulin sensor was prepared by thermal oxidation of a 20 nm thick iridium film deposited on a p-Si–SiO_2–Ti–Pt structure used for the preparation of glucose sensor.

Electrochemical characterization of sensors

For the electrochemical characterization of the amperometric glucose and insulin sensor, the Pt and Ir_xO_y working electrodes were connected to a potentiostat (PalmSens, Palm Instruments BV, Netherlands). A three-electrode arrangement was used, where a conventional liquid-junction Ag/AgCl electrode (Metrohm) was utilized as a reference electrode and a platinum wire as a counter electrode. The swelling/shrinking behavior of the temperature-responsive PNIPAAm hydrogel was studied at different temperatures (28.6 - 42.2 °C) using an impedance measurement system IM6e (Zahner Elektrik GmbH, Germany).

References

[1] K. Szaciłowski. "Digital information processing in molecular systems". *Chemical Reviews* 108 (2008), 3481–3548.

[2] J. Andréasson and U. Pischel. "Smart molecules at work–mimicking advanced logic operations". *Chemical Society Reviews* 39 (2010), 174–188.

[3] J. Andréasson and U. Pischel. "Molecules with a sense of logic: A progress report". *Chemical Society Reviews* 44 (2015), 1053–1069.

[4] E. Katz and V. Privman. "Enzyme-based logic systems for information processing". *Chemical Society Reviews* 39 (2010), 1835–1857.

[5] E. Katz, A. Poghossian, and M. J. Schöning. "Enzyme-based logic gates and circuits-analytical applications and interfacing with electronics". *Analytical and Bioanalytical Chemistry* 409 (2017), 81–94.

[6] Y. Benenson. "Biomolecular computing systems: Principles, progress and potential". *Nature Reviews. Genetics* 13 (2012), 455–468.

[7] Y.-H. Lai, S.-C. Sun, and M.-C. Chuang. "Biosensors with built-in biomolecular logic gates for practical applications". *Biosensors* 4 (2014), 273–300.

[8] J. Wang and E. Katz. "Digital biosensors with built-in logic for biomedical applications - biosensors based on a biocomputing concept". *Analytical and Bioanalytical Chemistry* 398 (2010), 1591–1603.

[9] U. Pischel, J. Andréasson, D. Gust, and V. F. Pais. "Information processing with molecules - Quo vadis?" *ChemPhysChem* 14 (2013), 28–46.

[10] A. Poghossian, E. Katz, and M. J. Schöning. "Enzyme logic AND-Reset and OR-Reset gates based on a field-effect electronic transducer modified with multienzyme membrane". *Chemical Communications* 51 (2015), 6564–6567.

[11] A. Poghossian, K. Malzahn, M. H. Abouzar, P. Mehndiratta, E. Katz, and M. J. Schöning. "Integration of biomolecular logic gates with field-effect transducers". *Electrochimica Acta* 56 (2011), 9661–9665.

[12] E. Katz and S. Minko. "Enzyme-based logic systems interfaced with signal-responsive materials and electrodes". *Chemical Communications* 51 (2015), 3493–3500.

[13] Y. Xiang, X. Qian, Y. Zhang, Y. Chen, Y. Chai, and R. Yuan. "A reagentless, disposable and multiplexed electronic biosensing platform: Application to molecular logic gates". *Biosensors and Bioelectronics* 26 (2011), 3077–3080.

[14] M. Krämer, M. Pita, J. Zhou, M. Ornatska, A. Poghossian, M. J. Schöning, and E. Katz. "Coupling of biocomputing systems with electronic chips: Electronic interface for transduction of biochemical information". *The Journal of Physical Chemistry C* 113 (2009), 2573–2579.

[15] A. Poghossian, M. Krämer, M. H. Abouzar, M. Pita, E. Katz, and M. J. Schöning. "Interfacing of biocomputing systems with silicon chips: Enzyme logic gates based on field-effect devices". *Procedia Chemistry* 1 (2009), 682–685.

[16] E. Katz, J. Wang, M. Privman, and J. Halámek. "Multianalyte digital enzyme biosensors with built-in Boolean logic". *Analytical Chemistry* 84 (2012), 5463–5469.

[17] K. Radhakrishnan, J. Tripathy, and A. M. Raichur. "Dual enzyme responsive microcapsules simulating an "OR" logic gate for biologically triggered drug delivery applications". *Chemical Communications* 49 (2013), 5390–5392.

[18] J. Liu, H. Zhou, J.-J. Xu, and H.-Y. Chen. "Dual-biomarker-based logic-controlled electrochemical diagnosis for prostate cancers". *Electrochemistry Communications* 32 (2013), 27–30.

[19] M. Gamella, A. Zakharchenko, N. Guz, M. Masi, S. Minko, D. M. Kolpashchikov, H. Iken, A. Poghossian, M. J. Schöning, and E. Katz. "DNA computing systems activated by electrochemically-triggered DNA release from a polymer-brush-modified electrode array". *Electroanalysis* 29 (2017), 398–408.

[20] E. Katz, J. M. Pingarrón, S. Mailloux, N. Guz, M. Gamella, G. Melman, and A. Melman. "Substance release triggered by biomolecular signals in bioelectronic systems". *The Journal of Physical Chemistry Letters* 6 (2015), 1340–1347.

[21] M. Zhou, N. Zhou, F. Kuralay, J. R. Windmiller, S. Parkhomovsky, G. Valdés-Ramírez, E. Katz, and J. Wang. "A self-powered "sense-act-treat" system that is based on a biofuel cell and controlled by boolean logic". *Angewandte Chemie* 51 (2012), 2686–2689.

[22] D. Molinnus, M. Bäcker, H. Iken, A. Poghossian, M. Keusgen, and M. J. Schöning. "Concept for a biomolecular logic chip with an integrated sensor and actuator function". *Physica Status Solidi A* 212 (2015), 1382–1388.

[23] D. Rolka, A. Poghossian, and M. J. Schöning. "Integration of a capacitive EIS Sensor into a FIA system for pH and penicillin determination". *Sensors* 4 (2004), 84–94.

[24] M. Beyer, C. Menzel, R. Quack, T. Scheper, K. Schügerl, W. Treichel, H. Voigt, M. Ullrich, and R. Ferretti. "Development and application of a new enzyme sensor type based on the EIS-capacitance structure for bioprocess control". *Biosensors and Bioelectronics* 9 (1994), 17–21.

[25] C. Menzel, T. Lerch, T. Scheper, and K. Schügerl. "Development of biosensors based on an electrolyte isolator semiconductor (EIS) -capacitor structure and their application for process monitoring. Part I. Development of the biosensors and their characterization". *Analytica Chimica Acta* 317 (1995), 259–264.

[26] M. H. Abouzar, A. Poghossian, A. G. Cherstvy, A. M. Pedraza, S. Ingebrandt, and M. J. Schöning. "Label-free electrical detection of DNA by means of field-effect nanoplate capacitors: Experiments and modeling". *Physica Status Solidi A* 209 (2012), 925–934.

[27] A. Poghossian, M. Weil, A. G. Cherstvy, and M. J. Schöning. "Electrical monitoring of polyelectrolyte multilayer formation by means of capacitive field-effect devices". *Analytical and Bioanalytical Chemistry* 405 (2013), 6425–6436.

[28] A. Poghossian and M. J. Schöning. "Label-free sensing of biomolecules with field-effect devices for clinical applications". *Electroanalysis* 26 (2014), 1197–1213.

[29] G. Z. Garyfallou, L. C. de Smet, and E. J. Sudhölter. "The effect of the type of doping on the electrical characteristics of electrolyte–oxide–silicon sensors: pH sensing and polyelectrolyte adsorption". *Sensors and Actuators B: Chemical* 168 (2012), 207–213.

[30] A. Poghossian, M. Bäcker, D. Mayer, and M. J. Schöning. "Gating capacitive field-effect sensors by the charge of nanoparticle/molecule hybrids". *Nanoscale* 7 (2015), 1023–1031.

[31] J. R. Siqueira, M. H. Abouzar, M. Bäcker, V. Zucolotto, A. Poghossian, O. N. Oliveira, and M. J. Schöning. "Carbon nanotubes in nanostructured films: Potential application as amperometric and potentiometric field-effect (bio-)chemical sensors". *Physica Status Solidi A* 206 (2009), 462–467.

[32] D.-H. Kwon, B.-W. Cho, C.-S. Kim, and B.-K. Sohn. "Effects of heat treatment on Ta_2O_5 sensing membrane for low drift and high sensitivity pH-ISFET". *Sensors and Actuators B: Chemical* 34 (1996), 441–445.

[33] A. S. Poghossian. "The super-Nernstian pH sensitivity of Ta_2O_5-gate ISFETs". *Sensors and Actuators B: Chemical* 7 (1992), 367–370.

[34] F. Moseley, J. Halámek, F. Kramer, A. Poghossian, M. J. Schöning, and E. Katz. "An enzyme-based reversible CNOT logic gate realized in a flow system". *The Analyst* 139 (2014), 1839–1842.

[35] D. Molinnus, M. Sorich, A. Bartz, P. Siegert, H. S. Willenberg, F. Lisdat, A. Poghossian, M. Keusgen, and M. J. Schöning. "Towards an adrenaline biosensor based on substrate recycling amplification in combination with an enzyme logic gate". *Sensors and Actuators B: Chemical* 237 (2016), 190–195.

[36] W. F. Young and A. W. Stanson. "What are the keys to successful adrenal venous sampling (AVS) in patients with primary aldosteronism?" *Clinical Endocrinolody* 70 (2009), 14–17.

[37] P. Collste, B. Brismar, A. Alveryd, I. Björkhem, C. Hårdstedt, L. Svensson, and J. Ostman. "The catecholamine concentration in central veins of hypertensive patients - an aid not without problems in locating phaeochromocytoma". *Acta Chirurgica Scandinavica, Supplementum* 530 (1986), 67–71.

[38] E. L. Bravo, R. C. Tarazi, F. M. Fouad, D. G. Vidt, and R. W. Gifford. "Clonidine-suppression test: A useful aid in the diagnosis of pheochromocytoma". *New England Journal of Medicine* 305 (1981), 623–626.

[39] G. P. Rossi, R. J. Auchus, M. Brown, J. W. M. Lenders, M. Naruse, P. F. Plouin, F. Satoh, and W. F. Young. "An expert consensus statement on use of adrenal vein sampling for the subtyping of primary aldosteronism". *Hypertension* 63 (2013), 151–160.

[40] T. Dekkers, J. Deinum, L. J. Schultzekool, D. Blondin, O. Vonend, A.R.R.M. Hermus, M. Peitzsch, L. C. Rump, G. Antoch, F.C.G.J. Sweep, S. R. Bornstein, J. W. M. Lenders, H. S. Willenberg, and G. Eisenhofer. "Plasma metanephrine for assessing the selectivity of adrenal venous sampling". *Hypertension* 62 (2013), 1152–1157.

[41] A. L. Ghindilis, A. Makower, C. G. Bauer, F. F. Bier, and F. W. Scheller. "Determination of *p*-aminophenol and catecholamines at picomolar concentrations based on recycling enzyme amplification". *Analytica Chimica Acta* 304 (1995), 25–31.

[42] F. Lisdat, U. Wollenberger, A. Makower, H. Hörtnagl, D. Pfeiffer, and F. W. Scheller. "Catecholamine detection using enzymatic amplification". *Biosensors and Bioelectronics* 12 (1997), 1199–1211.

[43] J. Szeponik, B. Möller, D. Pfeiffer, F. Lisdat, U. Wollenberger, A. Makower, and F. W. Scheller. "Ultrasensitive bienzyme sensor for adrenaline". *Biosensors and Bioelectronics* 12 (1997), 947–952.

[44] Y. Benenson, B. Gil, U. Ben-Dor, R. Adar, and E. Shapiro. "An autonomous molecular computer for logical control of gene expression". *Nature* 429 (2004), 423–429.

[45] M. E. Caldorera-Moore, W. B. Liechty, and N. A. Peppas. "Responsive theranostic systems: Integration of diagnostic imaging agents and responsive controlled release drug delivery carriers". *Accounts of Chemical Research* 44 (2011), 1061–1070.

[46] S. Mailloux, J. Halámek, and E. Katz. "A model system for targeted drug release triggered by biomolecular signals logically processed through enzyme logic networks". *The Analyst* 139 (2014), 982–986.

[47] I. Tokarev and S. Minko. "Stimuli-responsive hydrogel thin films". *Soft Matter* 5 (2009), 511–524.

[48] T. Khaleque, S. Abu-Salih, J. R. Saunders, and W. Moussa. "Experimental methods of actuation, characterization and prototyping of hydrogels for bioMEMS/NEMS applications". *Journal of Nanoscience and Nanotechnology* 11 (2011), 2470–2479.

[49] M. Bäcker, M. Raue, S. Schusser, C. Jeitner, L. Breuer, P. Wagner, A. Poghossian, A. Förster, T. Mang, and M. J. Schöning. "Microfluidic chip with integrated microvalves based on temperature- and pH-responsive hydrogel thin films". *Physica Status Solidi A* 209 (2012), 839–845.

[50] A. Richter, S. Klatt, G. Paschew, and C. Klenke. "Micropumps operated by swelling and shrinking of temperature-sensitive hydrogels". *Lab on a Chip* 9 (2009), 613–618.

[51] M. F. Smiechowski and V. F. Lvovich. "Iridium oxide sensors for acidity and basicity detection in industrial lubricants". *Sensors and Actuators B: Chemical* 96 (2003), 261–267.

[52] H. R. Murphy, K. Kumareswaran, D. Elleri, J. M. Allen, K. Caldwell, M. Biagioni, D. Simmons, D. B. Dunger, M. Nodale, M. E. Wilinska, S. A. Amiel, and R. Hovorka. "Safety and efficacy of 24-h closed-loop insulin delivery in well-controlled pregnant women with type 1 diabetes: A randomized crossover case series". *Diabetes Care* 34 (2011), 2527–2529.

[53] B. W. Bequette. "A critical assessment of algorithms and challenges in the development of a closed-loop artificial pancreas". *Diabetes Technology and Therapeutics* 7 (2005), 28–47.

[54] Medtronic. *MiniMed 670G System*. 24/04/2017. URL: `www.medtronic-diabetes.com/products/minimed-670g-insulin-pump-system,`.

[55] P. A. Bakhtiani, L. M. Zhao, J. El Youssef, J. R. Castle, and W. K. Ward. "A review of artificial pancreas technologies with an emphasis on bi-hormonal therapy". *Diabetes, Obesity and Metabolism* 15 (2013), 1065–1070.

[56] X. Yu, W. Lian, J. Zhang, and H. Liu. "Multi-input and -output logic circuits based on bioelectrocatalysis with horseradish peroxidase and glucose oxidase immobilized in multi-responsive copolymer films on electrodes". *Biosensors and Bioelectronics* 80 (2016), 631–639.

[57] E. Gdor, S. Shemesh, S. Magdassi, and D. Mandler. "Multienzyme inkjet printed 2D arrays". *ACS Applied Materials and Interfaces* 7 (2015), 17985–17992.

[58] O. B. Ayyub and P. Kofinas. "Enzyme induced stiffening of nanoparticle-hydrogel composites with structural color". *ACS Nano* 9 (2015), 8004–8011.

[59] Y. Huang, X. Ran, Y. Lin, J. Ren, and X. Qu. "Enzyme-regulated the changes of pH values for assembling a colorimetric and multistage interconnection logic network with multiple readouts". *Analytica Chimica Acta* 870 (2015), 92–98.

[60] L. Wang, W. Lian, H. Yao, and H. Liu. "Multiple-stimuli responsive bioelectrocatalysis based on reduced graphene oxide/poly(N-isopropylacrylamide) composite films and its application in the fabrication of logic gates". *ACS Applied Materials and Interfaces* 7 (2015), 5168–5176.

[61] L. Ma and A. Diao. "Design of enzyme-interfaced DNA logic operations (AND, OR and INHIBIT) with an assaying application for single-base mismatch". *Chemical Communications* 51 (2015), 10233–10235.

[62] T. Miyake, E. E. Josberger, S. Keene, Y. Deng, and M. Rolandi. "An enzyme logic bioprotonic transducer". *APL Materials* 3 (2015), 014906.

[63] S. Liu, L. Wang, W. Lian, H. Liu, and C.-Z. Li. "Logic gate system with three outputs and three inputs based on switchable electrocatalysis of glucose by glucose oxidase entrapped in chitosan films". *Chemistry - An Asian Journal* 10 (2015), 225–230.

[64] M. Ikeda, T. Tanida, T. Yoshii, K. Kurotani, S. Onogi, K. Urayama, and I. Hamachi. "Installing logic-gate responses to a variety of biological substances in supramolecular hydrogel-enzyme hybrids". *Nature Chemistry* 6 (2014), 511–518.

[65] J. Guo, J. Zhuang, F. Wang, K. R. Raghupathi, and S. Thayumanavan. "Protein and enzyme gated supramolecular disassembly". *Journal of the American Chemical Society* 136 (2014), 2220–2223.

[66] J. Chen and L. Zeng. "Enzyme-amplified electronic logic gates based on split/intact aptamers". *Biosensors and Bioelectronics* 42 (2013), 93–99.

[67] W. Liu, L. Wu, S. Yan, R. Huang, X. Weng, and X. Zhou. "Graphene oxide-based fluorescent detection of DNA and enzymes using Hoechst 33258 and its use for dual-output fluorescent logic gates". *Analytical Methods* 5 (2013), 3631.

[68] S. Domanskyi and V. Privman. "Design of digital response in enzyme-based bioanalytical systems for information processing applications". *The Journal of Physical Chemistry. B* 116 (2012), 13690–13695.

[69] E. Kim, Y. Liu, W. E. Bentley, and G. F. Payne. "Redox capacitor to establish bio-device redox-connectivity". *Advanced Functional Materials* 22 (2012), 1409–1416.

[70] M. Zhou and J. Wang. "Biofuel cells for self-powered electrochemical biosensing and logic biosensing: A Review". *Electroanalysis* 24 (2012), 197–209.

[71] S. Perez Rafael, A. Vallée-Bélisle, E. Fabregas, K. Plaxco, G. Palleschi, and F. Ricci. "Employing the metabolic "branch point effect" to generate an all-or-none, digital-like response in enzymatic outputs and enzyme-based sensors". *Analytical Chemistry* 84 (2012), 1076–1082.

[72] T. K. Tam. "Switchable biocatalytic electrodes controlled by biomolecular computing systems." *International Journal of Unconventional Computing* 8 (2012), 367–381.

[73] M. Pita. "Switchable biofuel cells controlled by biomolecular computing systems". *International Journal of Unconventional Computing* 8 (2012), 391–417.

[74] K.-W. Kim, B. C. Kim, H. J. Lee, J. Kim, and M.-K. Oh. "Enzyme logic gates based on enzyme-coated carbon nanotubes". *Electroanalysis* 23 (2011), 980–986.

[75] M. Zhou, F. Wang, and S. Dong. "Boolean logic gates based on oxygen-controlled biofuel cell in "one pot"". *Electrochimica Acta* 56 (2011), 4112–4118.

[76] M. Zhou, X. Zheng, J. Wang, and S. Dong. "A self-powered and reusable biocomputing security keypad lock system based on biofuel cells". *Chemistry* 16 (2010), 7719–7724.

[77] S. Sivan, S. Tuchman, and N. Lotan. "A biochemical logic gate using an enzyme and its inhibitor. Part II: The logic gate". *Biosystems* 70 (2003), 21–33.

[78] S. Sivan and N. Lotan. "A biochemical logic gate using an enzyme and its inhibitor. 1. The inhibitor as switching element". *Biotechnology Progress* 15 (1999), 964–970.

[79] A. Arkin and J. Ross. "Computational functions in biochemical reaction networks". *Biophysical Journal* 67 (1994), 560–578.

[80] Y. Jia, R. Duan, F. Hong, B. Wang, N. Liu, and F. Xia. "Electrochemical biocomputing: A new class of molecular-electronic logic devices". *Soft Matter* 9 (2013), 6571–6577.

8 Development and characterization of a field-effect biosensor for the detection of acetoin (*Biosensors and Bioelectronics,* 115, (2018), *in press*)

D. Molinnus, L. Muschallik, L. Osorio Gonzalez, J. Bongaerts, T. Wagner, T. Selmer, P. Siegert, M. Keusgen and M. J. Schöning

Published in: *Biosensors and Bioelectronics,* Vol. 115, (2018), *in press.*

Submitted: 2018-03-06; Accepted: 2018-05-10; Published: 2018-05-18

8.1 Abstract

A capacitive electrolyte-insulator-semiconductor (EIS) field-effect biosensor for acetoin detection has been presented for the first time. The EIS sensor consists of a layer structure of Al/p-Si/SiO_2/Ta_2O_5/enzyme acetoin reductase. The enzyme, also referred to as butane-2,3-diol dehydrogenase from *B. clausii* DSM 8716^T, has been recently characterized. The enzyme catalyzes the (*R*)-specific reduction of racemic acetoin to (*R,R*)- and *meso*-butane-2,3-diol, respectively. Two different enzyme-immobilization strategies (cross-linking by using glutaraldehyde and adsorption) have been studied. Typical biosensor parameters such as optimal pH-working range, sensitivity, hysteresis, linear concentration range and long-term stability have been examined by means of constant-capacitance (ConCap) mode measurements. Furthermore, preliminary experiments have been successfully carried out for the detection of acetoin in diluted white wine samples.

8.2 Introduction

Acetoin and diacetyl are widely distributed in various beverages, and are also used in foods and cosmetics as flavouring and fragrance, as well as in chemical synthesis [1–4]. These compounds are products of fermentative metabolism in different microorganisms. Acetoin can be formed, e.g., in most bacteria from pyruvate and is thus a product of carbohydrate metabolism, or from diacetyl while NAD(P)H serves as a cofactor of the enzyme acetoin reductase [5, 6].

During the fermentation process of alcoholic beverages, such as beer or wine, acetoin plays an important role in their quality due to its buttery-like taste, although acetoin is not pungent smelling [7].Typical acetoin concentrations in alcoholic beverages are in the range of 10 μM to 50 μM in beer, 500 μM in white wine and 150 μM in red wine [7–9]. The detection of acetoin content during the fermentation process could control the quality of alcoholic beverages due to its involvement in the wine bouquet or its influence in the beer flavor. Furthermore, the acetoin concentration during beer storage is used as a parameter to establish the degree of the beer‘s maturity [8]. Precise detection of the acetoin level can be used to avoid unnecessary maturation time [7, 10]. Hence, its control of concentration change during the fermentation course could help assess the fermentation process, as well as the maturation process.

Several methods have already been described for the detection of acetoin, mainly colorimetric techniques, like the Voges-Proskauer test, which is the most commonly applied procedure for the detection of acetoin in analytical microbiology or gas chromatography [11, 12]. However, none of these techniques provide the advantages that can be achieved by using a biosensor which offers a faster analytical approach and that does not need additional trained staff.

Capacitive EIS sensors are field-effect devices that are used for the detection of surface-potential changes, e.g., due to pH alterations [13]. These changes can also be induced by, e.g., enzymatic reactions [14–17], and binding of charged molecules, like DNA [18–21]. These sensors can also be applied for the development of enzyme logic gates [22–24]. Furthermore, EIS sensors have many advantages over conventional analytical methods such as small size, low weight and fast response time, and they are easy and cost-effective in fabrication [25–27]. Furthermore, due to the miniaturized sensor layout, only a small sample volume is necessary for the measurement. Additionally, with an array of different modified EIS sensors, several analytes can be detected simultaneously.

In this study, we report on the development of a chip-based biosensor for the acetoin detection for the first time. The sensor is based on a pH-sensitive capacitive EIS field-effect structure consisting of an Al/p-Si/SiO_2/Ta_2O_5 layer set-up. The chip was modified using a recently introduced acetoin reductase from *B. clausii* DSM 8716^T [28] accountable for the reduction of acetoin in the presence of NADH as a cofactor [29]. The local pH shift induced by the enzymatic reaction resulted in the modulation of the flat-band potential of the field-effect biosensor, arising in a shift of the capacitance-voltage (C-V) curve of the EIS structure. Two immobilization strategies, namely adsorptive binding and cross-linking by forming cross-linkages between the enzyme molecules, have been investigated to attach the acetoin reductase to the pH-sensitive Ta_2O_5 surface of the EIS-sensor chip. Characteristic biosensor parameters such as linear concentration

range, pH optimum of the field-effect sensor with the immobilized enzyme, sensitivity, lower and upper detection limit, hysteresis and long-term stability will be discussed. In addition, the newly developed acetoin biosensor was applied for measurements in real samples such as white wine.

8.3 Experimental

8.3.1 Materials

Acetoin and the cofactor NADH were acquired from Sigma-Aldrich (USA), as well as glutaraldehyde, glycerol and NaCl. TRIS-HCl buffer (0.2 mM) was purchased from Carl Roth (Germany). The respective pH values of the buffer solution were adjusted by addition of 0.1 M NaOH or 0.1 M HCl. The enzyme acetoin reductase from *B. clausii* (∼380 U/mL) is produced in our institute as described before [28].

8.3.2 Preparation of the sensor structures

The applied capacitive EIS sensor consists of the following layer stack: a p-doped silicon substrate with a thickness of ∼400 μm and a specific resistance of ρ = 5 - 10 Ωcm, a 30 nm thermally grown SiO_2 insulating layer and a 60 nm thick Ta_2O_5 gate-insulator layer (for that 30 nm Ta is deposited by electron-beam evaporation, followed by a thermal oxidation step). A rear-side contact, consisting of a 300 nm thick aluminum layer is deposited by electron-beam evaporation and annealed afterwards. As a final step, the wafer is separated into 1 cm x 1 cm chips with a diamond saw. Fig. 8.1 shows the EIS-sensor set-up with the different layers. Detailed information about the sensor‘s fabrication process is described in [27]. The Ta_2O_5 layer as gate insulator has been selected because of its well-known excellent pH behavior and high permittivity but also because of its chemical stability [30, 31].

The acetoin EIS biosensor was developed by modifying the Ta_2O_5 surface with the enzyme acetoin reductase. Immediately before modification, each sensor was cleaned in acetone, isopropanol and deionized water for 5 minutes, respectively. Two different immobilization strategies have been investigated. As first immobilization method, the enzyme acetoin reductase is adsorptively bound to the sensor surface. For this, ∼80 μL of acetoin reductase solution was dropped onto the sensor surface. For the second immobilization procedure, cross-linking is performed by formation of cross-linkages between the enzyme molecules, where the membrane cocktail consisting of 48 μL glutaraldehyde (2 vol%) / glycerol (10 vol%) solution and 32 μL of enzyme solution was mixed. 80 μL of the membrane cocktail was pipetted onto the Ta_2O_5 surface. After drying of the different prepared EIS sensors, they were mounted into a homemade measuring cell, sealed by an O-ring to protect the rear-side contact and to define the contact area of the EIS sensor with the analyte solution (∼0.5 cm^2). Before measurements, the sensors were stored at 4 °C in the dark.

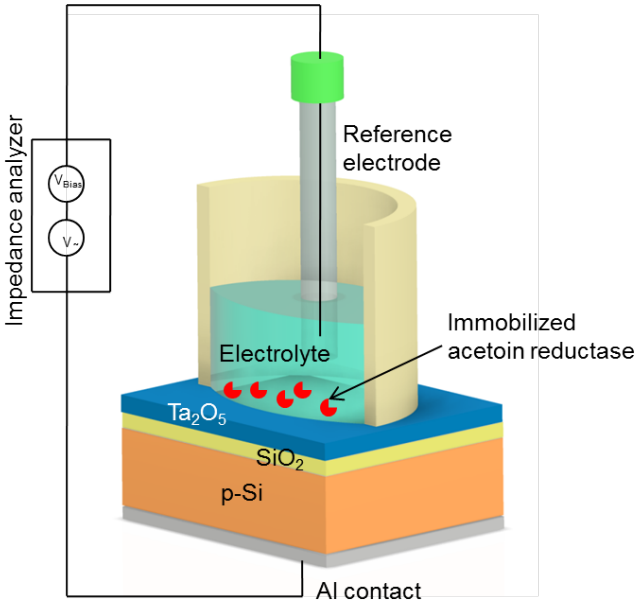

Fig. 8.1: Schematic of the measurement set-up with the Al-p-Si-SiO_2-Ta_2O_5 EIS sensor modified with the enzyme acetoin reductase for the detection of acetoin.

8.4 Measurement principle

Fig. 8.1 illustrates the measurement set-up with the developed acetoin field-effect biosensor. For the electrochemical characterization of the acetoin biosensor chip, C-V (capacitance/voltage) and ConCap (constant capacitance) measurements were performed by connecting the EIS chip with an impedance analyzer IM6 (Zahner Elektrik, Germany). Before performing ConCap measurements, C-V curves of each sensor chip, in a gate-voltage range between -2 V and 2 V with steps of 100 mV were recorded to define a fixed capacitance value (in the linear range of the depletion region, ~60% of the maximum capacitance) using a feedback-control circuit. With the help of ConCap measurements, potential and/or charge changes at the Ta_2O_5 surface can be detected in real time. An external liquid-junction Ag/AgCl electrode (Metrohm, Germany) filled with 3 M KCl was applied as the reference electrode. The C-V- and ConCap measurements were carried out at a frequency of 120 Hz. A 20 mV ac (alternating current) voltage has been applied between the Ag/AgCl reference electrode and the rear-side Al contact, to measure the capacitance. The measurement principle for the detection of acetoin using the capacitive field-effect sensor is based on the enzymatic reaction as depicted in equation 1.1. (R)- and (S)-acetoin will be reduced by the *R*-specific enzyme acetoin reductase to (*R*,*R*)-2,3-butanediol and *meso*-butanediol, respectively, while NADH serves as a cofactor and will be oxidized to NAD^+ (nicotinamide adenine dinucleotide).

$$acetoin + NADH + H^+ \xrightarrow{\text{acetoin reductase}} 2,3-butanediol + NAD^+ \qquad (8.1)$$

As a result of this enzymatic reaction, the hydrogen-ion concentration decreases,

and this pH change can be detected by the pH-sensitive Ta_2O_5 transducer surface of the field-effect sensor. The resulting change in the flat-band potential of the sensor is recorded and corresponds to the measured acetoin concentration. All measurements were performed in a dark Faraday cage at room temperature. Before starting the measurements, the sensor chip was incubated in 0.2 mM TRIS-HCl buffer solution (pH 7.1) containing 150 mM NaCl for 2 h. All solutions contained 500 μM of the cofactor NADH and all measurements were performed in 1 mL analyte solution containing different acetoin concentrations varying from 1 μM to 500 μM. The pH value of the solutions used was additionally controlled by a pH meter (Mettler-Toledo, Germany).

8.5 Results and discussions

8.5.1 Electrochemical characterization of the capacitive acetoin biosensor

Before surface modification, the functionality and pH sensitivity of the bare EIS-sensor chip was studied. Therefore, the pH sensitivity of each sensor was determined in the ConCap measurement mode with standard pH buffer solutions (Titrisol, Merck, Germany). The result of a typical ConCap-measurement of a bare EIS-sensor chip is presented in Fig. 8.2, for the pH values of 7-8-9-8-7-6-5-6-7, respectively. Each pH value has been recorded for 5 minutes. As the pH buffer solution is changed, an immediate signal step is perceived. This result shows that the EIS sensor is highly reproducible as demonstrated for pH 7.0, which was measured three times within this measurement cycle, yielding a potential at this pH value that is always -179 $\pm$ 5 mV. The corresponding calibration curve is shown in the inset figure of Fig. 8.2 and demonstrates a nearly Nernstian pH sensitivity of 55.9 mV/pH, as described in literature [27].

Additionally, different acetoin concentrations in the range between 30 μM and 90 μM were tested with the bare sensor chip (i.e., without the immobilized enzyme) (data not shown). The variation of the acetoin concentration only resulted in negligible potential changes of less than 3 mV, which can be related to slight pH variations of the analyte and drift effects of the sensor chip itself. In a further experiment, the EIS-sensor chip modified with the enzyme acetoin reductase was also examined with regard to its original pH sensitivity in Titrisol buffer solutions of different pH values (identical procedure as performed in Fig. 8.2). The sensor modified by the enzyme possesses a similar sensitivity of 55.7 mV/pH as for the bare EIS sensor. Thus, the immobilized enzyme has no influence on the pH response of the pH-sensitive Ta_2O_5-transducer layer.

The immobilization of the enzyme onto the sensor surface is always an essential step in the development of a biosensor. Several immobilization methods such as adsorptive binding, covalent bonding, entrapment or cross-linking have been discussed in literature (Sassolas et *al.* 2012). For the immobilization of the enzyme acetoin reductase, two different immobilization methods were investigated, in particular, adsorptive binding and cross-linking by using glutaraldehyde to form a stable membrane which is drop-coated onto the sensor surface. Biosensor chips were prepared with each immobilization method.

The influence of the enzyme immobilization on the sensitivity of the capacitive acetoin EIS-biosensor chip was studied at different acetoin concentrations ranging between

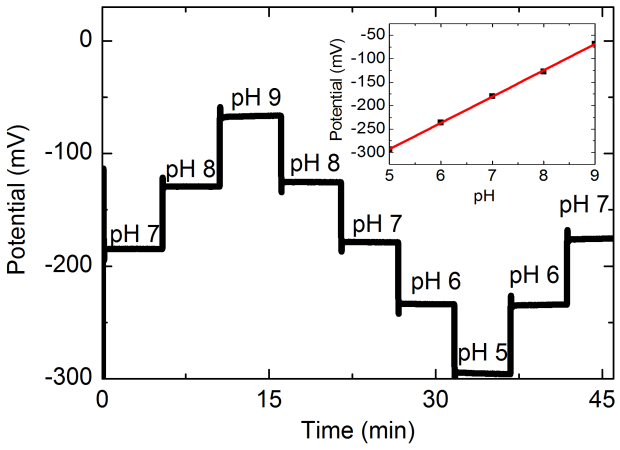

Fig. 8.2: Typical ConCap measurement for different pH values of Titrisol buffer solution of a bare EIS sensor; the inset figure depicts the resulting calibration curve with an average slope of 55.9 mV/pH between pH 5 and pH 9.

30 μM and 90 μM in 0.2 mM TRIS-HCl buffer solution, containing 150 mM NaCl and 500 μM NADH at pH 7.1. Fig. 8.3a) shows the results of the mean values of the sensitivities. The two bars depict the mean values of the sensitivities obtained from each three individual sensors modified using adsorptive binding and cross-linking, respectively. The highest sensitivity has been observed with the sensors modified by means of cross-linking with a mean sensitivity of 65 mV/dec, while the sensors modified using adsorptive immobilization only have a mean sensitivity of 27 mV/dec. These results demonstrate that although the adsorption method causes little to no enzyme inactivation, the enzymes are probably loosely attached to the sensor surface resulting in less amount of enzymes, which are fixed on the surface and hence, a lower acetoin sensitivity was achieved. Therefore, for the subsequent experiments, the sensor was modified by applying the cross-linking method for the immobilization of the enzyme.

To investigate the lower and upper detection limit of the developed biosensor chip towards acetoin, ConCap measurements were furtherly performed in the acetoin concentration range between 1 μM and 500 μM. Fig. 8.3b) shows an S-shaped calibration curve, as typically expected for electrochemical biosensors. The sensor signal is plotted versus the logarithmic acetoin concentration. A linear behavior in the acetoin concentration range between 10 μM and 90 μM with a sensitivity of 65 mV/dec is given. A saturation effect is resulting for acetoin concentrations higher than 150 μM. Due to the enzymatic reaction, the pH increase close to the sensor surface might lead to an enzyme inhibition due to the pH dependence of acetoin reductase's activity (see also Fig. 8.4). Note that a shift in the biosensor signal of about 65 mV for varying acetoin concentrations corresponds to a pH shift from originally pH 7.1 to about pH 8.2 at the biosensor surface. This is defined by the pH sensitivity of the Ta_2O_5 layer with immobilized enzyme of about 56 mV/pH as described above. On the other side, the curve starts to get flat at low acetoin concentrations (<10 μM) that defines the detection limit of the

biosensor set-up.

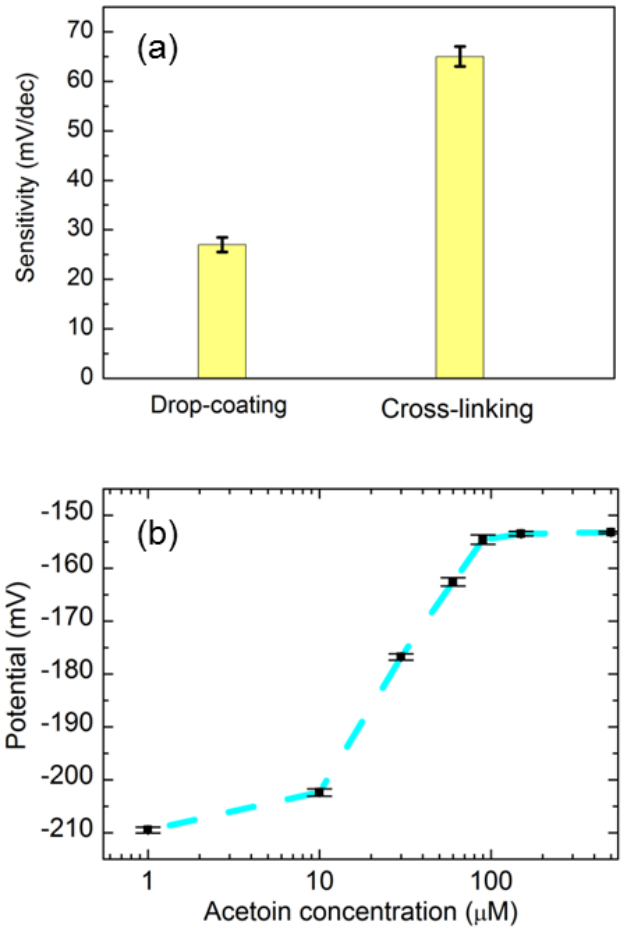

Fig. 8.3: (a) Mean values of the sensitivity with standard deviation (set of three series of measurements for each immobilization method) for the capacitive acetoin EIS-biosensor chip recorded in buffer solution with different acetoin concentrations from 30 μM to 90 μM. (b) Calibration plot with standard deviation obtained with the capacitive, cross-linked acetoin EIS-biosensor chip measured in the acetoin concentration range between 1 μM and 500 μM.

To study the pH influence on the sensitivity of the developed capacitive acetoin EIS biosensor in more detail, measurements in the ConCap mode were performed by variation of the pH of the buffer solution over a range from pH 6.5 to pH 8.0. Different acetoin concentrations ranging from 30 μM to 90 μM (buffer solution) were taken into account for the measurement. Fig. 8.4a) summarizes the mean values and their standard deviations of the sensitivity obtained for three individual acetoin biosensors determined at each pH value. Maximum response with a sensitivity of 65 $\pm$ 4 mV/dec could be reached at a pH value of $\sim$7.1, which is also consistent with the pH optimum of the used acetoin reductase ($\sim$pH 7.0) for the given reaction [28].

Fig. 8.4b) demonstrates an example of a ConCap measurement of the acetoin biosen-

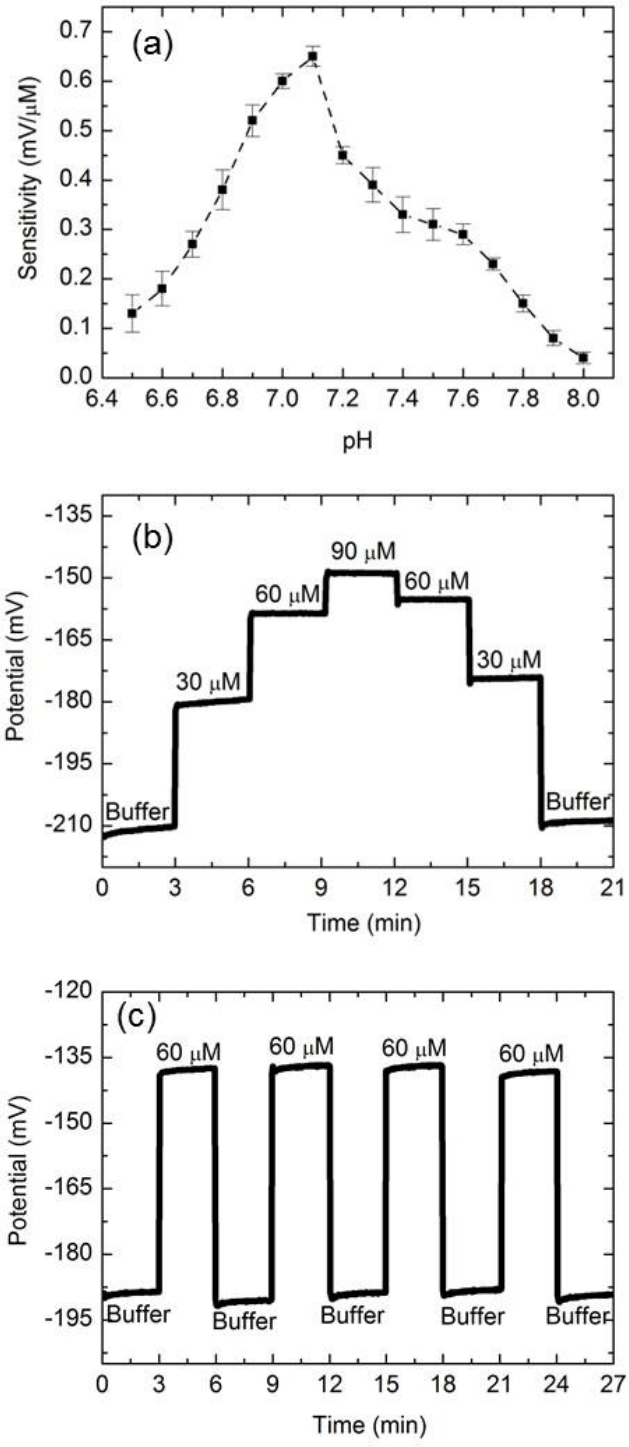

Fig. 8.4: (a) Mean values of the sensitivity with standard deviation (set of three series of measurements) for three fabricated capacitive acetoin EIS biosensors recorded in TRIS-HCl buffer containing 150 mM NaCl in the pH range between pH 6.5 and pH 8.0 with different acetoin concentrations from 30 μM to 90 μM. (b) Typical ConCap-calibration measurement of different acetoin concentrations in the range from 30 μM to 90 μM measured by the acetoin biosensor chip. (c) Reproducibility measurement of buffer solution alternating with 60 μM acetoin.

sor with regard to its hysteresis behavior and response time. Acetoin concentrations were varied starting with a concentration of 30 μM up to 90 μM and then decreasing the concentration again down to 30 μM. Each concentration was recorded for 3 min and was varied in steps of 30 μM. A clear dependence of the sensor signal on the acetoin concentration is observed. The sensor signal is increasing with an increase of the acetoin concentration due to the decrease of the H^+-ion concentration as discussed in equation 8.1 affected by the biocatalytic reaction. Furthermore, the sensor output is almost the same in the upward and downward series of the performed measurement with a small hysteresis of less than 5 mV. In contrast to standard measurement techniques for the detection of acetoin [12], the response time $t_{90\%}$ is only about 25 s by using the developed acetoin EIS biosensor.

To proof the reproducibility of the developed acetoin biosensor chip, the sensor signal of the measurement performed in TRIS-HCl buffer solution at pH 7.1 was recorded in alternation with an acetoin concentration of 60 μM in the ConCap mode. Fig. 8.4c) shows exemplarily the results obtained with one sensor, when this cycle is repeated four (60 μM acetoin) and five (buffer) times, respectively. The sensor signal is increased to a value of -137 $\pm$ 1 mV with each acetoin concentration step and again decreased when measured in buffer solution to a value of -189 $\pm$ 1 mV. This experiment again underlines that the sensor delivered reproducible and reversible results independent of the titration direction, only with a small hysteresis of $\sim$1 mV.

The stability of a biosensor often limits its use to a certain number of measurements, and losses of sensitivity are caused due to either the decrease of the applied enzyme activity or the enzyme leakage out from the sensor surface after a certain time. Therefore, the biosensor's stability has been studied over a time period of 5 days (see Fig. 8.5).

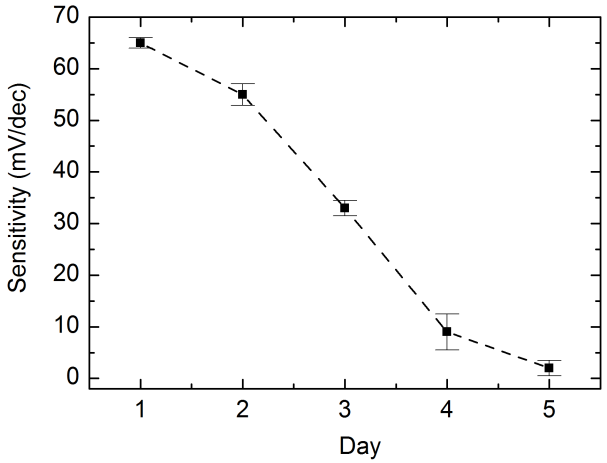

Fig. 8.5: Long-term stability of the acetoin biosensor. Mean values of the sensitivity with standard deviations of three individual biosensors recorded in buffer solution at different days (day 1 to day 5) with different acetoin concentrations from 30 μM to 90 μM.

At each day, different acetoin concentrations between 30 μM and 90 μM were measured in buffer solution. Three individual biosensor chips were tested. Between the

measurements, the sensors were stored under dry conditions in the refrigerator at 4 °C. The results of mean values of the obtained sensitivities with their standard deviations are overviewed in Fig. 8.5.

Within the first two days, the biosensors show good sensitivities of about 65 mV/dec and 55 mV/dec, respectively. However, after two performed measurement days, the sensitivity starts to decrease rapidly to a value of 3 mV/dec at day 5. These results are comparable to results obtained, when the pure enzyme activity was investigated in solution without immobilization [28].

8.5.2 Application of the acetoin biosensor chip in wine

The aim of the newly developed capacitive acetoin EIS biosensor is to control and monitor fermentation processes to avoid unnecessary storage of beer or wine. Therefore, such biosensor chip should be able to detect acetoin in real fermentation samples.

In this study, preliminary experiments have been performed in diluted white wine samples (alcohol 10 vol%) to verify the ability of the acetoin biosensor. The pH value of white wine was about pH 3.3. After dilution with TRIS-HCl buffer solution (pH 7.1) containing 150 mM NaCl (wine to buffer mixture of 1:50), the pH value was about pH 3.8. Therefore, the pH value was adjusted to pH 7.1, the optimum working pH of the field-effect sensor with the immobilized enzyme, by addition of 0.1 M NaOH. Different acetoin concentrations between 1 μM and 500 μM were spiked to the wine-buffer mixture. As already demonstrated for the buffer solution containing varying acetoin concentrations (see Fig. 8.3), Fig. 8.6a) depicts again a typical S-shaped calibration curve obtained in the wine-buffer mixture with the potential recordings depending on the logarithmic acetoin concentration. Here, a linear behavior was reached in the acetoin concentration range between 10 μM and 90 μM with an average sensitivity of 40 mV/dec. Note that the average sensitivity is somewhat lower than for the acetoin measurements in buffer without wine (65 mV/dec). On the other hand, the sensitivity and detection limit of the developed biosensor is sufficient to detect acetoin in the industrially relevant concentration range. For the detection of higher concentrations, the sample might be diluted if necessary.

Fig. 8.6b) demonstrates exemplarily a ConCap response of the acetoin biosensor in buffer solution and wine-buffer mixture, both at pH 7.1, without acetoin or spiked with different acetoin concentrations (30 μM to 90 μM). The sensor signal obtained in each solution was recorded for 3 min. Again, with increasing acetoin concentrations, the biosensor signal raises, clarifying the clear dependence of the biosensor signal in wine-buffer mixtures with spiked acetoin content. Interestingly, an increase in the biosensor signal was also observed for the pure wine-buffer mixture (without additionally spiked acetoin). The shift in contrast to the sensor signal in buffer might be explained due to the naturally present acetoin content in that sample. These experiments in wine-buffer mixture underline that the developed acetoin biosensor can detect different acetoin concentrations even in real samples.

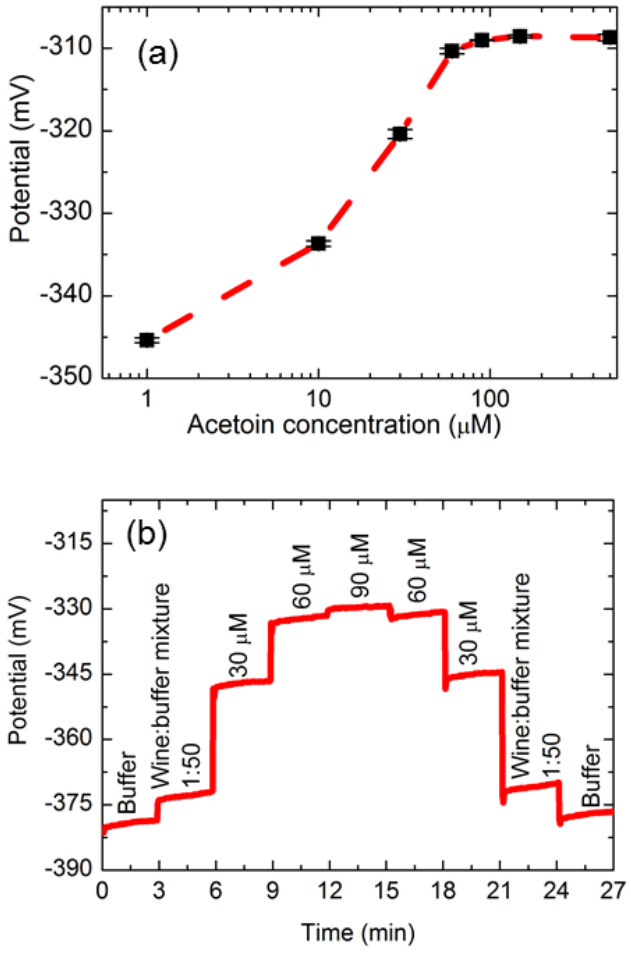

Fig. 8.6: (a) Calibration plot with standard deviation obtained with the capacitive acetoin EIS biosensor measured in a concentration range between 1 μM and 500 μM in a wine-buffer mixture (1:50). (b) ConCap measurement of different acetoin concentrations in a wine-buffer mixture (1:50) in the range from 30 μM to 90 μM measured by the acetoin biosensor chip.

8.6 Conclusions

A capacitive EIS field-effect biosensor has been modified by a recently introduced acetoin reductase. Due to the immobilized enzyme, racemic acetoin will be converted to (*R,R*)-2,3-butanediol and *meso*-butanediol, respectively, in a H^+-consuming reaction resulting in a pH change that can be detected by the EIS sensor. The acetoin biosensor has been characterized regarding the immobilization method and the pH optimum. The developed biosensor depicted the highest sensitivity through immobilization of the enzyme via cross-linking by using glutaraldehyde at a pH value of 7.1. Furthermore, reproducible measurement results could be achieved at different acetoin concentrations in the range between 10 μM and 100 μM with an average acetoin sensitivity of 65 mV/dec. The sensor shows a long-term stability of around two days, which should be further im-

proved. Ongoing experiments are dealing with the stabilization of the enzyme‘s activity. Moreover, first experiments in white wine have been carried out where acetoin concentrations between 10 μM and 90 μM could be successfully detected, giving a hint that the sensor can be applied to real fermentation solutions. In future experiments, possible cross-sensitivity effects towards diacetyl and acetylbutanediol shall be investigated, especially for diacetyl, which is also an important flavor in beer and responsible for the buttery taste [32]. Additionally, the obtained results in real samples, such as wine or beer, should be compared with already established measurement methods, like gas chromatography.

Thus, both substances (acetoin and diacetyl) can be used as indicator for different fermentation processes and could prove the quality of alcoholic beverages. By applying Boolean operations (such as **AND**, **OR**, **NAND**,...) [33, 34] and by defining a threshold voltage of the particular biosensor signal (depending on the fermentation process), the overall sensor read-out could give an indication of the status of the fermentation course. Because diacetyl and acetoin are both key indicators whether beer has been adequately matured, or if the fermentation time of wine is successfully completed. By detecting both parameters, the fermentation could be stopped at the right time to avoid unnecessary fermentation or maturation time to accelerate the process. Furthermore, the unpleasant buttery-like flavor, which occurs due to exceeded fermentation/maturation process, can be avoided.

Acknowledgments

The authors thank the Ministry of Innovation, Science and Research of the state of North Rhine-Westphalia for financial support (funding program FH-Struktur 2016). The authors thank A. Poghossian for valuable discussions and H. Iken for the preparation of the EIS sensor chips.

References

[1] E. C. Hahn, A. A. Suleiman, G. G. Guilbault, and J. R. Cavanaugh. “A piezoelectric crystal detector for determination of acetoin in air”. *Analytica Chimica Acta* 197 (1987), 195–202.

[2] A. M. Lawson, R. A. Speers, and J. Zhu. “Chemical and sensory detection of diacetyl in strawberry juice”. *Food / Nahrung* 39 (1995), 323–327.

[3] P. C. Vasavada and C. H. White. “A screening method of bacteriat reduction of diacetyl”. *Journal of Dairy Science* 60 (1977), 1854–1857.

[4] Z. Xiao, X. Wang, Y. Huang, F. Huo, X. Zhu, L. Xi, and J. R. Lu. “Thermophilic fermentation of acetoin and 2,3-butanediol by a novel *Geobacillus* strain”. *Biotechnology for Biofuels* 5 (2012), 88–89.

[5] T. M. Cogan, M. O‘Dwod, and D. Mellericj. “Effect of pH and sugar on acetoin production from citrate by leuconostoc lactis”. *Applied Microbiology and Biotechnology* 41 (1981), 1–8.

[6] M. Huang, F. B. Oppermann-Sanio, and Steinbüchel A. "Biochemical and molecular characterization of the *Bacillus subtillis* acetoin catabolic pathway". *Journal of Bacteriology* 181 (1999), 3837–3841.

[7] P. Romano and G. Suzzi. "Origin and production of acetoin during wine yeast fermentation". *Applied Microbiology and Biotechnology* 2 (1996), 309–315.

[8] A. D. Haukeli and S. Lie. "Formatoin and removal of acetoin during yeast fermentation". *Journal of the Institute of Brewing* 81 (1975), 58–64.

[9] G. Reed and T. W. Nagodawithana. *Yeast technology second edition.* Dordrecht: Springer Netherlands, 1991.

[10] L. Vann and J. D. Sheppard. "Development of a biosensor for measurement of diacetyl in beer". *Transactions of the ASAE* 48 (2005), 2223–2228.

[11] M. Levine. "On the significance of the Voges-Proskauer reaction". *The Journal of Interfectious Diseases (J. Bacteriol)* 2 (1916), 153–164.

[12] E. L. Speck and E. Freese. "Control of metabolite secretion in *Bacillus subtilis*". *Journal of General Microbiology* 78 (1973), 261–275.

[13] A. Poghossian, D.-T. Mai, Y. Mourzina, and M. J. Schöning. "Impedance effect of an ion-sensitive membrane: Characterisation of an EMIS sensor by impedance spectroscopy, capacitance–voltage and constant–capacitance method". *Sensors and Actuators B: Chemical* 103 (2004), 423–428.

[14] A. Poghossian, T. Yoshinobu, A. Simonis, H. Ecken, H. Lüth, and M. J. Schöning. "Penicillin detection by means of field-effect based sensors: EnFET, capacitive EIS sensor or LAPS?" *Sensors and Actuators B: Chemical* 78 (2001), 237–242.

[15] M. J. Schöning, D. Brinkmann, D. Rolka, C. Demuth, and A. Poghossian. "CIP (cleaning-in-place) suitable "non-glass" pH sensor based on a Ta_2O_5-gate EIS structure". *Sensors and Actuators B: Chemical* 111-112 (2005), 423–429.

[16] J. R. Siqueira, D. Molinnus, S. Beging, and M. J. Schöning. "Incorporating a hybrid urease-carbon nanotubes sensitive nanofilm on capacitive field-effect sensors for urea detection". *Analytical Chemistry* 86 (2014), 5370–5375.

[17] M. Thust, M. J. Schöning, J. Vetter, P. Kordos, and H. Lüth. "A long-term stable penicillin-sensitive potentiometric biosensor with enzyme immobilized by heterobifunctional cross-linking". *Analytica Chimica Acta* 323 (1996), 115–121.

[18] M. H. Abouzar, A. Poghossian, A. G. Cherstvy, A. M. Pedraza, S. Ingebrandt, and M. J. Schöning. "Label-free electrical detection of DNA by means of field-effect nanoplate capacitors: Experiments and modeling". *Physica Status Solidi A* 209 (2012), 925–934.

[19] T. S. Bronder, A. Poghossian, S. Scheja, C. Wu, M. Keusgen, D. Mewes, and M. J. Schöning. "DNA immobilization and hybridization detection by the intrinsic molecular charge using capacitive field-effect sensors modified with a charged weak polyelectrolyte layer". *ACS Applied Materials and Interfaces* 7 (2015), 20068–20075.

[20] A. Poghossian, M. Thust, P. Schroth, A. Steffen, H. Lüth, and M. Schöning. "Penicillin detection by means of silicon-based field-effect structures". *Sensors and Materials* 13 (2001), 207–223.

[21] B. Veigas, E. Fortunato, and P. V. Baptista. "Field effect sensors for nucleic acid detection: Recent advances and future perspectives". *Sensors* 15 (2015), 10380–10398.

[22] D. Molinnus, A. Poghossian, M. Keusgen, E. Katz, and M. J. Schöning. "Coupling of biomolecular logic gates with electronic transducers: from single enzyme logic gates to sense/act/treat chips". *Electroanalysis* 29 (2017), 1840–1849.

[23] A. Poghossian, K. Malzahn, M. H. Abouzar, P. Mehndiratta, E. Katz, and M. J. Schöning. "Integration of biomolecular logic gates with field-effect transducers". *Electrochimica Acta* 56 (2011), 9661–9665.

[24] A. Poghossian, M. Bäcker, D. Mayer, and M. J. Schöning. "Gating capacitive field-effect sensors by the charge of nanoparticle/molecule hybrids". *Nanoscale* 7 (2015), 1023–1031.

[25] A. Poghossian and M. J. Schöning. "Label-free sensing of biomolecules with field-effect devices for clinical applications". *Electroanalysis* 26 (2014), 1197–1213.

[26] V. Scherbahn, M. T. Putze, B. Dietzel, T. Heinlein, J. J. Schneider, and F. Lisdat. "Biofuel cells based on direct enzyme-electrode contacts using PQQ-dependent glucose dehydrogenase/bilirubin oxidase and modified carbon nanotube materials". *Biosensors and Bioelectronics* 61 (2014), 631–638.

[27] M. J. Schöning, N. Näther, V. Auger, A. Poghossian, and M. Koudelka-Hep. "Miniaturised flow-through cell with integrated capacitive EIS sensor fabricated at wafer level using Si and SU-8 technologies". *Sensors and Actuators B: Chemical* 108 (2005), 986–992.

[28] L. Muschallik, D. Molinnus, J. Bongaerts, M. Pohl, T. Wagner, M. J. Schöning, P. Siegert, and T. Selmer. "(R,R)-Butane-2,3-diol dehydrogenase from *Bacillus clausii* DSM 8716^{T}: Cloning and expression of the bdhA-gene, and initial characterization of enzyme". *Journal of Biotechnology* 258 (2017), 41–50.

[29] D. Molinnus, L. Muschallik, J. Bongaerts, T. Selmer, T. Wagner, P. Siegert, M. Keusgen, and M. J. Schöning. "Development of a biosensor for the detection of acetoin during wine fermentation". *Proceedings* 1 (2017), 718.

[30] E. Atanassova and D. Spassov. "Electrical properties of thin Ta_2O_5 films obtained by thermal oxidation of Ta on Si". *Microelectronics Reliability* 38 (1998), 827–832.

[31] C. Chaneliere, J. L. Autran, R. Devine, and B. Balland. "Tantalum pentoxide (Ta_2O_5) thin films for advanced dielectric applications". *Materials Science and Engineering: R: Reports* 22 (1998), 269–322.

[32] T. Wainwright. "Diacetyl- a review: Part I - Analytical and biochemical considerations: Part II - Brewing experience". *Journal of the Institute of Brewing* 79 (1973), 451–470.

[33] E. Katz, A. Poghossian, and M. J. Schöning. "Enzyme-based logic gates and circuits-analytical applications and interfacing with electronics". *Analytical and Bioanalytical Chemistry* 409 (2017), 81–94.

[34] E. Katz, V. M. Fernández, and M. Pita. "Switchable bioelectrocatalysis controlled by pH changes". *Electroanalysis* 27 (2015), 2063–2073.

9 Concluding remarks and perspectives

Biocomputing implies the application of logic principles known from digital electronics in combination with biology. Here, one or more (bio)chemical input signals can be detected and due to Boolean operations, basing on biochemical processes, one output signal according to the binary notation, consisting of **0** and **1** corresponding to a YES/NO answer, is delivered. They are already many concepts of biologic gate systems with the idea for their application in e.g., medicine when a rapid diagnosing of a disease is required. In this case, several biomarkers are detected and depending on the output pattern(s), a certain disease can be diagnosed. But up to now, so far developed concepts often use all-photonic detection methods to read out an output signal, which makes it quite difficult to combine several different logic gates in one system. Due to photoreaction, irreversible operations are formed which can be problematic for creating resetting and recycling devices without adding chemicals. Since the chemical reaction occurs in the analyte solution, and by applying e.g., fluorescence markers or other dyes, the analyte is affected and hence, the following reactions can be falsified. Furthermore, by applying optical detection methods, the analyte solution has to be prepared before measurements that is time-consuming and not sustainable when every second counts for the patient.
Hence, the initial situation led to the development of different concepts of biologic gates integrated on electrochemical transducers for label-free detection. Such systems allow the design of novel digital biosensors with direct electrical output signals corresponding to the input signals. Three different digital biosensors are conceptualized for a possible application in medicine or food industry with realizing of "proof-of-principle" experiments.

As first concept, a BioLogicChip has been developed combining a "sense-act-treat" function integrated on one chip. The BioLogicChip is developed to diagnose a specific disease depending on a particular biomarker or on the combination of different biomarkers (serving as input signal). At the same time, with the same device, a certain amount of drug that is necessary can be administered. Here, multiple biochemical input signals can be detected simultaneously and due to Boolean operations (**AND, OR,** etc.), the actuator is triggered to release a substance. Furthermore, the amount and time of the drug release is monitored by the addition of a drug sensor.

This concept has been exemplarily demonstrated as "artificial pancreas" and is proposed as closed-loop drug-release system triggered by an enzyme logic gate. The glucose level of the patient is determined by a chip-based biosensor. This amperometric sensor is designed as enzyme-based **AND** logic gate with the inputs glucose and oxygen. The chip-based amperometric glucose sensor exhibits a linear behavior in the milimolar concentration range. Furthermore, preliminary studies were carried out of the enzyme

AND gate biosensor. As a result, in the absence of either or both input signals, no chemical reaction occurs, no output is generated, resulting in an output signal of logic **0**. Only in the presence of both inputs (oxygen and glucose), the enzymatic reaction can be completed, thus, an output current (as logic **1**) is generated which could be used to address the actuator.

A temperature-dependent hydrogel (poly-(N-isopropylacrylamide) (PNIPAAm)) is characterized with regard to its possible application as actuator. Therefore, the impedance of the interdigitated circular electrode with the deposited hydrogel was measured at temperatures between 28 °C and 42 °C. At lower temperatures, the impedance is constant that implies the swelling state of the hydrogel. At higher temperatures than the phase-transition temperature (>34 °C), the impedance is sharply increased corresponding to the collapsed state. Due to the swelling and shrinking characteristic of the hydrogel, switching between "ON" and "OFF", a certain amount of a drug (here, e.g., insulin) can be released, which is additionally monitored. In contrast to conventional systems, the BiologicChip provides an additional chip-based Ir_xO_y sensor for the detection of insulin. Successful experiments with insulin concentrations in the nano- to micromolar concentration range were carried out.

- Perspectively, all three individual components, such as the amperometric sensor with the enzyme-based **AND** logic gate, the temperature-dependent hydrogel using as actuator and the chip-based Ir_xO_y sensor for the detection of insulin, should be combined into one system, onto one chip. Moreover, this chip, which is based on biomolecular logic principles, should be integrated into a microfluidic system to realize the closed-loop drug-release system. However, there are still some challenges which have to be considered, such as the generated current from the glucose **AND** logic gate has to be amplified resulting in a sufficiently high current to address the actuator. This could be either done by an external amplification source or by a (bio)chemical amplification of the sensor signal. In addition, the temperature-dependent hydrogel should be further developed to be feasible to release a defined amount of a certain drug. For the future, the hydrogel could be used as a valve to separate the drug into a chamber of the microfluidic system. It could be also possible to further modify the hydrogel in a way that the medical drug is already incorporated into the hydrogel and due to the shrinking effect, a defined amount of the drug will be washed out automatically.

- In future, the BioLogicChip could be developed as e.g., point-of-care (POC) diagnostic device for the application in emergency rooms, operation rooms, or any situation in which a rapid result is required and a fast administration of the drug is necessary. Such a device would be developed with the advantages of low-cost, lightweight and portability, and requires a minimum of sample preparation. The challenge in the developing of POC systems is the integration of the blood collection from the patient, sample pre-treatment (if necessary), analyte-specific reaction, signal production, signal detection and reporting of the results. All these different components have to be compatible with each other. Especially, with the

higher amount of individual devices integrated into one system, the compatibility is getting extremely ambitious.

- Another strategy could be the development of the BioLogicChip as an implantable device. In this case, the whole system has to be miniaturized for an implantation under the skin. With such system, the blood glucose level of the patient could be monitored continuously to make the life of diabetes patients saver and more comfortable. If the glucose level increases, a certain amount of insulin will be released automatically, depending on the glucose level. However, there are some challenges to be solved. The main challenge is the miniaturization of the system. The glucose sensor as well as the insulin sensor should have a high sensitivity but their size should be as small as possible. Additionally, after some time, the amount of insulin, which is integrated in the BioLogicChip will decrease and flow into the human's body, as desired. Hence, it has to be refilled. Either insulin has to be injected into the system from outside of the body, or the whole BioLogicChip has to be replaced. Additionally, the developed device has to be biocompatible (a task which has not yet been solved for the last 30 years), it has to be always reliable and may not bring harm to the human's body.

The main part of the thesis was spent for the development and improvement of a digital adrenaline biosensor that is introduced as second concept. This biosensor is of high interest for medical applications, in particular to support adrenal vein sampling (AVS). People with adrenal gland tumors have to undergo the AVS procedure to diagnose primary aldosteronism, which is the most frequent cause of hypertension. Since AVS is a technically demanding procedure in which correct cannulation of the right adrenal veins is quite sophisticated due to their small size, adrenaline could serve as a biomarker due to its concentration difference between adrenal veins ($\gtrsim$100 nM) and peripheral blood ($\lesssim$5 nM). Therefore, the sensor should be able to detect the adrenaline concentration difference in adrenal blood and peripheral blood to proof the position of the catheter and hence, to facilitate and to accelerate the medical examination. For the realization of the adrenaline biosensor, a commercially available galvanic oxygen sensor is modified by a laccase/pyrroloquinoline quinone-dependent glucose dehydrogenase (PQQ-GDH) bi-enzyme system to realize the substrate-recycling principle in order to amplify the biosensor signal. In a first reaction step, adrenaline is oxidized by the enzyme laccase to adrenochrome under oxygen consumption, followed by the second reaction where adrenochrome is catalyzed by the enzyme PQQ-GDH again back to adrenaline in the presence of glucose. Here, the oxygen consumption is the measured quantity. The sensor has been studied in both buffer solution as well as in Ringer's solution and exhibited that it has a high activity in a wide pH range. A lower detection limit of 1 nM at physiological pH values (pH 7.4) and at 30 °C could be achieved. In addition, the sensitivity of the adrenaline biosensor has been studied towards different catecholamines present in blood or artificial ones such as noradrenaline, dobutamine and dopamine. The sensor is almost insensitive against the artificial dobutamine. A sensor signal at a concentration of 10 nM and 50 nM for noradrenaline and dopamine, respectively, has been observed. However, the detectable concentrations of noradrenaline and dopamine

are much higher than their concentrations in adrenal venous blood and hence, they have no influence on the sensor signal during medical adrenaline measurements. Finally, the developed adrenaline biosensor has been successfully examined in blood plasma samples spiked with adrenaline concentrations between 1 nM and 150 nM. These experiments demonstrate that the sensor enables the detection of adrenaline at concentrations corresponding to adrenal- and peripheral blood. Additionally, "proof-of-principle" experiments of the digital adrenaline biosensor have been performed. This biosensor is structured as two concatenated enzyme-based **AND** logic gates with the enzyme laccase, which is part of the first **AND** logic gate and PQQ-GDH in combination with the second **AND** logic gate. With this digital adrenaline biosensor, a rapid qualitative analysis about an elevated or normal adrenaline concentration in the body fluids can be given, by definition of a personally tailored threshold level separating the logic **0** and **1** values. With the help of the digital adrenaline biosensor, the physician can control and correct the position of the catheter, if necessary. This would accelerate and facilitate this complicated medical investigation. Furthermore, since AVS procedure is usually controlled by a computer tomography scan, with a faster insertion of the catheter into the right vein, the patient will be exposed less time to the radiation.

In a continues study, the adrenaline biosensor is further developed as miniaturized chip-based biosensor system consisting of a platinum thin-film sensor chip fabricated by means of conventional silicon- and thin-film technology and modified with the enzyme PQQ-GDH. With this chip-based biosensor, the bioelectrocatalytical measurement principle for the recycling reaction of adrenaline is generated, to amplify the sensor signal. By an applied potential of +450 mV to the working electrode *vs.* the Ag/AgCl reference electrode, adrenaline will be first oxidized at the electrode surface to adrenochrome, followed by the second reaction, where adrenochrome is reduced back to adrenaline, catalyzed by the immobilized enzyme PQQ-GDH while glucose will be reduced to gluconolactone. The amperometric chip-based biosensor has been characterized regarding the working pH-, temperature- and glucose-concentration optimum, respectively. Here, a lower detection limit of 1 nM at physiological pH value of pH 7.4 and at 30 °C with a glucose concentration of 20 mM could be achieved. Long-term stability of the adrenaline biosensor has been studied over 10 days. Also the chip-based biosensor has been tested for its sensitivity towards other catecholamines such as noradrenaline, dopamine and dobutamine. The highest sensitivity has been observed during measurements with adrenaline. Finally, preliminary studies in blood plasma were successfully carried out. The sensor was able to detect the adrenaline-concentration difference between adrenal blood and peripheral blood from patients suffering from an adrenal gland tumor with hypokalemic hypertension, which favors its application to support the AVS.

This biosensor has a high potential for the application as POC system during AVS in the operation room to proof the correct position of the catheter. There are two possible application methods (fields) which can be beneficial for the physician:

- The first one is the idea to further develop this chip-based biosensor as a kind of smart adrenaline hand-held device (as known from a glucose biosensor). Thus,

it would be possible to measure adrenalin concentrations location-independently. That means, directly, next to the patient, the blood drained during AVS can be verified regarding its adrenaline concentration and depending on the output signal, the physician has the chance to correct the catheter, if necessary, directly during the medical examination. This has the advantage that the patient has to undergo only once this painful AVS procedure, because the physician can be sure that the finally collected blood is from the desired adrenal vein.

- The second idea is the integration of the digital adrenaline biosensor into the catheter, which is used to diagnose adrenal gland tumors during AVS. Furthermore, the biosensor could be coupled with an indicator lamp, fixed on the catheter. Depending on the catheter position and hence, depending on the adrenaline concentration, the lamp starts to flash. If there is a low adrenaline concentration corresponding to peripheral blood, the light flashes e.g., "red" indicating that the physician has to additionally correct the position of the catheter, until the light is "green". The latter corresponds to a high andrenaline concentration in adrenal glands. In this case, the adrenaline biosensor has to be further miniaturized because the diameter of such a catheter is less than 1 cm. A big challenge is here that the biosensor has to be biocompatible because it has direct contact to the patient's blood in the body. Basic prerequisite is that it must not lead to health impairment of the patient.

For both ideas, the biosensor has to be distinctly miniaturized. All three electrodes, such as reference-, counter- and working electrode, should be integrated onto one chip to make the biosensor easier to handle. As a consequence, this miniaturization can have an influence on the biosensor's sensitivity and should be compensated by e.g., a higher loading of the enzyme PQQ-GDH onto the sensor surface to reach a higher activity. Also, in this thesis, measurements were performed in blood plasma. The aim is, however, to measure adrenaline without pre-treatment of the blood. The biosensor's behavior can be different during measurements in whole blood and has to be studied first. In general, the developed adrenaline biosensor has to undergo clinical studies to proof the functionality of the device to different situations with different patients a number of times. Additionally, for medical devices, approval regulations (such as Food and Drug Administration regulations or European Medicines Agency) have to be considered.

After demonstrating biologic gates based on amperometric biosensors, enzyme-based logic gates based on field-effect EIS (electrolyte-insulator-semiconductor) biosensors have been presented. A novel biosensor has been developed for the detection of acetoin during fermentation processes (e.g., fermentation of beer or wine). Since acetoin is pale to yellow and is indicated by a buttery-like taste and a pleasant yogurt-creamy order, it can influence the taste and hence, the quality of alcoholic beverages. The detection of acetoin during fermentation processes could monitor and control the quality of alcoholic beverages due to its involvement in the wine bouquet or its influence in the beer flavor.

The introduced field-effect EIS biosensor consists of a layer structure of Al/p-Si/SiO_2/Ta_2O_5 and has been modified by the enzyme acetoin reductase (butane-2,3-diol dehydrogenase from *Bacillus clausii* DSM 8716^T) for the catalytic reaction of racemic

acetoin to (R,R)-2,3-butanediol and meso-butanediol, respectively. This reaction results in a pH change due to the H^+-ion consumption. The biosensor exhibits a linear concentration behavior at acetoin concentrations between 3 mM and 90 mM. Two different immobilization strategies have been compared, namely adsorptive binding and cross-linking (by forming cross-linkages between the enzyme molecules using glutaraldehyde). The highest sensitivity has been reached with the biosensors modified by means of cross-linking method. A pH optimum at pH 7.1 has been obtained. The long-term stability of this biosensor has been investigated over five days. Here, the developed biosensor showed a long-term stability of around two days. Additionally, with this biosensor it was possible to detect spiked acetoin concentrations in real white wine samples.

Acetoin has a broad usage and is mainly found in food and drinks to enhance the flavor of the products such as breakfast cereals, cheese, chewing gum, fats and oils, puddings or sweet sauces. Therefore, the fast detection of acetoin by the developed biosensor could – besides the fermentation process – also facilitate the monitoring of the production of different food products, to fulfill the requirements as independent control system. The following tasks, however, have to be addressed first:

- Since the developed chip-based biosensor shows a long-term stability of only two days, the enzyme‘s activity has to be further stabilized to apply the sensor more often (e.g., one week).
- This biosensor should be examined regarding its cross-sensitivity towards diacetyl or acethylbutanediol, two compounds that are also present during fermentation processes.
- Furthermore, since acetoin and diacetyl attribute to the beer- and wine flavor, the biosensor should be further developed to realize a digital acetoin/diacetyl biosensor by applying Boolean operations. As a variant, a more complex logic gate has to be developed by immobilization of a second enzyme onto the biosensor surface for the detection of diacetyl. Depending on the desired buttery-like taste of the certain alcoholic beverage, a threshold value has to be defined (below this threshold value, a logic **0** is generated, and above this value, a logic **1** is given). Thus, a “YES/NO” answer should be delivered about the status of the fermentation process.

In summary, several concepts of biologic gates integrated on different transducers for a rapid label-free detection of certain biomarkers were demonstrated in this thesis. In contrast to the most developments on molecular logic gates discussed in literature – which are mostly biomolecular logic gates based on optical output signals such as e.g., fluorescence – the presented concepts take benefit from electrical output signals. This has the advantage that multiple logic devices can be implemented together in the same analyte. The application of electronic transducers instead of optical signal-reading devices is highly promising to move from “proof-of-concept” studies to finally ready-to-use logic devices with direct electrical output. Furthermore, more complex logic

gate devices can be build up. A gate-to-gate communication can be realized without influencing or changing the analyte solution. Furthermore, a desired logic gate can be electrochemically and independently addressed and it is possible to switch between the "ON" and "OFF" state of the single logic gate within the network.

For the future, the combination of biomolecular logic principles with electronic transducers should be further extended, to enable the establishment of new multifunctional sensor- and actuator principles. An example of the functionality of such biosensor platform is exemplarily demonstrated in Fig. 9.1.

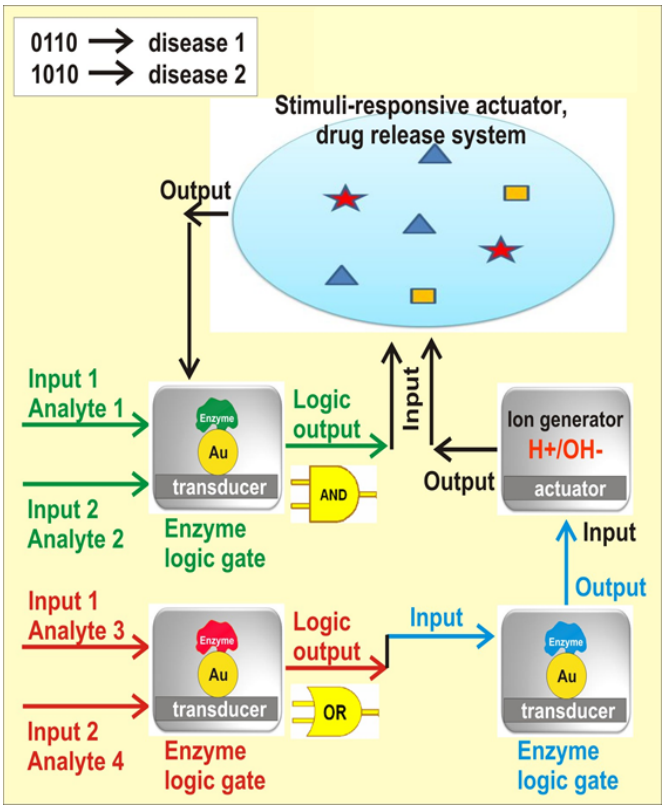

Fig. 9.1: Schematic of a biosensor platform in combination with actuators and logically triggered drug-release system(s).

One of the advantages of biomolecular logic systems with electronic transducers is their combination with stimuli-responsive materials, like hydrogels; therewith, an actuator function can be triggered depending on the output signal of the logical operation. With those a biosensor chips, an array of electrical and/or light-addressable chemical or biochemical sensors modified with corresponding biomolecules, such as enzymes or antibodies, can detect several analytes (e.g., biomarkers) as well as selected reactions (e.g., enzyme cascades), and with the help of Boolean operations a logic output signal can be generated. The read-out bio-/chemical signals correspond to mathematic algorithms consisting of "**0**" and "**1**". For a possible application in medicine, the resulting bit pattern correlates with a certain disease (disease 1: **0110**; disease 2: **1010**). In this case,

with this biosensor chip, in combination with logical principles, a specific diagnose with high reliability can be provided: for example, different biomarkers indicating cancer (e.g., pancreas cancer, breast cancer) can be determined. Furthermore, with the same system, the required medication should be released (e.g., Taxol or Vincristine). Hence, a new generation of biosensors in combination with actuators together with logically triggered drug-release systems could be developed, to result in closed-loop intelligent sense/act/treat biochips. These logic biochips are considered as highly attractive as new generation of digital biosensors for the application in personalized medicine and theranostics.

Nonetheless, to obtain these goals, there are several remaining challenges which have to be considered and finally solved:

- With the development of more complex biomolecular logic gates in combination with electronic transducers, the chemical cross-reactivity could be an issue for systems that are more complex than the ones described herein as "proof-of-principle" examples. Therefore, the used biomolecules and bioreceptors have to be selected carefully to avoid undesired sensor signals.

- Due to the small size of the desired biosensor platform, each individual sensor has to be miniaturized, which can influence its sensitivity behavior as well as its stability in operation.

The further development of such a biosensor platform to a programmable diagnostic computer is conceivable in the future. The device might be, for example, implanted into the human's body, consisting of an integrated sensor technology which is able to respond automatically to metabolic variations. Furthermore, it could diagnose symptoms and release a prompt and certain amount of a drug for the treatment of the patient with the integrated actuator function. Such diagnostic device could be equipped with specific bioreceptor arrangements corresponding to the biomarkers for the diagnosis of diseases, which are typical for certain risk patients (with e.g., cardiovascular dysfunction due to living conditions such as smoking, obesity, or family burden). The integrated computer has to be programmed depending of the used bioreceptor/biomarker combination to select the measurement principle (such as amperometry or potentiometry) with defined threshold values dependent on the patient conditions. This intelligent biocomputer is able to diagnose and distinguish between e.g., a heart failure or sporty overexertion, dizziness or brain tumor etc. In addition, the biosystem should be easily adapted to the patient in a personalized way by choosing the right combination of bioreceptors/biomarkers. For such personalized biocomputing systems, attention should be paid to e.g., pre-existing condition and family burden: both, patient monitoring/treatment in a critical medical condition and a timely early diagnosis, might be possible. The whole humanity would benefit from such an essential step in the development of a medical expert system in a form of an implantable biocomuter.

10 Zusammenfassung

In der vorliegenden Arbeit wurden verschiedene Konzepte mit biologischen Schaltungen, die auf elektronischen Transducern integriert sind, entwickelt. Damit können neuartige digitale Biosensoren aufgebaut werden, die in Abhängigkeit der Eingangssignale ein elektrisches Ausgangssignal generieren.

Als erstes Konzept wird ein "BioLogicChip" vorgestellt, der die "Sense-act-treat"-Funktion auf einem Chip kombiniert. Mit diesem BioLogicChip soll es möglich sein, eine bestimmte Krankheit abhängig von spezifischen Biomarkern zu diagnostizieren. Gleichzeitig soll mit diesem Chip eine bestimme Menge des benötigten Wirkstoffs dem Patienten verabreicht werden können. In dieser Arbeit wurde das Konzept exemplarisch als "künstliche Pankreas" dargestellt, bei der die Glukosekonzentration mit Hilfe eines Chip-basierten Biosensors bestimmt wird. Der Glukosesensor wurde als logische **AND**-Schaltung konzipiert, mit Glukose und Sauerstoff als Eingangssignale. Nur wenn beide Eingangssignale gleichzeitig vorhanden sind, kommt es zur Reaktion und ein Strom wird generiert. Dieser Strom kann dann zur Adressierung des impedimetrischen Sensors genutzt werden, auf dem ein temperaturabhängiges Hydrogel immobilisiert ist. Dieses Hydrogel dient, auf Grund seiner Quell- und Schrumpf-Eigenschaft, als Aktuator und kann somit zwischen "AUF" und "ZU" schalten. Damit kann eine bestimmte Menge eines Wirkstoffs (z.B. Insulin) freigesetzt werden. Um das Hydrogel auf seine Aktuatorfunktion zu prüfen, wurde die Impedanz bei verschiedenen Temperaturen (28 °C - 42 °C) untersucht. Unterhalb der Phasenübergangstemperatur ist der Impedanzwert konstant, was dem aufgequollenen Zustand des Hydrogels entspricht. Bei höheren Temperaturen (34 °C) steigt die Impedanz an und entspricht dem kollabierten Zustand. Im Gegensatz zur konventionellen "künstlichen Pankreas", wird bei dem BioLogicChip die Freisetzung des Wirkstoffs durch den Aktuator zusätzlich sensorisch überprüft. Hierbei dient ein Chip-basierter Ir_xO_y-Sensor zur Insulinmessung im nano- bis mikromolaren Konzentrationsbereich.

Als zweites Konzept wurde ein digitaler Adrenalinbiosensor entwickelt, der die Nebennierenvenenkatheteruntersuchung (AVS) unterstützen soll. Mit diesem Sensor sollen die Adrenalinkonzentrationsunterschiede zwischen Nebennierenblut und peripherem Blut gemessen werden, um so die Position des Katheters zu überprüfen. Zur Entwicklung des Adrenalinbiosensors wurde eine 2-Enzymmembran (bestehend aus Laccase und Pyrroloquinolinchinon-abhängiger Glukose-Dehydrogenase (PQQ-GDH)) auf einem Sauerstoffsensor fixiert. Damit findet das Substraterecycling-Prinzip Anwendung, wodurch das Sensorsignal verstärkt wird. Im ersten Reaktionsschritt wird Adrenalin mit Hilfe der Laccase unter Sauerstoffverbrauch zu Adrenochrom oxidiert. Anschließend wird das entstandene Adrenochrom wieder über die PQQ-GDH zurück zu Adrenalin

reduziert, bei gleichzeitiger Oxidation von Glukose. Der verbrauchte Sauerstoff wird mittels O_2-Sensor gemessen und ist proportional zur Adrenalinkonzentration. Mit dem Adrenalinsensor konnte in Puffer- und Ringerlösung eine untere Nachweisgrenze von 1 nM bei pH 7,4 und 30 °C erreicht werden. Außerdem wurde die Querempfindlichkeit gegenüber anderen Katecholaminen (Noradrenalin, Dopamin, Dobutamin) überprüft. Bei den natürlich vorkommenden Katecholaminen konnte ein Sensorsignal erst bei 10 nM Noradrenalin und 50 nM Dopamin erfasst werden; gegenüber künstlichem Dobutamin war der Sensor unempfindlich. Zusätzlich konnten gespikte Adrenalinproben (1 nM - 150 nM) im Blutplasma untersucht werden. Die Experimente zeigten, dass Konzentrationen im Nebennierenblut und peripheren Blut detektiert werden können. Außerdem wurden mit dem digitalen Adrenalinsensor "Proof-of-principle"-Experimente aus zwei aufeinanderfolgenden logischen **AND**-Schaltungen durchgeführt (Laccase als erste logische **AND**-Schaltung; PQQ-GDH als zweite logische **AND**-Schaltung). Mit diesem digitalen Adrenalinbiosensor kann eine schnelle, qualitative Analyse über die Adrenalinkonzentration im Blut erfolgen; der Arzt kann die Position des Katheters überprüfen und gegebenenfalls korrigieren.

Im weiteren Verlauf wurde der Adrenalinbiosensor hinsichtlich seiner Miniaturisierbarkeit weiterentwickelt. Dazu wurde ein Chip-basierter Platinsensor mit dem Enzym PQQ-GDH modifiziert, um das bioelektrokatalytische Messprinzip zu ermöglichen, um so Adrenalin zu recyclen und das Sensorsignal zu verstärken. Der Chip-basierte Adrenalinbiosensor wurde bezüglich pH-, Temperatur- und Glukose-Optimum charakterisiert. Dabei konnte eine untere Nachweisgrenze von 1 nM bei einem physiologischen pH-Wert von pH 7,4, bei 30 °C und bei einer Glukosekonzentration von 20 mM erreicht werden. Darüber hinaus wurde die Langzeitstabilität des Biosensors über zehn Tage untersucht. Zusätzlich wurde die Sensitivität des Chip-basierten Biosensors gegenüber verschiedener Katecholaminen (Noradrenalin, Dopamin und Dobutamine) validiert. Die höchste Empfindlichkeit wurde bei Messungen mit Adrenalin erreicht. Es konnten erfolgreich erste Messungen in Blutplasma durchgeführt werden. Mit dem entwickelten Adrenalinbiosensor konnte außerdem die Konzentrationsdifferenz zwischen Nebennierenblut und peripherem Blut gemessen werden.

Neben logischen Schaltungen mit amperometrischen Sensoren wurden auch logische Schaltungen mit Feldeffekt-Sensoren am Beispiel eines Acetoinbiosensors entwickelt. Dieser soll für die Bestimmung verschiedener Acetoinkonzentrationen (z.B. in der Fermentation von Bier und Wein) eingesetzt werden. Der Feldeffekt-Sensor wurde mit Hilfe des Enzyms Acetoinreduktase modifiziert, wodurch razemisches Acetoin zu (R,R)-2,3-Butandiol und Meso-Butandiol katalytisch umgesetzt wird. Bei dieser Reaktion werden H^+-Ionen verbraucht. Der entwickelte Sensor zeigt ein lineares Verhalten bei Acetoinkonzentrationen zwischen 3 mM und 90 mM. Die höchste Sensitivität des Acetoinbiosensors konnte bei pH 7,1 erreicht werden. Es wurde die Langzeitstabilität über fünf Tage überprüft. Darüber hinaus wurden gespikte Acetoinkonzentrationen in Weißwein gemessen. Zukünftig könnte der Sensor als digitaler Acetoin/Diacecyl-Biosensor weiterentwickelt werden, da beide Substanzen zum Geschmack von Bier/Wein beitragen. Boole'sche JA/NEIN-Aussagen würden so den Status der Fermentation abbilden.

List of publications

Publications in peer-reviewed journals

[1] J. R. Siqueira, D. Molinnus, S. Beging, and M. J. Schöning. "Incorporating a hybrid urease-carbon nanotubes sensitive nanofilm on capacitive field-effect sensors for urea detection". *Analytical Chemistry* 86 (2014), 5370–5375.

[2] A. J. Bandodkar, D. Molinnus, O. Mirza, T. Guinovart, J. R. Windmiller, G. Valdés-Ramírez, F. J. Andrade, M. J. Schöning, and J. Wang. "Epidermal tattoo potentiometric sodium sensors with wireless signal transduction for continuous non-invasive sweat monitoring". *Biosensors and Bioelectronics* 54 (2014), 603–609.

[3] D. Molinnus, M. Bäcker, H. Iken, A. Poghossian, M. Keusgen, and M. J. Schöning. "Concept for a biomolecular logic chip with an integrated sensor and actuator function". *Physica Status Solidi A* 212 (2015), 1382–1388.

[4] D. Molinnus, M. Sorich, A. Bartz, P. Siegert, H. S. Willenberg, F. Lisdat, A. Poghossian, M. Keusgen, and M. J. Schöning. "Towards an adrenaline biosensor based on substrate recycling amplification in combination with an enzyme logic gate". *Sensors and Actuators B: Chemical* 237 (2016), 190–195.

[5] L. Muschallik, D. Molinnus, J. Bongaerts, M. Pohl, T. Wagner, M. J. Schöning, P. Siegert, and T. Selmer. "(R,R)-Butane-2,3-diol dehydrogenase from *Bacillus clausii* DSM 8716^{T}: Cloning and expression of the bdhA-gene, and initial characterization of enzyme". *Journal of Biotechnology* 258 (2017), 41–50.

[6] D. Molinnus, A. Poghossian, M. Keusgen, E. Katz, and M. J. Schöning. "Coupling of biomolecular logic gates with electronic transducers: from single enzyme logic gates to sense/act/treat chips". *Electroanalysis* 29 (2017), 1840–1849.

[7] D. Molinnus, G. Hardt, P. Siegert, H. S. Willenberg, A. Poghossian, M. Keusgen, and M. J. Schöning. "Detection of adrenaline in blood plasma as biomarker for adrenal venous sampling". *Electroanalysis* 30 (2018), 937–942.

[8] D. Molinnus, L. Muschallik, L. O. Gonzalez, J. Bongaerts, T. Wagner, T. Selmer, P. Siegert, M. Keusgen, and M. J. Schöning. "Development and characterization of a field-effect biosensor for the detection of acetoin". *Biosensors and Bioelectronics* 115 (2018), in press.

[9] D. Molinnus, G. Hardt, L. Käver, H. S. Willenberg, J.-C. Kröger, A. Poghossian, M. Keusgen, and M. J. Schöning. "Chip-based biosensor for the detection of low adrenaline concentrations to support adrenal venous sampling". *Sensors and Actuators B: Chemical* 272 (2018), 21–27.

Proceedings

[1] D. Molinnus, A. Bartz, M. Bäcker, P. Siegert, H. Willenberg, A. Poghossian, M. Keusgen, and M. J. Schöning. "Detection of adrenaline based on substrate recycling amplification". *Procedia Engineering* 120 (2015), 540–543.

[2] D. Molinnus, G. Hardt, L. Käver, H. S. Willenberg, A. Poghossian, M. Keusgen, and M. J. Schöning. "Detection of adrenaline based on bioelectrocatalytical system to support tumor diagnostic technology". *Proceedings* 1 (2017), 506.

[3] D. Molinnus, L. Muschallik, J. Bongaerts, T. Selmer, T. Wagner, P. Siegert, M. Keusgen, and M. J. Schöning. "Development of a biosensor for the detection of acetoin during wine fermentation". *Proceedings* 1 (2017), 718.

[4] D. Molinnus, G. Hardt, P. Siegert, H. S. Willenberg, F. Lisdat, A. Poghossian, M. Keusgen, and M. J. Schöning. "Adrenaline bi-enzyme sensor using signal amplification principle to support adrenal venous sampling". *Proceedings* 1 (2017), 717.

Oral and poster presentations

[1] D. Molinnus, A. Poghossian, M. Keusgen, and M. J. Schöning. *Concept for a biomolecular logic chip with an integrated sensor actuator function.* EnFI 2014. Jülich, Germany. 14. - 15.07.2014.

[2] D. Molinnus, A. Poghossian, M. Keusgen, and M. J. Schöning. *Konzept eines biomolekularen Logic-Chip mit integrieter Sensor- und Aktuatorfunktion.* 9. Deutsches BioSensor Symposium 2015. München, Germany. 11. - 13.03.2015.

[3] D. Molinnus, A. Bartz, M. Bäcker, P. Siegert, H. S. Willenberg, A. Poghossian, M. Keusgen, and M. J. Schöning. *Toward adrenaline biosensor based on an enzymatic logic gate.* EnFI 2015. Hannover, Germany. 06. - 07.07.2015.

[4] D. Molinnus, A. Bartz, M. Bäcker, P. Siegert, H. S. Willenberg, A. Poghossian, M. Keusgen, and M. J. Schöning. *Detection of adrenaline based on substrate recycling amplification.* Eurosensors 2015. Freiburg, Germany. 06. - 09.09.2015.

[5] D. Molinnus, M. Sorich, P. Siegert, H. S. Willenberg, A. Poghossian, and M. J. Schöning. *Enzymbasierter Adrenalinbiosensor für den unterstützenden Einsatz in der Tumordiagnostik - Fiktion oder Realität.* 12. Deutsche Nebennierenkonferenz 2016. Rostock, Germany. 12. - 14.02.2016.

[6] D. Molinnus, M. Sorich, P. Siegert, H. S. Willenberg, F. Lisdat, A. Poghossian, M. Keusgen, and M. Schöning. *A high-sensitive digital adrenaline biosensor.* EnFI 2016. Wildau, Germany. 04. - 05.07.2016.

[7] D. Molinnus, M. Sorich, P. Siegert, H. S. Willenberg, F. Lisdat, A. Poghossian, M. Keusgen, and M. J. Schöning. *High-sensitive and low detection limit adrenaline biosensor using substrate recycling amplification.* IMCS 2016. Jeju Island, Korea. 10. - 13.07.2016.

[8] D. Molinnus, M. Sorich, P. Siegert, H. S. Willenberg, F. Lisdat, A. Poghossian, M. Keusgen, and M. J. Schöning. *Towards a digital adrenaline biosensor assisting adrenal venous sampling procedure*. Kurt Schwabe Symposium 2016. Mittweida, Germany. 04. - 07.09.2016.

[9] D. Molinnus, M. Sorich, P. Siegert, H. S. Willenberg, F. Lisdat, A. Poghossian, M. Keusgen, and M. J. Schöning. *Towards a digital adrenaline biosensor: a useful tool for AVS (Adrenaline Vein Sampling)*. Micro and Nanosystems in Biochemical Analysis 2016. Warschau, Polen. 12. - 14.10.2016.

[10] D. Molinnus, L. Käver, P. Siegert, H. S. Willenberg, F. Lisdat, A. Poghossian, M. Keusgen, and M. J. Schöning. *Substrate recycling principle for the detection of adrenaline to support adrenal vein sampling*. EBS 2017. Potsdam, Germany. 20. - 23.03.2017.

[11] D. Molinnus, G. Hardt, L. Käver, H. S. Willenberg, F. Lisdat, A. Poghossian, M. Keusgen, and M. J. Schöning. *Detection of adrenaline based on substrate recycling principle to support adrenal vein sampling*. 60. Deutscher Kongress für Endokrinologie 2017. Würzburg, Germany. 15. - 17.03.2017.

[12] D. Molinnus, G. Hardt, L. Käver, H. S. Willenberg, A. Poghossian, M. Keusgen, and M. J. Schöning. *High-sensitive adrenaline biosensor based on bioelectrocatalysis to support tumor diagnosis*. EnFI 2017. Marburg, Germany. 28. - 29.08.2017.

[13] D. Molinnus, G. Hardt, L. Käver, H. S. Willenberg, A. Poghossian, M. Keusgen, and M. J. Schöning. *Detection of adrenaline based on bioelectrocatalytic systems to support tumor diagnostic technology*. Eurosensors 2017. Paris, France. 03. - 06.09.2017.

[14] D. Molinnus, L. Muschallik, J. Bongaerts, T. Selmer, T. Wagner, P. Siegert, M. Keusgen, and M. J. Schöning. *Development of a biosensor for the detection of acetoin during wine fermentation*. I3S 2017. Barcelona, Spain. 27. - 29.09.2017.

[15] D. Molinnus, G. Hardt, P. Siegert, H. S. Willenberg, F. Lisdat, A. Poghossian, M. Keusgen, and M. J. Schöning. *Adrenaline bi-enzyme sensor using signal amplification principle to support adrenal venous sampling*. I3S 2017. Barcelona, Spain. 27. - 29.09.2017.

[16] D. Molinnus, A. Poghossian, M. Keusgen, and M. J. Schöning. *Towards digital biosensors with enzyme logic gates for biomedical applications*. Biodetection and Biosensors 2017. Cambridge, England. 10. - 11.10.2017.

[17] D. Molinnus, A. Poghossian, M. Keusgen, and M. J. Schöning. *Enzyme based biologic gates for biomedical applications*. Nanoscale Science and Technology 2017. Hammamet, Tunesia. 27. - 29.10.2017.

[18] D. Molinnus, L. Muschallik, M. Jablonski, J. Bongaerts, T. Wagner, T. Selmer, P. Siegert, M. Keusgen, and M. Schöning. *Development and characterization of a field-effect biosensor for the detection of acetoin during fermentation processes*. EnFI 2018. Wittenberg, Germany. 01. - 03.07.2018.

Acknowledgment

On this journey, I want to express my deep gratitude for the outstanding support in different ways of pleasant people to enable this dissertation.

I am wholehearted thankful to all these people.

First and foremost, I want to take this opportunity to express my heartful gratitude to Prof. Dr. Michael J. Schöning for giving me the opportunity to carry out this exciting topic and being a member in your team of the Institute of Nano- and Biotechnologies at FH Aachen, Campus Jülich. Thank you for trusting and believing in me and giving me the big chance to carry out my Masterproject in the group of Prof. Dr. Joseph Wang in the US. But more importantly, I am much obliged for your seemingly tireless support, guidance and discussions during the entire time of this work. I am very thankful giving me the opportunity to present this scientific work at numerous conferences gaining experience and getting in touch with other scientists.

It is my great pleasure to thank Prof. Dr. Michael Keusgen in the same way for giving me the opportunity to graduate at the University of Marburg under his supervision. I want to thank you for your always helpful discussions, your advices and great support throughout the entire time of working on this thesis.

I am deeply thankful Prof. Dr. Arshak Poghossian for your untiring willingness not only to correct and improve publications but more important for having always an open mind to discuss and to question all my "scientific thoughts". Your scientific experience and energy has always been a source of inspiration. After finishing my thesis, I hope you can more enjoy your retirement.

My special thanks belongs to Prof. Dr. Holger Willenberg who came with this interesting topic to our institute. I want to thank you for this excellent cooperation. You gave me a great inside into this medical topic, and you had always an open mind for all my questions for a better understanding in this field. I would like to express my sincere thanks for your continuous interest, your support and proof-readings. And last but not least, thank you for the opportunity to carry out the measurement sessions in your lab and being such generous in blood donations.

I am in short of words to thank Prof. Dr. Joseph Wang for giving me the opportunity to carry out my Masterproject in the Laboratory of Nanobioelectronics at University of California, San Diego. Without this experience, I would never have thought about doing a Ph.D. You inspired and motivated me in order to venture this essential step.

I want thank Prof. Dr. Petra Siegert to support me in the biotechnological part ("acetoin") of my thesis, for the great collaboration, proof-reading publications and many discussions together with Prof. Dr. Thorsten Selmer, Prof. Dr. Johannes Bongaerts and Prof. Dr. Torsten Wagner. Especially, I want to thank Lukas Muschallik to support me in all the biological questions to provide the enzyme acetoin reductase, even spontaneously.

It is my great pleasure to thank Prof. Dr. Evgeny Katz (Department of Chemistry and Biomolecular Science, Clarkson University Potsdam, USA) to inspired me for working on this special topic. I am thankful for our outstanding collaboration to create a brilliant Review Article together. In the same way I want to thank Prof. Dr. Fred Lisdat (Biosystems Technology, University of Applied Sciences Wildau) for many discussions and collaboration.

I wish to thank all the students who contributed to this work in a number of ways with their research projects, bachelor or master thesis. Namely, Alexander Bartz, Maren Sorich, Cyrill Winzen, Ichrak Keroumi, Larissa Käver, Laura Osorio Gonsalez und Gabriel Hardt. I am really thankful for the friendly and trustful working atmosphere.

I want to thank the former Ph.D students at the INB: Dr. Sebastian Schusser, Dr. Christina Huck, Dr. Matthias Bäcker and Dr. Frederik Werner. You all helped me to facilitate the start in this new scientific world. I also want to thank all the members of the biosensoric lab, especially Heiko Iken, David Rolka and Stefan Beging for being the good souls in the lab and to keep always an open mind for any support. In a same way, I want to thank Dr. Elke Börmann-El Kholy being my office mate. My special thanks goes to Jan Oberländer for having fruitful discussions during many coffee breaks in the last years, to support me in each manner and to give me a better understanding for working with LaTeX. But specially, thank you that I can always count on you.

I also want to take this opportunity to express my deep gratitude to my family whose affecting, blessing and guidance have always been a source of inspiration for me. I am thankful for your tremendous moral boosting and sacrifice me self-reliant, positive and optimistic human being. Finally, I want to thank all my friends for supporting me and to encourage me during this dissertation. Especially, many thanks to my Jülich friends to make me feel like at home.

Denise Molinnus

Curriculum vitae

The curriculum vitae is not part of the online version.

The curriculum vitae is not part of the online version.